UNIVERSITY OF CAPE TOWN

Department of Civil Engineering

CHLORIDE TRANSPORT THROUGH CONCRETE AND IMPLICATIONS FOR RAPID CHLORIDE TESTING

Prepared by: Thomas J Gardner

in partial fulfilment of the requirements of MSc (Eng)

Submitted: March 2006

DECLARATION

I declare that this dissertation is my own, unaided work. I have used the Harvard Method of citation for referencing each significant contribution to, and quotation in, this dissertation. It is being submitted, as partial fulfilment of MSc (Civil Engineering), to the University of Cape Town, South Africa. It has not been submitted before for any other degree or examination at any other University or Tertiary Institution.

_____

Thomas Jayson Gardner
March 2006

ABSTRACT

The transport properties of concretes are key parameters affecting the serviceability of structures in chloride environments. Rapid chloride test methods are used to efficiently assess and categorise concrete to be used in chloride environments. These rapid tests are generally migration tests and rely on the application of an electrical field to accelerate the diffusion of chloride ions through a concrete specimen.

An experimental investigation was conducted in order to analyse the effect of an applied electrical field on the measured transport coefficients of mortars, and chloride binding capacity. Split cell diffusion and migration tests were conducted on mortar samples and the respective transport coefficients determined. This was followed by a chloride binding test, using the equalisation method, in order to determine the specimens' chloride binding capacity.

It was found that:

- Measured migration coefficients are generally an order of magnitude higher than measured diffusion coefficients.
- Binder systems with higher chemical chloride binding potential (e.g. Ground granulated Corex slag) showed the highest discrepancy between measured migration and diffusion coefficients.
- The discrepancy between the two parameters decreases with increased initial chloride concentration.
- The application of an electrical field lowers the chloride binding capacity of cementitious matrices – having greatest effect on chemical chloride binding capacity.
- The chloride binding capacity of the matrix appears to be permanently altered by the application of an electrical field.

Rapid chloride testing affects the behaviour of chloride ions within the matrix. The results of rapid chloride tests should, therefore, not be used to calculate diffusion coefficients of concretes to be used in long-term prediction models unless the tests have been calibrated for this purpose.

The Bulk Diffusion Test (BDT) and three rapid chloride tests:

- The Rapid Chloride Permeability Test (RCPT);
- The Rapid Migration Test (RMT); and
- The Chloride Conductivity Test (CCT),

were critically reviewed through literature review and laboratory trials.

The BDT was found to be the test most representative of in-service chloride diffusion. Due to its lengthy test duration, it is not suited for quality assurance purposes in practice. However, this test should be used for long-term research studies and in obtaining transport parameters for long-term serviceability prediction.

The RCPT should not be used for rapid chloride testing of concretes due to thermal effects and the many other variables affecting electrical current measurement though concrete.

The RMT and CCT are both well suited for the rapid characterisation of concretes, with the CCT being minimally impacted by electrical field application due to its relatively instantaneous testing time.

ACKNOWLEDGEMENTS

I am very grateful to both of my supervisors for the knowledge and skills I have learnt as a result of their ongoing efforts in research and teaching.

I would like to thank Professor MG Alexander for his guidance and support throughout this study. His encouragement, probing questions and positive attitude, even in the direst of situations, was very motivating and greatly appreciated.

I would like to thank Dr K Stanish for his constant feedback and availability in answering my numerous questions throughout the study. His expertise in the field of chloride transport was of great benefit in shaping the study and analysing the results.

I would also like to thank:

- Professor Y Ballim, of the University of the Witwatersrand, who provided much input, especially in the analysis of the many micrographs we obtained, for which I am very grateful.

- Professor K Scrivener and Professor S Diamond for their specialist opinions and constructive criticisms of the SEM study.

- Professor C Andrade for the consultation at the beginning of the study. Her experience and advice was most useful in avoiding many potential problems.

- Doctor J Mackechnie for his opinions and knowledge of the Chloride Conductivity Test.

I would like to thank the National Research Foundation, the Cement and Concrete Institute (CNCI), the Harry Crossley Foundation, and the KW Johnston and Weine trusts for the research funding and scholarships that made this study possible.

Finally, a thank you to the many lab technicians and managers that assisted me, including:

C May and E Witbooi in the UCT Concrete Lab,
H Divey at the UCT Chemical Engineering Lab and
M Waldren at the UCT Electron Microscope Unit

TABLE OF CONTENTS

LIST OF FIGURES

Chapter 2

Chapter 3

Chapter 4

Chapter 5

Chapter 6

Chapter 7

Chapter 8

Appendix 1

Appendix 3

LIST OF TABLES

1. INTRODUCTION

The transport properties of concrete are of primary importance in designing structures intended to remain in service for extended periods of time. Significant capital expenditure is required to repair and rehabilitate deteriorating structures. Increased construction of high-rise buildings and structures during the twentieth century resulted in substantially increased use of reinforced concrete. Due to lack of technical knowledge or application of existing knowledge, severe deterioration of many of these concrete structures occurred. This significantly lowered their effective service lives - costing large sums of money to repair or replace.

Preventing chloride ingress in saline environments is an important aspect of concrete durability. Chloride ions break down the naturally-occurring passivating layer surrounding embedded reinforcing bars. Depassivation of the reinforcing steel results in corrosion. If left untreated, eventual cracking and spalling of the concrete results. Chloride ions enter and are transported through the cementitious matrix predominantly by diffusion – the movement of ions from a high concentration to a low concentration. As concrete is a porous, permeable material, the transport properties of the hardened concrete can be controlled through correct mix design and construction practice. Various test methods have been developed in order to assess and categorise concrete mixes to be used in chloride environments. These include:

- The Bulk Diffusion Test (BDT)
- The Rapid Chloride Permeability Test (RCPT)
- The Rapid Migration Test (RMT)
- The Chloride Conductivity Test (CCT)

The RCPT, RMT and CCT are categorized as rapid chloride test methods. These rapid tests involve applying an electrical field to a concrete specimen in order to accelerate the transport process. This accelerated transport process is termed migration. Chloride ions are, however, not inert and interact with and become immobilised by the cement matrix. This is termed chloride binding. The effect of accelerating the transport process, using an electrical field, on the binding behaviour of chloride ions and the measured transport properties is unclear. Little could be found in the literature on the effects of rapid chloride testing (and electrical field

application in particular) on the chloride binding behaviour and measured transport properties.

Diffusion and migration coefficients are used to measure a medium's ability to facilitate ion transport. These transport coefficients are generally accepted measures of a concrete's ability to resist chloride ingress. These coefficients can be calculated using theory and the results of rapid chloride testing. Relationships between diffusion and migration have been established and formulae such as Fick's Laws and the Nernst-Plank equation proposed. However, these equations are based on fundamental theory. A question that arises is whether the application of electrical fields during rapid (migration) testing may impart a number of further variables due to the complexity of cement chemistry and the associated pore solution.

Diffusion coefficients are necessary when predicting the long-term serviceability of a structure in a chloride environment. Due to the relationships between migration and diffusion coefficients, these are used interchangeably. Migration coefficients are the measures of choice because of the accelerated rate at which migration coefficients can be obtained from rapid testing. However, little research could be found relating actual measured migration coefficients to diffusion coefficients, or analysing the effect of electrical field application on the ion-matrix interaction (chloride binding). These complex processes are not reflected in diffusion and migration theory. Therefore, research into this area is necessary in order to determine whether the proposed relationships between migration and diffusion coefficients hold in practice.

Research into these areas of rapid chloride testing would provide further understanding of the limitations of these test procedures - providing further knowledge to allow better interpretation of measured transport properties. This would lead to better understanding and application of reinforced concrete in chloride environments.

Objectives

The objectives of the study include:

- Critical review of present rapid chloride test methods in order to become familiar with the test methods the degree to which an electrical field is employed (time and magnitude) and its role in the analysis of results.

- Identification of areas within the test methods requiring better understanding

- Experimentally determining whether further work is required to develop the effectiveness of CCT sample saturation, and any potential negative effects of oven drying and sample size on the CCT

From the critical literature and rapid chloride test review, further research objectives were identified:

- Analysing the effect of an electrical field and initial chloride solution concentration on measured transport properties

- Investigating the test variability associated with each initial concentration and particular binder system

- Assess the possible effect of electrical field application on chloride binding behaviour and potentially isolate the mechanism most affected – chemical versus physical chloride binding.

Plan of Development of Dissertation

PART 1 – Literature Review

The theory behind diffusion and migration is presented in Chapter 2. This is followed by a brief discussion of concrete microstructure pertaining to ion transport. Here, cementitious hydration products and the pore structure of the cementitious matrix and concrete are discussed. Chloride binding is then discussed in Chapter 4. Reported changes in microstructure due to chloride ingress are also presented. As supplementary cementitious materials alter the microstructure of concrete and change ionic transport properties, these aspects of chloride transport are discussed as a closing to the foundation literature review.

PART 2 – Critical Review of Present Rapid Chloride Test Methods

The fundamentals of chloride transport were then used to critically review current rapid chloride testing practice. Literature pertaining to the test methods chosen for review was analysed. Trial tests were carried out in the laboratory to assess the test

procedures. An experimental investigation was conducted to identify areas within the Chloride Conductivity Test requiring further research and development. These areas are discussed in Chapter 5.

PART 3 – Experimental Research

Considering the fundamentals of cement and concrete chemistry and chloride transport, coupled with the results of the critical review of present test methods, an experimental study was formulated. The research strategy and details of the study are presented in Chapter 6.

Results of the diffusion and migration tests to determine the impact of electrical field application on the transport properties of mortars are then presented in Chapter 7. These tests are closely linked to the chloride binding test results, also presented in Chapter 7. The results of the broadly scoped Scanning Electron Microscopy (SEM) investigation are then presented and discussed in Chapter 8.

Finally, conclusions are drawn and recommendations are made in Chapter 9.

A flow chart of the Plan of Development of the dissertation is presented on page 5.

Scope and Limitations

A literature review is presented focusing on aspects of ions transport relevant to chloride ions and concrete. Ion transport theory is discussed in general and then applied to concrete technology. The nature of concrete microstructure and its interaction with chloride ions is presented and used to assess the relevance of the various ion transport theories presented. Four widely-used chloride test methods were then critically reviewed. The conclusions from the literature review regarding chloride transport theory and its application to concrete formed the basis of the rapid chloride test review. Areas requiring further development were identified from this review.

Indicative tests were conducted on the sample preparation procedure of the CCT. This was done to determine whether further work in this area was required. The tests were conducted on one concrete mix only, at one water-binder ratio.

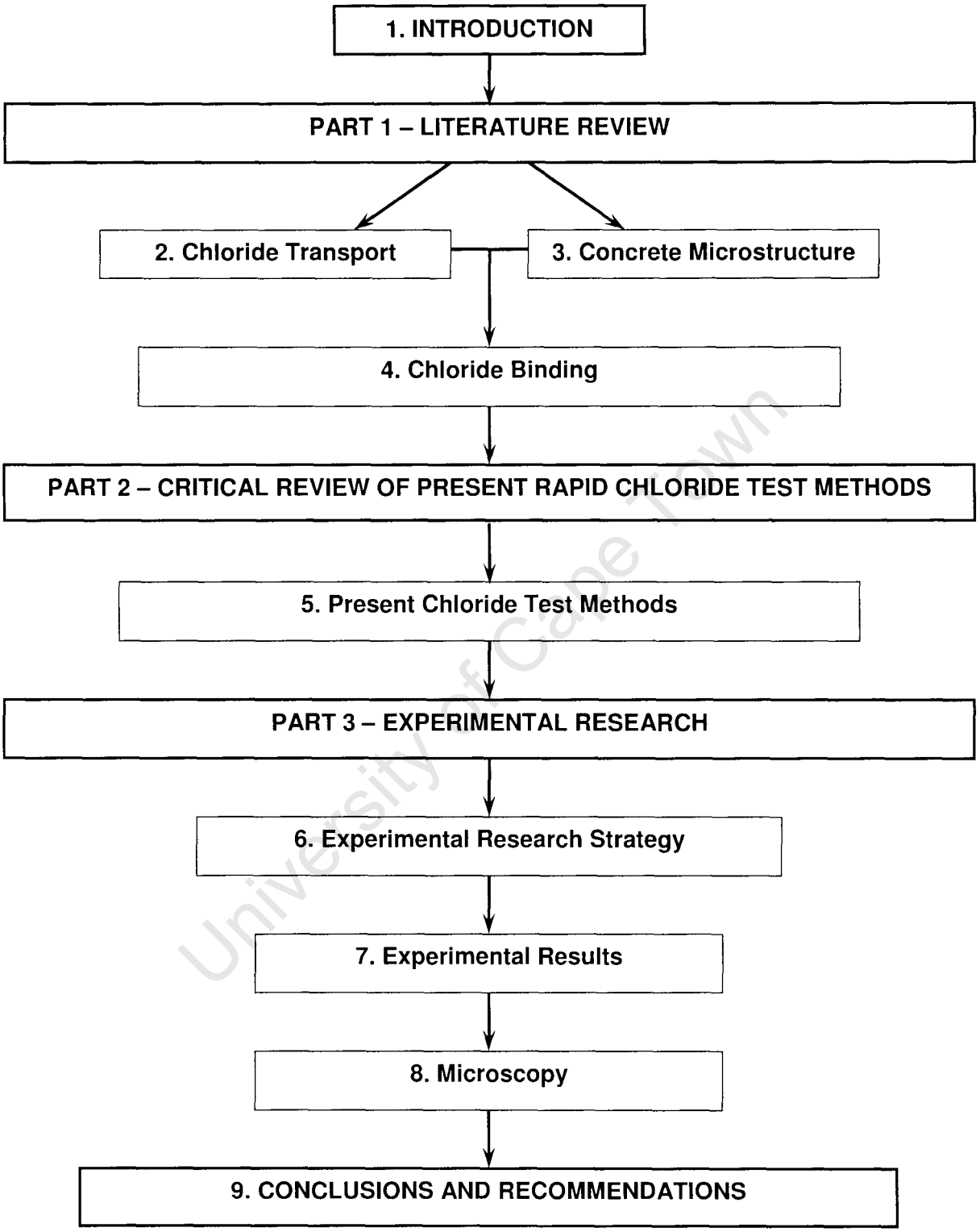

Rapid chloride testing of concrete is dependent on the use of an electrical field to accelerate the diffusion process. However, insufficient information could be found regarding the effect of electrical field application on chloride ion behaviour and measured transport coefficients. An experimental study was then devised to investigate this as this was identified as a generic area requiring further understanding.

As most rapid chloride test methods make use of electrical fields, the effect of the electrical field on chloride ion transport was experimentally investigated in the laboratory. Mortar samples were used in order to eliminate significant edge-effects, interfacial transition zone effects and particle packing effects from the study. As 5 mm thick specimens were used, results may have been significantly affected by these variables. Three initial chloride concentrations were used in these diffusion and migration experiments. These were selected in order to cover the relatively broad range of values used in the various standard tests. Concentrations below 1 M chloride concentration were not considered as these low levels are seldom found in standard tests and a change in chloride binding behaviour occurs at these levels. This would possibly confound the diffusion and migration tests results. In total, results from 36 split cell diffusion and 36 split cell migration tests were analysed.

Following the tests on electrical field application, tests to verify the chloride binding characteristics of South African cement extenders were conducted. Ground granulated Corex slag and condensed silica fume were used as cement extenders. Water to binder ratio was not varied as this was not a variable requiring investigation in this study.

PART 1 – LITERATURE REVIEW

The literature review discusses theory regarding chloride ion transport and its application to concrete. Fundamentals are discussed and then used to investigate chloride binding phenomena, changes in the microstructure as a result of chloride ingress and the use of supplementary cementitious materials. A wealth of literature exists regarding chloride ingress and concrete. The literature review was an integral part of this study in order to critically assess various works and draw state-of-the-art conclusions. Many conclusions drawn in the literature review pertain to associated rapid chloride tests. These will be discussed in greater detail in Part 2, where four widely-used rapid chloride test methods are critically reviewed.

2. CHLORIDE TRANSPORT

When concrete is placed in a chloride environment, such as a marine structure, chlorides may enter the concrete in three main ways:

- Capillary absorption
- Permeation
- Diffusion

Capillary absorption occurs when surface moisture and liquids are drawn into the concrete by capillary suction, typically through cyclical wetting and drying of the concrete. This, however, only affects a shallow portion of the concrete and will not generally affect the concrete to the level of the reinforcement. However, if the concrete is of extremely poor quality or the reinforcing cover is very low, it may be possible for capillary absorption to bring chlorides directly to the level of the reinforcing steel. Capillary suction does lower the effective distance that the ions have to subsequently travel to reach the reinforcing steel.

Permeation as result of a ***hydraulic pressure gradient*** could drive fluids (and ions) into the concrete microstructure. However, the pressure required to do this is great and will be of concern in instances such as deep sea oil rigs and tunnel linings. This ion ingress can be avoided with good design and casting practice. This mechanism is seldom experienced in normal practice.

Diffusion is the movement of ions due to a concentration gradient. This is a relatively slow process but is of most concern. Diffusion usually allows chloride ions to reach the level of the reinforcing steel within the life span of the structure.

[Tang, 1996; Stanish *et al*, 2000]

Once sufficient chlorides reach the level of reinforcement, the chloride threshold required for corrosion will eventually be surpassed and corrosion will begin. In real systems, diffusion is a highly complex phenomenon, and is further discussed below.

2.1 Diffusion

Diffusion is the phenomenon whereby molecules in a gas or a liquid will move from a high concentration to a low concentration in order to achieve system equilibrium. Diffusion in ideal media follows Fick's Laws:

Fick's First Law – Steady state diffusion

$$J = -D \frac{dC}{dx} \qquad \textbf{(2.1)}$$

Where J – Flux of ions ($g/m^2/s$)
D – Diffusion Coefficient (m^2/s)
C – Ion Concentration (g/m^3)
x – Distance from 'upstream' face (m)

Fick's Second Law – Non steady state diffusion

$$\frac{\partial C}{\partial t} = -D \frac{\partial^2 C}{\partial x^2} \qquad \textbf{(2.2)}$$

Where t – time (s)

These laws, however, only apply to molecules in ideal gases and solutions. Ions behave in a similar fashion, but are charged. The charge carried by the ions results in complex ion-solvent and ion-ion interactions.

Ion-Solvent Interaction

Ions occur due to dissolution. This is the result of ionic crystals interacting with water molecules. As the solvent's molecules collide with the solid ionic lattice, ions become displaced as they are offered a superior energetic state by interacting with the water molecules. This can be seen in Figure 1. These ongoing interactions result in considerable energy expenditure – *solvation energy* (Bockris and Reddy, 1998).

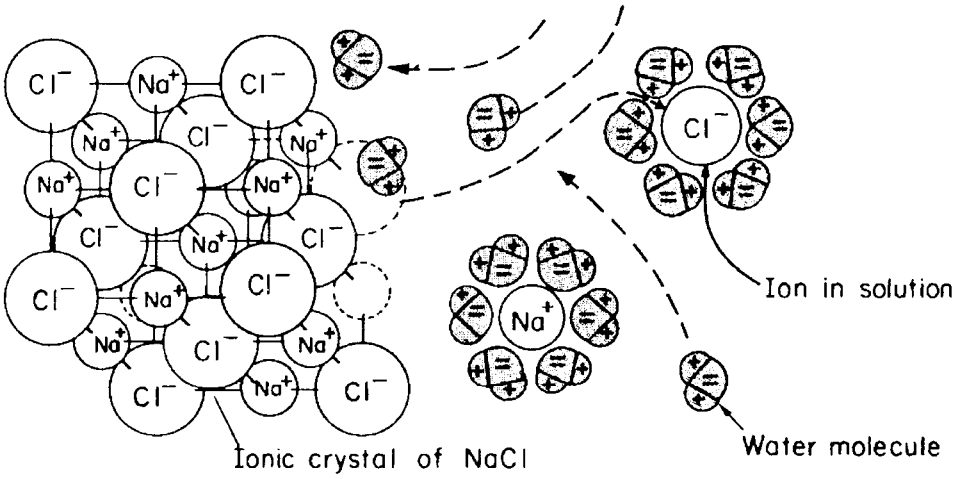

Figure 1: Dissolution of ions and the use of solvation energy (Bockris and Reddy 1998).

As NaCl dissolves, water molecules become attracted to the ions, electrochemically. These molecules are effectively bound to the ions and move with them. The solvation number is "the number of water molecules that remain with an ion for at least one movement" in the solution (Bockris and Reddy, 1998). For chloride it is 1 ±1 and for sodium it is 5 ± 1. The "binding" of these molecules effectively removes them from the solution and affects ion mobility. For sodium ions to move, approximately 5 water molecules must also be moved. Therefore, chloride ions are more mobile than sodium ions in solution (Bockris and Reddy, 1998). This effect also results in a lower number of free water molecules in the solution. This lowers the dissolving potential of the solution and decreases the mobility of the ions. These impacts are quantifiably represented by the ***activity coefficient*** (Bockris and Reddy, 1998).

Ion-Ion Interaction

The presence of ions in the vicinity of an ion impacts on the behaviour and movement of that ion. This ion-ion interaction affects the drift of ions under both diffusion and migration circumstances. This mutual interaction of all ions in the solution is dependent on "the mean distance apart of the ions" (technically the ionic density or concentration) because the strength of the interionic fields is distance dependent. The concentration or ionic population density is dependent on the solution or, more specifically, the electrolyte and the extent to which it gives rise to ions in solution (Bockris and Reddy, 1998).

These parameters impact on the behaviour of diffusing ions and result in deviations from ideal diffusion behaviour. These parameters can be used in diffusion and migration formulae (to be discussed later) but are generally disregarded. This is due to their complexity and the difficulties of accurate measurement – especially in instances where numerous ions are present (such as in the case of concrete pore solution).

The Activity Coefficient

The activity coefficient is a correction factor used when applying ideal behaviour to real environments. The activity coefficient takes ion-ion and ion-solution interaction into account. The lower the activity coefficient of the ions, the lower the potential the ions have for transport or diffusion (Bockris and Reddy, 1998). The measurement of activity coefficients is difficult and is affected by other present ions. This makes the use of the activity coefficient in practice inefficient – to be discussed later.

2.2 Diffusion Formulae – derivation and theory[1]

Chemical potential is defined as the potential for an ion to move or be transported. According to Bockris and Reddy, (1998) "The gradient of chemical potential resulting from a non-uniform concentration is equivalent to a driving force for diffusion and produces a diffusion flux". In ideal systems, the classic thermodynamic formula for the chemical potential of a nonelectrolyte solute is given by:

$$\mu_i(ideal) = \mu_i^0 + RT \ln c_i \qquad \textbf{(2.3)}$$

Where μ_i is the chemical potential
μ^0_i is the chemical potential in the standard state
c_i is the concentration of the solute in mole fraction units
T is absolute temperature
R is the gas constant, 8.314 J/(mol.K)

[1] The majority of the mathematical derivations are adapted from Tang (1996). Supplementary references are given where relevant.

However, experiments have shown that even in dilute solutions,

$$\mu_i - \mu_i^0 \neq RT \ln c_i \qquad \textbf{(2.4)}$$

To treat nonideal electrolytic solutions, an empirical correction factor, f_i, is introduced as a modifier of the concentration term. So,

$$\mu_i - \mu_i^0 = RT \ln c_i f_i = RT \ln c_i + RT \ln f_i \qquad \textbf{(2.5)}$$

Here $\mu_i - \mu_i^0$ is the chemical potential change arising from ion interactions.

The effective concentration ($c_i f_i$) has become known as the *activity*, a_i, of the species *i*. The correction factor, f_i, is the ***activity coefficient***.

For ideal solutions (of infinite volume where ion-ion and ion-solvent reactions do not exist), the activity coefficient is unity. Experimental results have provided values for the activity coefficient of ions in solution. The trend seen in Figure 2 shows the effect of concentration on the extent of ion-ion interaction. This has direct implications for diffusion behaviour. As the concentration of the NaCl solution rises from zero to approximately 1 molal, the activity coefficient drops to a local minimum of approximately 0.66. This implies that the chemical potential of the ions drops considerably due to increased ion-ion interaction at around 1 molal concentration. Molal – Molar conversions are given in Table 1.

Table 1: Molar versus molality and root molality values - 0.5 to 5 M

Molar (M)	Molal (m)	Root Molal (√m)	Molar (M)	Molal (m)	Root Molal (√m)
0.5	0.51	0.71	**3**	**3.19**	**1.79**
1	**1.02**	**1.01**	3.5	3.77	1.94
1.5	1.54	1.24	**4**	**4.36**	**2.09**
2	**2.08**	**1.44**	4.5	4.97	2.23
2.5	2.63	1.62	**5**	**5.60**	**2.37**

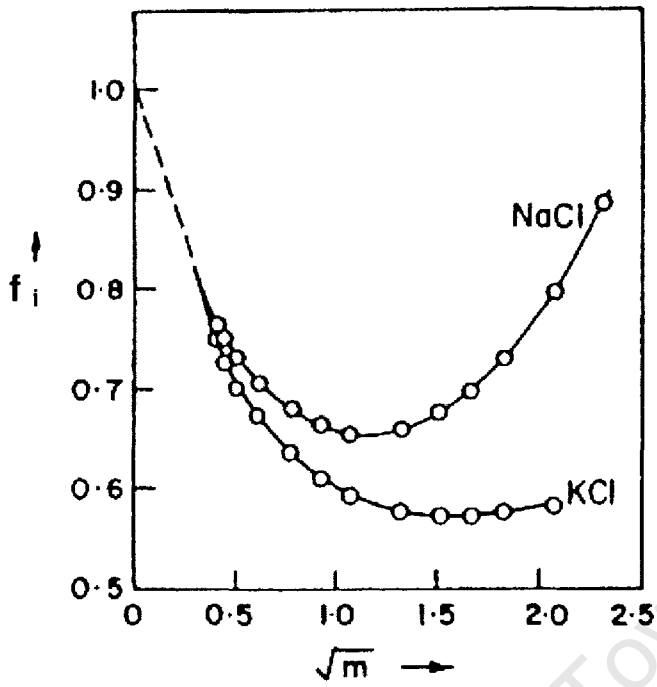

Figure 2: The effect of varying concentration on the activity coefficient (f_i) of NaCl and KCl in solution (Bockris and Reddy, 1998)

Although many researchers employ Fick's Laws in describing diffusion behaviour, Tang (1996) states the equation

$$v = -B\frac{\partial \mu}{\partial x} + u'\frac{\partial \phi'}{\partial x} = -BRT\left(\frac{\partial \ln c}{\partial x} + \frac{\partial \ln f_i}{\partial x}\right) + u'\frac{\partial \phi'}{\partial x} \qquad \textbf{(2.6)}$$

or

$$v = -BRT\frac{\partial \ln c}{\partial x}\left(1 + \frac{\partial \ln f_i}{\partial \ln c}\right) + u'\frac{\partial \phi'}{\partial x} \qquad \textbf{(2.7)}$$

where u' is the ion mobility

v is the average velocity of chloride ion movement

Φ' is the counter electric field

f_i is the empirical correction factor for non-ideal behaviour

c is the concentration

x is the distance from the initial ionic front to some point in the medium

B is the proportionality factor (diffusion coefficient independent of T)

T is the absolute temperature in Kelvin

R is the gas constant, 8.314 J / (mol·K)

This equation takes ion-ion and ion-cation interaction into account. In contrast to Fick's Law, this equation accounts for the force due to the chemical potential gradient ***and*** the drag force due to cations. Due to crystal dissolution, there are as many cations in solution as there are anions. As the chloride ions move, a counter electric field between the chloride ions and the sodium ions creates a "draw back" force. This must also be overcome during transport.

Now replacing BRT with D (the diffusion coefficient), a single measure of diffusion capacity, independent of time, is obtained. Hence, the flux (flow rate of ions through a unit area of solution) is given by:

$$J_d = cv = -D\frac{c\partial \ln c}{\partial x}\left(1+\frac{\partial \ln f_i}{\partial \ln c}\right)+cu'\frac{\partial \phi'}{\partial x} \qquad \textbf{(2.8)}$$

or

$$J_d = -D\frac{\partial c}{\partial x}\left(1+\frac{c}{a}.\frac{\partial a}{\partial c}\right)+cu'\frac{\partial \phi'}{\partial x} \qquad \textbf{(2.9)}$$

as $c_i f_i$ = a (the activity coefficient), as previously discussed.

Hence, in theory, an activity coefficient may be used as a variable describing diffusion behaviour. However, the numerous possible combinations of ions in the concrete pore solution makes its use inefficient, if not impossible. As it is difficult to solve the terms $\frac{c}{a}.\frac{\partial a}{\partial c}$ and $cu'\frac{\partial \phi'}{\partial x}$, they are often neglected. The equation thus reduces to Fick's First Law (2.1). The primary characteristics of ion behaviour are, thus, ignored. Ions are treated as simple, uncharged particles moving through an ideal solution. Ignoring ion activity may, therefore, lead to erroneous predictions and experimental flaws. Although one can use Fick's Law, an understanding of the limitations thereof and of ion characteristics is imperative to accurately researching and testing chloride transport in concrete. Prediction models may be calibrated using long term in situ measurements. However, using diffusion coefficients which do not account for ion activity and changes thereof may lead to incorrect calculations of long-term prediction. Literature exploring the practical relationship between ion activity and long-term prediction of concrete performance could not be found.

2.3 Diffusion Coefficients

A practical solution to the theoretical considerations presented above is to use an effective diffusion coefficient, D_{eff}. Effective diffusion coefficients are used to describe diffusion through concrete – a porous medium containing a non-ideal solution. Effective diffusion coefficients are generally obtained from experimental data from diffusion tests. The effective diffusion coefficient indirectly accounts for ion-solvent, ion-ion and ion-media interactions. Over and above the fundamental chemical interactions, the effective diffusion coefficient also accounts for the permeability of the concrete system as it is not an ideal porous medium and varies in porosity and permeability – both spatially and in time.

There are a number of ways to calculate these diffusion coefficients.

Non-steady State Diffusion (NSS)

As ions begin to move through the concrete microstructure, they are under non-steady state conditions. The microstructure is complex and leads to three-dimensional diffusion that is highly dependent on the pore structure and local concentrations. Chloride binding affects the process by removing a significant amount of ions from the pore solution.

Nonsteady state (NSS) diffusion coefficients and steady state (SS) diffusion coefficients are very different. This is predominantly due to chloride binding. During NSS, the flux is dependent on the free chloride concentration gradient in the concrete. Here,

$$\frac{\partial c_t}{\partial t} = \frac{\partial c}{\partial t} + \frac{\partial c_b}{\partial t} = \frac{\partial c}{\partial t}\left(1 + \frac{\partial c_b}{\partial c}\right) = D_{eff}\frac{\partial^2 c}{\partial x^2} \qquad \textbf{(2.10)}$$

Where c_b is the concentration of bound chlorides

c is the free chloride concentration in the pore solution

c_t is the total chloride concentration

x is the depth measured from the exposure face

NSS diffusion is characterised by Fick's second law (modified to account for chloride binding):

$$\frac{\partial c}{\partial t} = \frac{D_{eff}}{1 + \frac{\partial c_b}{\partial c}} \cdot \frac{\partial^2 c}{\partial x^2} = D_{nss} \frac{\partial^2 c}{\partial x^2} \qquad \textbf{(2.11)}$$

Where D_{nss} is the effective non-steady state diffusion coefficient

The SS and NNS diffusion coefficients are thus related by

$$D_{nss} = \frac{D_{ss}}{\varepsilon\left(1 + \frac{\partial c_b}{\partial c}\right)} \qquad \textbf{(2.12)}$$

Where ε is the porosity

Chloride binding is a complex phenomenon and the chloride binding capacity ($\frac{\partial c_b}{\partial c}$) of the matrix changes with chloride concentration, the non-steady state diffusion coefficient is, therefore, not constant. For this reason, researchers using split cell diffusion tests generally limit themselves to steady state investigations and use the steady state diffusion coefficient as a basis for comparison.

Steady State Diffusion (SS)

In specimens of relatively small thickness, ions will eventually reach the opposing face of the specimen – termed the "breakthrough point" and the time taken termed "time to breakthrough". The majority of chloride binding occurs at relatively low concentrations (as binding sites are available) and local equilibrium would have been reached by the time breakthrough is reached. Therefore, from this point on diffusion is steady state. Here the concentration gradient is assumed to be linear (Figure 3) and equations (2.3) to (2.8) can be applied. The diffusion coefficient can be calculated from the time to breakthrough or from the concentration gradient during steady state conditions.

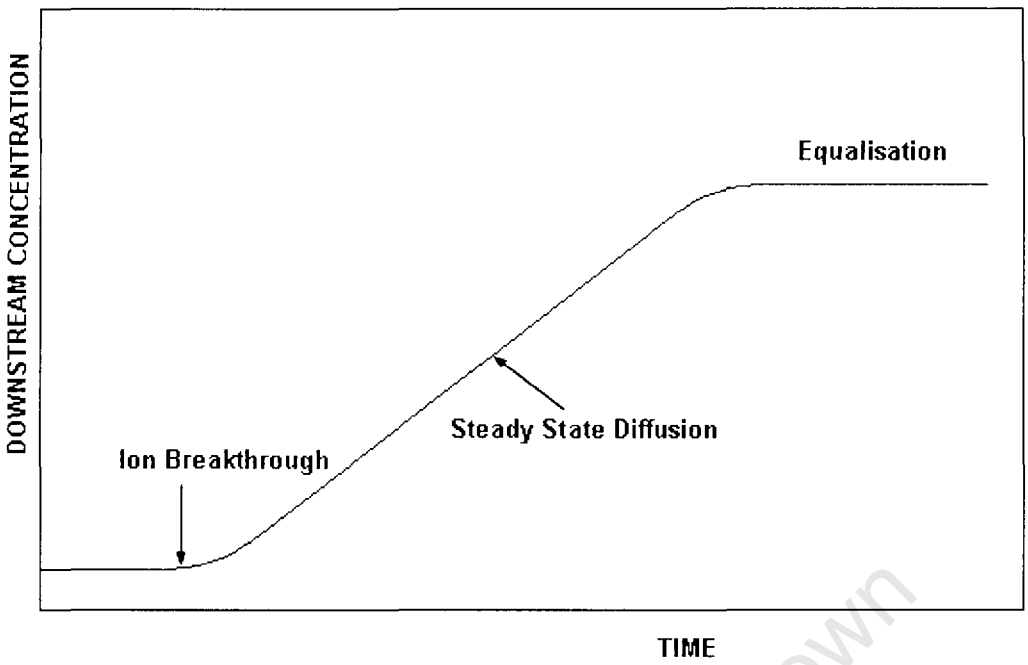

Figure 3: Theoretical profile of concentration with time at the opposing face of a concrete specimen

Researchers have formulated various diffusion experiments. Two typical designs predominate with both involving two cells, separated by a concrete sample.

1. **Equal compartment split cell diffusion test**

This comprises two cells of equal volume separated by a concrete, mortar or cement paste sample. One cell initially contains chlorides while the other does not. The concentration of each cell is then monitored with time. In this case, the upstream concentration does not remain constant and must be monitored to obtain dc/dt. See Figure 4.

MacDonald and Northwood (1995) used the following equation in their research to determine the effective concrete diffusion coefficient:

$$c_2 = \frac{D_{eff}.A.c_1}{V.l}.t \qquad \textbf{(2.13)}$$

Where:

c_1 and c_2 are the concentrations of chloride ions in cells 1 (upstream) and 2 (downstream) respectively.

D_{eff} is the effective diffusion coefficient of the hardened mortar

A is the cross sectional area

V is the volume of cell 2 (initially non-chloride containing cell)

l is the thickness of the disc

t is time

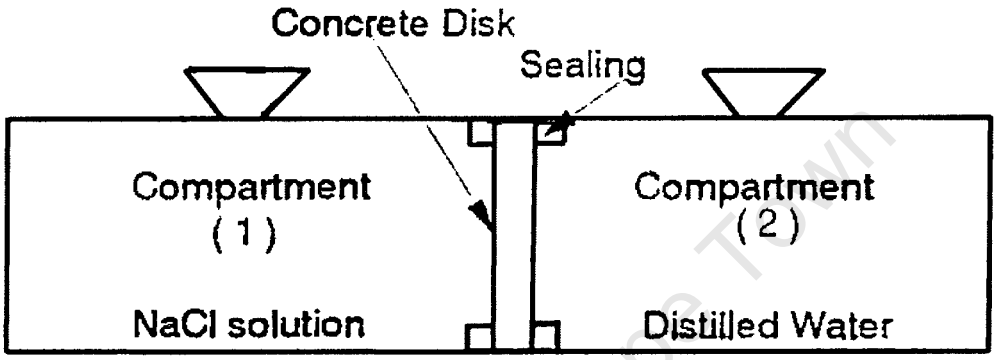

FIG. 1.

Figure 4: Two compartment diffusion cell used by Dehghanian and Arjemandi (1997)

Dehghanian and Arjemandi (1997) and Tang (1996) used a similar equation – all obtained from an average finite difference solution to Fick's Law. Here, a finite interval ($t_{n+1} - t_n$) method is used to calculate effective diffusion coefficients. This is preferable to the differential equation, in practice, as maturity (continued hydration) will affect the diffusion coefficients calculated at different times, causing them to become smaller with time.

2. Split cell diffusion test with infinitely large upstream chloride reservoir

As an alternative to the previously discussed cell configuration, the upstream cell may be much larger than the downstream cell to ensure that the upstream cell experiences negligible concentration loss. In this case, only the downstream cell must be monitored. The method of analysis is not affected. c_1 simply remains constant.

In both instances, dc/dx converges to zero as the test progresses. The rate of diffusion, therefore, theoretically converges to zero also. The second cell configuration is generally preferred as it makes the calculation of the diffusion coefficient relatively simple - based on the linear dc/dt obtained after breakthrough.

2.4 Migration

For quality control purposes, rapid chloride testing is a necessity. Due to the slow nature of diffusion, researchers and practitioners accelerate the diffusion process with the use of an electrical potential difference, applied across a concrete specimen. This is generally termed chloride migration.

General Migration Theory

An external electrical field will cause ions to move at an average velocity, v_m, of:

$$v_m = u\frac{\partial \phi}{\partial x} \qquad \textbf{(2.14)}$$

where u is the ion mobility

$\partial\varphi/\partial x$ is the strength of the electrical field

Einstein related mobility to the ion valence (z) and a general diffusion coefficient by:

$$u = D.\frac{zF}{RT} \qquad \textbf{(2.15)}$$

where F is Faraday's constant, 96480 J/(V.mol)

z is the ion valence

If N is the number density of ions in solution, the number of ions passing through an area A in time Δt is given by $(A \,.\, v_m.\, \Delta t)N$. The flux of ions can then be calculated by

$$J_m = \frac{(A.v_m.\Delta t).N}{A\Delta t} = N.v_m \qquad \text{(no. of chlorides / } m^2_{\text{solution}} \text{ . s)} \qquad \textbf{(2.16)}$$

or

$$J_m = c.v_m = c.D.\frac{zF}{RT}.\frac{\partial \phi}{\partial x} \qquad (g_{Cl}/\ m^2{}_{solution}\ .\ s) \qquad \textbf{(2.17)}$$

where c is the concentration of free chlorides.

In general, the external electrical field is constant, i.e. $\frac{\partial \phi}{\partial x} = \frac{U}{l}$ (where U is the externally applied electrical potential difference).

Hence, $J_m = D\frac{zFU}{RTl}c$ **(2.18)**

A criticism of the above derivation is the lack of consideration of an activity coefficient. The assumption is that the externally applied electrical field is so great that the internal ion interactions are insignificant. However, in terms of chloride binding phenomena, the impact of increased ion energy on ion-ion interaction and ion-concrete interaction is unclear and cannot be assumed to be insignificant.

Non - Steady State Migration

Non-steady state ion movement is inherently complex. The three dimensional cementitious matrix has varying permeability and porosity. Chloride binding further complicates the fundamental process. However, the majority of rapid chloride test methods are founded on non-steady state migration and diffusion theory.

In the non-steady state phase

$$\frac{\partial c}{\partial t} = -\frac{D_0}{1+\frac{\partial c_b}{\partial c}}.\frac{zFU}{RTL}\frac{\partial c}{\partial x} = -D_{nssm}.\frac{zFU}{RTL}\frac{\partial c}{\partial x} \qquad \textbf{(2.19)}$$

If the chloride front moves a discrete distance x_f in time t and can only reach a maximum concentration of c_0 (the bulk solution or upstream concentration), then equation 2.19 becomes:

$$D_{nssm} = \frac{D_0}{\left(1 + \frac{\int_0^{c_b} c_b}{\gamma_b c_0 \int_0^{} dc}\right)} = \frac{RTL}{zFU} \frac{\int_o^{x_f} dx}{\int_0^t dt} \qquad \textbf{(2.20)}$$

After integrating dc_b from 0 to c_b, dc from 0 to $\gamma_b c_0$ and dx from 0 to x_f we obtain

$$D_{nssm} = \frac{D_0}{\left(1 + \frac{c_b}{\gamma_b c_0}\right)} = \frac{RTL}{zFU} \frac{x_f}{t} \qquad \textbf{(2.21)}$$

where γ_b lies between 0 and 1 and is effectively an activity coefficient relating to chloride binding during migration.

From chloride binding theory

$$\frac{c_b}{\gamma_b c_0} = K_b \frac{W_{gel}}{\varepsilon} \qquad \textbf{(2.22)}$$

where K_b is a chloride binding constant during NSS migration ($m^3_{solution}/kg_{gel}$)
W_{gel} is the hydrated gel content of the concrete (kg_{gel}/m^3)
ε is the porosity of the concrete

$$K_b = \frac{f_b}{1000} (\gamma_b c_0)^{\beta - 1}$$

in which f_b and β are adsorption binding constants

This leads to the final solution

$$D_{nssm} = \frac{D_0}{\left(1 + K_b \frac{W_{gel}}{\varepsilon}\right)} \quad (m^2 / s) \qquad \textbf{(2.23)}$$

D_{nssm} is relatively constant whereas D_{nss} is not, as previously stated.

Steady State Migration

In certain rapid chloride tests, a steady state process occurs. Here, the flux is independent of distance and time, provided that the concentration of the "upstream" solution remains constant or that the reservoir is large enough to ensure that changes are insignificant.

In this case, the diffusion coefficient can be calculated by

$$D = \frac{JRTL}{zFUc} \qquad \textbf{(2.24)}$$

This is a form of the Nernst-Planck equation, usually given as:

$$J = -D\frac{zFU}{RTL}c \qquad \textbf{(2.25)}$$

In turn,

$$D_{ssm} = \frac{RTL}{zFUc} J_{concrete} = \frac{RTL}{zFUc} J_{0m}.\varepsilon = D_0\varepsilon = D_{ss} \qquad \textbf{(2.26)}$$

Where D_{ssm} is the steady state migration coefficient

D_{ss} is the steady state diffusion coefficient

J_{om} is the migratory flux through the pore solution

D_0 is the diffusion coefficient per unit cross sectional area of pore solution

The diffusion coefficient obtained from the steady state migration test is therefore the same as that for the steady state diffusion test – not accounting for the effect of chloride binding (if any).

This would indeed occur if the concentration of the solutions and pore solution is high enough to complete chloride binding during the saturation process – prior to the test. This would ensure that little non-steady state phenomena occur due to binding. These circumstances may be desirable as they effectively rule out significantly unpredictable variables such as chloride binding, local equilibria within the sample and three-dimensional ion flow through the cementitious matrix. However, these variables are important in retarding chloride ingress, in practice.

2.5 Migration Coefficients

Halamickova *et al* (1995) and McGrath and Hooton (1996) based their calculation of migration coefficients on the time to breakthrough of chloride ions. Using the modified version of Fick's Second Law:

$$\frac{dc}{dt} = D\left(\frac{d^2c}{dx^2} - \frac{zFU}{RT}\frac{dc}{dx}\right) \qquad \textbf{(2.27)}$$

with the following conditions:

Boundary condition:	$c = c_0$, $x = 0$, $t > 0$
Initial condition:	$c = 0$, $x > 0$, $t = 0$
Infinite point condition:	$c = 0$, $x =$ infinity, $t =$ large

the exact analytical solution was obtained:

$$\frac{c}{c_0} = \frac{1}{2}\left[e^{kx}erfc\left(\frac{x+kDt}{2\sqrt{Dt}}\right) + erfc\left(\frac{x-kDt}{2\sqrt{Dt}}\right)\right] \quad \text{where } k = \frac{zFU}{RT} \qquad \textbf{(2.28)}$$

The term in the square brackets depends solely on the time to break through. The coefficient of migration was thus calculated using the time to breakthrough. The experimental setup used allowed this to be easily obtained. Samson *et al* (2003) used the same approach but calculated the migration coefficient using a fitted chloride profile.

The Nernst-Planck equation (2.25) is commonly used to calculate steady state migration coefficients (Basheer *et al*, 2003; Yang and Su, 2002; Andrade, 1993; McGrath and Hooton, 1996). This is generally done over finite time intervals and is best suited for the split cell diffusion test where the upstream concentration does not change. It can be used for equal volume split cell diffusion tests, with finite time steps, however changing upstream concentration may introduce complicating variables in the form of varying activity coefficients.

As the migration coefficient will change with time (concrete maturity, chloride binding effects on migration and on pore structure), deciding which value is representative can be problematic. The migration coefficient also depends strongly on the pore structure and chemical composition of the concrete (chloride binding effects). Hence, various values are reported in the literature:

	Migration Coefficient (m^2/s)		
	CEM I	**GGBS**	
Luo *et al*, 2003	3.02×10^{-12}	1.95×10^{-12}	(70 % GGBS concrete)
Basheer *at al*, 2002	7.3×10^{-12}	3×10^{-12}	(50 % GGBS concrete)
Yang and Cho, 2003	13.4×10^{-12}	6.07×10^{-12}	(25 % GGBS concrete)

GGBS coefficients are, on average, approximately half of those reported for CEM I concretes, a reflection of their superior transport properties (to be discussed later).

2.6 Transport Coefficients of Cementitious Matrices

Due to the numerous methods and analysis techniques available to analyse diffusion and migration coefficients of cementitious matrices, a range of values are quoted in the literature. Fundamental trends will be discussed here. Transport coefficients of the various binder systems are discussed in Chapter 4.

2.6.1 Transport coefficients and water binder ratio

As transport mechanisms are a function of the permeability and tortuosity of the matrix, as well as the amount of specific chemical constituents, transport coefficients are a function of water-binder ratio.

Figure 5 shows the trend reported by MacDonald and Northwood (1995) obtained from split cell diffusion tests of ordinary Portland cement (OPC) pastes. It is interesting to note the significant difference between the distribution of permeability with water-cement ratio (Figure 6) and that of diffusivity and water-binder ratio. The relationship reported by Neville (1981) shows a sharp exponential increase between the 0.55 to 0.65 w:c range. The change in diffusivity with w:c, although exponential, is more consistent across all w:c ratios, without a sharp, sudden increase. This implies that the diffusivity of the cementitious matrix is more sensitive to changes in the binder content of the mix than to permeability, tortuousity, etc.

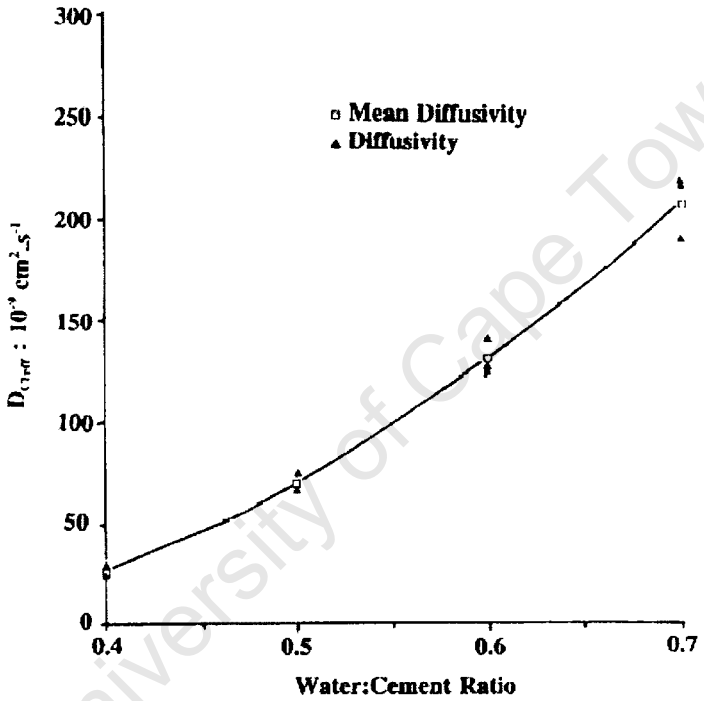

Figure 5: Diffusivity as a function of water binder ratio of an OPC paste (MacDonald and Northwood, 1995)

Figure 7 was compiled using data from Yang and Cho (2003) and Tang and Nilsson (1996) and shows the effect of water-binder ratio on the steady-state migration coefficient. As with diffusivity, the migration coefficients increase steadily with increasing water-binder ratio. From the data shown, it appears that the migration characteristics of OPC mixes are more sensitive to changes in water-binder ratio than blends. The mortar specimens used by Tang and Nilsson showed significantly lower migration coefficients. This is surprising as mortars are generally more porous than concretes (due to lack of coarse aggregate). It is possible that this occurred due

to lack of edge- and interfacial transition zone effects in the mortar specimens (to be discussed later). The effect of supplementary cementitious materials can also be seen in Figure 7. This will be discussed in greater detail in Chapter 4.

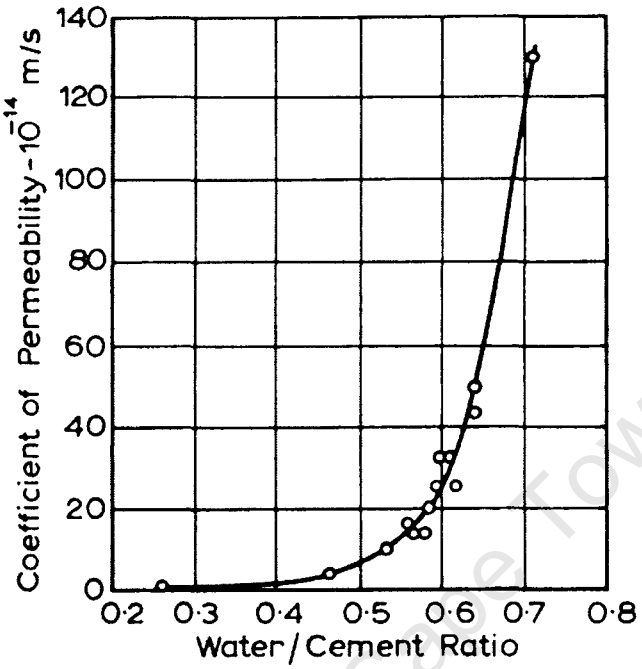

Figure 6: Permeability as a function of water binder (Neville, 1981)

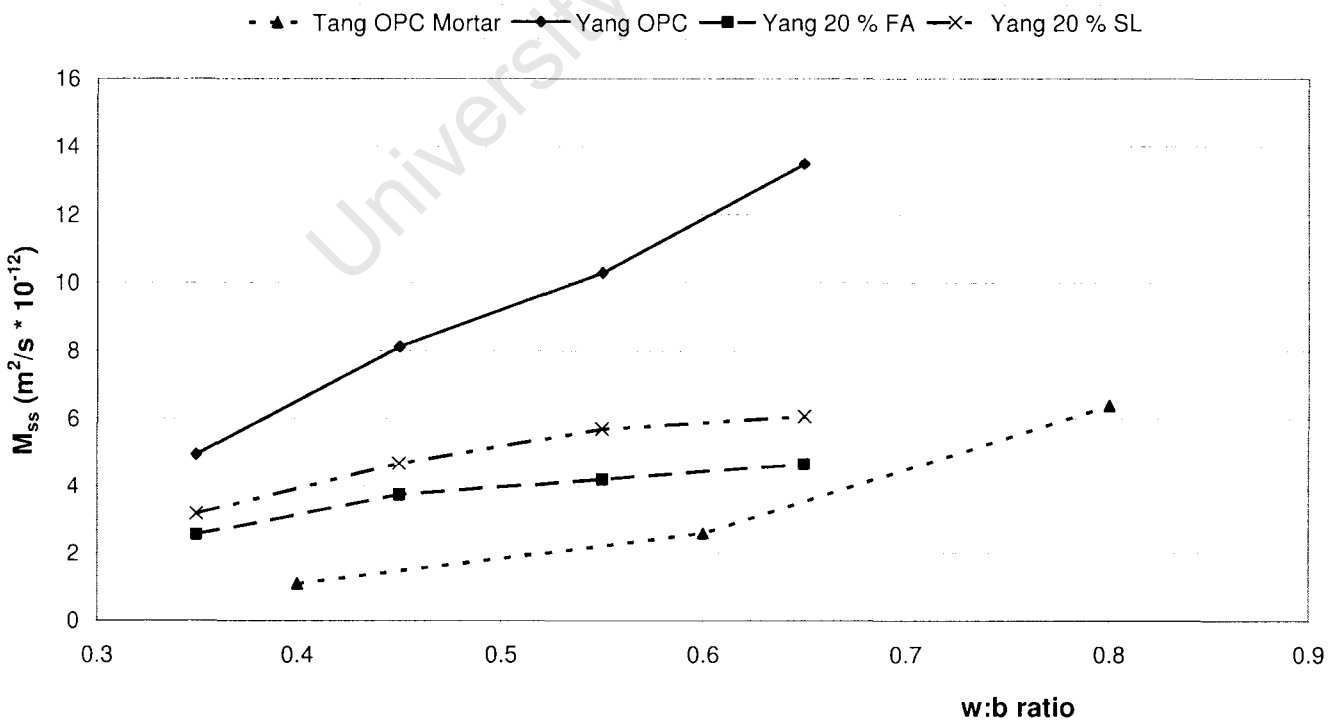

Figure 7: The effect of water binder ratio on the steady state migration coefficient

2.6.2 Migration coefficients and applied voltage

Figure 8 shows the effect of applied voltage on measured migration coefficients. Firstly, it can be noted that the steady-state migration coefficient is generally greater than the non-steady state migration coefficient. This is expected, due to the greater influence of chloride binding on the non-steady state process. Secondly, the measured steady state migration coefficients vary significantly with applied voltage. This implies that the voltage may affect either the ion activity or the ion-matrix interaction. This variation with applied potential difference must be accounted for when considering results reported in the literature and when comparing concretes tested at different potential differences. It is, therefore, desirable to use the same potential difference for all steady state tests.

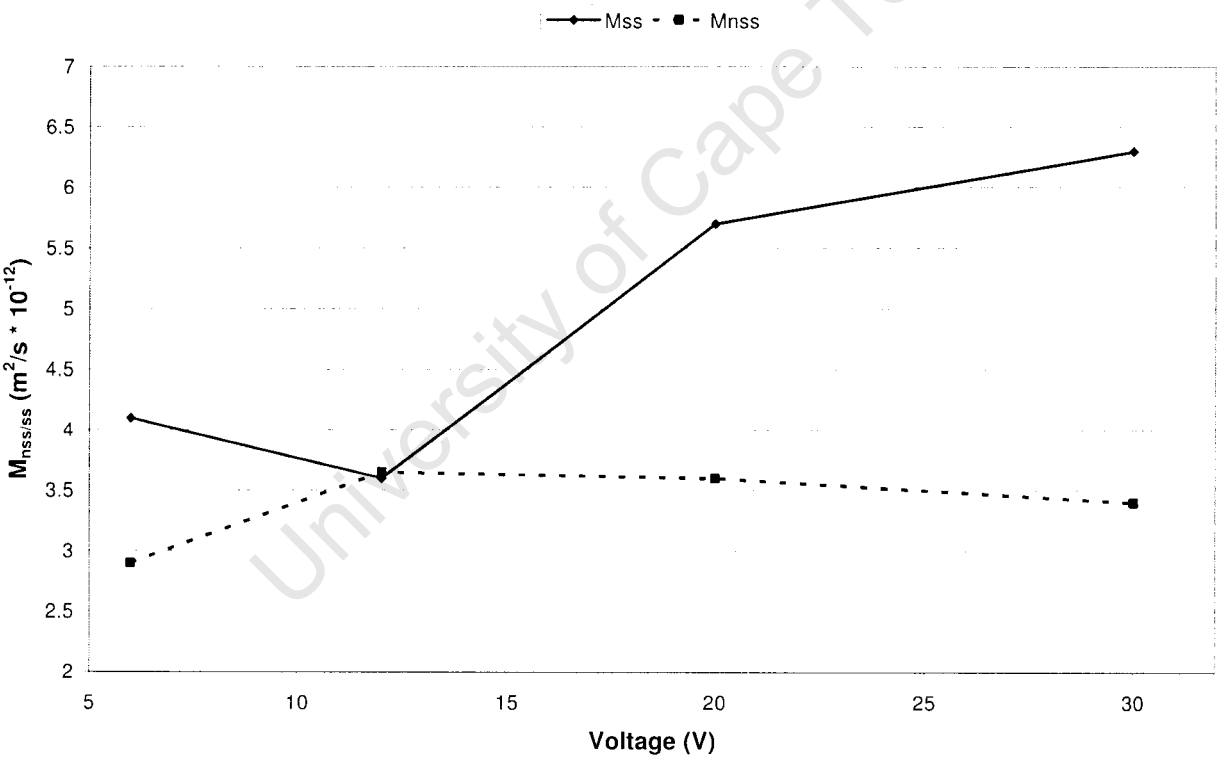

Figure 8: The effect of applied voltage on the measured migration coefficients (Compiled using data from McGrath and Hooton, 1996)

As the measured migration coefficient is affected by a change in voltage, it can also be concluded that the application of an electrical field would affect the measured transport properties.

2.6.3 Diffusion and migration coefficient comparison

Figure 9 shows reported diffusion and migration results for a particular OPC concrete. It can be seen, from the values reported by Tang and Nilsson (1992), that the non-steady state migration coefficients are higher than the observed non-steady state diffusion coefficients. This implies that the electrical field may affect the ion-matrix interactions and the chloride binding capabilities of the matrix. This will be discussed in greater detail in Chapter 4.

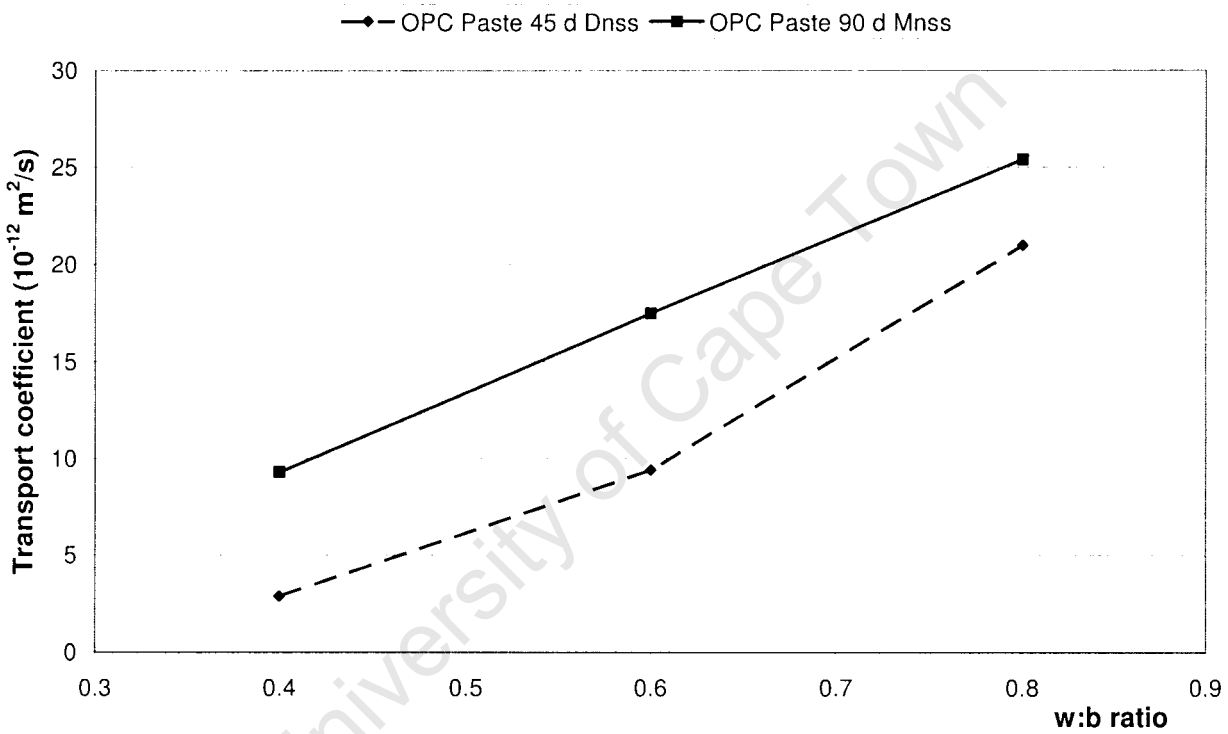

Figure 9: Differences between diffusion and migration coefficients (compiled using data from Tang and Nilsson, 1992)

2.7 Conclusions

Fick's Law is generally used to describe ion diffusion through solutions. The activity coefficient plays an important role in applying the theoretical formulae (Fick's Laws) to practical situations. Here, an activity coefficient or effective diffusion coefficient is used to account for non-ideal behaviour (ion-ion and ion-solution interaction). However, the activity coefficient is difficult to measure and is dependent on the

combination of ions in the pore solution of concrete. Hence, it is typically disregarded and an effective diffusion coefficient used to measure the concrete's capacity to facilitate chloride ion transport. This must be considered in analysing results obtained from diffusion and migration experiments, as differing starting concentrations and pore solution compositions may give rise to differing results.

Various methods of determining diffusion coefficients exist. These depend on the experimental setup and whether non-steady state or steady state transport is being analysed. This must be considered when interpreting values of diffusion and migration coefficients given in the literature.

Non-steady state diffusion coefficients are affected by chloride binding (to be discussed later) and are, therefore, not constant. Steady state diffusion coefficients are said to be relatively constant as the majority of chloride binding occurs at low concentrations during the non-steady state phase. This, and its implications, is to be explored further.

The application of an electric potential difference across a sample accelerates the diffusion process (termed migration) and alters the behaviour of the ions and ion-matrix interaction. The Nernst-Plank equation is used to describe migration behaviour. Steady state diffusion and migration coefficients were shown to be theoretically equal. However, research shows that measured diffusion and migration coefficients may be significantly different.

As concrete is a complex matrix of varying constituents and morphologies, it is necessary to understand the nature of concrete microstructure when applying theories to practice. As transport processes are dependent on ion-ion, ion-solvent, and ion-media interaction, the chemical and physical properties of concrete must be understood. These will be discussed in the following chapter.

3. CONCRETE MICROSTRUCTURE

3.1 Cementitious Hydration Products

Cement is manufactured from ground shale, limestone, iron ore and siliceous sand. These raw materials are passed through a kiln where they are heated to approximately 1450 °C. The resulting clinker is then ground to a desired fineness together with approximately 5 % gypsum. The resulting cement contains several compounds.

Alite is basically tricalcium silicate (C_3S). It makes up between 45 – 65 % of Ordinary Portland Cement (OPC).
Belite is essentially dicalcium silicate (C_2S) and makes up 10 – 35 % of OPC.
Tricalcium Aluminate (C_3A) makes up 4 – 10 % of OPC.
Celite is tetracalcium aluminoferrite (C_4AF) and makes up approximately 5 - 10 % of OPC. (Soroka, 1993; Neville, 1981, Addis and Owens, 2001)

The properties of the four major constituents of ordinary Portland cement (OPC) have a great effect on the resulting concrete. These constituents hydrate with water to form the primary hydration products, calcium silicate hydrates and aluminates. The hydration of OPC is described by the following chemical reactions (Addis and Owens, 2001)

$$2C_3S + 6H \rightarrow C_3S_2H_3 + 3CH \quad (3.1)$$
$$2C_2S + 4H \rightarrow C_3S_2H_3 + CH \quad (3.2)$$
$$C_3A + CH + 12H \rightarrow C_4AH_{13} \quad (3.3)$$
$$C_4AF + 4CH + 22H \rightarrow C_4AH_{13} + C_4FH_{13} \quad (3.4)$$

Where S represents silicate
C represents calcium oxide
A represents alumina
F represents ferric oxide
And H represents water

Calcium hydroxide for reactions 3.3 and 3.4 are provided by reactions 3.1 and 3.2.

3.1.1 Calcium Silicate Hydrates

As seen in equations 3.1 and 3.2, C_3S undergoes hydration to produce $C_3S_2H_3$. Released lime separates out as $Ca(OH)_2$. It is uncertain whether C_2S and C_3S result in the same ultimate hydration product. Physical observations have indicated that several distinct calcium silicate hydrates may be present. This polymorphic material is referred to as CSH gel.

C_3S and C_2S have differing rates of hydration. This is shown in Figure 10. It must be noted that these rates are for the pure forms of the silicates. In cements, the silicates contain traces of impurities (oxides present in the clinker), which affect the nature of the calcium silicate hydrates. CSH usually contains small amounts of Mg, Al, Fe, and other ions.

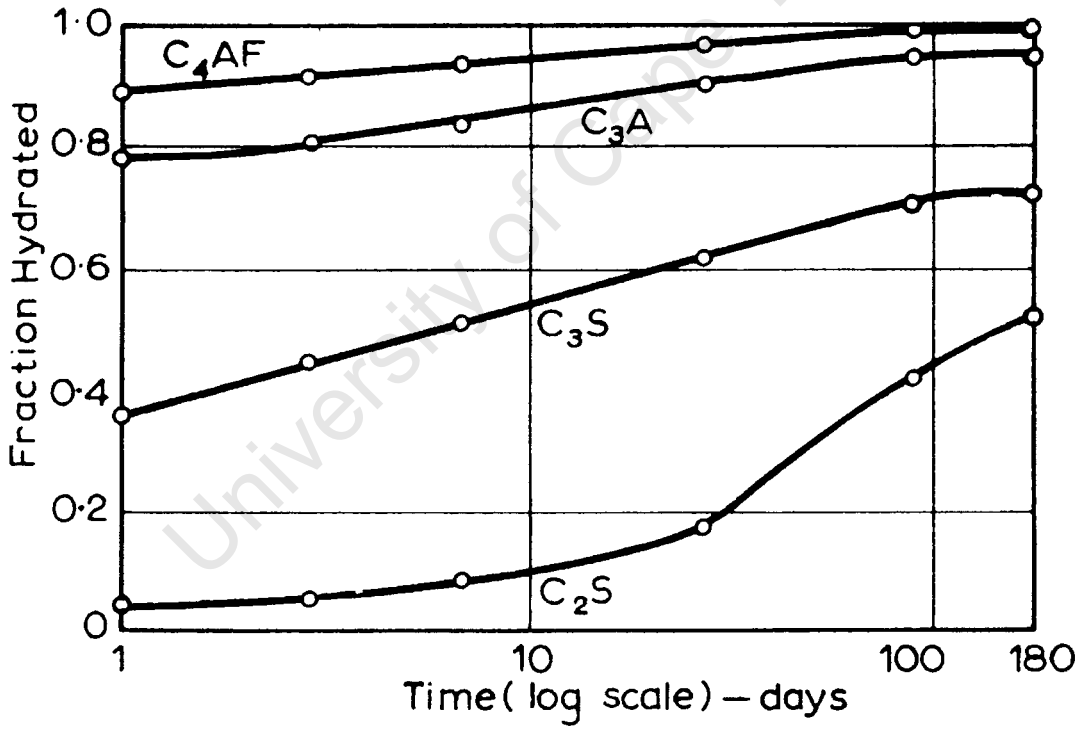

Figure 10: Hydration curves of various constituents (Neville, 1981)

Aitcin *et al* (1987) and Gleize *et al* (2003) - as referenced by Diamond (1976 and 1986) - identified four differing morphologies of CSH occuring in varying degrees. These are commonly referred to as:

Type I - A fibrous, acicular (needle-like[2]) form. This type is predominantly found in immature paste but can be found at much later ages in cements of relatively high silica content. See Figure 11.

Type II - A reticular or honey-comb like network. See Figure 12.

Type III - A dense, irregular network. See Figure 13.

Type IV - A dense, solid formation, generally attributed to inner hydrate, often found on the interior of Hadley Grains (Hadley *et al*, 2000).

The $Ca(OH)_2$ liberated by the hydration reactions is deposited randomly in large voids and recesses as thin hexagonal plates (Figure 14) that later merge into a massive deposit. With continued hydration, this phenomenon further decreases the macro porosity.

Figure 11: Type I CSH – fibrous, acicular

[2] As defined by the Readers Digest Great Illustrated Dictionary, 1984.

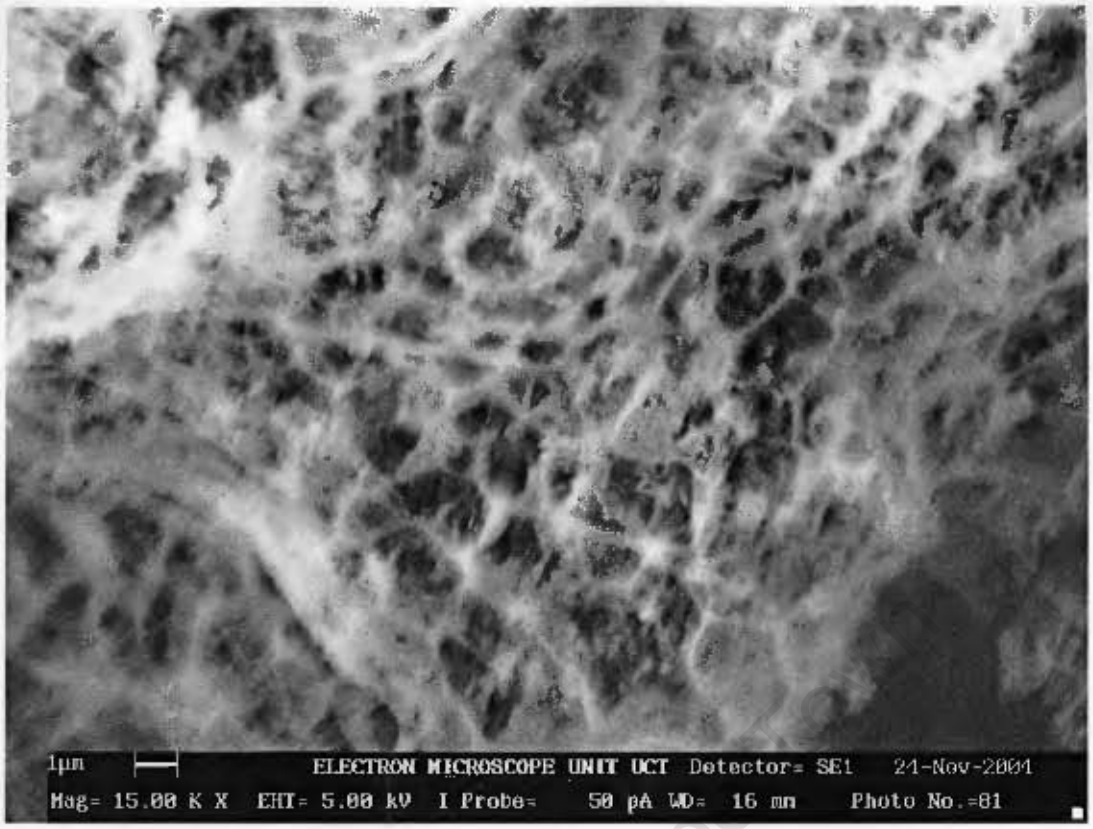

Figure 12: Type II CSH gel, a honeycomb like network

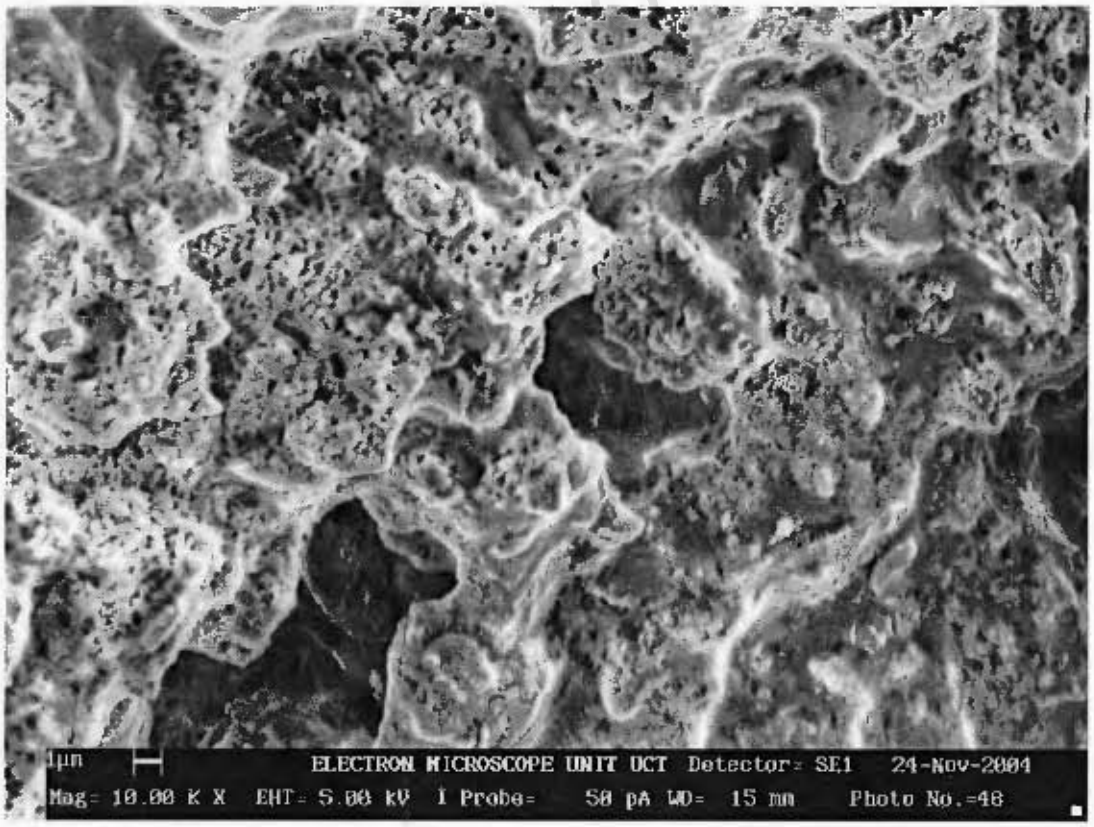

Figure 13: Dense Type II and Type III CSH

Figure 14: Large hexagonal plate deposits of Calcium Hydroxide in a macropore

3.1.2 Tricalcium Aluminate Hydrate and Gypsum

The reaction of C_3A with water results in a flash set. Gypsum is incorporated to counteract this phenomenon. Gypsum and C_3A react forming insoluble calcium sulphoaluminate ($3CaO.Al_2O_3.3CaSO_4.31H_2O$). Eventually a tricalcium aluminate hydrate is formed, which is preceded by a metastable $3CaO.Al_2O_3.CaSO_4.12H_2O$. As more C_3A comes into solution the sulphate content decreases continuously, changing the composition.

Apart from its small contribution to early age strength, C_3A has few long-term benefits and is attacked by sulphates and expands. C_3A is however useful in the manufacture of cement as it acts as a flux. It also possesses chloride-binding properties.

The aluminate phase has many forms. This is dependent on the amount of heavy metals present in the mix (Fe^+, Ba^+, etc) and anions present. A general formula for the aluminate phase is

$[Ca_2(Al,Fe)(OH)_6]^+ x^-.mH_2O$ (Birin-Yauri and Glasser, 1998)

C_4AF hydrates to form tricalcium aluminate hydrate (C_3AH) and $CaO.Fe_2O_3$. aq., an amorphous phase. Fe_2O_3 may also be found in solid solution in the tricalcium aluminate hydrate. It is the ability of this phase to bond with any anion (x^-) - to balance interlayer forces - that makes this compound of great importance to chemical chloride binding.

The hydration products collectively form the cement gel in hardened concrete. It is through this gel that ions must travel during transport. It is therefore equally important to understand the structure, as well as the composition, of the cement paste fraction.

3.2 Pore Structure – Nature and Measurement

Concrete is a porous medium. As hydration proceeds, hydration products diffuse away from their initial source, coming into contact with other hydrating grains, forming an erratic network of hydration products and pores. It is through this network of pores that ions can be transported. Most diffusion and migration theory applies to unobstructed paths in solutions. Concrete, however, interacts with ions in, or transported through, the pore network. Durability parameters and transport mechanisms are influenced by porosity (total pore volume), pore segmentation and tortuousity.

3.2.1 Pore Structure of Cementitious Systems

The hydration process gives rise to the solid network of cement gel. This network consists of various hydration products, unhydrated cement particles, aggregate particles, calcium hydroxide deposits, some minor components and water.

Electrostatic forces during the fresh phase and subsequent particle packing gives rise to numerous voids within the microstructure. Water filled spaces within the cement paste are collectively referred to as ***capillary pores***. Interstitial voids within the gel itself are known as ***gel pores*** (Figure 15). [Neville, 1981]

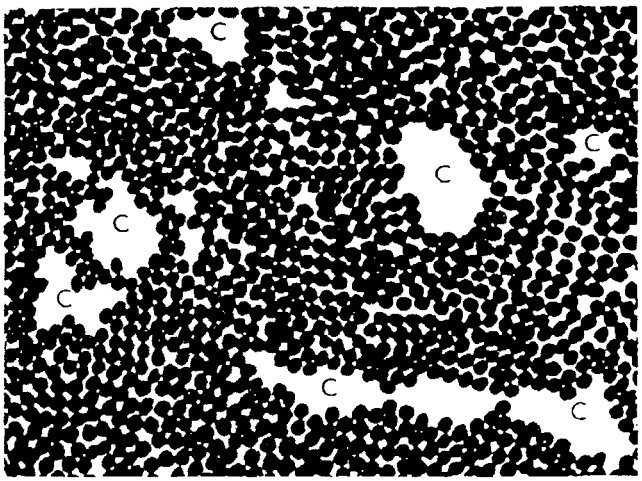

Figure 15: Simplified Powers Model of paste pore structure showing interstitial spaces (gel pores) and capillary pores (marked C). [Neville, 1981]

Gel Pores

Gel pores make up approximately 28 % of the total pore volume (Hearn *et al*, 1994). This value is dependent on binder characteristics, but is independent of the water-binder ratio and degree of hydration, indicating that continued hydration results in a gel of similar properties and that it does not affect existing paste structure (Neville, 1981). Gel pores range in size from 1 to 3 nm (Neville, 1981; Mehta, 1986; referred to by Hearn *et al*, 1994). Gel "particles are mostly fibrous, and bundles of such fibres form a cross-linked network containing some more or less amorphous interstitial material" (Neville, 1981). This network may densify to produce varying gel morphologies – as discussed. However, the irregular nature of the gel pores would remain.

Capillary Pores

"Capillary pores represent that part of the gross volume which has not been filled by the products of hydration" (Neville, 1981). Capillary pore size ranges from 10 to 1000 nm (Neville, 1981; Mehta, 1986 - referred to by Hearn *et al*, 1994). Capillary pores are relatively lengthy pores of irregular spacing, diameter, shape and connectedness.

In contrast to gel pores, the capillary pore fraction is dependent on the water–binder ratio and the degree of hydration of the cementitious binders. As the hydration products occupy more volume than the original cement particles, the capillary pore volume will reduce with continued hydration (Neville, 1981). Due to their size and position within the microstructure, these pores may become completely enclosed by continued hydration. This is dependent on initial water-binder ratio and degree of hydration. An initial water-binder ratio of 0.38 or less is sufficient to result in the effective elimination of capillaries, rendering the paste impermeable (Hearn *et al,* 1994). Table 2 gives the time required for capillaries to become segmented (not eliminated) as a function of water-cement ratio. In practice, these values are dependent on mix design (certain supplementary cementitious materials refine pore structure), placing temperature (which increases the hydration rate but results in a coarser pore structure) and curing practice - which also affects pore refinement (Hearn *et al*, 1994).

Table 2: Approximate age at which capillary pores become segmented (discontinuous) (Powers, 1958, as referred to by Hearn et al, 1994 and Neville, 1981)

W/C ratio by mass	Time Required for Capillary Discontinuity
0.40	3 days
0.45	7 days
0.50	14 days
0.60	6 months
0.70	1 year
Over 0.70	Impossible

Entrained air bubbles

Entrained air bubbles occur in the mix intentionally (air entraining admixtures) or naturally as the mix water and aggregate particles contain small amounts of air (Figure 16). These generally fall into the 1 to 50 μm size range (Mehta, 1986; referred to by Hearn *et al*, 1994). The voids are initially air filled but may become filled with water at a later stage depending on the prevailing conditions. The air pressure within these voids results in distorted spherical shapes, often surrounded by a relatively dense layer of hydration products, as result of the diffusion forces acting against the air pressure. This may cause them to become cut off from the capillary pores.

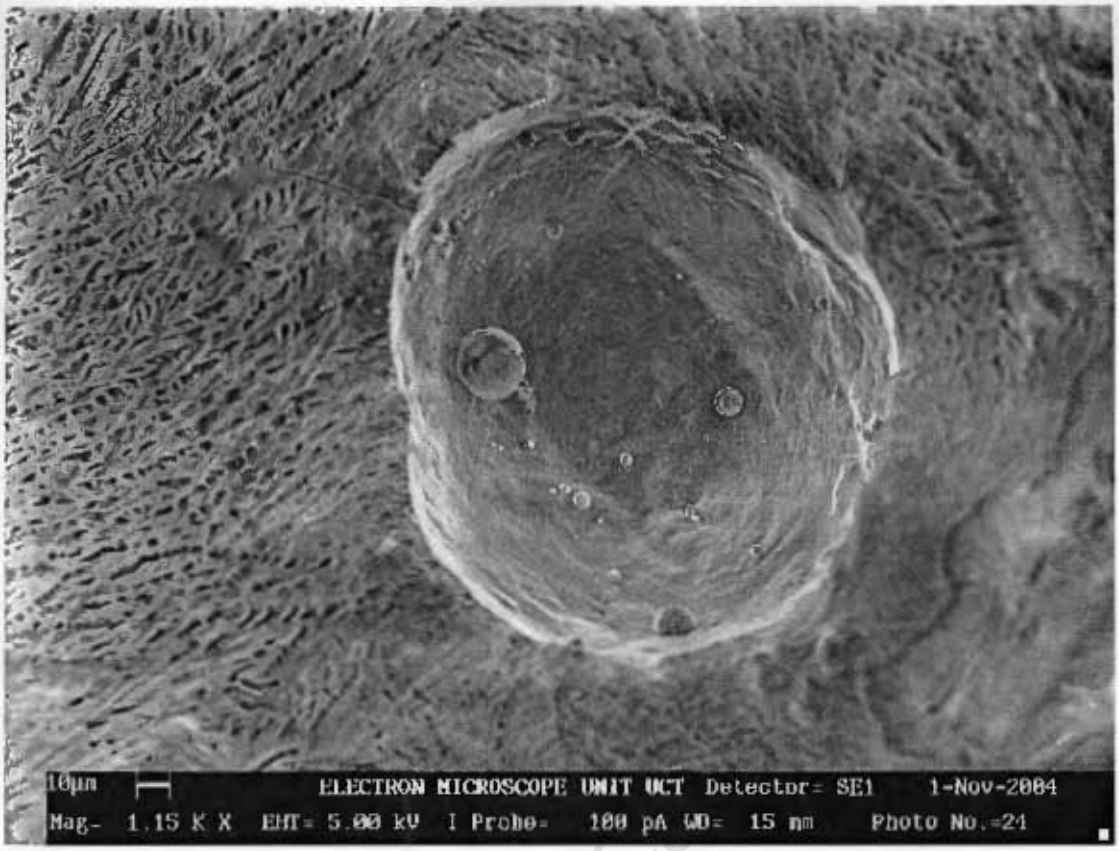

Figure 16: SEM micrograph of an entrained air void effectively cut off from the capillary pore network (smooth pore walls versus porous fracture surface – left)

Entrapped air voids

Entrapped air voids occur as result of poor compaction of the fresh concrete mix. These pores range in size from 1 to 3 mm, or more (Mehta, 1986; referred to by Hearn *et al*, 1994). These also take the form of distorted spheres due to air pressure. They may also be cut off from the capillary pore fraction.

Bleed lenses

During setting, settlement of the mix occurs under gravity, causing solid, heavier particles to sink within the mix. This displaces mix water upwards to be deposited as a thin film on the top surface. This is known as bleeding – giving rise to bleed water. As this bleed water moves through the mix, towards the surface, it may be trapped under aggregate particles and steel bars, etc. If it is not subsequently removed it

remains as a void in the hardened matrix. This type of void is referred to as a ***bleed lens***. Good mix design can eliminate the formation of bleed lenses.

Discussion

Although the gel pores make up approximately 28 % of the total pore volume (Hearn *et al*, 1994), their size makes the movement of water through them highly unlikely. Water molecules are only an order of magnitude smaller than these pores, and electrostatic forces would hinder the movement of water molecules and chloride ions through these three dimensional spaces. They are, therefore, unlikely to influence chloride test methods and pore structure measurements. Suryavanshi and Swamy (1998) noted that permeability and durability have been attributed to the volume of pores larger than a specific diameter. They refer to numerous research results:

Researchers	**Limiting pore diameter**
Mehta and Manmohan (1980)	132 nm
Goto and Roy (1981)	150 nm
Feldman (1981)	118 nm
Mehta (1981)	60 nm
Page *et al* (1981)	100 nm

These limits are far greater than the domain of the gel pores.

Capillary pores, therefore, constitute an important aspect of transport studies. Capillary pores are accessible to, and able to facilitate, water and ion transport. Their occurrence is dependent on water-binder ratio and degree of hydration. Mix design and curing practice would impact on these properties, altering transport properties.

3.2.2 The Interfacial Transition Zone (ITZ)

Although few normal aggregates have porosities greater than 5 % by volume (Hearn *et al,* 1994), the coarse and fine aggregate volumes may impact on pore structure in other ways. Increased aggregate fraction effectively lowers paste fraction. This, in turn, lowers the total porosity of the particular concrete. However, an increase in

aggregate fraction may be detrimental to the concrete's transport properties due to the occurrence of interfacial transition zones.

The interfacial transition zone is as a result of particle packing inefficiencies (termed the "wall effect"), one-sided hydration product growth and water entrapment (Scrivener, 2004; Scrivener, 1996; Delegrave *et al*, 1997; Liao *et al*; 2004). This zone extends up to 20 μm from the aggregate interface (Hearn *et al*, 1994; Scrivener, 2004; Figure 17). This phenomenon leaves a zone adjacent to the aggregate particles that is deficient in cement grains. This zone is also occupied by water due to the thin film that surrounds aggregate particles resulting from electrostatic forces. The cement grain deficit leaves further space that can only be occupied by water. As hydration proceeds, hydration products occupy this region. However, the local increase in water-binder ratio results in a more porous and permeable zone seen in Figure 18. Scrivener (2004) stated that "this 15-20 μm zone ... appears to be minor compared to the bulk paste, but it in fact makes up some 20-30 % of the total paste volume in a typical concrete." This is in agreement with statements made by Delegrave (1997).

Scrivener (1996) conducted analysis of BSEM images of concrete samples penetrated by Wood's metal in order to quantify the transition in porosity form the aggregate interface outwards. These results are in accordance with Elsharief *et al* (2003) and Neville (1995) showing a significant increase in porosity (up to 15 % higher) in the < 20 μm range. Using Wood's metal, Scrivener showed that the ITZ is penetrated preferentially to the bulk cement paste. Scrivener concluded that her study "gives direct evidence for the fact that the higher porosity in the ITZ results in this porosity being more interconnected and confirms that the ITZ has an important effect on the transport properties of concrete."

Neville (1995) presented porosity results as a function of distance from an aggregate particle (Figure 19). This clearly shows that a significantly higher porosity (three times higher) results nearer to the aggregate paste interface compared to the bulk cement paste. This is in accordance with Figure 17 presented by Scrivener (2004) where this porosity transition can clearly be seen.

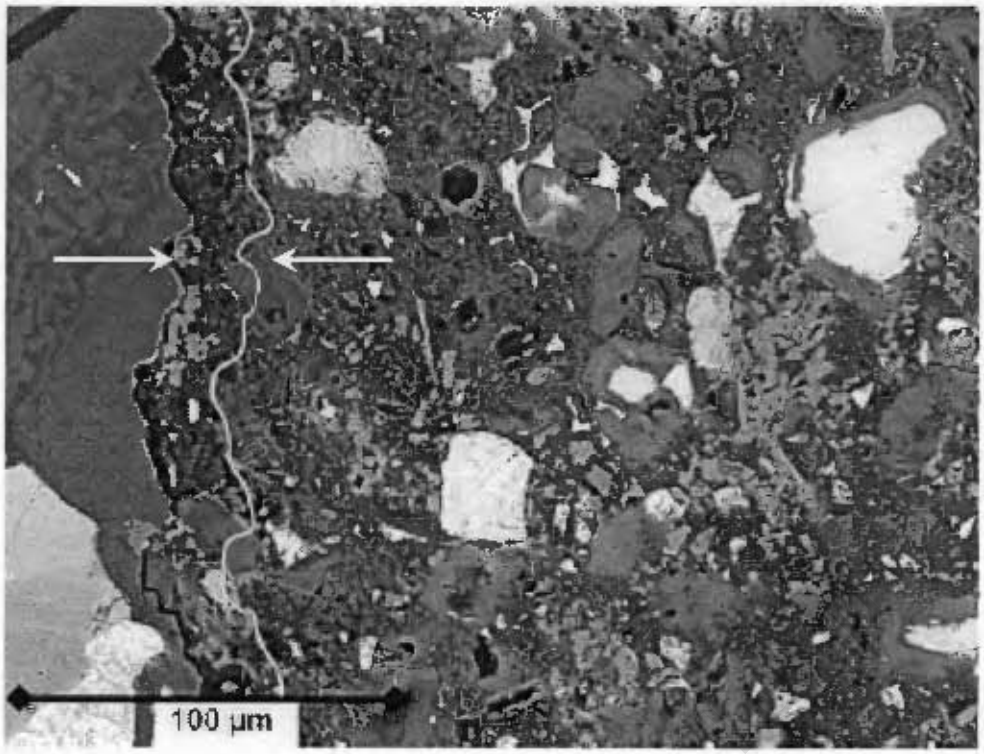

Figure 17: A backscattered scanning electron micrograph of the ITZ – outlined in white (Taken from Scrivener, 2004)

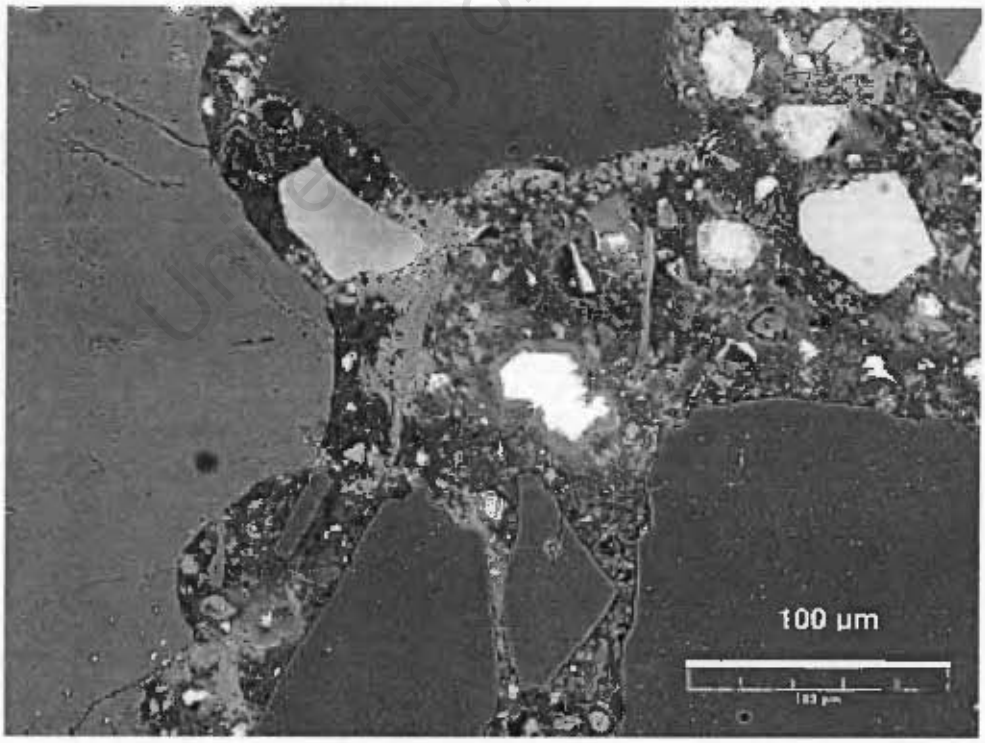

Figure 18: Irregular particle packing around and near aggregate particle results in irregular gel density (Scrivener, 2004)

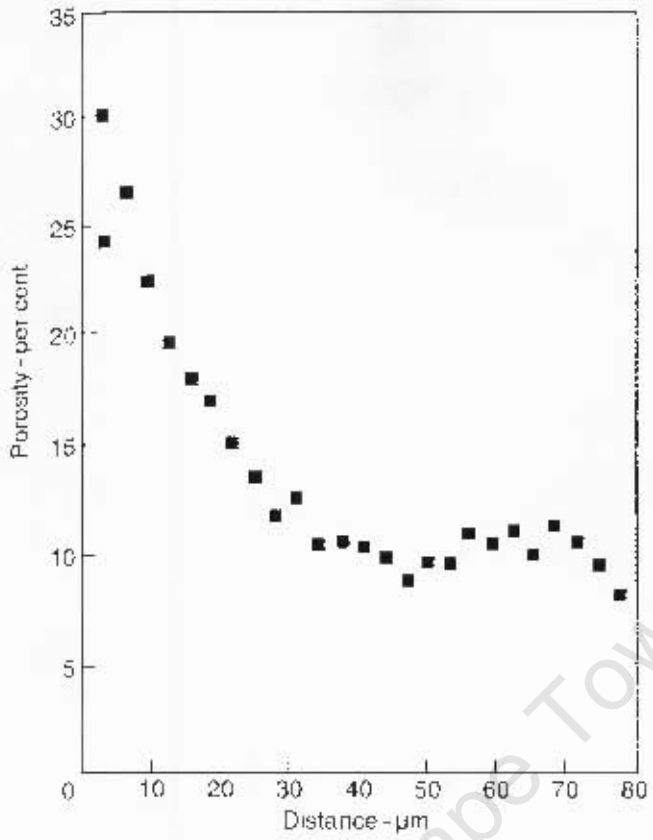

Figure 19: Porosity as a function of distance from a coarse aggregate particle (Neville, 1995)

Diamond (2004; 2003; 2001) has challenged the hypothesis of the relatively consistent formation of an ITZ surrounding all aggregate particles. His SEM investigations have led him to believe that particle-packing variations do cause areas of increased porosity, however, these areas occur irregularly. A distinct boundary separates these patches from the denser hardened cement paste. This can be seen in Figures 20 and 21. Diamond (2004) also presented evidence that calcium hydroxide deposits can be found in the ITZ region (see Figure 22). This forms a dense layer around the aggregate particle. However, it is believed that calcium hydroxide preferentially deposits in large voids and macro pores. If excessive calcium hydroxide is present in the pore solution, and not used up by supplementary cementitious binders, it will deposit in the ITZ, as this is a region of relatively high porosity. The occurrence of calcium hydroxide in one ITZ, or in the ITZs of one concrete mix, is insufficient evidence to support its deposition in all instances of ITZ formation. The occurrence of these large $Ca(OH)_2$ deposits is evidence that the ITZ actually exists.

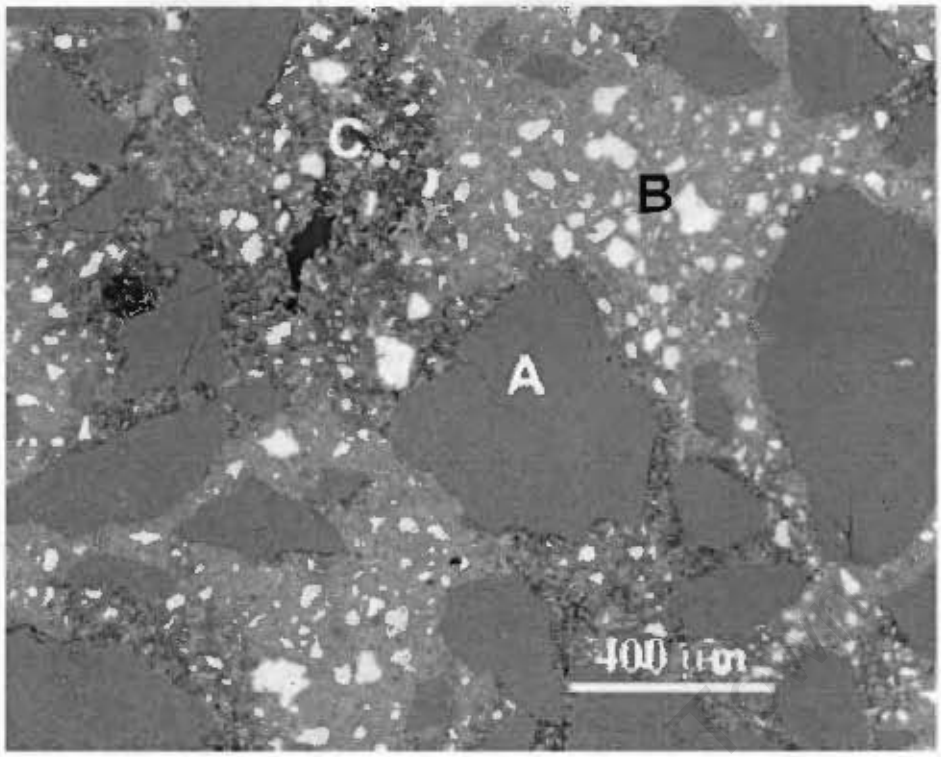

Figure 20: SEM micrograph showing patches of porous hcp (C), within dense hcp (B), surrounding aggregate particles (A), inconsistent with the general ITZ model (Diamond, 2003)

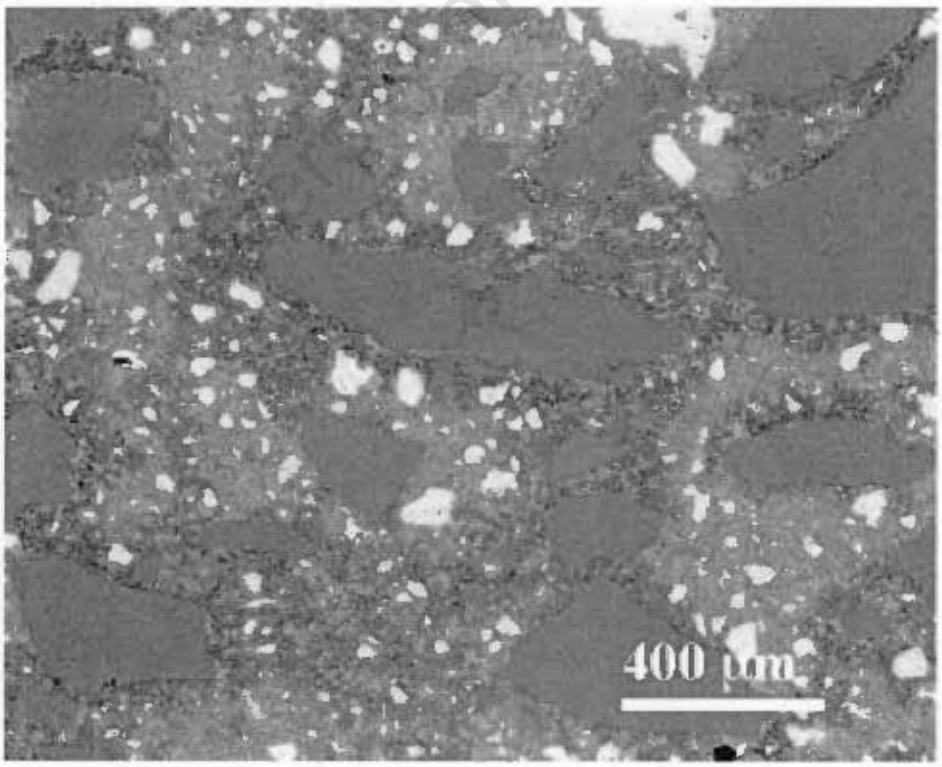

Figure 21: This lower magnification view does, however, show resemblance to the general model of ITZ occurrence (Diamond, 2003)

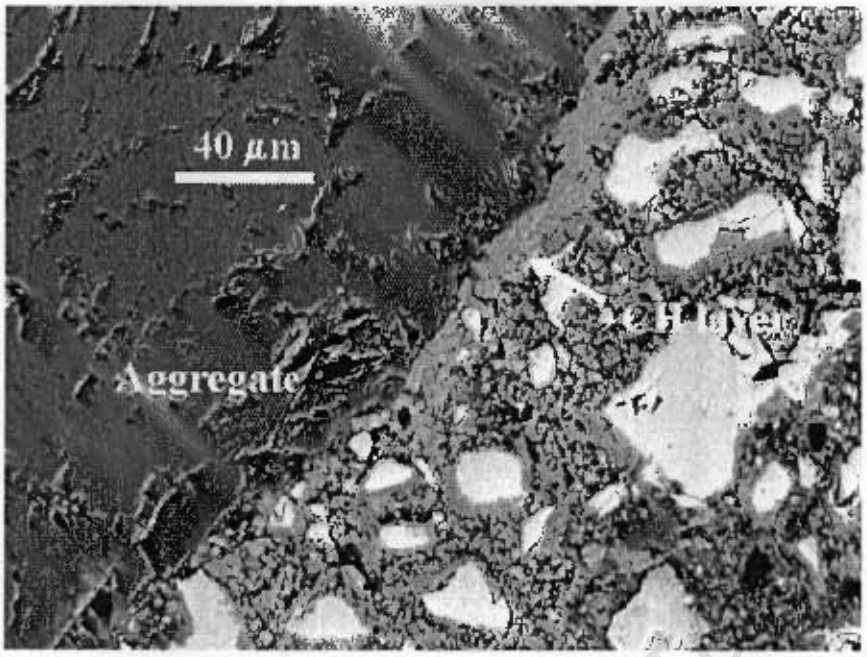

Figure 22: Calcium hydroxide deposit in the ITZ region (Diamond, 2004)

ITZ's, Aggregate Volume Fraction and Percolation

The formation of an ITZ has obvious implications in applying fundamental paste research to mortars and then to concretes. The sand or aggregate content has been proven to be the predominant parameter governing the effect of the ITZ. An isolated aggregate particle could exist, with its ITZ, and have no impact on bulk transport properties. However, once a critical amount of aggregate has been added to the mix, a greater number of aggregate particles become closer in proximity. This causes the ITZ to become merged, resulting in continuous pathways of decreased resistance to penetration. This is termed percolation (Halamickova, 1995; Winslow, 1994; Scrivener, 1996; Ollivier *at al*, 1995). Figure 23 shows the potential impact of coarse aggregate fraction on ITZ percolation. Aggregate's ITZs can be isolated (a) and not affect transport properties greatly. As aggregate content increases, the ITZs begin to merge (b) until they form continual pathways through the concrete (c).

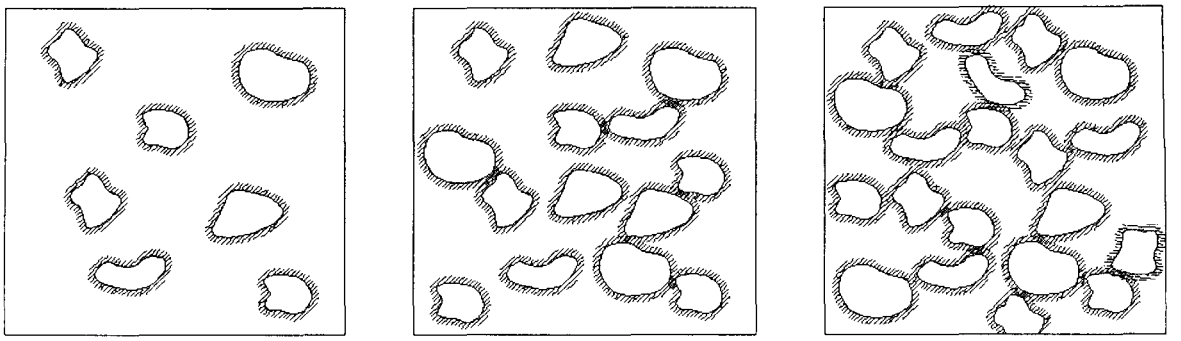

Figure 23: The coarse aggregate volume fraction can cause ITZ percolation (Alexander and Mindess, 2005).

Halamickova *et al* (1995) studied the impact of sand content on transport behaviour (diffusion coefficients). Key results can be found in Table 3.

Table 3: Affect of sand content on diffusion transport characteristics (Adapted from Halamickova et al, 1995)

Sand Volume	Degree of Hydration	Average D_{eff}	C_v
(%)	(%)	($m^2/s \times 10^{-11}$)	(%)
0	55 – 56	2.96	4.6
35	70 – 73	0.96	3.7
45	70 – 72	1.79	0.5
55	70 - 73	0.84	2.4

It can be seen that for the 0.5 water-cement ratio, water-cured mortars used in the above study, an irregularity occurs between 35 and 55 % sand content. It is at this level that the pore structure is negatively affected to the extent that percolation occurs, doubling the effective diffusion coefficient. The same trend was observed for a 0.4 water-cement ratio. The reason for the subsequent decrease is uncertain. It may be due to the significant decrease of accessible transport volume as paste is replaced by relatively impermeable aggregate particles.

Winslow *et al* (1994) showed using MIP that the impact of increased aggregate content in mortars increased the mortars' accessible porosity. These results can be

seen in Figure 24. Here, it seems that a critical volume fraction is present between 45 and 48 %, where a significant jump in the derivative (of porosity versus volume fraction) occurs.

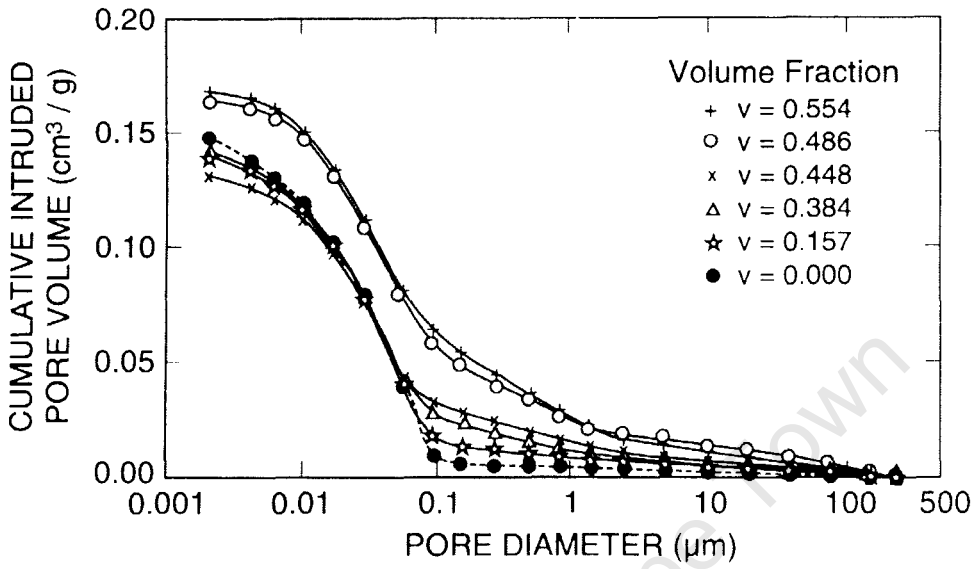

Figure 24: Mercury intrusion of different sand volume fractions shows a critical percolation volume fraction between 45 and 48 % (Winslow *et al*, 1994)

Yang and Su (2002) set out to quantify the effects of the ITZ on chloride diffusion. It was found that "the approximate chloride migration coefficient of ITZ is about 2.83, 1.76 and 1.55 times [that] of the matrix migration coefficient for [an] ITZ with [a] thickness of 20, 40 and 50 μm, respectively." These results were obtained from a combined experimental and modelling technique. Migration rates were obtained as a function of aggregate volume fraction. A model was then employed in order to relate these values to modelled ITZ fractions.

Basheer *et al* (2005) found that air permeability increased with aggregate size. This would indicate that particle packing inefficiencies are increased and the tortuousity of the ITZ paths formed by larger aggregates decreases – which could have a negative impact on the durability of the concrete. However, in terms of fine aggregate content, it was found that increased fine aggregate content decreased air permeability – this was attributed to increased tortuousity. It was also shown that carbonation increased with aggregate size.

Elsharief *et al* (2003) found, using BSEM, that by decreasing the aggregate size, porosity is reduced and the amount of unhydrated cement grains surrounding the coarse aggregate particles (i.e. in the ITZ's) increased. Ollivier *et al* (1994) agreed with this statement and noted that the local increase in w:b ratio resulted in greater porosity. It was noted that the hydration products found in this region were better formed and oriented due to their freedom to diffuse efficiently.

Principallo *et al* (2003) used electrical conductivity to analyse the impact of aggregate fraction increases. It was found that a percolation pathway was established once the coarse aggregate fraction had exceeded 60 %. This can be seen in Figure 25.

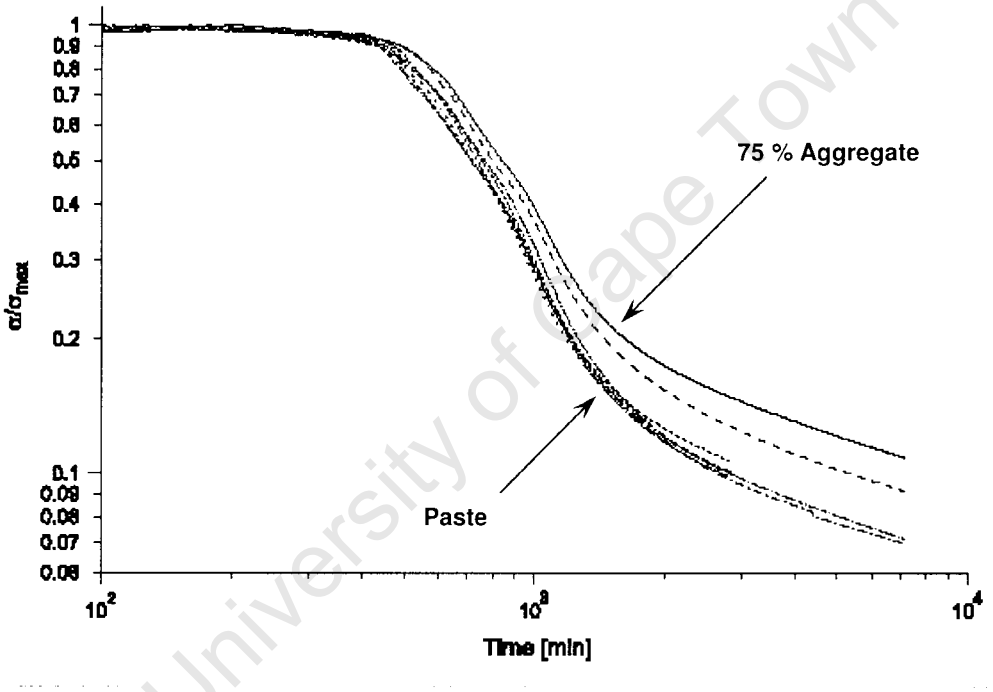

Figure 25: Normalised electrical conductivity as a function of time and aggregate content (Principallo *et al*, 2003)

Discussion

The nature and impact of the ITZ phenomenon is dependent on aggregate volume fraction, aggregate size and mix constituents (due to calcium deposition in ITZ regions). It is clear that this has the potential to impact on the global pore structure and the concrete's transport properties. It is important to consider these effects when designing and analysing laboratory specimens. Concretes and mortars containing a

large coarse aggregate proportion may encourage percolation to occur. Hence, a poor reflection of the true paste properties would result when conducting global tests.

The characterisation of concretes, mortars and pastes requires a representative sample to be obtained and tested. Hence, the larger the sample, the more representative the test results. However, practicality and other limitations dictate that relatively small samples are tested. It is therefore important to ensure that percolation does not occur through the sample due to the size or nature of the sample dimensions. This phenomenon is exhibited in Figure 26.

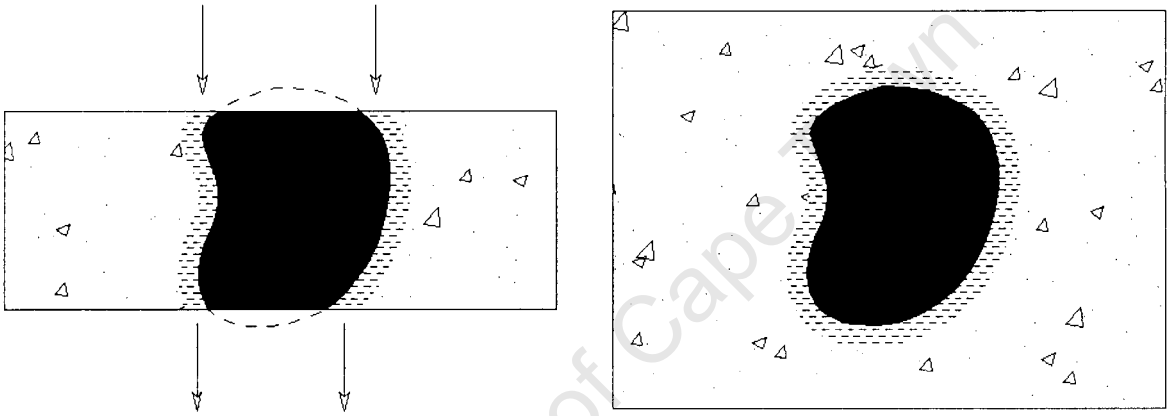

Figure 26: Potential percolation occurrence (a) - as result of sample size and ITZ – avoidable with larger sample size (b)

3.3 Measurement and Comparison of Hardened Concrete Pore Structure

Various methods are available to measure the size distribution, interconnectedness and amount of capillary pores. Techniques such as scanning electron microscopy, BET surface area, bulk porosity, sorptivity, mercury intrusion porosimetry and, more recently, three-dimensional X-Ray (Scrivener – personal communication, 2003) are being utilised to gain a greater understanding of capillary microstructure. However, these methods yield significantly differing quantifications.

To reiterate, it is the accessible pore fraction and the degree to which this fraction is interconnected that is of interest and importance to ion transport and to durability studies as a whole. It is therefore necessary to be able to quantify this accessible pore fraction, its permeability properties and physical characteristics (e.g. tortuosity).

3.3.1 Total Porosity

A measure of porosity gives an indication of the volume of solution available to facilitate chloride transport. It is also necessary for chloride binding calculations (to be discussed later).

Mass loss on drying

The free water fraction constitutes that volume of porosity available for transport of ions and liquids. This total accessible porosity can be determined by mass loss upon drying at 105 ˚C. Porosity is thus calculated by equation 3.1.

$$n = \frac{V_p}{V_T} = \frac{\frac{\Delta m}{\Delta \rho_{solution}}}{\frac{m_c}{\rho_c}} \qquad (3.1)$$

where n is total (accessible) porosity

V_p is volume of pores in sample

V_T is total volume of sample

Δ m is mass loss on drying

(Δ) $\rho_{solution}$ is the density of solution occupying the pore space before drying (or the change in solution density in the case of solvent displacement)

m_c is the mass of the concrete sample

ρ_c is the density of the concrete

The thermal cracking and shrinkage that the sample undergoes during oven drying may, however, significantly disrupt the microstructure. It is hypothesised that this may expose previously inaccessible water sources such as isolated capillaries and water filled entrained air voids (Chatterji, 2001).

Samaha and Hover (1992) noted that

> "Slow drying under relatively moderate environmental conditions caused only minor alterations of the pore structure and the occurrence of some discrete, unconnected shrinkage cracks which may not affect mass transport. ... ... When the concrete is oven-dried, however, severe microcracking results. It has been observed that such cracks are usually uniformly distributed throughout the specimen and cover both paste and paste-aggregate interface regions."

Samaha and Hover (1992) found that samples oven-dried at 100 ˚C exhibited an increase in charge passed in the RCPT test up to 7 times that obtained for control specimens. Care should, therefore be taken when oven-drying samples. Increased temperature and increased rate of temperature gain results in severe microcracking that would significantly affect subsequently measured transport properties.

Organic solvent displacement

The sample is weighed and immersed in an organic solvent (e.g. isopropyl alcohol or acetone). The solvent displaces the accessible water within the microstructure. This water collects at the bottom of the container (the solvent can be dried using suitable molecular sieves). The sample remains submerged until a constant mass is obtained. The accessible porosity can then be calculated using equation 3.1.

This method is often used to avoid excessive thermal microcracking, where further tests have to be conducted on the sample or its microstructure (e.g. MIP). The drawback to this technique is that it may take several weeks to dry a sample the size of a "small saw cut prism" (Halamickova *et al,* 1995). Samples may also be crushed prior to drying (Stanish, 2002). This accelerates the process but introduces microcracking. SEM work on fractured surfaces conducted as part of this research showed some, but relatively insignificant, evidence of microcracking after sample preparation by crushing.

3.4 Conclusions

The amount and nature of the predominant hydration products will impact on the behaviour of chloride ions as they are transported through the microstructure. Calcium silicate hydrate (CSH), calcium aluminate hydrate (C_4AH_{13}) and calcium ferrous hydrate (C_4FH_{13}) are the primary hydration products. Calcium hydroxide (CH) is the primary by-product of the hydration reactions. Hydration rate differences amongst the various products must be considered when analysing rapid test results of concretes of different ages. Tricalcium silicate hydrates at a faster rate than dicalcium silicate. Over 60 % of C_3S is hydrated by 28 day age, while less than 20 % of C_2S is hydrated. At 90 days age approximately 70 % of C_3S and 40 % of C_2S is hydrated. This has direct implications on test timing and the ability of such rapid tests to give a good representation of long term behaviour.

The microstructure of cement paste, mortars and concrete is complex and irregular. The capillary pore fraction (pore diameters ranging from 10 to 1000 nm) is capable of facilitating chloride ion transport. The smaller gel pores are too small to facilitate chloride ion transport. Hence, the capillary pore fraction may be termed the accessible pore fraction for chloride transport and may be used for the purposes of chloride binding calculations (to be discussed later). Mass loss on drying at 105 ˚C and organic solvent displacement are suitable ways of calculating the accessible (capillary) pore fraction. Where thermal cracking must be avoided (in pore size distribution analysis, for example), organic solvent displacement is a more suitable technique. However, oven drying at 105 ˚C is acceptable where the bulk porosity of the specimens is required.

The occurrence of ITZ's may cause percolation through specimens. This should either be accounted for or avoided. The sand-to-binder and maximum-aggregate-size-to-minimum-sample-dimension ratios are important measures in controlling the potential effect of ITZ's on the results of transport tests. The impact of ITZ's and the limiting ratio values are mix specific and should be obtained from trial experiments.

4. CHLORIDE BINDING

Chloride ions interact with the hydration products as they are transported through the cement matrix. This results in the immobilisation of a portion of the chloride ions. This phenomenon is loosely referred to as chloride binding. Chloride binding can be categorised by two general mechanisms: ***chemical binding*** and ***physical adsorption***. These two mechanisms lead to the depletion of free ions in the pore structure. A cementitious binder's potential to bind chloride ions can have an influence on expected resistance to chloride-induced corrosion. The removal of free chloride ions lowers the amount of migrating ions, reducing their concentration in the pore water, thus slowing the diffusion process.

No clear distinction is made between chemical and physical binding in the literature. The phenomena are collectively referred to as chloride binding in literature. In obtaining a fundamental understanding of chloride transport behaviour – especially when applied to chloride extraction – a distinction must be made between reversible and irreversible chloride binding. For this reason, the two theories – chemical and physical - are dealt with separately.

Work has been conducted on chlorides incorporated in the mix water of concrete (Rasheeduzzafar *et al*, 1992; Enevoldsen *et al*, 1994; Arya *et al*, 1990; Al-Hussaini *et al*, 1990). However, in this case, the chloride ions formed during the dissolution of the NaCl become intricately bound in the hydration products and influence the morphology of the microstructure. This removes most chemical and physical binding sites before the concrete element's service life begins. These binding mechanisms differ from those occurring during chloride ingress into hardened concrete. It has been noted and is generally understood that the use of salt water as mix water should be avoided when reinforcement is employed (Neville, 1995). Therefore, no studies on chlorides introduced in the mix water were considered in this work.

4.1 Physical Binding - Adsorption

The majority of publications on the subject of chloride binding make reference to both mechanisms of chloride binding – chemical and physical. Adsorption is generally mentioned during the introduction and then not discussed again.

CSH is the primary hydration product in the cement paste. Its large surface area allows a significant amount of physical adsorption to take place. Physical adsorption is dependent on local equilibrium between the pore solution and ions adsorbed onto the pore walls through Van Der Waal's forces. This has been shown by the strong correlation between chloride binding and the Cl^- / OH^- ratio (Kayali and Haque, 1995). Hence, ion substitution must occur and competition between differing ions results. It has also been shown (Sergi *et al*, 1992) that this ratio also has important implications on the threshold value for corrosion to be initiated. Corrosion and chloride binding are both influenced by the competition between various ions to occupy available adsorption sites on the surface of the CSH gel and reinforcing steel in order to maintain local equilibrium.

Tang and Nilsson (1993) conducted a desorption test as part of their study on chloride binding. A crushed mortar was mixed with NaCl solution and the concentration of chloride ions allowed to equalize. The amount of bound chlorides was calculated by finding the difference between the initial solution concentration and that at equilibrium. The sample was then removed from the solution and placed in deionized water. Again, equilibrium was reached as ions were desorbed. The desorption isotherm was found from a number of samples. The results can be seen in Figure 27. Tang and Nilsson (1993) concluded that at chloride concentrations lower than 0.05 mol/l only monolayer adsorption occurs. At concentrations above 0.05 mol/l complex adsorption occurs. Between 0.01 and 0.05 mol/l a transition zone occurs. It was found that the Freundlich isotherm best represented the results at concentrations above 0.01 mol/l. The non-linear portion of the curve in Figure 30 indicates this. And, the Langmuir isotherm best represented results at concentrations below 0.01 mol/l. These isotherms will be discussed later. It was noted from the results that the desorption isotherm has the same slope as the adsorption (binding) isotherm. However, the ordinate axis is higher. Hence, as desorption is monitored, the samples would have a greater amount of bound chlorides at a given concentration as the irreversibly bound ions would remain bound. Tang and Nilsson

speculated that this might indicate that some ions have become chemically bound to the hydration products and could not be desorbed. Their study showed that both physical and chemical processes were occurring simultaneously.

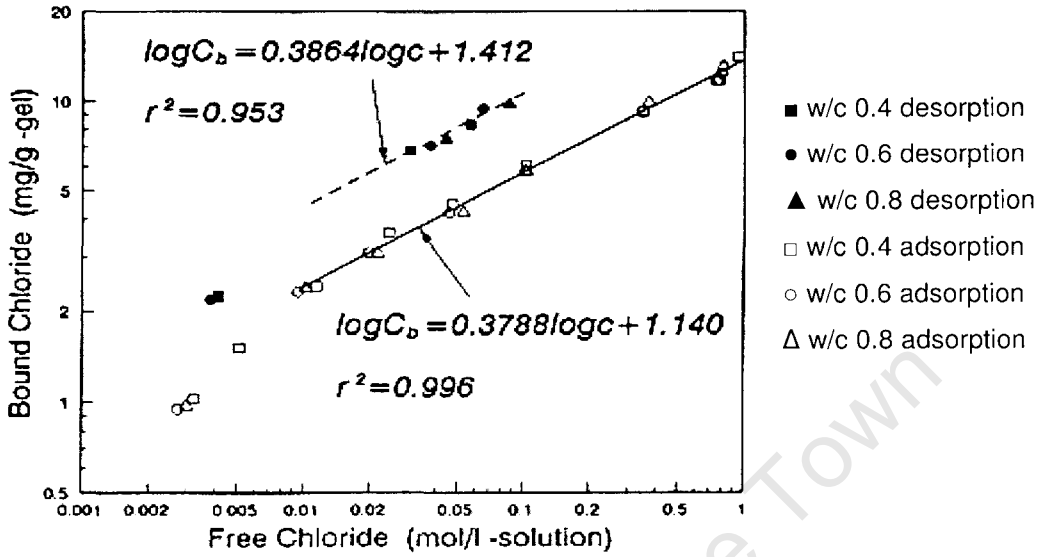

Figure 27: Freundlich Isotherm obtained by Tang and Nilsson (1993). Desorption is also shown (the dotted line).

4.2 Chemical binding

Chemical chloride binding mechanisms are complex and have not yet been clearly defined in the literature. One of the primary hypotheses is that the chloride ions react with the alumina-containing hydration products to form Friedel's Salt.

Jensen *et al* (2000) found that chloride binding is strongly influenced by aluminate and sulphate content of the cement. They introduced a parameter called "the equivalent C_3A content" for comparison of binders' chemical chloride binding potential:

$$(C_3A)_{eq} = C_3A + 0.556\ C_4AF - 1.98\ CS \qquad (4.1)$$

where C_3A, C_4AF and CS refer to the weight percentages of these constituents. A higher equivalent C_3A equivalent would imply that a higher chloride binding capacity exists.

After the hydration of the calcium aluminates, two main alumina phases exist: mono-ferrite $[AF_m]$[3] and tri-ferrite $[AF_t]$[4]. These phases are then capable of binding available ions and are generally known to react with sulphates in the mix, to form ettringite (calcium sulpho aluminate hydrate), early on in the hydration process. Once sulphate reserves are exhausted, a significant amount of AF_m remains, partially balanced by hydroxide ions and partially by sulphates. Chloride ingress would make a significant amount of chloride ions available to substitute for the hydroxide ions in the interlayer spaces. Chloride binding, hence, occurs more readily in the AF_m phase (Jones *et al*, 2003). Hewlett (1998) notes that as concrete matures, the amount of the AF_t phase declines while the amount of AF_m phase increases. Chloride binding would, thus, be expected to increase with maturity. The AF_m phase has varying structural forms depending on the chemical environment in which it is found. A general formula is given by:

$[Ca(Al,Fe)(OH)_6]^+ X^-.mH_2O$ (Birin-Yauri and Glasser, 1998)

$[Ca_2Al(OH)_6]^+$ main layer and $[X^-, nH_2O]$ interlayers

(Rapin *et al*, 2002; Jones *et al*, 2003)

The anions (indicated by an *X* in the equations above) balance the positively charged layer unit in the interlayer spaces. These anions are generally OH^-, Cl^-, I^-, Br^-, NO_3^-, SO_4^{2-}, or CO_3^{2-}. Thus, as chlorides diffuse through the cement matrix, anion exchange may occur between the highly reactive chloride ions and the more inert anions found in the interlayer spaces, especially OH^- ions. The formation of Friedel's Salt results when the anion exchange is predominantly characterized by Cl^- substitution. This would be the predominant phenomenon in a chloride-rich environment. The structure and composition of Friedel's Salt, thus, varies according to the inherent ions found in the interlayer spaces and the amount of substitution that has taken place. The anion's size and polarisability, in turn, determines the amount of interlayer water molecules and the layer stacking sequence. The following Friedel's salt compositions, among others, have been identified:

Rapin *et al* (2001); Jensen *et al* (2000) $3CaO.Al_2O_3.CaCl_2.10H_2O$

---

[3] AF_m is calcium aluminoferrite, monosubstituted

[4] AF_t is calcium aluminoferrite, trisubstituted

Birin-Yauri and Glasser (1998) $Ca_2Al(OH)_6Cl.2H_2O$

The predominant source of chloride ions is NaCl. Salt dissociates into Na^+ and Cl^- ions in water. As charge equilibrium must be maintained, ion exchange must occur. OH^- are generally displaced due to their low reactivity in comparison to Cl^- ions. Thus,

$$[Cl^-]_{bound} = [OH^-]_{released}$$ (Jones *et al*, 2003)

It is uncertain whether chemical chloride binding is reversible, or to what extent. It is plausible that more reactive sulphate ions may substitute for chloride ions in the same way as chloride ions initially substituted for hydroxide ions (Justnes, 1998). As chloride ions become locked in interlayer spaces, it would be more difficult to undo chemical binding than physical adsorption due to the increased electrostatic forces of the Friedel's salt crystal lattice.

Illustrations of Friedel's Salt deposits can be found in Figures 28 to 30. These were obtained from scanning electron microscopy on fractured bulk diffusion test samples. Figure 31 shows a typical Friedel's Salt EDX distribution – used to analyse the elemental structure of a compound.

As discussed, a competition exists between sulphates and chloride in reacting with the alumino-ferrite phases (Csizmadia *et al*, 2001). It has been shown that chloride can only react with the alumino-ferrite phases once available sulphates have been exhausted through forming ettringite or complex alumino ferrite sulphate hydrate (Emanuelson and Hansen, 1997). Sulphates are present in cement (gypsum), and can penetrate into concrete due to their presence in seawater, groundwater and other effluents carried in concrete pipelines. Subsequent ingress is undesirable as ettringite formation is expansive and leads to deterioration of the concrete through cracking. Hence, sulphate ingress should be avoided.

Figure 28: Secondary and backscattered SEM of a small Friedel's Salt deposit in a GGCS mortar

Figure 29: Secondary SEM of clustered Friedel's Salt formations

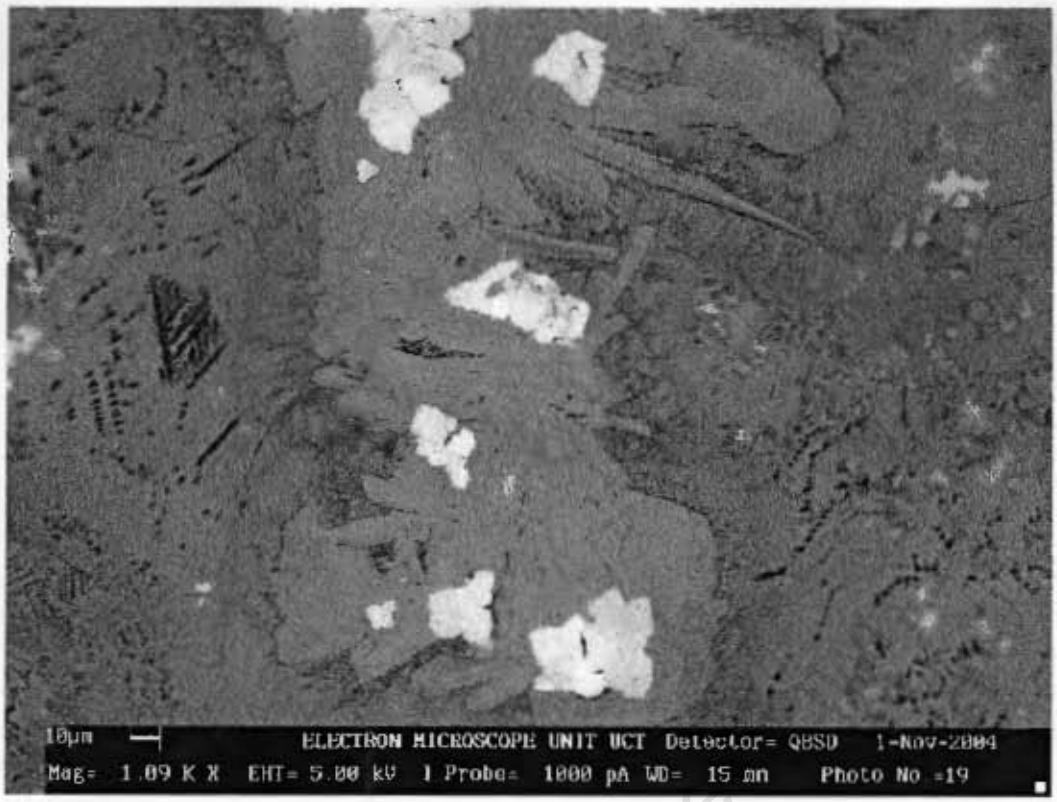

Figure 30: BSEM of clustered Friedel's Salt formations (bright coloured deposits)

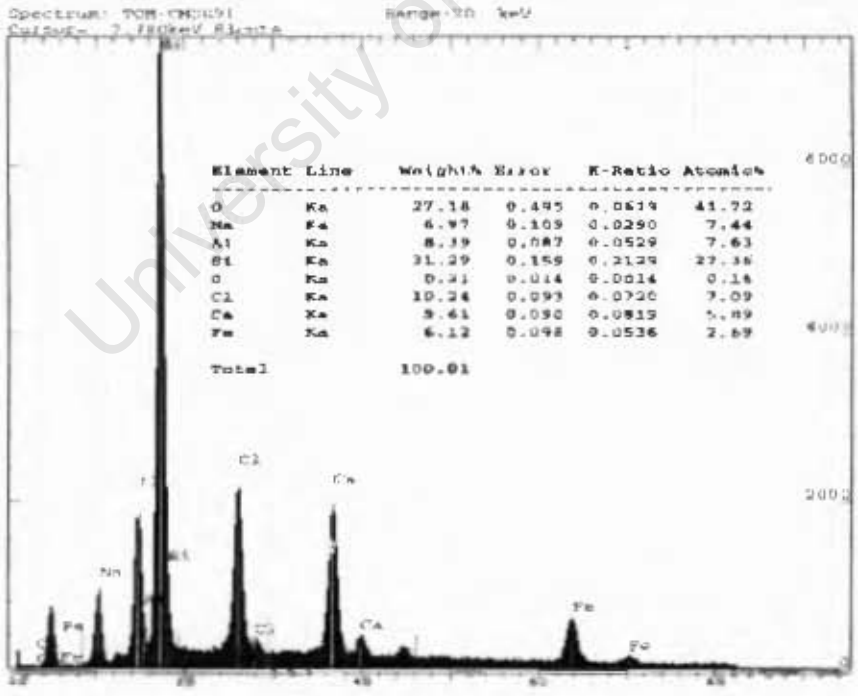

Figure 31: EDX of singular Friedel's Salt crystal showing distinct Al, Si, Cl and Fe peaks

Discussion

Due to the complexities of measuring the chloride ion interactions with the cement gel, it is difficult to distinguish between physical adsorption and chemical binding. As physical adsorption is dependent on local ion and charge equilibrium, it is plausible that almost all physically bound chlorides can be extracted by continually removing chlorides from the pore water. However, it is equally plausible that a portion of chemically bound chloride ions can also be removed. Those ions bound in alumina phases - through ion substitution - may not be completely locked in the alumina matrices or may be displaced by subsequent sulphate ingress. No studies could be found exploring the effect of subsequent sulphate ingress on the existing Friedel's salt deposits.

As chloride levels seldom drop to negligible levels in chloride environments, it is not plausible that a significant amount of bound ions could be unbound naturally. They, therefore, could not contribute to corrosion but do deplete the chloride binding capacity of the concrete. In the case of sulphate ingress, unbound chlorides may contribute to corrosion. Further work exploring this phenomenon is required.

In designing for and predicting the service life of a concrete structure, two variables appear to be necessary to characterise chloride binding capacity:

- Chemical binding capacity - The alumina content and total binder content gives an indication of the amount of alumina available to chemically bind chlorides. The chemical binding studies discussed show clear evidence of chemical binding occurrence and its dependence on cement content and composition.

- Physical adsorption capacity – The internal surface area of the matrix available to physically adsorb chloride ions.

These two factors are in some ways complimentary and in others competitive. An increase in binder content would densify the matrix while providing more alumina for chloride binding. Densification would lower the total pore surface area, lowering the adsorption potential. This would, too, make less gel available for interaction with the

chloride ions present in the pore solution. Hence, more alumina would be present, but not necessarily available to the chloride ions in the pore solution.

4.3 Chloride Binding Isotherms

Chloride binding isotherms are used to characterise the gel's ability to bind ions at increasing chloride concentrations. These isotherms do not distinguish between adsorption and chemical binding, but give a global indication of the gel's ability to interact with and immobilise chloride ions.

Two isotherms are commonly used to express the relationship between free and total chlorides at a particular temperature. These are:

The Langmuir Isotherm (Glass *et al*, 1998):

$$c_t = c_b + M_{Cl} V c_f \qquad (4.2)$$

Where c_b is the bound chloride ions

c_t is the total concentration of chloride ions

M_{Cl} is the atomic mass of chlorine

V is the pore solution volume

c_f is the free chloride concentration

And the Freundlich Isotherm (Glass *et al*, 1997):

$$c_b = \kappa (c_f)^{\frac{1}{n}} \qquad (4.3)$$

Where κ and n are constants dependent on binding capacity.

These isotherms were developed to describe gas adsorption onto solids. The Langmuir isotherm was derived for the adsorption of a monolayer of gas onto a solid, whereas the Freundlich isotherm is an empirical description of the multi-layer adsorption process (Glass *et al*, 1997).

Glass *et al* (1997) found that the Langmuir isotherm predicted the relationship between total and free chloride concentration more accurately, but the Freundlich isotherm was superior when applied to instances where a high level of chloride binding occurred (e.g. where a supplementary cementitious material was used, with high chloride binding capacity).

Tang and Nilsson (1993) stated that the relationship found in their study obeyed the Freundlich isotherm at free chloride concentrations higher than 0.01 mol/l and that it obeyed the Langmuir isotherm at concentrations lower than 0.05 mol/l. This implies that at low concentrations, monolayer adsorption occurs. At concentrations above 0.05 M, complex adsorption involving multiple, interacting adsorption layers occurs. This corresponds to the findings of Glass *et al* (1997).

The isotherm expressions are based on adsorption theory only. The relative accuracy of the isotherm's ability to represent chloride binding is, therefore, surprising as the isotherms do not take chemical chloride binding into account. However, the binding constants obtained from the fitting process can be used to categorise the cementitious binders' total chloride binding capacity or behaviour.

4.4 Chloride Binding and Temperature

As a substantial portion of chloride binding involves chemical binding, it can be assumed that binding is temperature dependent (hence, the term "isotherm"). Jensen *et al* (2000) showed that the influence of temperature on binding is dependent on cement composition. They showed that for cement paste with 20 % C_3A substitution, more chloride became bound at 20 ˚C than at 4 ˚C and 35 ˚C. They gave no reason for this.

Friedel's salt stability is also temperature-dependent. At 28˚C, the salt undergoes a "polymorphic phase transition from a low temperature monoclinic [alpha] form to a high temperature rhombohedral [beta] form" (Jensen *et al*, 2000). This may, in some way, be responsible for the change in binding behaviour experienced between 4 ˚C and 35 ˚C. Binding experiments should thus be performed in a controlled environment at constant temperature.

4.5 Chloride Binding and Electrical Fields

The only study found in literature concerning the impact of electrical fields on chloride binding was done by Castelotte *et al* (1999). Castelotte *et al* analysed the amount of bound chloride in migration samples using X-ray fluorescence to obtain the amount of total chlorides and a leaching method to extract and analyse the amount of free chlorides. The results obtained can be seen in Figure 32. The presence of an electrical field suppressed chloride binding considerably at lower concentrations (< approx 97 g/l) but enhanced chloride binding at higher concentrations (> approx 97 g/l). Castelotte *et al* attributed this to two possible mechanisms. One plausible reason may be decreased contact time between any given ion and the matrix due to the acceleration of the transport process. This hypothesis also hinges on a further hypothesis that binding is not instantaneous and increases with exposure time. This phenomenon would, however, be apparent at all concentrations. Another consideration may be that the electrical field alters the double layer potential of the pore walls, affecting the interaction between the matrix and the chloride ions.

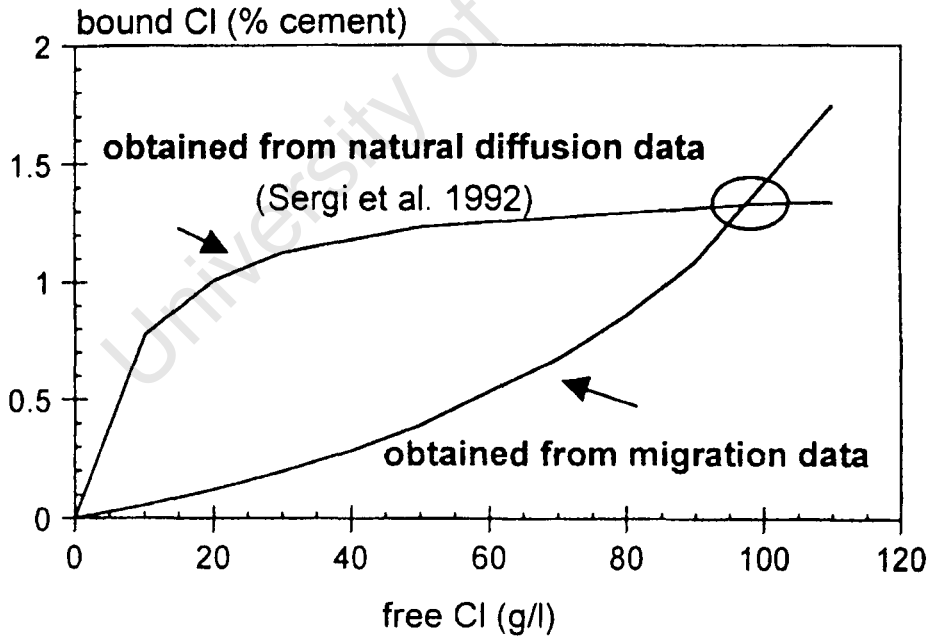

Figure 32: The effect of electrical fields on the binding behaviour of chloride ions (Castelotte et al, 1999)

It is unclear whether electrical field application affects ion activity. If it does in some way, both of these reported hypotheses may also be dependent on ion activity effects. However, the local minimum in chloride ion activity lies at approximately 1 M concentration (Figure 2, p.14). Hence, the trend observed by Castelotte *et al* cannot be fully attributed to ion activity. It is, however, clear that the electrical field alters the interaction behaviour of the ions. This directly influences the chloride binding behaviour and, hence, would impact on the observed effective migration coefficients from migration tests.

The use of a leaching method, however, may yield unrepresentative results as changes in the pore water chloride concentration and pH may result in a significant amount of chlorides to become unbound. The results may have been more meaningful if Castelotte *et al* had carried out both the diffusion and migration binding analysis using the same method or an improved method.

4.6 Measurement of Chloride Binding

Chloride binding can be measured using either the equilibrium method or pore expression.

Equilibrium method

The equilibrium method is a relatively simple and unintrusive method of measuring chloride binding. Generally, a sample of concrete or mortar, either whole or crushed, is submerged in a chloride solution. The concentration of the solution is monitored until it equalizes. At this point, it is assumed that the pore solution and external solution are in equilibrium, i.e.

$$[Cl^-]_{\text{pore solution}} = [Cl^-]_{\text{external solution}} = [Cl^-]_{\text{free}} \qquad (mg_{\text{chlorides}} / ml) \qquad (4.4)$$

Mass balance can then be done to calculate the amount of bound chlorides. If the sample is saturated when initially submerged, the porosity of the sample must be obtained in order to conduct the mass balance. In mass terms,

$$Cl^-_{\text{initial}} = Cl^-_{\text{external solution}} + Cl^-_{\text{pore solution}} + Cl^-_{\text{bound}} \qquad (g) \qquad (4.5)$$

Alternatively, a total chloride test can be conducted on the sample. In this case

$$[Cl^-]_{total} = [Cl^-]_{external\ solution} + [Cl^-]_{bound} \qquad (mg / g_{concrete} \text{ or mass } \%) \qquad (4.6)$$

Again, the external solution is assumed to be equal in concentration to the internal pore solution.

This method had the advantage of not disrupting the microstructure during analysis. It does, however, rely on the assumption that equilibrium between the pore and external solution occurs and is maintained. The time consuming nature of obtaining equilibrium is a primary disadvantage. However, in crushed samples (d < 2.36 mm), this may only take 6 weeks (Stanish, K. – personal communication).

Pore Expression

Pore expression is a widely used technique for the analysis of pore solutions. The sample is placed in the expression device and compressed in a compression machine. This effectively destroys the microstructure as it squeezes the pore solution out of the sample. The collected solution can then be analysed as representative of the pore solution. This generally yields the free chloride concentration. Total chloride analysis can then be conducted on a second sample in order to calculate the amount of bound ions, i.e.

$$[Cl^-]_{total} = [Cl^-]_{expressed\ solution} + [Cl^-]_{bound} \qquad (mg / g_{concrete} \text{ or mass } \%) \qquad (4.7)$$

Due to the high pressures used and associated destruction of the microstructure, this method has been criticised. Glass and Buenfeld (1995) and Glass, *et al* (1996) found that the chloride concentrations of the expressed pore solutions were, surprisingly, higher than the storage solution. The expressed pore solution chloride concentration was found to be 30 % higher than the storage solution. They hypothesized that the destruction of the microstructure and compressive forces resulted in the disruption of loosely bound or adsorbed chloride ions. Nagataki *et al* (1992) and Tritthart's (1989) results were in accordance with Glass and Buenfeld's results.

4.7 Impact of chloride ingress on microstructure

The transport of chloride ions through a cementitious matrix is accompanied by a chemical and physical interaction between the chloride ions and the cement gel. Any alterations in the concrete matrix brought about by chloride ingress must be understood in order to more accurately predict a structure's short- and long-term performance. Suryavanshi and Swamy (1998) noted that a significant amount of research into the microstructural alteration caused by the incorporation of chlorides in the mix water exists. They went on to note that "there is very little reported data in the literature on changes in the microstructure of structural concrete due to chloride penetration."

The addition of sodium chloride during mixing has been shown to decrease the coarser pore fraction (D > 100 nm) while increasing the finer pore fraction (D < 100 nm). This is generally attributed to the formation of a denser CSH gel in the presence of chlorides (Suryavanshi *et al*, 1995; Young, 1974).

Midgley and Illston (1984) found that penetration of an aqueous sodium chloride solution into OPC mixes resulted in a reduction in number of the pores around the 80 nm diameter range. They concluded that chloride ion penetration alters pore size distribution – the greater the chloride concentration present, the smaller the observed pores. Midgley and Illston also found that at a 0.71 w:b ratio, more CSH was produced in the presence of chlorides.

Suryavanshi and Swamy (1998) cast reinforced concrete slabs and employed a surface coating on half of the slab in order to prevent chloride penetration. The slabs were then exposed to cyclical ponding of 4 % NaCl solution. MIP was conducted on representative specimens of the concrete mortar (in order to avoid skewed results due to the presence of coarse aggregate particle, due to the small required MIP sample size). Their cumulative pore size distribution results can be seen in Figure 33 (Slab S1 had a w:b of 0.45 and S2 a w:b of 0.6). Overall pore reductions were noted for all samples subjected to chloride ingress. Suryavanshi and Swamy reported that this reduction became less severe at increased water-cement ratios.

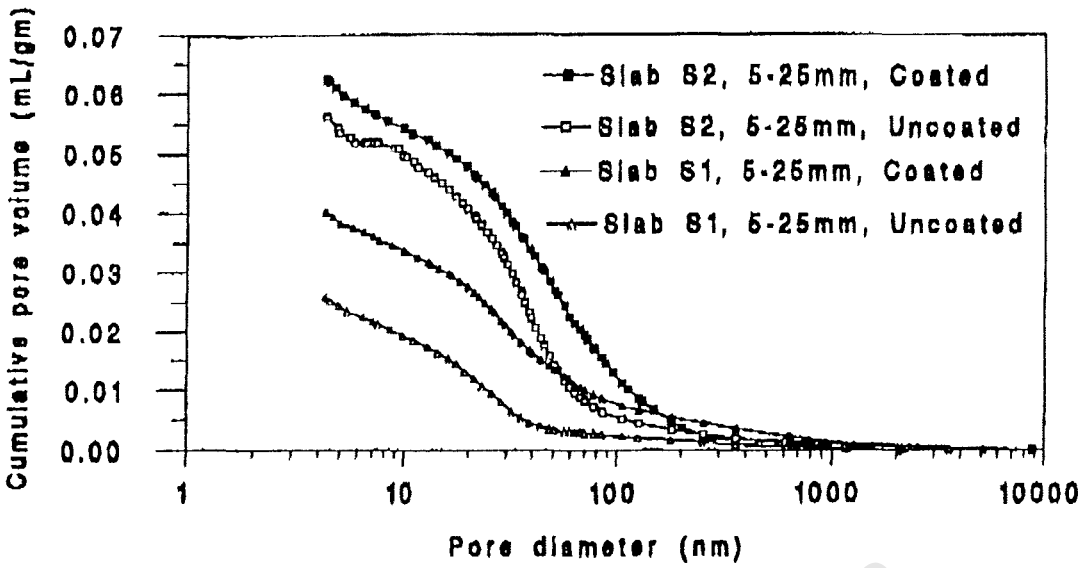

Figure 33: Impact of penetrating chlorides on the pore size distribution of concrete (Suryavanshi and Swamy, 1998).

Total accessible pore volume was also quantified. This showed a marked decrease in porosity with chloride ingress – 3 % decrease in the 0.45 w:b ratio mix. This decrease became less apparent at higher w:b ratios. The numerical results are in Table 4.

Table 4: Porosity effect of chloride ingress (Suryavanshi and Swamy, 1998)

Slab	W:B Ratio	Location (Sample depth range)	Total Accessible Pore Volume	Porosity
			mL/g	%
S1	0.45	5 – 25 mm uncoated	0.0257	5.61
S1	0.45	5 - 25 mm coated	0.0401	8.41
S2	0.6	5 – 25 mm uncoated	0.0562	11.13
S2	0.6	5 – 25 mm coated	0.0624	12.16

Differential pore volume plots were analysed to identify the pore ranges most affected. It was shown that both the coated and the uncoated samples contained nearly identical pore volumes in the 30 nm and below diameter range.

Suryavanshi and Swamy then used differential thermal analysis (DTA) and thermo-gravimetric analysis (TGA) in order to study the effects on hydration products and

precipitates formed after chloride ingress. It was found that NaCl ingress accelerates the hydration process. The hydration products formed preferentially deposit in the coarser pore fraction. It was also found that a significant amount of Friedel's Salt and calcium chloride deposited in the coarser pore fraction, as well as an increase in the amount of calcium chloride formed. These factors would certainly alter the pore structure of the matrix. It was concluded that "chloride intrusion reduces both the accessible pore volume and porosity, and such reductions appear to decrease with increasing W/C ratio." This may be due to less unhydrated cement being present at lower w:c ratios.

Castelotte *et al* (1999) conducted a study to quantify the effect of migration tests on the pore structure of concrete. They compared diffusion samples to migration samples. It was found that, in the case of diffusion, a decrease in total porosity was apparent and attributed to a decrease in capillary pores ($D < 5$ µm). The application of an electrical field resulted in an increase in total porosity, when compared to control samples not exposed to chloride ingress. This increase was most apparent in the smallest capillary pores ($D < 0.05$ µm) and was attributed to dissolution and removal of Portlandite and ettringite (through ion migration). An initial decrease in porosity was noted, due to the formation of Friedel's Salt near the cathode, however, "the total porosity increases after the passage of sufficient electrical charge".

Castelotte et al (1999) did not use control samples in order to identify the natural densification of microstructure with continued hydration. They used the initial pore distributions of the sample (prior to chloride ingress) as reference curves. As some of their diffusion tests lasted as long as 360 days, a significant reduction in total porosity would be expected purely due to continued hydration. Comparing diffusion results to migration results, without quantifying and eliminating continued hydration effects in the analysis, would not be correct.

4.8 Influence of Supplementary Cementitious Materials

Supplementary cementitious materials are incorporated into concrete mixes due to their properties and economic benefits. Their chemical compositions are of great importance as these have the capacity to change the chemistry, microstructure and resulting performance of the concrete. Due to the nature of chemical binding, varying cementitious binder compositions can change the binding potential of a concrete mix.

It is therefore important to understand the composition of various binder systems and their effect on chloride binding.

The South African binders found in Table 5 - Ordinary Portland Cement (OPC); Ground Granulated Corex Slag (GGCS); Ground Granulated Blastfurnace Slag (GGBS); Fly Ash (FA) and Condensed Silica Fume (CSF) - will be considered due to their widespread use and properties.

Table 5: Typical South African cement and cement extender compositions (Mackechnie et al, 2003, Mackechnie and Alexander, 2000 and Addis and Owens, 2001)

Oxides	OPC	GGCS	GGBS	FA	CSF
CaO	67.2	37.2	34.0	4.7	0.6
SiO_2	22.3	30.8	35.5	54.1	92
Al_2O_3	4.4	16.0	15.4	32.9	1.5
MgO	1.01	13.7	9.4	1.3	0.6
TiO_2	0.22	0.51	1.2	1.7	-
Fe_2O_3	3.4	0.87	0.98	3.3	1.2
MnO	0.08	0.09	0.88	-	-
K_2O	0.56	0.35	0.87	0.6	0.6
Na_2O	0.21	0.12	0.16	0.6	-
SO_3	0.58	3.19	2.49	0.4	-

4.8.1 Ground Granulated Blastfurnace Slag (GGBS)

GGBS is a by-product of the blastfurnace process used to produce iron. It comprises mainly silica and alumina from the iron ore and lime added as a fluxing agent. The slag is rapidly cooled, giving a reactive, glassy state. This product is then milled to form GGBS. (Addis and Owens, 2001)

The use of GGBS as a supplementary cementitious extender results in a decrease in porosity of cement pastes and concrete (Soroka, 1993). This is illustrated by Figure 34, and leads to an improved durability, but is highly dependent on the amount of GGBS substituted. It is important to locate the optimum substitution percentage in

order to achieve improved results. High substitution percentages (> 60 %) have been shown to result in higher porosity than midrange values (Soroka, 1993).

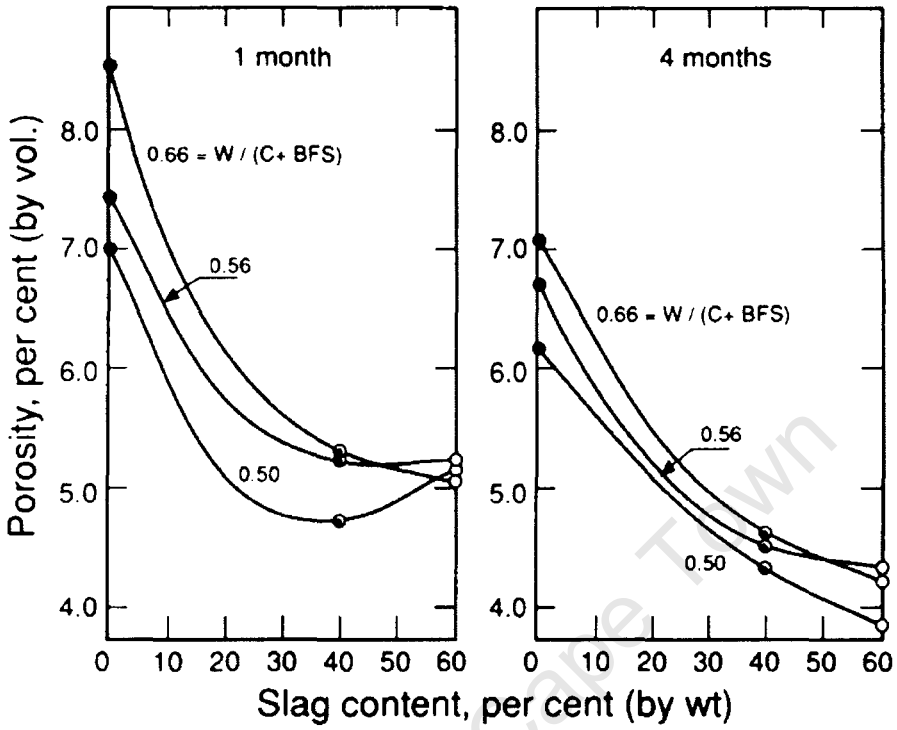

Figure 34: Effect of GGBS content and water-binder ratio on concrete porosity (Soroka, 1993).

GGBS is beneficial in terms of chloride binding due to its chemical composition. The amount of CSH gel would increase slightly when employing GGBS as an extender due to its marginally higher silica content (Table 5). However, the amount of aluminium oxide present is far greater in a GGBS-containing mix. As this is fundamental to chemical chloride binding (the formation of Friedel's Salt), the addition of GGBS increases the chemical binding potential. This has been reflected in a number of studies (Dhir *et al,* 1996; Glass *et al*, 1997; Birnin-Yauri and Glasser, 1998). Dhir *et al* (1996) conducted chloride ingress binding experiments on 6-week-old crushed samples by submerging the samples in NaCl solution until solution equilibrium was reached. The w:b ratios were kept constant at 0.55. Figure 35 shows that the chloride binding capacity increases significantly with GGBS replacement. Dhir *et al* found that for a replacement level of 66.7 % GGBS, the chloride binding capacity was approximately 5 times that of the OPC control when exposed to a 5 M sodium chloride solution. This large increase in chloride binding capacity would

dramatically lower the free chloride concentration in the matrix, resulting in an even lower rate of diffusion and, hence, a longer service lifespan.

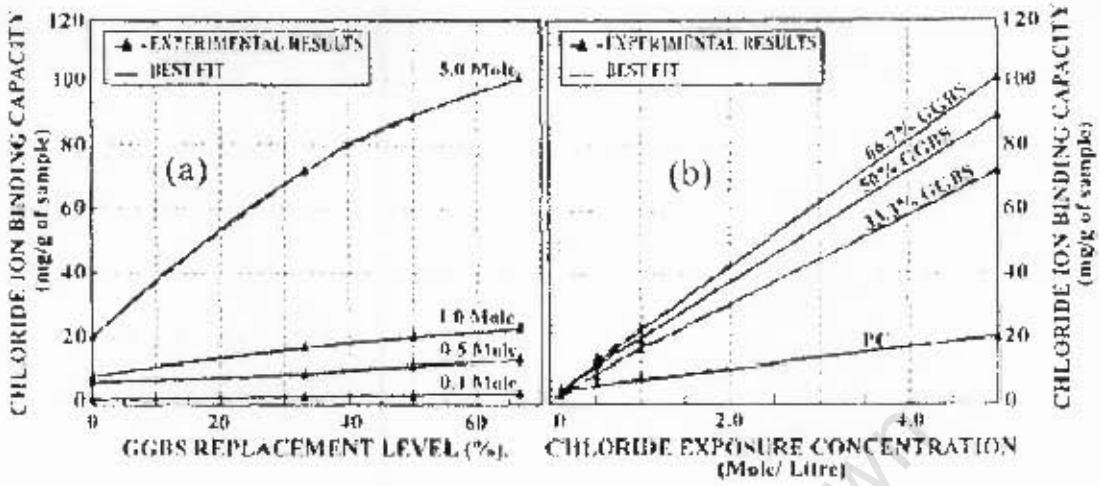

Figure 35: The effect of GGBS replacement on the chloride binding capacity of concretes (Dhir et al, 1996)

Dhir *et al* (1996) proposed the following formula for calculating the chloride ion binding capacity of GGBS-containing concrete:

$$C_b = (-22.21G^2 + 39.45G + 3.36)X + (6.84G^2 - 6.40G + 3.64) \qquad (6.1)$$

Where C_b = chloride ion binding capacity in mg/g of concrete

G = GGBS/total binder ratio

X = Chloride solution concentration in mole/litre

Dhir *et al* (1996) also found that intrinsic permeability remained relatively unchanged with increased GGBS replacement (Figure 36). However, chloride diffusion decreased by an order of magnitude from 0 % to 33% replacement while chloride binding capacity increased three times over the same replacement interval. This led Dhir *et al* to conclude that the observed changes in chloride diffusion were as a result of the high alumina content of GGBS and the consequent formation of Friedel's Salt – chemically binding a significant portion of the chloride ions.

Luo *et al* (2003) found similar results, that of a large increase in the chloride binding capacity of GGBS containing mortars. They also found that the presence of

sulphates decreases the chloride binding capacity. This is due to the competition between sulphate and chloride ions to occupy binding sites available in the microstructure. Luo *et al* conducted Differential Thermal Analysis (DTA), X-Ray Diffraction (XRD) and SEM to analysis the presence and degree of Friedel's Salt formation. GGBS's ability to form Friedel's Salt is shown in Figure 37 where the Friedel's Salt peak is found at approximately 360 °C. Luo *et al* did not label their axes. However, for DTA, these are usually from 0 to 1000 °C for the horizontal and endothermal differential (presumably °C) for the vertical. In the OPC mix, the Friedel's Salt peak is not apparent whereas when GGBS is substituted, it is clear. It was found that GGBS has a superior ability to form Friedel's Salt, increasing its chemical binding capabilities. Luo *et al* (2003) conducted an SEM study to verify this and found an abundance of Friedel's Salt crystal formed with the C-S-H gel. Examples of these crystals can be seen in Figure 38.

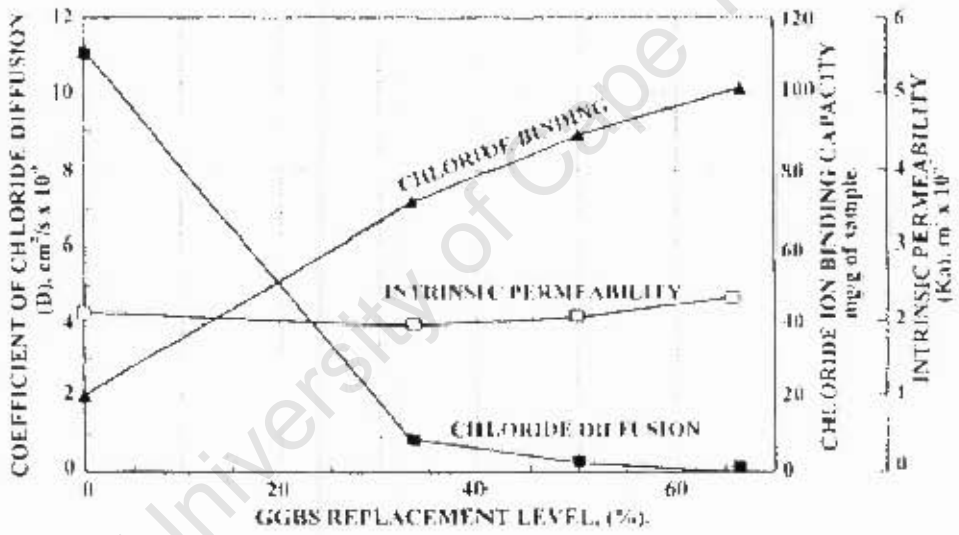

Figure 36: The effect of GGBS replacement on permeability, chloride binding capacity and chloride diffusion (Dhir et al, 1996)

Polder and Peelen (2002) conducted resistivity experiments on concretes at 0.45 w:b exposed to weekly cycles of 24 hours 3 % NaCl ponding followed by 6 days drying at 50 °C. Figure 39 shows that the 50 % GGBS concrete exhibited superior resistivity – followed by the CEM V/A (25 % GGBS and 25% FA). Polder and Peelen (2002) concluded that concretes made with high and intermediate levels of GGBS substitution (25 – 75 %) "show less chloride penetration, lower probabilities of corrosion and higher electrical resistivities than concrete made with CEM 1".

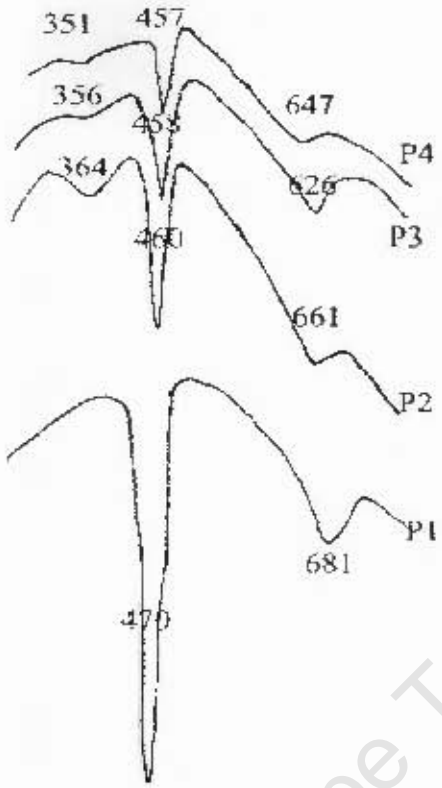

Figure 37: DTA of cement pastes with varying GGBS replacement levels. P1 - OPC; P2 - 70 % GGBS; P3 - 65 % GGBS and 5 % Calcium Sulphate and P4 - 65 % GGBS and 5 % Sodium Sulphate (Luo et al, 2003)

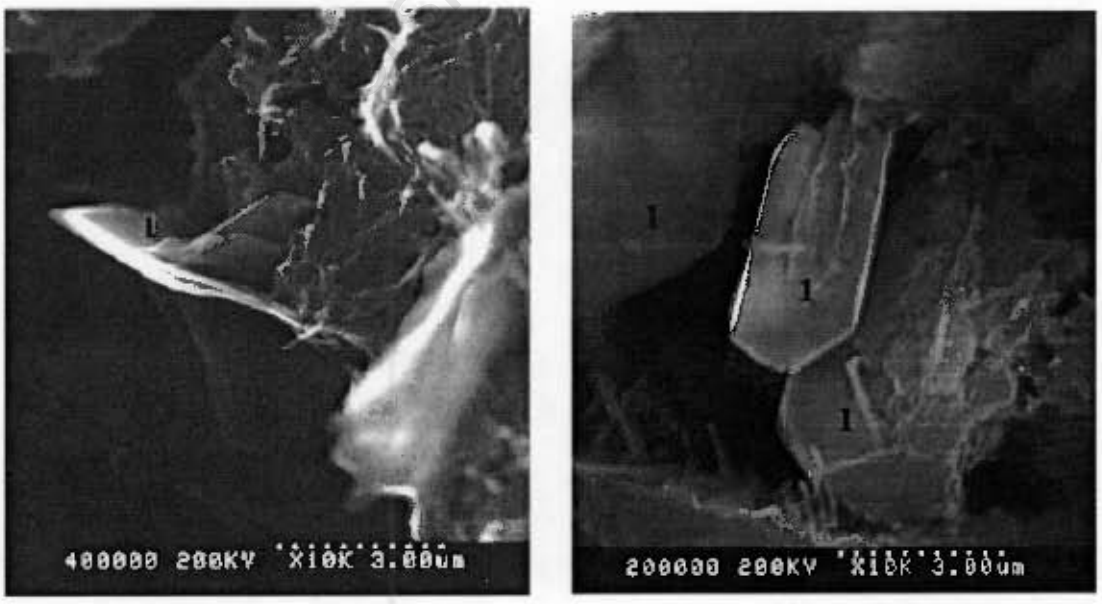

Figure 38: SEM micrographs of Friedel's Salt found in GGBS paste (Luo et al, 2003)

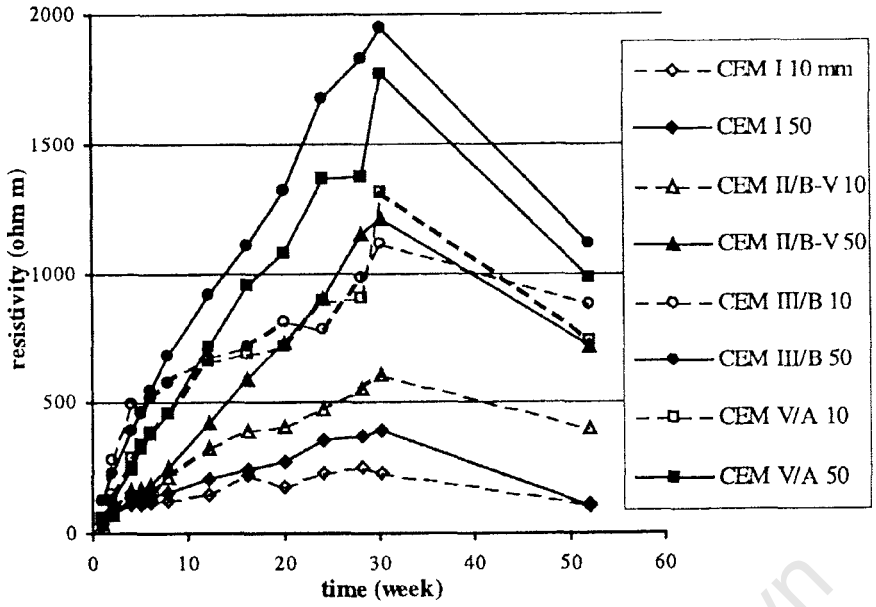

Figure 39: The effect of GGBS (CEM III/B) and FA (CEM II/B-V) substitution on concrete resistivity (Polder and Peelen, 2002)

Mangat and Molloy (1995) conducted a study on samples exposed to 6 hour wetting and drying cycles of seawater with varied exposure time. This was in tandem with samples stored in the tidal zone of the North Sea, and samples stored in a seawater tank for 270 days. The researchers report conflicting results. It was found that GGBS replacement does not affect chloride binding close to the surface of the concrete. However, at greater penetration depths, it was found that GGBS replacement results in a ***reduction*** of bound chlorides. This was noted in both their abstract and conclusions, but is in contrast to most other binding data and studies. However, within the paper, it is noted: "the 60 % gbs mix has far superior chloride binding capacity." It may be possible that the authors did not measure the reduction of bound chlorides as a percentage of total chlorides or as related to free chlorides. The total chloride content may have decreased due to the physical and chemical alteration of the microstructure through the use of GGBS.

Dehghanian and Arjemandi (1997) found that GGBS replacement did not influence the chloride diffusion rate. They also found that for w:b ratios above 0.55, chloride diffusivity increases were exacerbated by higher GGBS contents. This is in conflict with research previously presented, as chloride binding would impact on chloride diffusion rates by lowering the concentration of the chloride penetration front. It is possible that this trend changes at higher water-binder ratios due to the exponential

increase in porosity experienced at these levels. Dehghanian and Arjemandi did not give possible reasons for their results.

GGBS has consistently been reported to possess superior chloride binding capabilities. The use of GGBS is, therefore, encouraged, in order to combat the transport of harmful chloride ions through the cementitious matrix.

4.8.2 Ground Granulated Corex Slag (GGCS)

Ground granulated Corex Slag is a relatively new addition to the suite of available cementitious binders. It is a by-product of the Corex™ process used by Voest-Alpine at the Saldanha Steel plant in the Western Cape, South Africa.

GGCS generally has a similar chemistry and characteristics as Ground Granulated Blastfurnace Slag (GGBS). However, GGCS is faster reacting. It is general practice to attribute GGCS with the characteristics of GGBS – although, perhaps, not rightly so.

GGCS is generally used at a 50 % replacement level (Mackechnie *et al,* 2003). This is the optimum level for structural and durability advantages. The use of GGCS in salt environments is highly recommended. The joint effects of a denser microstructure and vastly improved chloride binding capacity allows a lower grade of concrete and a lower cover depth to be used. Alternatively, with relatively standard concrete grades and covers, the service life of the concrete and the structure improves dramatically. It can be seen from iso-conductivity curves, Figure 40, that GGCS and GGBS behave very similarly in terms of chloride transport.

4.8.3 Condensed Silica Fume (CSF)

Condensed Silica Fume is a by-product of the ferrosilicon smelting process. The reduction of quartz at 2000 ˚C in the process produces SiO gas. Some of this gas escapes and oxidises in air to form SiO_2, the other portion is condensed into very small, spherical silica particles (Addis and Owens, 2001; Soroka, 1993).

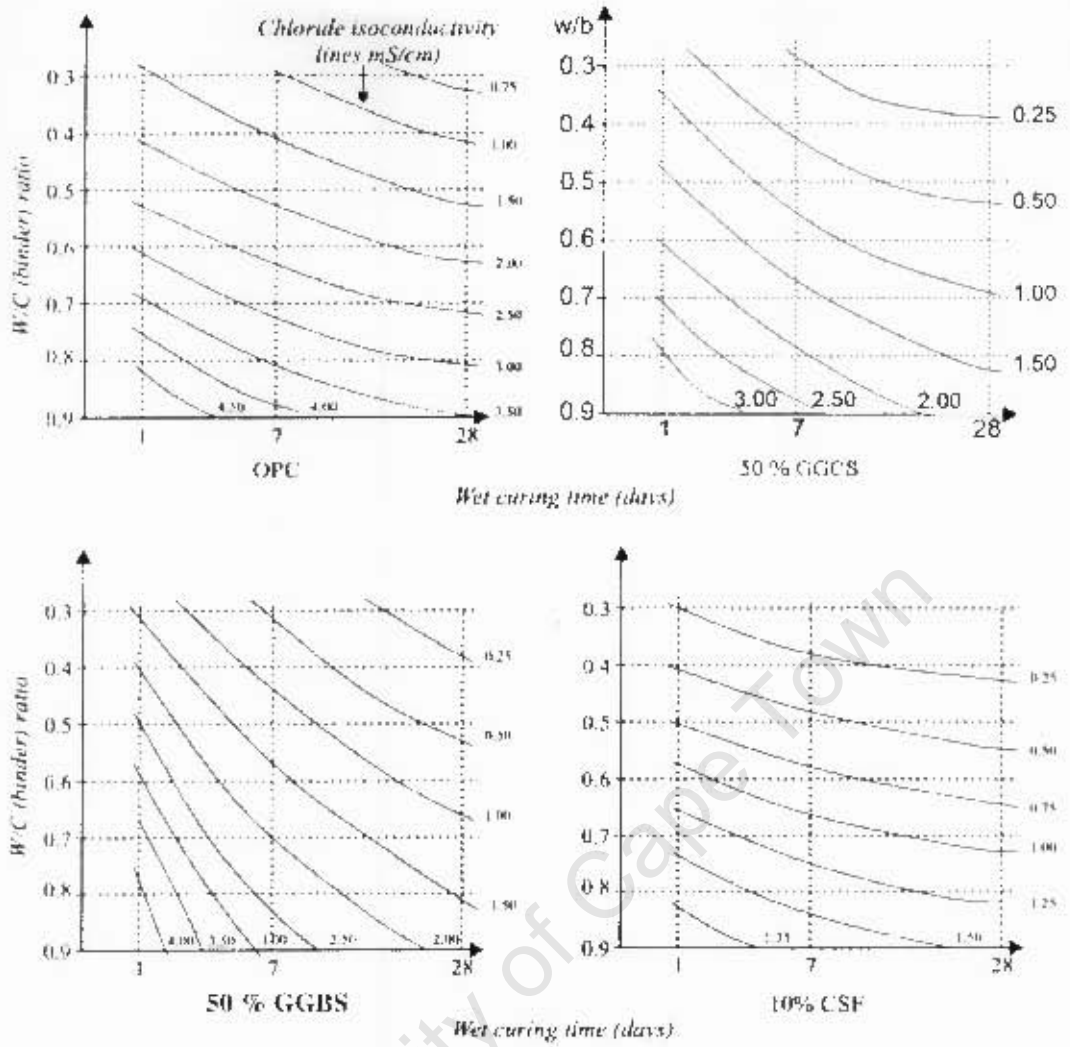

Figure 40: Chloride Iso-conductivity curves for various cement extenders [Adapted from Mackechnie *et al* (2003) and Alexander *et al* (1999)]

Its use as a cement extender greatly improves microstructure and pore structure. A significant benefit of using CSF is its high silica content. The by-products of the initial CSH reaction react with the additional silica provided by the CSF, hence forming more CSH gel. This has a beneficial impact on the transport properties of the concrete.

In the study by Mangat and Molloy (1995), previously discussed, it was concluded that concretes containing silica fume "show negligible chloride binding capacity." This is shown in Figure 41, where the chloride binding capacity of concrete containing 15 % CSF is clearly lower than 60 % GGBS, 25 % PFA and OPC concretes.

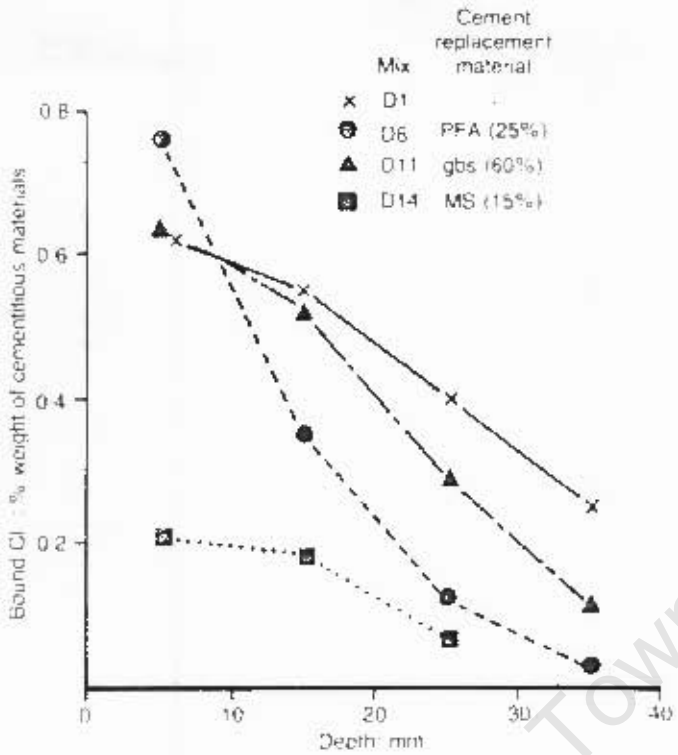

Figure 41: Chloride binding capacity of CSF concrete (MS in the diagram)

(Manget and Molloy, 1995)

Arya and Xu (1995) conducted a study on concretes at 0.55 w:b. Their results indicated that a CSF containing mix exposed to the same NaCl solution as other mixes exhibited a higher pore solution chlorice concentration than the other concretes. This indicated that the chloride binding capacity of the CSF containing mix is inferior to the other mixes. These results are shown in Figure 42.

Arya and Xu (1995) also measured the pore solution OH^- concentration of the various concretes. These results are shown in Figure 43. The 10 % CSF concrete exhibited a significantly lower concentration of OH^- ions in its pore solution. This is in line with work by Tritthart (1989). The lower OH^- concentration results from the uptake of OH^- ions during the hydration of CSF. This lowers the pH (creating more favourable chlorice binding conditions). The loss of OH^- ions in the pore solution will result in chloride ions being favoured for available binding sites in order to maintain local equilibrium (Tritthart, 1989). However, research shows that CSF containing mixes have inferior chloride binding capacity. This indicates that chemical binding (aluminate content) is more effective in immobilizing chloride ions than adsorption.

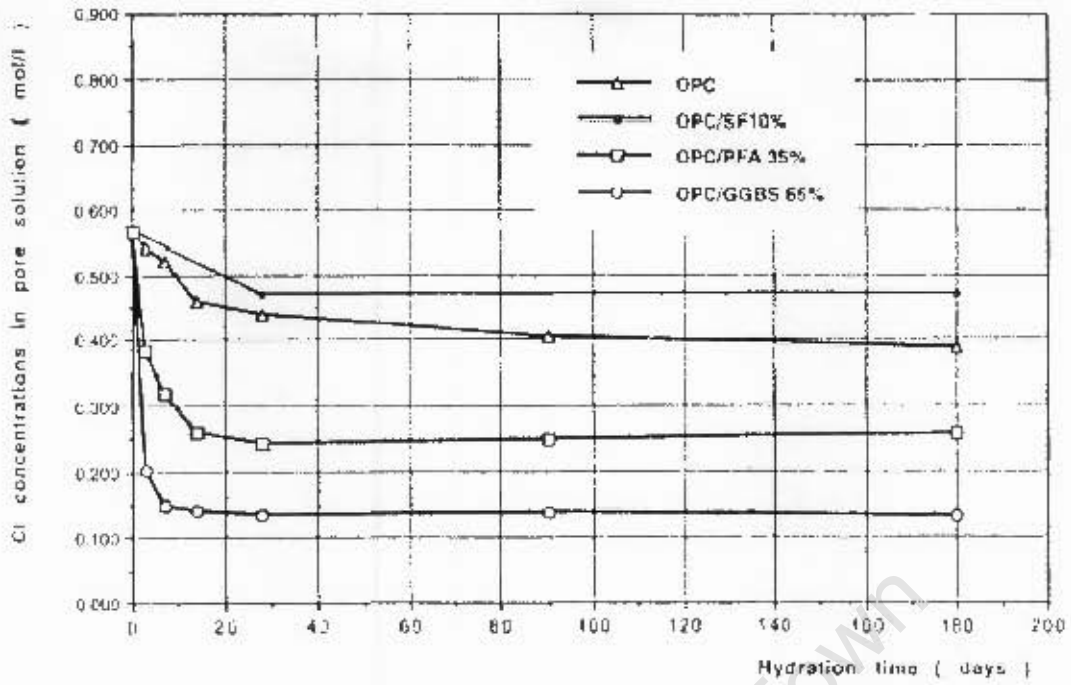

Figure 42: Pore solution chloride concentration of different extender mixes exposed to a 3 % chloride solution (Arya and Xu, 1995)

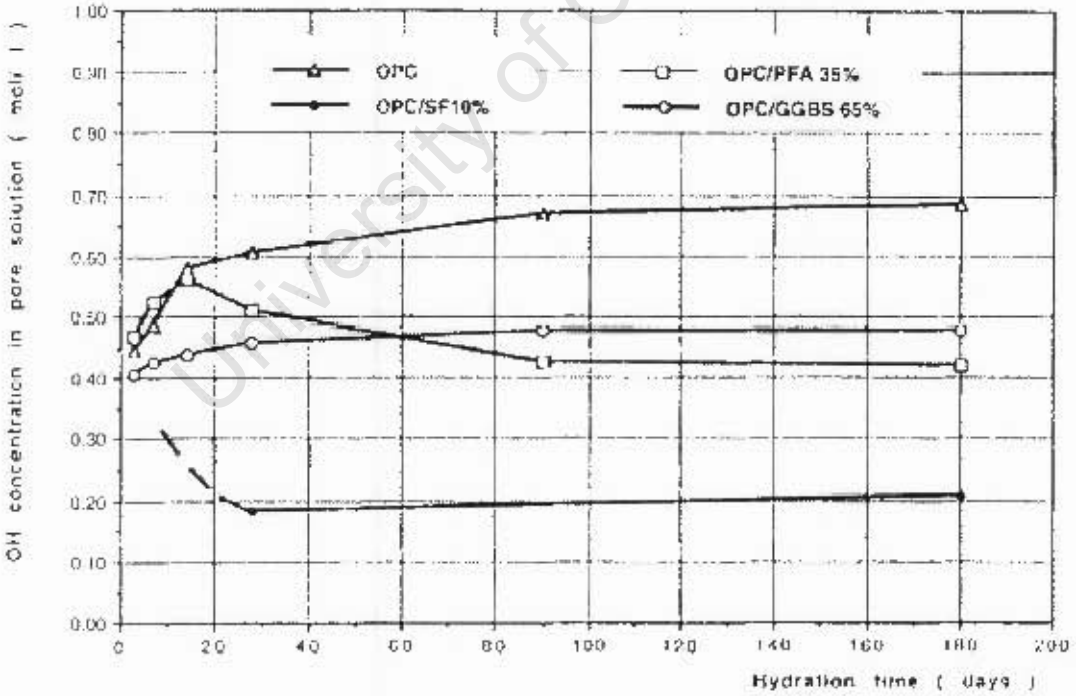

Figure 43: Pore solution OH concentration of various extender mixes exposed to a 3 % chloride solution (Arya and Xu, 1995)

Arya *et al* (1990); Delagrave *et al* (1997); and Page and Vennesland (1982) have also shown that CSF replacement results in a reduction of chloride binding capacity (Referred to by Justnes, 1998). Thus, the positive impact of CSF replacement on OH^- ion removal does not outweigh the negative impact of reduction in alumina content and gel densification on chloride binding capacity.

An advantage of using CSF lies in its effect on the pore structure of concrete. Permeability and sorptivity tests show that the pore structure of the cement matrix becomes finer with CSF replacement (Alexander *et al*, 1999). This can be seen in Figure 44. The resulting dense matrix can combat chloride transport only through lowering the effective diffusion area and increasing constrictivity and tortuosity. This is the reason that many researchers have incorrectly found silica fume to be a desirable extender in chloride environments (Detwiler *et al*, 1994; Khedr and Abou-Zeid, 1994; Neville, 1995). During a concrete's service life, loading, creep, shrinkage and corrosion induced microcracking can be expected. In these instances, a CSF concrete's physical ability to combat chloride transport would be compromised. It is therefore preferable to have a degree of chemical chloride binding capacity.

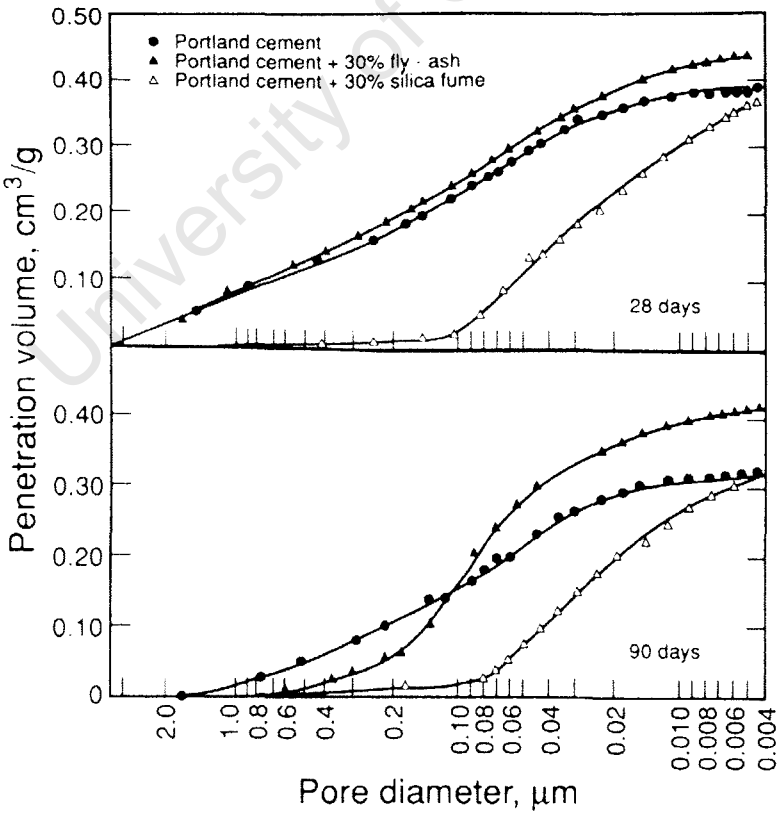

Figure 44: The effect of CSF and Fly Ash substitution on the pore size distribution of cement paste (Soroka, 1993)

It is hypothesised that the reduction in chloride binding capacity is a result of two mechanisms:

- Substitution of CSF (from 5 to 15 % typically) will lower the amount of alumina in the mix available for hydration, and, subsequently for chloride binding.
- The densification of the CSH gel lowers the effective pore surface area in the microstructure. This would significantly lower the physical binding potential as well as lowering the chemical binding potential by making AF_m phases less accessible.

4.8.4 Fly Ash

Fly ash is formed during coal combustion. Coal impurities such as quartz and clay are fused together during the process and form glassy, spherical particles. The flue gas stream carries these away where they are collected using electrostatic precipitators. This compound is generally known as fly ash (US and SA) or pulverised fly ash (UK) (Soroka, 1993).

Fly ash comprises mostly silica and alumina (Table 5, p. 69). This chemical composition makes it useful as a supplementary cementitious extender. Fly ash lacks necessary CaO content to act as a hydraulic binder. Hence, the hydration of fly ash relies on the calcium hydroxide by-product of the cement hydration process. Fly ash is, therefore, categorised as a latent hydraulic binder. The high silica content of fly ash reacts with the CH by-product to form further CSH gel. This densifies the matrix to some extent. The spherical nature of fly ash particles aids in particle packing efficiency. This further improves the density of the matrix. The relatively high alumina content of fly ash is beneficial to chemical chloride binding.

Figure 44, presented previously, clearly shows the latent hydraulic property of FA and the densifying effect FA has on pore structure. The benefits of FA replacement only become apparent after 28 days. This is due to the latent hydraulic property of FA. This is of concern as most quality assurance tests are conducted at the standard 28-day age. Hence, FA is inherently disadvantaged. It is therefore imperative that practitioners understand FA technology in both design and testing of FA concretes. It can also be seen in Figure 44 that the microporosity of the cement paste benefits significantly from FA replacement. Between 28 and 90 days, significant densification

of the pore structure occurs as the silica rich FA reacts with the CH cement hydration by-product to form further CSH within the already established cement gel pore structure.

Ngala *et al* (1995) conducted a study on the effects of FA replacement on porosity, chloride diffusivity (D_{cl}) and oxygen diffusion (D_o). Cement pastes were mixed at 0.4; 0.5; 0.6 and 0.7 w:b ratios. The samples were wet cured at 38 ˚C for ten weeks to ensure sufficient hydration of the FA. The results can be found in Table 6.

Table 6: The effect of fly ash replacement of diffusion and porosity at 0.5 w:b (Adapted from Ngala et al, 1995)

	Oxygen Diffusion	Chloride Diffusion	
Mix	D_o ($x10^{-12}m^2/s$)	D_{cl} ($x10^{-12}m^2/s$)	Capillary Porosity (%)
OPC	10.40	7.80	8.36
30 % FA	6.67	0.43	5.31

It is interesting to note that the chloride diffusivity decreases significantly more than the oxygen diffusivity with FA replacement. The reduction in oxygen permeability is expected due to the densified pore structure of the FA/OPC matrix shown by the significant decrease in capillary porosity. The higher decline in chloride diffusivity is a result of both the less permeable matrix, as well as the increased chloride binding capacity of the matrix. This is due to the high alumina content of the FA.

Thomas and Matthews (2004) conducted experiments on concrete prisms subjected to marine environments for a duration of 10 years. The samples were profiled to determine the effect of FA on the ingress of chlorides into concrete. The samples had a w:b of approximately 0.55. As can be seen in Figure 45, FA significantly reduces the observed chloride profiles. This indicates that the movement of the chloride front through the concrete is significantly retarded.

Thomas and Matthews (2004) also investigated the effect that FA replacement has on the depth of the threshold chloride concentration (0.4 % by mass of cement). Figure 46 shows that with a small amount of FA replacement, a significant reduction in chloride penetration, and hence build up to critical chloride threshold, can be achieved. Figure 46 also indicates the marginal improvements that are experienced

with FA replacement from 30 % to 50 % by mass of cement. The optimum FA replacement level is generally regarded as 30 % due to limiting amounts of CH available for hydration.

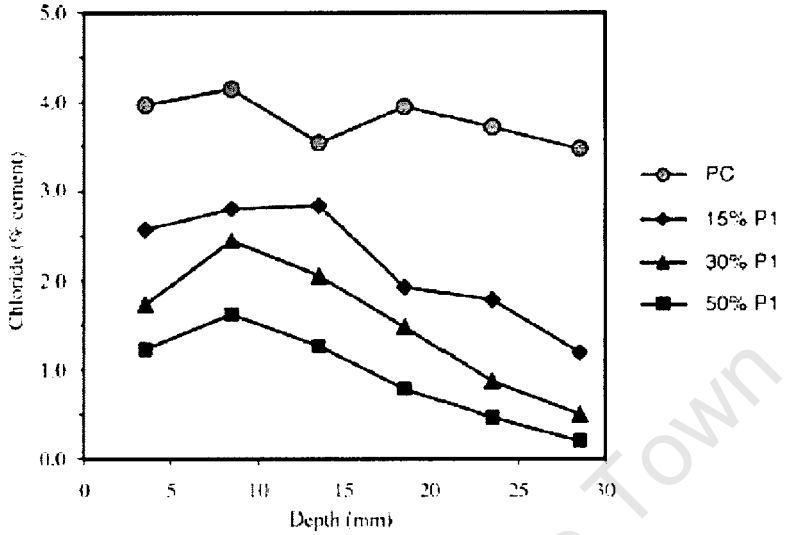

Figure 45: The effect of FA on chloride profiles, as observed in concretes exposed to marine conditions for 10 years (Thomas and Matthews, 2004)

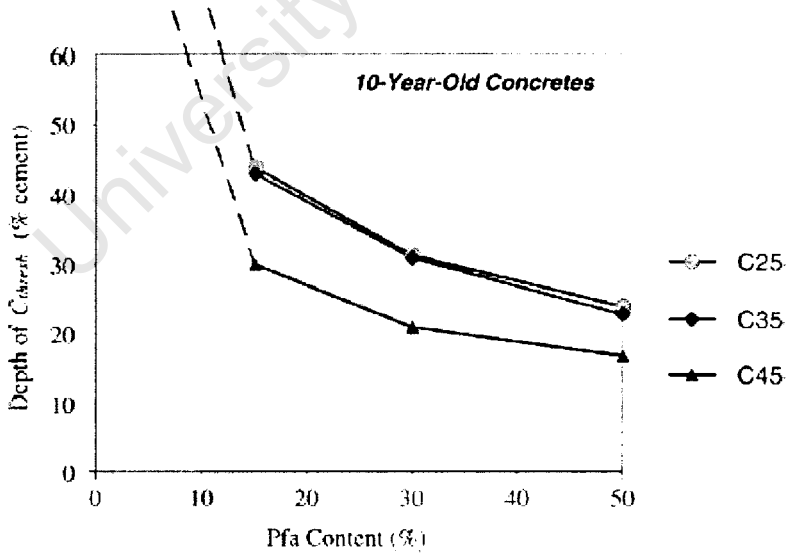

Figure 46: The effect of FA replacement on the depth of critical chloride threshold and time (Thomas and Matthews, 2004)

4.8.5 Supplementary Cementitious Materials and Transport Properties

Changes in pore structure and chemical composition brought about by the use of supplementary cementitious extenders affect the resulting transport properties of the matrix. A denser, less permeable matrix would retard the transport of ions, as would a mix containing more chloride binding compounds.

The superior binding capacities of Fly Ash and GGBS retard the movement of ions through the matrix (Figure 47). Hence, the migration coefficients are significantly lower that those of OPC mixes for various w:b ratios. Figure 48 shows the effect of CSF replacement on the migration coefficients. A large change is experienced from 0 to 6 % substitution, indicative of the influence CSF replacement has on the pore structure of the matrix. This change is from the densification of the cement gel. The retardation of ion movement is physical as opposed to chemical. This is undesirable, however, as should microcracking occur in a CSF concrete, there would be no opposition to ion flow.

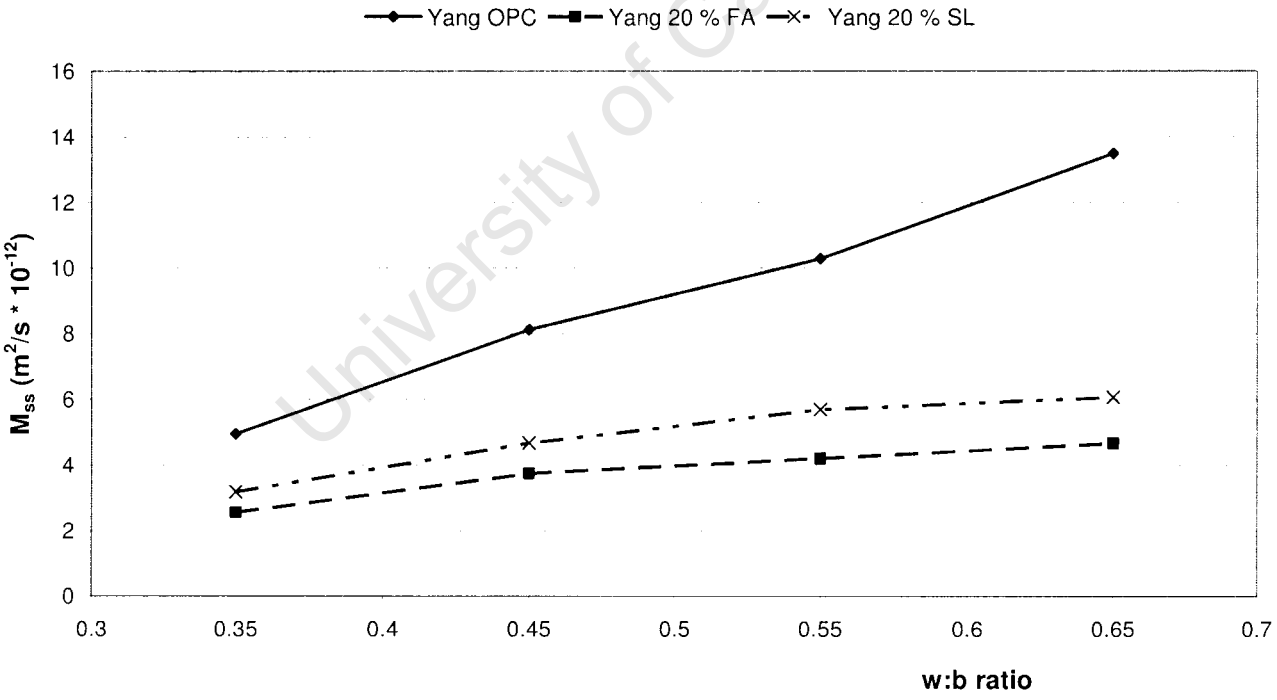

Figure 47: The effects of FA and GGBS substitution on the steady state migration coefficient (M_{ss}) of concrete (compiled using data obtained from Yang and Cho, 2003)

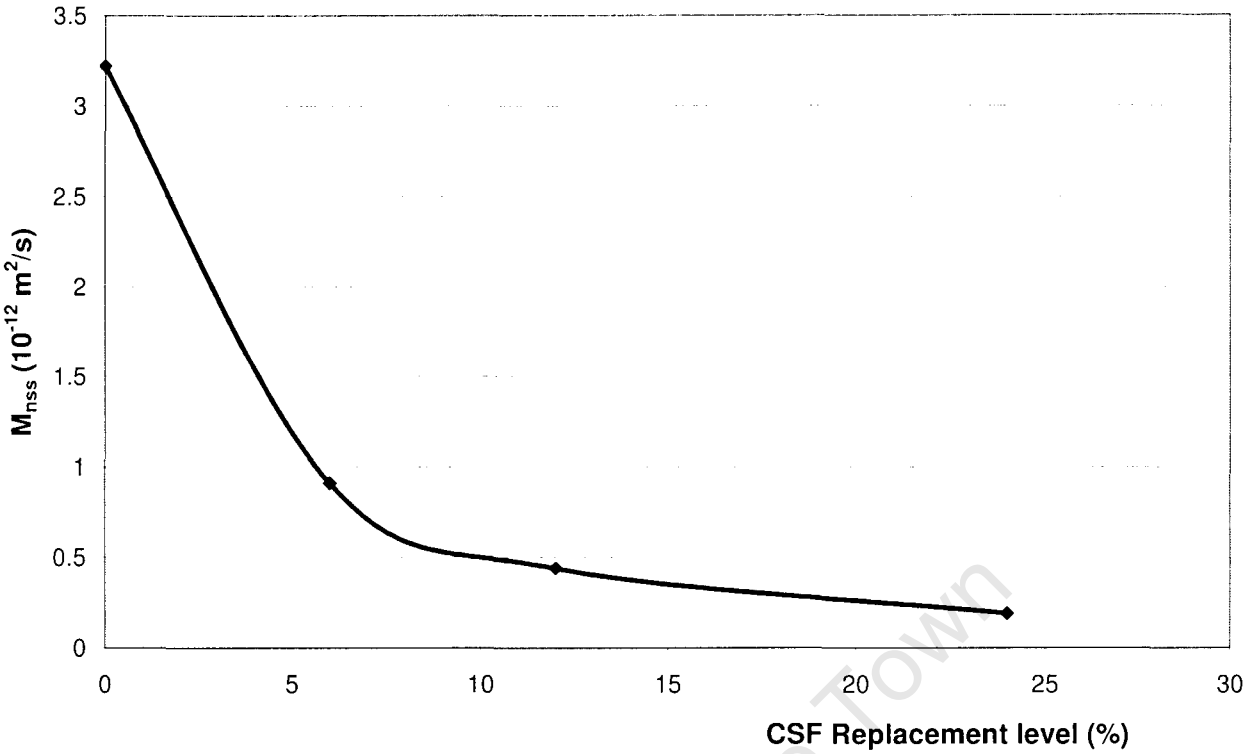

Figure 48: The effect of CSF replacement on the non-steady state migration coefficient (M_{ss}) (compiled using data from Tang, 1996)

4.9 Conclusions

Chemical and physical binding removes a significant amount of chloride ions from the pore solution. This has a positive impact on the durability of the structure by decreasing diffusion rates through decreasing the chloride front concentration. Chloride binding is dependent on the constituents of the mix (aluminates) – for chemical binding - and the paste volume fraction – for adsorption. Chemical binding results in the formation of Friedel's Salt. Binding is dependent on local electrostatic equilibria between the gel of the pore walls and the pore solution. Ion substitution occurs during both chemical and physical binding. Generally, chloride ions substitute for hydroxide ions in order to maintain electrostatic equilibria. Competition, however, exists between chloride ions and sulphate ions for binding sites. It could be expected that other ions in the pore solution may also compete for binding sites. Only studies comparing chloride and sulphate binding potentials could be found in the literature.

The chloride binding capacity of a binder system is generally expressed as an isotherm. The Freundlich isotherm best represents chloride binding behaviour above 0.01 M and the Langmuir isotherm below 0.01 M. A transition zone exists between 0.01 and 0.05 M as monolayer adsorption occurs below 0.01 M becoming complex, multi-layer adsorption above 0.05 M. This must be accounted for when analysing chloride binding results of specimens exposed to a solution of low chloride concentration.

Chloride binding is temperature dependent. Hence, any chloride binding tests should be conducted at constant temperature and compared to tests conducted at a similar temperature. Electrical fields have been shown to affect chloride binding capacity – suppressing chloride binding at concentrations below 97 g/l (2.7 M) and enhancing chloride binding at concentrations above 2.7 M. It is uncertain whether the 2.7 M boundary indicates a fundamental shift in the impact of the electrical field on ion activity and binding behaviour, or whether this is an arbitrary value dependent on specimen characteristics and experimental setup.

Chloride binding can be measured using pore expression or equilibrium techniques. The pore expression technique is widely used but has received significant criticism. The equilibrium technique takes the same amount of time to perform and is concluded to be the preferred method for the purposes of this study.

In order to correctly rate concretes for use in chloride environments, chloride binding must be considered and factored into quality control tests. Even though chloride binding is a complex process, micro scale and macro scale measurements are possible and can be used to categorize concretes. However, care must be taken in correctly distinguishing between total, free and bound chlorides. Disruption of the microstructure may significantly affect results.

The lack of available research on the topic suggests that further work into the impacts of chloride ingress on pore structure and permeability is needed. Based on the limited literature found, the penetration of chlorides into concrete results in chemical alterations that impact on the pore distribution and total porosity of the matrix. A decrease in porosity and refinement of the coarse capillary pore fraction generally results – with pores below 0.05 μm diameter being most affected. The use of electrical fields (migration testing) promotes the dissolution and removal of precipitates, effectively increasing the total porosity and capillary pore fraction. Even

though chloride ingress results in the formation of Friedel's Salt, it appears that the impact of this phenomenon on the pore structure is inferior to the leaching of precipitates.

The use of supplementary cementitious binders changes the binding capacity of concrete. This can be either detrimental or beneficial to the durability, depending on the extender and the substitution percentage used. It is important that current rapid chloride tests sufficiently represent these characteristics in comparatively rating concrete durability.

GGCS enhances chloride binding capacity chemically through the addition of further alumina to the mix. This slows the diffusion process by lowering the amount of free chloride ions available to facilitate reinforcement corrosion. GGCS has similar properties to GGBS. Fifty-percent GGBS replacement results in an increase in chloride binding capacity of approximately five times that of CEM 1, decreasing the diffusion coefficient of the concrete by an order of magnitude. The diffusion coefficients of a 0.55 w:b GGBS mix lie in the $0 - 1 \times 10^{-12}$ range.

CSF densifies the cementitious matrix immensely due to its high silica content (> 90 %), fineness and particle shape. Its very low alumina content (approximately 2 %) results in a loss of chloride binding capacity with CSF replacement. This is detrimental to concrete durability against chlorides as CSF mixes may have less than 50 % chloride binding capacity than a CEM 1 mix at the same w:b. The significantly denser microstructure slows the diffusion process physically. A non-steady state diffusion coefficient of 5.4×10^{-11} has been reported for a 10 % CSF concrete at 0.52 w:b. This was lower than the CEM 1 control, which had a non-steady state diffusion coefficient of 7.3×10^{-11}. However, any form of microcracking would be detrimental to a microstructure with low chemical binding capability.

FA, like GGCS and GGBS, improves the chloride binding capacity chemically and also has diffusion coefficients that are generally an order of magnitude lower than CEM 1 controls. FA also refines the pore structure of the matrix, providing a physical impediment to chloride transport. As FA is a latent hydraulic binder, standard 28-day tests do not give a true reflection of FA concrete's properties. This factor must be considered when employing FA and analysing standard test results.

Rapid chloride tests should draw a distinction between free and bound chloride ions or give an indication of chloride binding capacity. This is an important consideration, especially in evaluating cement extenders. By employing a suitable cement extender such as GGCS or FA, significant retardation of the diffusion process would occur through chloride binding.

PART 2 – CRITICAL REVIEW OF PRESENT RAPID CHLORIDE TEST METHODS

5. PRESENT CHLORIDE TEST METHODS

As established, chloride ingress into reinforced concrete is detrimental to the durability and lifespan of a structure. In order to combat this ingress, a suitable concrete mix design must be used. In order to gauge the chloride transport properties of concrete, a number of tests have been developed for use in the laboratory or as quality control measures in practice. Of the various tests, four were chosen for evaluation, based on their use as standard tests and the differing theories and methods represented. These were:

The Bulk Diffusion Test (BDT)
The Rapid Migration Test (RMT)
The Rapid Chloride Permeability Test (RCPT)
The Chloride Conductivity Test (CCT)

A literature review of the test methods was conducted, followed by an experimental review where the tests were critically assessed in the laboratory.

5.1 Bulk Diffusion Test (NordTest NTBuild 443)

Cylindrical specimens (minimum 100 mm depth and 75 mm diameter) are saturated with limewater and then sealed on all sides except the top face, and submerged in a 2.8 M NaCl solution (Figure 49), for a minimum of 35 days. After this time chloride profiling is done, by grinding off 0.5 mm portions of the sample, to evaluate the performance of the specimen. The total chloride content is thus obtained. The error function of Fick's Second Law is then fitted to the curve and the diffusion value and surface concentration obtained. The detailed test method, apparatus and results analysis guidance can be found in: NTBUILD 202, 2nd Edition. Approved 1984-05. Concrete, Hardened: Chloride Content

Samples are water cured in saturated limewater, and are not required to be dried. Thus, the test does not require any sample preparation that may damage the sample's pore structure. Profiling of samples does require suitable grinding equipment with suitable tolerances to grind 0.5 mm layers. Saw cuts can be used on

low-grade samples due to increased penetration depth. This is not recommended, however, as sawing requires the use of water which may remove a significant amount of chlorides during the cutting process.

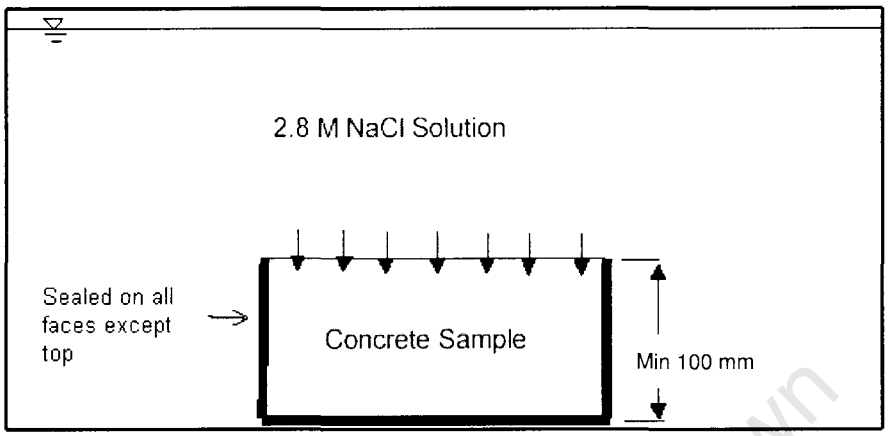

Figure 49: NordTest Setup (Hooton *et al*, 2001)

The large sample sizes prescribed (75 mm diameter cylinders with a depth greater than 100 mm) allows a variety of aggregate sizes and a large, representative concrete sample to be tested.

Chloride binding will impact on the depth of penetration and concentration gradient. This will, therefore, be reflected in the resulting penetration profile.

A primary criticism of this test is the length and variability of test duration. Depending on the quality of the concrete the test may be extended up to 90 days. This is not only unsuitable for quality control but significant microstructural change will occur during that time. This will include an increase in C_2S hydration and an increase in AF_m phase. Both these phenomena will influence the binding potential of the concrete. An associated decrease in porosity will also occur.

Whether the determination of total chloride concentration using digestion by acid solution is representative of the total amount of chlorides present is uncertain. The amount of chlorides extracted increases with nitric acid concentration as well as temperature. It has been shown that even aggressive conditions such as boiling nitric acid may lead to less than 90% of the actual chloride content being extracted (Glass *et al*, 1996). Others have attempted to address the chloride binding phenomena by isolating the free chloride ions. It is still common practice to assess bound versus free

chlorides by performing pore expression and analysing the expressed fluid as being representative of the pore solution. Again, this is uncertain, as discussed in Chapter 4.

Experimental Review

The following points were obtained after laboratory testing of mortar samples. The results were used in analysing the results of diffusion and migration tests carried out as part of the experimental work of the study. These will be presented in the Results section.

- The bulk diffusion test (BDT) is time consuming. It may, therefore, be used for research purposes but cannot be used as a quality assurance test. Results can only be obtained after approximately 120 days (4 months) from casting. This would not suit construction practice.

- Sample preparation is relatively simple as cylinders can be cast at the required diameter. A simple saw cut exposes the test face.

- The sides and base of the specimens are coated with at least 1 mm of thixotropic epoxy resin adhesive (Sikadur 31 was used). In some instances, the samples had to be re-epoxied in some places due to air bubbles forming – leaving channels through the epoxy. This may go unnoticed by operators in practice.

- The standard procedure of the test requires that, after epoxy coating, samples be submerged in saturated limewater until constant mass is reached. The mass of High Performance Concretes (HPC) and concretes with superior durability properties will take longer to stabilize than poorer concretes. This is not only time consuming but affects the degree of hydration. This would result in poorer concretes being tested at lower degrees of hydration than their superior counterparts. This will result in poor concretes looking poorer. Vacuum saturation is an alternative that may overcome these problems.

- Ideally a grinding machine should be used to profile the sample. This is costly, but worthwhile if a large number of BDT's are to be conducted. A

problem noted during the grinding of specimens was the difficulty in levelling the exposure face. Diamond tipped saws are not high precision instruments. This results in an angle between the exposure face and the longitudinal axis of the specimen being slightly different from ninety degrees. Profiling cannot, therefore, be conducted truly parallel to the exposure face unless the grinding machine is fitted with a levelling device. It is advised that the cylinders be ground true on another grinding machine before sample preparation begins - as with the strength testing of cylinders.

- Many researchers have utilised saw cuts in the analysis. Sawing, however, requires water, which would dissolve some of the chlorides present. Also, only large penetration depths can be analysed in this fashion. In HPC, the exposure depth will not be enough to allow sufficient samples to be obtained without long exposure periods.

- A further requirement of the test is titration apparatus. Many engineers may not have access to such equipment.

- The test allows sufficient time for supplementary cementitious materials to develop without accelerated curing methods. Fly ash, as discussed, exhibits a substantial portion of its superior durability enhancing properties after the 28-day period. The BDT is the only test that would show such changes.

5.2 Rapid Chloride Permeability Test

The RCPT involves placing a water saturated 50 mm thick, 100 mm diameter sample in a migration cell and applying a 60 V DC current for 6 hours (Figure 50). One cell of the migration device is filled with 3.0 % NaCl solution and the other with 0.3 M NaOH solution. The total charge passed is then determined and used to give a concrete rating.

The detailed test method, apparatus and results analysis guidance can be found in: ASTM C 1202 – 97. **Standard Test Method for Electrical Indication of Concrete's Ability to Resist Chloride Ion Penetration.** ASTM, USA.

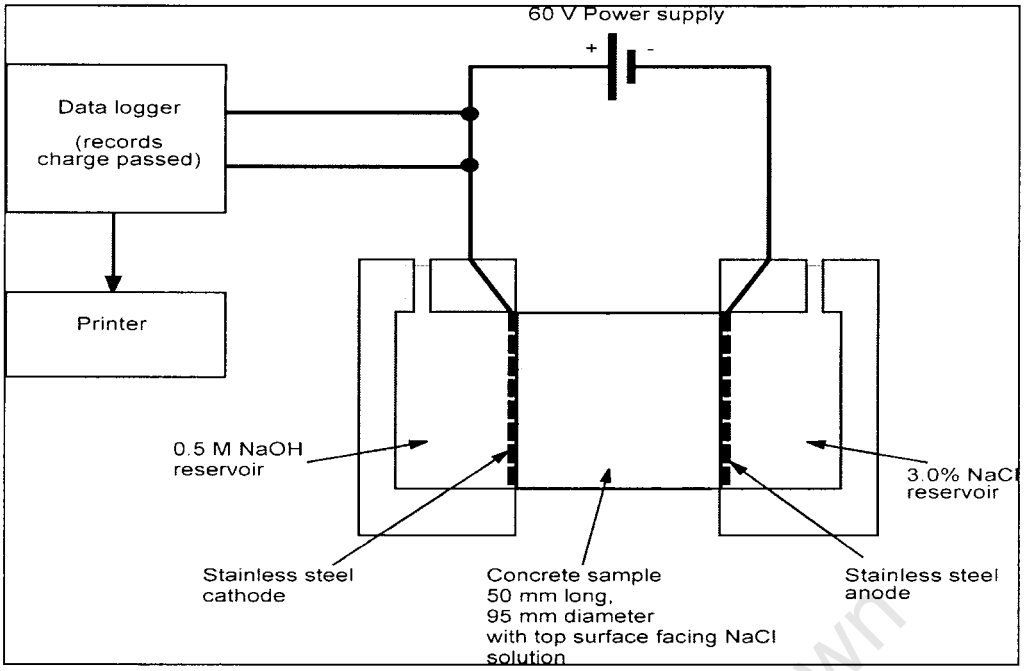

Figure 50: RCPT setup (Hooton *et al*, 2001)

ASTM C1202 – 97 clearly states in the opening clause that:

> "This test method is applicable to types of concrete where correlations have been established between this test procedure and long term chloride ponding procedures such as those described in AASHTO T 259."

This indirectly implies that the salt ponding test be conducted on all concrete types for correlation purposes. Considering that the Bulk Diffusion Test is an improvement of the salt ponding test, the code indirectly states that the BDT is preferable in obtaining a true fundamental representation of chloride ion transport behaviour to the RCPT.

As an electric current is employed, the test is affected by other ionic species present, pore solution alkalinity and the presence of steel reinforcement (as in the Rapid Migration Test).

The high voltage applied to the concrete for the required length of time can lead to a temperature increase within the concrete. This has two major implications. Firstly, the resistance of the concrete is affected. As the test relies on current passed at a constant voltage as a result, a decrease in resistance would affect results and make poor concretes look even worse. Secondly, as chloride binding is dependent on

temperature, the test results will not be representative of true chloride migration through a cementitious system. The chloride binding potential will be affected by the electric current (as in the Rapid Migration Test) and will also be impacted by the temperature rise. Feldman *et al* (1994) noted that the use of chloride ions in the RCPT is arbitrary as the same results were obtained using sodium hydroxide solutions for both the cathodic and anodic cells. This implies that the RCPT does not necessarily represent chloride binding in cementitious materials and, therefore, may not give a true representation of the actual behaviour of concretes in a chloride environment.

Warnings have been issued regarding the application of the RCPT to silica fume-containing concretes (Lane, 2000). It was reported that conventional CEM I concretes may have coulomb values of up to 15 times higher than silica fume- or slag-containing concretes. This was attributed to the extender's inherently high electrical resistivity and its influence on the conductivity of the pore solution. Ninety day salt ponding tests showed that the actual chloride ingress would only decrease by a factor of one or two.

Mackechnie and Alexander (2000) also showed that the RCPT results "fell into two distinct bands, OPC and FA concrete had high results while CSF, MK and SL concretes produced significantly lower results". They go on to state that FA containing concrete is unfairly disadvantaged in the RCPT as FA is a slow reacting extender and that testing on FA containing concretes should be conducted at 56 or 90 days. This further supports the research reported by Lane (2000) and strengthens the argument that the salt ponding test (and, hence, the Bulk Diffusion Test) is a preferable test method.

Feldman *et al* (1994) made measurements of the initial current or resistivity of the samples prior to the test, at room temperature. Using these measurements, the same ranking could be obtained for the samples, as that obtained from the actual test. Feldman noted that this method could replace the RCPT for those types of concrete. This procedure is similar to the Chloride Conductivity Test discussed below.

Experimental Review

The following points were obtained after laboratory testing of mortar samples.

- The RCPT is a rapid test. Apart from sawing samples to the required length and applying an epoxy coating, sample preparation is not time consuming.

- A high viscosity epoxy should be used (thixotropic epoxies hinder the sample from fitting snugly into the apparatus). This epoxy displaces air sufficiently so that air bubbles or channels are not formed.

- The apparatus for the test is relatively simple to build and maintain. It is not costly. Maintenance of the equipment (electrical connections, electrodes and seals) is very important. As the sample forms an intricate part of the apparatus, the seals should be of sufficient elasticity to form a good seal without the use of excessive effort.

- By the end of tests on 0.65 w/c mortars, the samples had generated a significant amount of heat. This not only affects the fundamental theory behind the test (by affecting the samples resistance) but may also lead to excessive evaporation of the solutions. Where data loggers are used, the test is allowed to complete itself unsupervised. Loss of solution due to increased evaporation would initially result in a change in concentration and eventually lead to a change in test area as the level drops below the top of the sample. It is possible to monitor temperature. Should the temperature rise to levels deemed excessive by the operator, the current generator could be automatically switched off – stopping the test prematurely.

- The test is non-steady state. This allows the chloride binding properties of the cementitious binders to be incorporated. As charge passed is the critical factor, loss of ions to chloride binding would affect the amount of charge able to pass through the matrix. However, the loss of a chloride ion generally results in the gain of a hydroxyl in pore solution – this would then be transported by the electrical potential difference and maintain current flow. This is due to ion substitution in both chemical and physical binding.

- Chloride binding is temperature dependent, as discussed in Chapter 4 – Chloride Binding. This would significantly affect the results of poor mixes, as these samples would suffer higher temperature gains, resulting in less chloride binding.

- The electrical field may affect chloride binding. The chloride solution employed in the RCPT is a 0.85 M NaCl solution, meaning that the electrical field would suppress chloride binding, according to Castelotte *et al* (1999).

The 50 mm length of sample allows a substantial amount of microstructure to be assessed. Percolation (ITZ surrounding large aggregate particles), coarse pores and aggregate size would not significantly affect the results of this test.

5.3 The Rapid Migration Test

This test employs an electric current and visual analysis. A 50 mm thick 100 mm diameter sample is placed in a migration cell (Figure 51). A 30 V potential difference is applied across the specimen for 18 hours. The specimen is then split longitudinally and a 0.1 N silver nitrate solution applied as a colorimetric indicator. In the presence of chlorides, the solution reacts to become silver chloride, which is white in colour. In the absence of chlorides, the solution turns a brown colour on reacting with hydroxide ions to form $Ag(OH)_2$. The colour change boundary, when using a 0.1 N silver nitrate solution, corresponds to a soluble chloride concentration of 0.15 % by mass of cement (Hooton *et al*, 2001). The depth of penetration is then used to determine a chloride ion diffusion coefficient (D) using the equation:

$$D = \frac{zFE}{RT} \cdot \frac{x_f}{t} \qquad (7.1)$$

where x_f is the penetration depth

z is the ion valence

F is Faraday's constant; 9.648 x 10^4 J / (V·mol)

E is the applied electrical voltage (V)

R is the gas constant; 8.314 J / (mol·K)

T is absolute temperature (K)

t is the time of voltage application

The detailed test method, apparatus and results analysis guidance can be found in: Tang, L. and Nilsson, L-O. (1992) **Rapid Determination of Chloride Diffusivity in Concrete by Applying an Electrical Field.** ACI Materials Journal, Vol. 89, No. 1, pp. 49 – 53. ACI, USA.

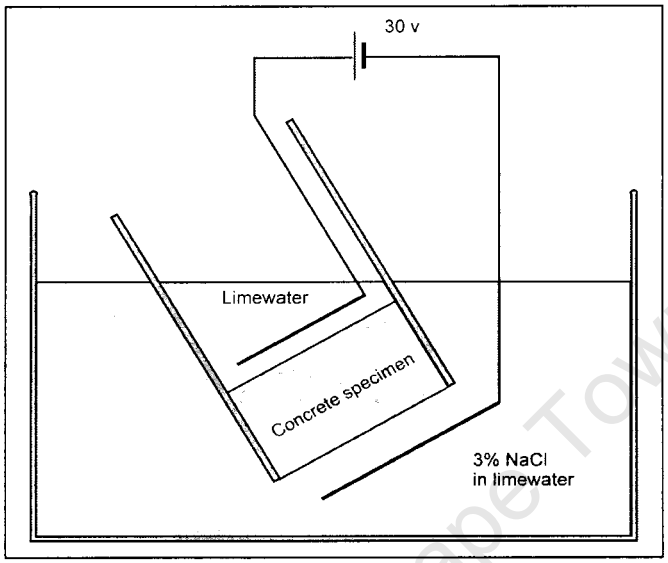

Figure 51: Rapid migration test setup (Hooton *et al*, 2001)

The application of an electric field accelerates the diffusion process by applying more energy to the ions. This energy may affect the binding potential of the ions due to their increased momentum and also changes in ion-ion, ion-solution and ion-medium interaction. The impact of an electrical field on both transport and binding mechanisms is not sufficiently established. As shown by Castelotte *et al* (1999) (Chapter 4), electrical fields do impact on binding behaviour. Therefore, the application of an electrical field in order to drive the chlorides into the concrete may affect the results obtained.

If another conductive ionic species is present, such as calcium nitrite (found in some admixtures), it is possible that this may carry the majority of the current (Mackechnie and Alexander, 2000). This would lower the impact of the electrical field on the chloride ions specifically and deem the results incomparable to those of concrete not containing such admixtures. Although the concentration of such ions in practice is generally low, they are commonly found in anodic-inhibiting admixtures. The presence of longitudinal reinforcing steel would short circuit the system directly. This test would also be sensitive to alkalinity effects as an increase in hydroxide ions

would result in a similar effect on the current carrying capacity of the chlorides. CSF would bias results due to its impact on the alkalinity of the pore solution and, hence, the conductivity.

The test duration and potential difference used may be varied. Depending on the concrete grade, varying durations or potential differences may be employed in order to obtain a more pronounced penetration depth, aiding measurement. Measurement is generally done with a steel rule to the nearest millimetre. Mackechnie and Alexander (2000) found that these values vary from 20 V for 12 hrs for low grade concretes to 60 V for 48 hrs for high strength concretes. These are based on the initial current passed – guidelines are given in certain standards (Hooton *et al*, 2001). It is uncertain whether ion behaviour and, hence, the results are sensitive to the magnitude of the applied potential difference.

Mackechnie and Alexander (2000) also noted that slower reacting materials such as FA would be inherently disadvantaged by such a test due to their slow reacting characteristics. Testing at 56 or 90 days is preferable for such mixes, even though it is impractical for quality control purposes. Slow reacting extenders and slow developing hydration products generally reach significant maturity after approximately 180 days but generally not before 28 days age. Rapid tests would, therefore, be a reflection of a substantially immature microstructure in terms of chemical composition and pore structure. ***Note: This point is true of all rapid chloride test methods conducted at 28 days age.***

Mackechnie and Alexander (2000) support the use of this test (as well as other rapid tests), suggesting that the results be corrected for long-term effects.

Experimental Review

The following points were obtained after laboratory testing of mortar samples.

- The sample preparation comments apply as in the RCPT.

- Mortars were assessed in this study. Consequently, a voltage of 10 V was applied across the samples, rather than 30 V. Hooton *et al* (2001) gave guidelines on applied voltage in order to avoid excessive heat formation. The

ability to use a low voltage circumvents the thermal problems associated with the RCPT.

- The non-steady state test exhibits chloride-binding characteristics in similar fashion to the bulk diffusion test. Significant binding would slow the chloride front progression, resulting in a shallower depth of penetration. The applied electrical field, however, would impact on binding as in the RCPT.

- As in the RCPT, voltage is controlled across the entire system and not across the specimens. Hence, the voltage values used in analysis would be greater than the actual voltage across the specimens – due to the resistance of the electrodes and solutions used.

5.4 Chloride Conductivity Test

The CCT involves the measurement of a sample's conductivity. A 25 mm thick, 68 mm diameter specimen is dried in an oven at 50˚C for seven days and pre-saturated via vacuum saturation with a 5 M NaCl solution. A migration cell is used, in which the sample is placed between two cells containing 5 M NaCl solution (Figure 55). A 10 V potential difference is applied across the sample and the corresponding current used to calculate the concrete's conductivity. The detailed test method, apparatus and results analysis guidance can be found in:

Alexander, M.G.; Mackechnie, J.R. and Ballim, Y. (1999). Research Monograph No. 2. **Guide to the use of durability indexes for achieving durability in concrete structures.** The University of Cape Town and The University of the Witwatersrand, SA.

Alexander, M.G.; Streicher, P.E. and Mackechnie, J.R. (1999). Research Monograph No. 3. **Rapid chloride conductivity testing of concrete.** The University of Cape Town and The University of the Witwatersrand, SA.

The most up-to-date test procedure can be found online at:

http://www.civil.uct.ac.za/research/materials/Durability%20Index%20Testing%20Manual.pdf

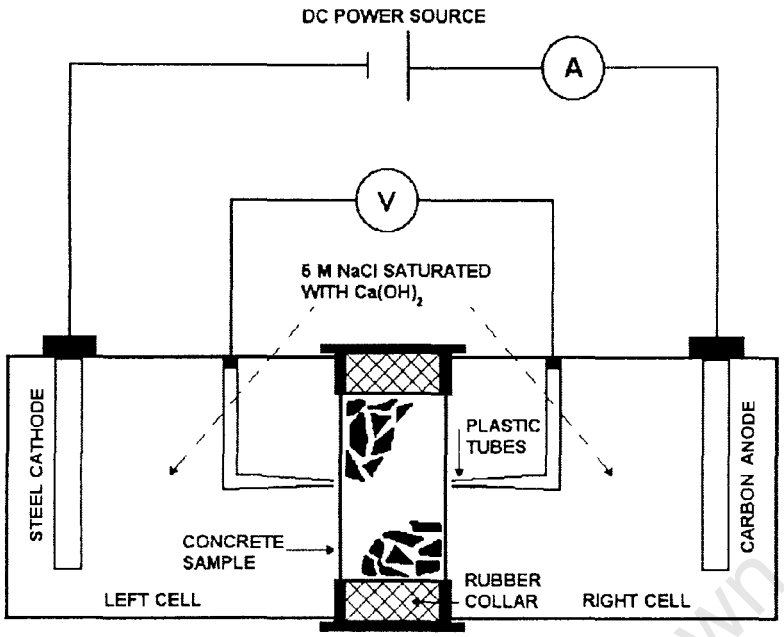

Figure 52: Chloride conductivity test apparatus (Alexander et al, 1999)

- Sample drying at 50°C, during specimen preparation, may result in microcracking, which could potentially affect the conductivity and transport properties. This requires investigation.

- Again, the application of an electric current may impede chloride binding and the presence of other ionic species and reinforcing steel may affect the results obtained. Even though the application of the current is relatively instantaneous, the effects of this are unknown and may affect the conductive behaviour of the ions.

- Vacuum saturation of high-grade concretes may be unsuccessful in completely saturating the samples with chloride solution, creating a chloride concentration gradient between the surface zone and the centre of the sample. This requires investigation.

- Should the presaturation process prove to be successful, almost all chloride binding would take place prior to the test. This was the aim of the test method, in order to obtain relatively equal solution conductivity throughout the sample and, hence, only measure the sample's conductivity. The test would, therefore, not take chloride binding into account and only be sensitive to

porosity and permeability effects. Hence, the test would be an ion permeability test and not account for chloride ion's unique binding behaviour – an important parameter.

Experimental Review

The following points were obtained after laboratory testing of mortar samples.

- The chloride conductivity test requires slightly longer specimen preparation time than the RCPT and the RMT. This is due to the oven drying procedure necessary for sample preparation, which takes 7 days. However, the actual test is instantaneous.

- As discussed in Chapter 3, drying at 50 °C may lead to microcracking and alterations in the pore structure. This would impact on the test results, which are based on the concrete's resistivity.

- As the CCT is a steady state test, all chloride binding would occur during sample saturation with 5 M chloride solution. The impact that the electrical field has on these bound chlorides and further binding are uncertain. It is plausible that the CCT only accounts for the density of the microstructure and not the chloride binding capabilities of the binder system.

- The vacuum saturation technique has also been questioned. It is uncertain whether the technique allows chloride to penetrate sufficiently evenly from the surface to the centre of the samples.

- These areas of uncertainty were experimentally investigated in this study. As this section of the study is directly linked to the CCT, the procedure and results are presented below.

5.5 Chloride Conductivity Test Developments

Four tests were conducted in order to identify possible areas of the CCT requiring further experimental investigation and development. These included:

Sample drying damage test
Sample size and percolation test
Chloride binding test (whether the CCT accounts for chloride binding)
Chloride saturation test (whether a chloride concentration gradient exists after saturation)

5.5.1 Concrete Mix designs

For the sample preparation, sample size and chloride binding tests, a CEM 1 concrete mix with a w:b of 0.5 was used.

For the chloride profile test, a 50 % GGCS concrete mix with a w:b of 0.5 was used. GGCS was used due to its hypothesized superior chloride binding capacity. Hence, this mix represented a fairly average mix for use in a chloride environment.

Greywacke aggregate of 9 mm nominal maximum size was used in both instances to avoid any potential ITZ effects due to the 25 mm specimen thickness.

5.5.2 Sample drying

The possible damage caused by oven drying in sample preparation was investigated. Specimens were prepared as directed in the standard test procedure. Four specimens were oven dried at 50 °C and four specimens were placed in propanol, until constant mass was obtained. The oven-dried samples were tested in the standard way after 7 days drying. The propanol-dried samples were placed in a 30 °C oven until, again, constant mass was obtained. These were vacuum saturated and tested. The test results were then compared. Results can be found in Figure 53.

Propanol drying resulted in a considerable decrease in the measured chloride conductivity of the samples. This may be as result of both decreased thermal stresses and associated microcracking and the accompanying ineffective sample saturation with 5 M NaCl solution. However, it is also possible that the oven-dried samples were more effectively dried than the propanol samples. This would have resulted in more sufficient chloride penetration during specimen preparation. The final dried masses of the specimens were not recorded and therefore cannot be

compared. This is recommended for future investigation. Also, CEM 1 mixes are not used in chloride environments. Had a 50 % GGCS mix been used, the oven-dried samples would have had a chloride conductivity of approximately 0.4 mS/cm^2. Comparing this to propanol dried 50 % GGCS specimens may have been more useful.

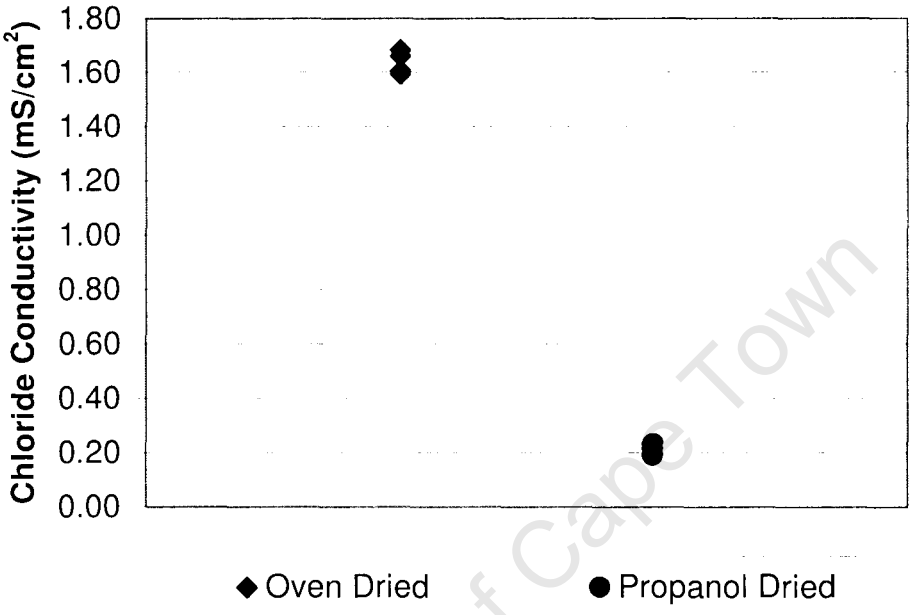

Figure 53: The effect of propanol drying on the measure chloride conductivity of CEM 1 specimens

5.5.3 Sample Size

It was hypothesised that, due to the possibility of the ITZ regions running from one face of the sample to the other, thinner samples would result in higher conductivities. The impact of sample size was analysed by testing samples (containing 9 mm aggregate) of 5 mm, 10 mm, 15 mm and 25 mm thickness. This gave ratios of minimum sample dimension to max aggregate size found in Table 7. Paste volume consistency was maintained by using the same coarse aggregate volume fraction in each mix. The test results obtained can be found in Figure 54.

Table 7: Maximum aggregate size to minimum sample dimension ratios for various disc thicknesses from a 9 mm aggregate mix

Sample Thickness (mm)	5	10	15	25
Maximum Aggregate Size / Minimum Sample Dimension (Approx)	0.5	1	1.5	2.5

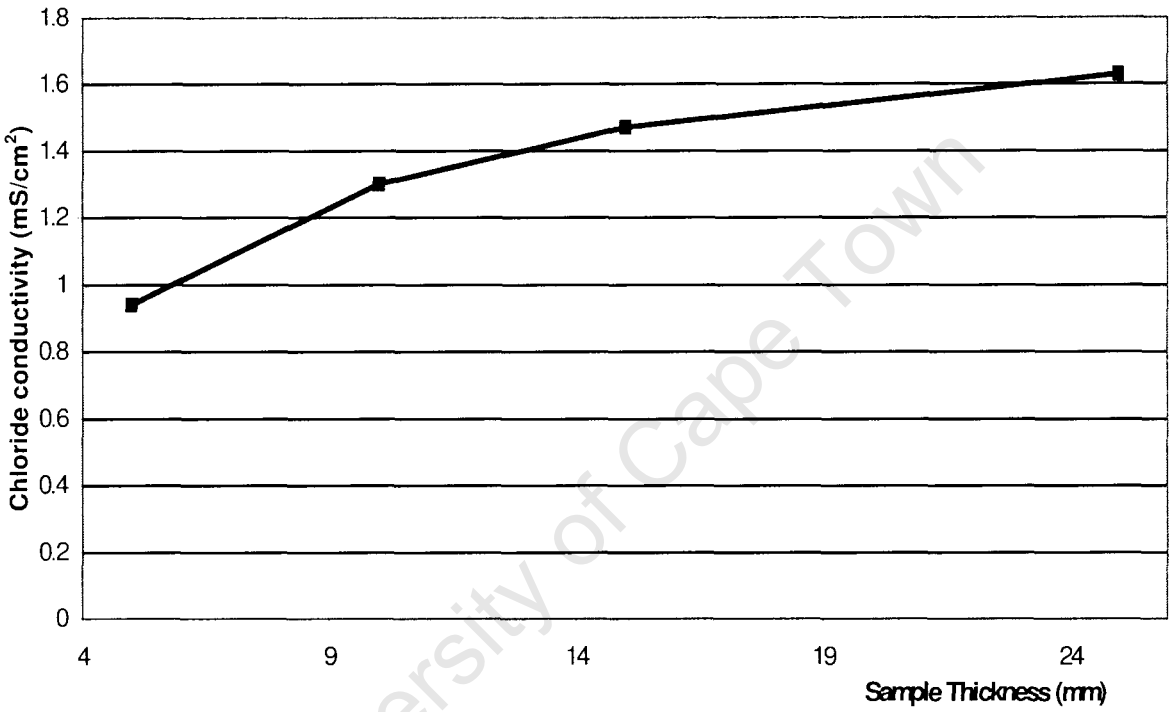

Figure 54: The effect of varying sample size on chloride conductivity test results

The results obtained indicated an opposite trend as to that which was expected. The chloride conductivity improved with thinner sample size and lower maximum aggregate size to minimum sample dimension (MASMSD). It is hypothesised that this is as a result of the sample preparation process. Oven drying at 50 °C would result in less cracking in thinner samples, as the thermal differential is lower, inducing lower thermal stresses in the samples. Hence, a lower amount of microcracking would occur in thinner samples – improving the measured conductivity of the samples.

Specimen saturation would also be more successful in thinner specimens. In thick specimens, a concentration gradient results in the specimens from the external faces to the centre (to be discussed). As a result, ions would preferentially be transported

through the outer regions of the specimen's cross sectional area. This would result in a lower effective migration area, decreasing the observed chloride conductivity. This was not apparent in the tested specimens. Hence, the impact of thermal cracking in larger specimens appears to outweigh the effect of insufficient specimen chloride saturation.

Streicher (1997) found a similar trend when developing the test. This was attributed to higher resistance in the cells due to increased distance and solution volume between the specimen faces and the electrodes. This may be possible; however, the magnitude of the drop in chloride conductivity for smaller specimens seems too large to be attributed to this phenomenon alone.

It is also possible that a smaller effective diffusion area was tested when using the smaller specimens. As a spacer was not used, an air bubble would occur in the conductivity cell when using specimen thinner than the standard 25 mm. Calculations show that a void of 75 ml would be formed in the 500 ml cell when using a 5 mm thick specimen. This would result in the solution level dropping approximately 15 mm from the top of the cells. Due to the rubber collar used in the apparatus, it is uncertain what the magnitude of this effect would be. However, in future studies, it is suggested that a spacer be used to eliminate this variable.

5.5.4 Chloride Binding

Due to presaturation with chloride solution and ion substitution, the majority (if not all) of chloride binding occurs before the chloride conductivity test is conducted. Hence, the conductivity reading would only take ion permeability into account and not ion – matrix interaction (chloride binding). This was analysed by conducting the test using NaOH instead of NaCl. The conductivity of the NaOH was matched to the conductivity of the 5 M NaCl, rather than using solutions of equal concentrations of ions. This would allow the impact of binding to be more easily exposed. A 5 M NaCl solution has a conductivity of approximately 260 000 µS. A NaOH solution concentration of 1.88 M gave the same solution conductivity. The results obtained can be found in Figure 55. The conductivity of the samples saturated with 1.88 M NaOH solution was approximately half that of the 5 M NaCl sample. This was unexpected. This may have occurred due to changes in the pore wall electrochemistry as result of the applied electrical field. Hydroxide ions do interact

with the matrix so it may have been preferable to use a more inert ion for the test – one that does not interact with any components of the matrix. It may be possible to use potassium hydroxide and measure the movement of potassium through the matrix. Potassium has a similar atomic mass to chlorides but would not react with the aluminate phases as negative ions do.

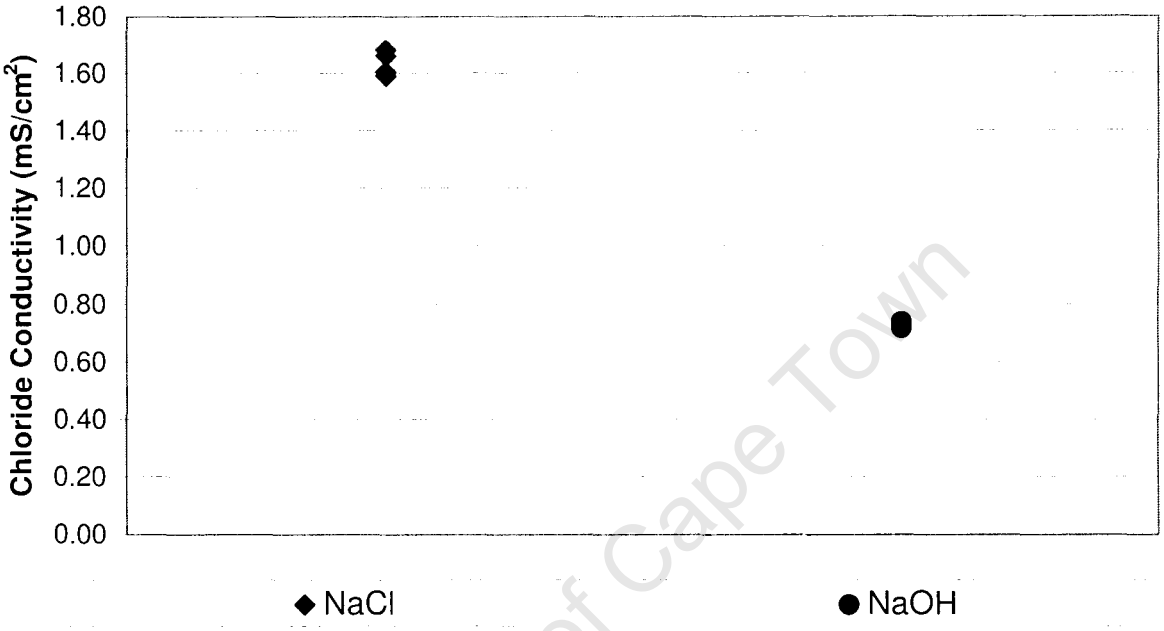

Figure 55: Chloride conductivity results for NaCl and NaOH solution tests with the same solution conductivity

5.5.5 Sample chloride saturation

Twenty-five millimetre specimens are vacuum saturated by 5 M NaCl solution. It is hypothesized that the time taken, and the action of chloride binding, results in a concentration gradient from the surface to the core of the samples. Specimens were prepared in the standard fashion but, instead of being tested, were profiled on a grinding machine. A modified milling machine was used to obtain alternate 0.5 mm profile samples from the specimens (this was sufficient to plot a representative concentration profile). These were then treated with nitric acid and titrated against silver nitrate to obtain the total chloride contents. Using an average binding capacity of 60 %, the total chloride values were translated into free chloride values – as this directly affects solution conductivity. The results can be found in Figure 56. A significant concentration gradient was present. It was also observed that very little

change in this gradient occurred after 7 days soaking. It can therefore be assumed that the sample is fully saturated with water, however, diffusion must now occur in order to transport chloride ions to the centre of the sample. This is a time consuming process and would not result in a uniform concentration gradient within the time required for rapid chloride testing. It was later found that Mackechnie and Alexander (2000) had obtained similar results for GGBS concretes, which were sliced and ground after testing. They also found that CSF concretes had "fairly uniform" concentration gradients – owing to their poor chloride binding capacity.

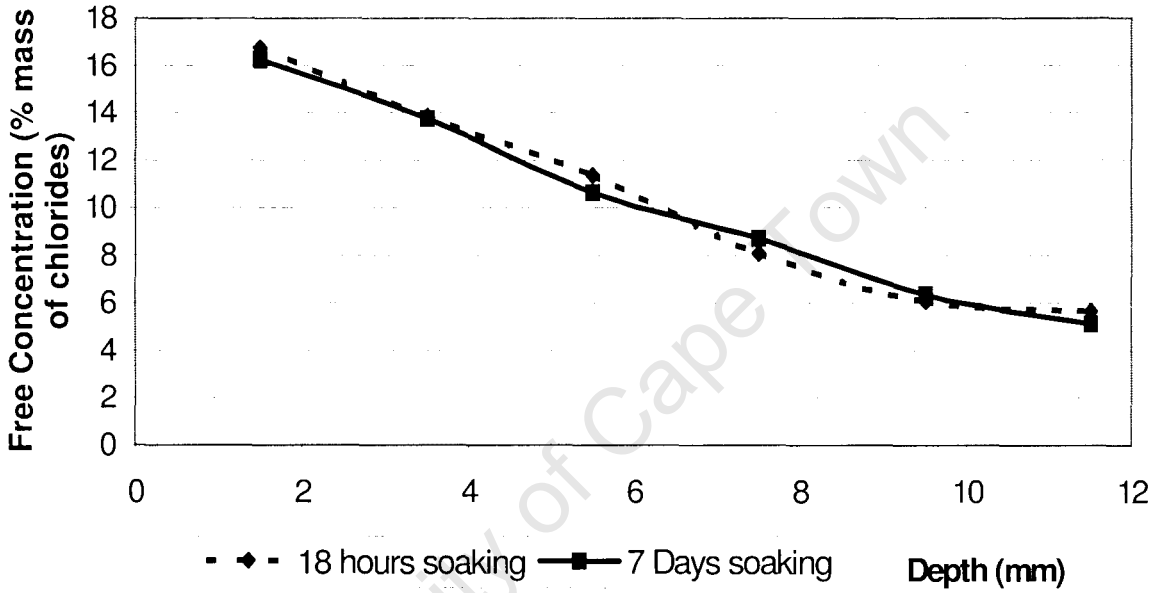

Figure 56: Free chloride concentration profile of chloride conductivity test sample prepared in the standard fashion and with 7 days 5 M NaCl soaking

Note: The concentration gradients were calculated assuming a two-dimensional concentration gradient (i.e. decreasing from the top of the sample to the centre and then increasing from the centre to the base). However, the concentration gradient is three-dimensional (i.e. decreasing from all sides to the centre). Hence, the results exhibited underestimate the magnitude of the true three-dimensional concentration gradient.

In order to determine the effect of this concentration gradient on the conductivity of the pore solution, bound chlorides had to be removed from consideration. A bound chloride to total chloride ratio of 40 % was assumed (consistent with literature – see Chapter 4). The free chloride concentration in the pore solution was thus calculated.

Chloride solution conductivity is dependent on concentration – as seen in Figure 57. Hence, a change in free chloride concentration from 16 to 6 % by mass of chlorides effectively halves the solution conductivity from 180000 µs to 78000 µs.

In effect, ions would preferentially be transported through the outer regions of the sample. This affects the area term in the conductivity equation, as well as limiting the portion of the sample actually represented by the test.

The chloride conductivity test does, inadvertently, account for the effect of chloride binding. The negative impact of a GGCS binder system on effective sample saturation would be far greater than the impact of an OPC mix. Hence, a greater concentration differential would result, resulting in a lower chloride conductivity – as can be expected from a GGCS containing mix.

The test, therefore, does not give a fundamental reflection of the ion transport behaviour due to the concentration gradient present and the resulting varying effective transport areas from test to test. Empirical relationships have, however, made it possible to use the test in estimating the performance of concrete in a marine or chloride environment.

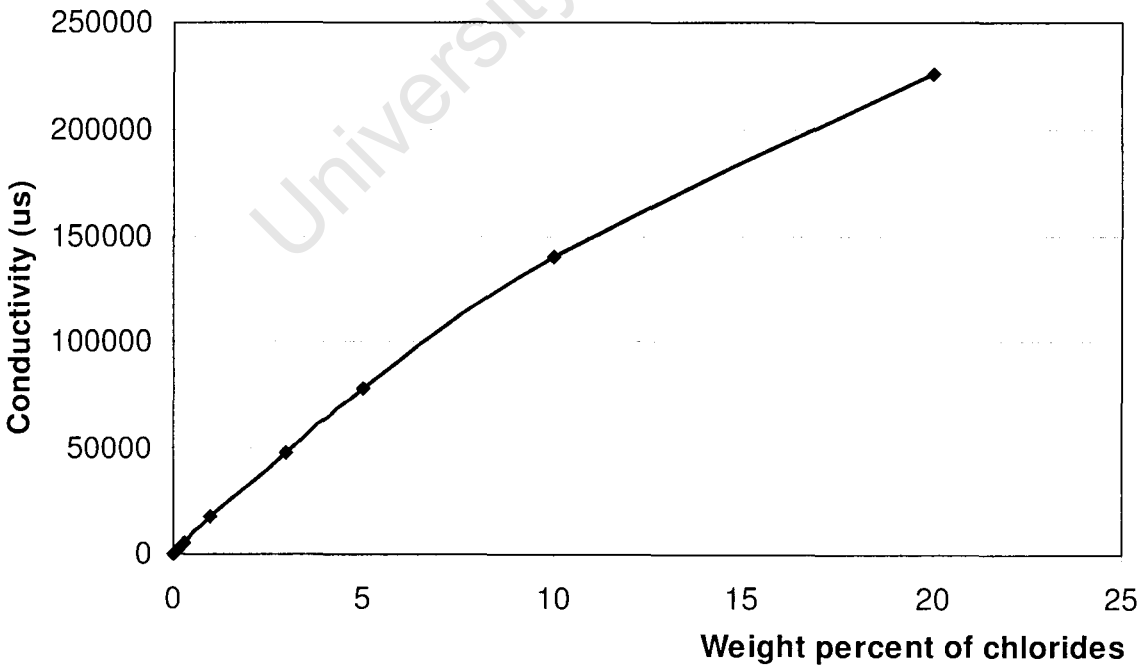

Figure 57: Chloride solution conductivity

5.6 Present Chloride Test Methods – Comparative Summary

The strengths and weaknesses of the four reviewed tests are summarised in Table 8.

Table 8: Rapid chloride test comparative summary

	BDT	RCPT	RMT	CCT
Sample Prep – Duration	Undefined: 2 days to weeks	Undefined: Days	Undefined: Days	8 Days
Sample prep – Damage?	Minimal	Minimal	Minimal	Significant
Test Duration	30 days to 90 days	6 hours	12 – 72 hours	Instant
Sample size	Ø = 75 mm t = 100 mm	Ø = 100 mm t = 50 mm	Ø = 100 mm t = 50 mm	Ø = 68 mm t = 25 mm
Apparatus	Grinder / Saw Titrator	Specific cell	Specific cell	Specific cell
Electrical field?	No	Yes	Yes	Yes
Results affected by test method?	No	Yes (Temperature)	No	No
Results negatively affected by binder system?	No	Yes (Pore solution chemistry)	Yes (Pore solution chemistry)	No
Results affected by other ionic species?	No	Yes	Yes	No
Effective in categorising latent hydraulic binders?	Yes	No	No	No

5.7 Conclusions

The Bulk Diffusion Test is most representative of fundamental chloride diffusion through concrete and is not affected by the unknown implications of using an electrical field to accelerate the diffusion process. However, the test is time consuming and is not suitable for quality assurance purposes. The test has, however, been used to calibrate most other test methods. This test is best suited for and should be used in long-term research projects.

The RCPT has fallen into disrepute. The test procedure results in variable effects on different mixes. This affects the results obtained. Improved tests have been developed and should be considered above the RCPT.

The Chloride Conductivity Test is a convenient rapid chloride test. Sample preparation does, however, require the use of an oven able to maintain 50 ˚C and vacuum saturation equipment. Although sample preparation does affect the microstructure of the samples, the test has been calibrated using the BDT and long-term tests on actual structures. Due to its simplicity, it is well suited for quality assurance purposes.

The chloride conductivity test is an effective rapid chloride test method. The test has a sound theoretical foundation. However, some areas of sample preparation do affect the fundamental properties of the samples – altering their behaviour.

These areas of uncertainty do not, however, impact on the test being an effective means of rapidly categorising concretes to be cast in chloride environments. The test has been calibrated using long-term in-situ measurements. This empirical relationship to actual chloride exposure specimens has taken account of microstructural damage during the drying process and ineffective sample saturation. The test can, therefore, be successfully used in practice.

The test is not suited, however, to fundamentally analysing chloride transport through concretes and mortars. The alterations made to the cementitious matrix during sample drying and the ineffective sample saturation makes obtaining a fundamental picture of ion permeability and chloride binding relationship difficult. Furthermore, microstructural damage during drying would preferentially affect certain binder

systems (especially CSF) and lower w:b mixes more negatively than others. Care must be taken when using this test on high performance and high strength concrete mixes as well as in fundamental studies of chloride transport. The BDT is better suited for fundamental studies.

The non-steady state Rapid Migration Test is an improvement of the RCPT and uses a superior analysis technique. Sample preparation does not affect the microstructure of the samples, is not complicated and does not require vacuum saturation equipment. The applied potential difference does not generate excessive temperature gains and the analysis technique is simple to perform. This test is therefore suited for quality assurance purposes.

It is necessary to have an appreciation for and understand the rapid tests' limitations - before utilising the results to make long term predictions of a concrete's potential service lifespan. It is equally necessary to consider the ease with which the tests can be carried out in testing laboratories – to ensure that consistent results can be obtained.

Rapid chloride test methods employ an electric current to accelerate the diffusion process, either under steady state or non-steady state conditions. As chloride binding is an important phenomenon in chloride transport, it is important to understand the impact of electrical fields on chloride binding capacity and the measured transport parameters. Further research into this area is required.

PART 3 – EXPERIMENTAL RESEARCH

6. EXPERIMENTAL RESEARCH STRATEGY

Four rapid chloride tests were individually reviewed and their respective strengths and weaknesses discussed. However, generic issues regarding theory and the measured relationship between diffusion properties and migration properties remained. The application of an electrical field across a cementitious sample has been reported to affect chloride binding (Castelotte *et al*, 1999). The increased energy transferred to the ions may hinder the cementitious system's binding potential, resulting in fewer bound ions. Alternatively, the activity of the ions may increase, resulting in a more excited and unstable state. This may increase the binding potential. It appears that the occurrence of these differing mechanisms is concentration-dependent and was hypothesised to significantly affect the observed transport coefficient when migration testing was conducted.

A research programme was devised, with the following objectives:

1. To determine whether the relationship between diffusion and migration given in the literature (i.e. Fick's Law and the Nernst-Plank equation) is representative of measured transport coefficients. As seen in Chapter 2, the Nernst-Plank equation is an extension of Fick's Law for use in migration testing, including constants accounting for the effect of the electrical field. However, chloride ion activity is disregarded. As the impact of an electrical field on ion activity is uncertain, it was hypothesized that differing initial concentrations may affect the measured results significantly. GGCS was used to determine the varying effects of increased binding capacity on the results and trends obtained for diffusion and migration coefficients, while CSF was used to determine the effects of decreased binding capacity.

2. To investigate whether initial chloride concentration in diffusion and migration tests significantly affects the results obtained and the test variability. As seen in Figure 2 (p. 14), a local minimum in ion activity occurs at approximately 1 M, which then increases rapidly as one approaches 5 M. Hence, small changes in solution concentration at 1 M would have less impact on ion activity than small changes at 5 M. It was hypothesized that this may affect the variability of the results obtained.

3. To investigate whether the application of an electrical field affects chloride binding phenomena and capacity. Castellotte *et al* (1999) showed that the application of an electrical field affects chloride binding potential, as discussed. Their work, however, only considered chloride concentrations up to 3 M. Due to the low change in chloride ion activity between 1 and 3 M, a significant change in behaviour was hypothesized to occur at 5 M concentration – as used in the CCT. GGCS and CSF were used in alternative binder systems to the CEM 1 control in an attempt to distinguish which binding phenomenon (physical or chemical) was most affected by the application of the electrical field.

The results of this investigation would have varying implications for each of the four tests reviewed. This will be discussed later.

In order to analyse the impact of an electrical field on transport properties and binding potential, diffusion and migration tests were used. This allowed diffusion and migration coefficients to be measured and analysed, followed by chloride binding tests on the same specimens. The chloride binding capacity of the specimens was investigated using an equalisation method. Differing binder systems were used to investigate the effect of electrical field application on adsorption versus chemical binding.

Cryogenic Backscattered and Secondary SEM was conducted on selected fractured samples in order to assess visually the occurrence and nature of Friedel's Salt deposits. Due to the scale and nature of fracture surface cryogenic SEM, definitive results could not be drawn from the microscopy study. However, interesting observations and trends were observed and will be discussed later.

Test Development

The nature of the transport tests (steady state versus non-steady state) and cells used would dictate which subsequent tests could be carried out on the samples and how the specimen would be analysed. Certain initial requirements and limitations had to be met and accounted for.

- The non-steady state diffusion coefficients of the mortars were obtained from the bulk diffusion test, which was conducted on all mortars. It was, therefore, unnecessary to conduct further non-steady state tests.

- The concentration in both cells (initial chloride containing "upstream" cell and non-chloride containing "downstream" cell) had to equalise. This was an initial requirement in order to analyse chloride binding in the specimen using a non-destructive, mass-balance technique.

- Using diffusion cells with infinitely large upstream chloride reservoirs could not be used as accurate mass-balance calculations would not have been possible for the chloride binding calculations.

- The specimen had to be relatively thin so that the diffusion process could be monitored within the time frame available for the study.

Finite volume split cell diffusion tests met these requirements.

- The cell volumes used were then required to be of sufficiently small size such that the amount of ions to be moved through the specimen for equalization to occur was minimised.

Using the concrete service life prediction model, Life365 (Thomas and Bentz, 2000), it was estimated that a 5 mm thick sample placed between two 120 ml cells would be sufficiently thin to allow equalisation to occur within the required timeframe. Trial tests, however, indicated that the time required for equalisation was far greater than that predicted. Accordingly, the analysis methods used had to be changed. This will be discussed later.

6.1 Diffusion Tests

Objective

To investigate the impact of electrical field application on measured transport parameters (namely the diffusion and migration coefficients), using coupled diffusion and migration tests.

An equal volume split cell diffusion test was used in order to determine the diffusion coefficients of the various mixes at various initial chloride concentrations. Initial concentrations of 1, 3 and 5 M were used in order to span the concentrations used in present rapid chloride test methods, and various ion activities.

In classic diffusion tests, a sample is placed between two cells. The "upstream" cell contains a chloride solution (not necessarily NaCl). The downstream cell generally contains 0.3 % by mass $Ca(OH)_2$ to prevent leaching of the pore solution or cementitious system.

The chloride ions diffuse through the sample due to the concentration gradient between the upstream and the downstream cells. The concentrations of both the upstream and downstream cells are monitored with time. Some characteristics of the concentration profile of the downstream cell with time can be seen in Figure 58.

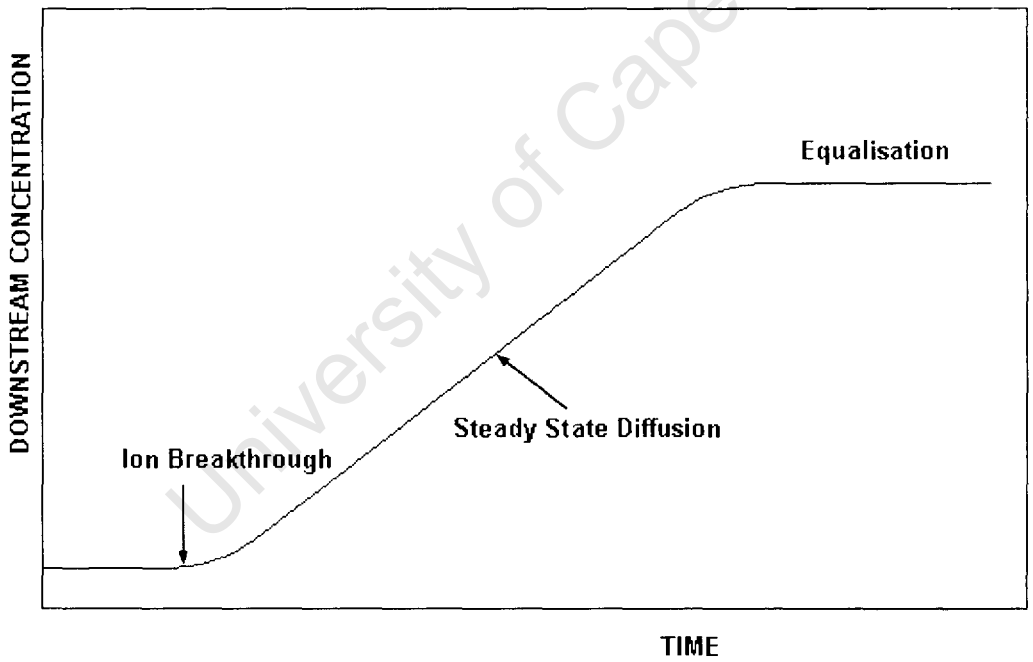

Figure 58: Theoretical concentration profile of the downstream diffusion cell reservoir

As ions penetrate and move through the sample in non-steady state diffusion, no change in concentration is observed in the downstream cell. Once chloride ions begin to reach the downstream face and enter the downstream cell, breakthrough occurs. From this point onwards, the system moves into steady state diffusion. If the upstream reservoir is of sufficient volume that negligible decrease in chloride

concentration is experienced, the downstream profile becomes linear. As the downstream reservoir begins to approach the upstream concentration, diffusion slows and eventually stops when the reservoir concentrations equalise.

In finite volume split cell diffusion tests, the downstream concentration-time profile has an inflection point rather than a linear portion. This is due to the continual decline in upstream reservoir chloride concentration. Different techniques must be used to analyse the two respective cell systems.

6.1.1 Cell Apparatus

The diffusion cell configuration can be seen in Figures 59 and 60. Diffusion cells were constructed using Polyvinyl Chloride (PVC). This would ensure sufficient accommodation of the highly concentrated salt solutions for the duration of the tests. The parts were clamped together using threaded brass rods and wing nuts. Seals were provided by silicon rubber, which was cast into recesses in the end plates and sample holder. Standard size PVC piping (90 mm OD, 76 mm ID) was used for the cells. The volumes of the upstream and downstream cells had to be optimised as the greater the cell volume, the greater the number of ions one would have to transport in order to reach equilibrium. The dimensions of the cells were 30 mm wide by 76 mm internal diameter. This allowed approximately 120 ml of solution to be accommodated initially (before sampling for concentration monitoring). A depth of 30 mm also allowed a sufficiently large hole to be drilled into the top of the cells to be used to extract solution samples for titration.

6.1.2 Sample Size

Five millimetre thick samples were used due to time constraints. In order to eliminate edge effects and the potential effects of Interfacial Transition Zones (ITZ's), mortar samples were used. The pit sand used was sieved and only particles passing the 2.360 mm sieve were used. This gave a ratio of minimum sample dimension to maximum aggregate size of approximately 2 - ensuring that sufficient paste fraction was in place for representative transport testing. In determining the sample diameter, both cell volumes and slenderness ratios had to be considered. Five millimetre thick mortar samples are fragile. A shock or jolt to a large thin sample could result in microcracking. A diameter of 50 mm was used in order to maintain some bending rigidity (this was verified in trial castings), while still having sufficient sample mass for

the various test requirements. Given the cell dimensions, a 50 mm sample diameter ensured that sufficient solution was available for sampling such that the level of solution would not fall below the upper limit of the sample.

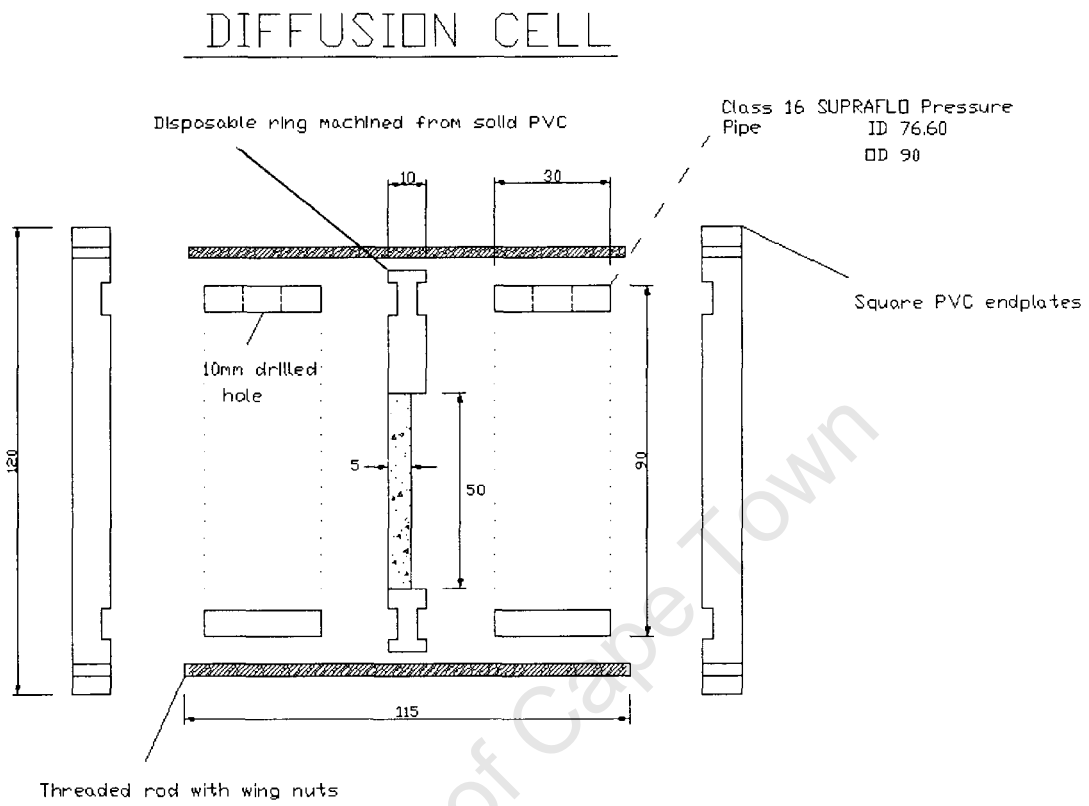

Figure 59: Cross section of the diffusion cell

The mortar samples were cast directly into the sample holders, which were slightly roughened with sand paper to ensure good mortar – PVC bond. Smooth PVC spacers were used to ensure clean and uniform finished faces were obtained. The samples were then cured for 7 days in a 100 % humidity environment before being submerged in saturated $Ca(OH)_2$ solution to avoid leaching. Curing at 100 % humidity ensured that no shrinkage of the specimens would occur. Shrinkage would have caused the samples to pull away from the sample holder, creating microscopic channels for chloride ions to move through.

6.1.3 Data Acquisition

As diffusion proceeded, the change in concentration of both solutions with time was measured. This was done by potentiometric titration of a 0.3 ml sample of each reservoir solution. Thus, diffusion coefficients could be calculated.

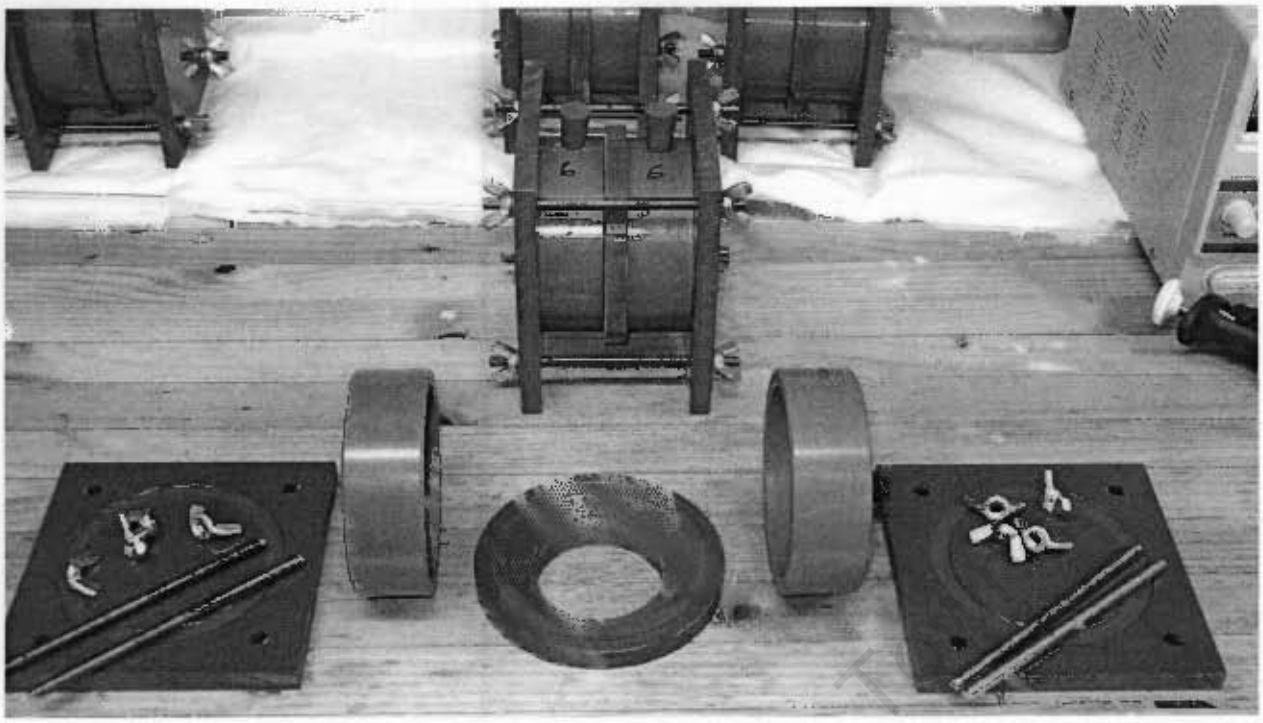

Figure 60: Diffusion cell components – photograph

6.1.4 Data Analysis

Table 9 shows the analysis procedure, methodologically. Numbers in square brackets in the text correspond to the numbers in the table. Spreadsheets showing the analysis of the numerous cells analysed can be found in Appendix 2.

Finite difference results can be obtained using Fick's First Law. However, these values are variable and generally decrease with time due to continued hydration and the interaction of chloride ions with the matrix. Effective diffusion coefficients are, therefore, generally calculated in order to account for these effects. This allows a single diffusion coefficient to be used, representing the observed flux through a particular specimen.

Using Fick's First Law, a prediction model was used to generate the data based on the starting conditions of each diffusion cell and a single diffusion coefficient.

$$J = -D_{eff} \cdot \frac{\Delta c}{l} \qquad (8.1)$$

where J is the flux through the downstream face of the specimen

D_{eff} is the effective diffusion coefficient

Δc is the concentration gradient across the specimen (the difference between the upstream and downstream concentration)

I is the thickness of the specimen

Using this finite difference equation with an arbitrary D_{eff}, the sample thickness (I) and the starting conditions (c_u = 1; 3 or 5 M respectively, c_d = 0, t = 0 – where c_u and c_d are the chloride concentrations in the upstream and downstream cells, respectively), a subsequent flux of chloride ions through the sample can be calculated [2]. This flux is then used to calculate the mass of chloride ions transported from the upstream cell to the downstream cell - resulting in a change in downstream concentration. The resulting "predicted" downstream chloride concentration [3] is calculated using the mass balance equation:

$$c_{d2} = \frac{J \cdot \Delta t \cdot A}{V} + c_{d1} \qquad (8.2)$$

where J is the flux through the downstream face of the specimen

Δt is the time interval

A is the cross sectional area of the specimen

V is the volume in the downstream cell

c_{d1} and c_{d2} are the chloride concentrations of the downstream cell at time t_1 and t_2 respectively

The "predicted" downstream concentrations using the arbitrary D_{eff} are then compared to the actual observed values.

A least-squares analysis was then done in which D_{eff} was varied to minimize the square of the errors between the observed downstream concentration data and the generated data [4]. This yielded a single effective diffusion coefficient (time independent) that could be used to categorise each sample [5]. Four cells were used per mix and starting concentration. Hence, four diffusion coefficients were obtained for each combination of mix type and starting NaCl concentration. These were then averaged to obtain a diffusion coefficient for each mix for a given initial concentration (The coefficients of variation are given in Chapter 7).

Table 9: Procedure of analysis

D_{eff}	Varied to obtain minimum least square error solution [5]			
Time	**Observed c_d (O)**	**Flux ($g/m^2/s$)**	**Predicted c_d (P)**	**Error Squared $(O-P)^2$**
0	0		0	
1	[1] Measured	[2] Calculated using single D_{eff} and starting conditions for each time step	[3] Calculated using flux obtained from arbitrary D_{eff}	
2	Measured			
3	Measured			
4	Measured			**[4] Sum is minimized**

6.2 Migration Tests

Objective

To obtain migration coefficients that could be directly compared to the diffusion coefficients obtained from the diffusion tests.

Identical cells to the diffusion cells discussed above were used for the migration test. Small slots were made at the top of the cell reservoirs, adjacent to the endplates. This allowed electrodes to be inserted into the cells, at a maximum distance from the samples (approximately 30 mm).

In previous migration experiments (Andrade and Sanjuan, 1994) steel electrodes were used and allowed to corrode. A problem with this methodology is the adsorption of chloride ions onto the products of corrosion found in the downstream solution. Stainless steel electrodes were only to be used in the cathodic chambers, as corrosion is not a concern here. In trial tests, carbon electrodes were used in the anodic chamber to buffer corrosion but they disintegrated over the duration of the test to form CO_2. Stainless steel anodes were then used for the actual tests. Minimal corrosion occurred at the 2 V potential-difference used. The electrodes were cut from stainless steel sheets and were 8 mm wide by 2 mm thick and protruded into the

reservoir solution to a depth of approximately 50 mm. The test was run at approximately 2 V. At this low voltage, the generation of Cl_2 gas was not foreseen. During the tests, an informal smell test was performed and chlorine gas could not be detected. There are no simple, practical tests for small scale chlorine gas evolution.

The tests were run for two weeks to ensure that sufficient data was obtained for prediction model analysis.

6.2.1 Data Analysis

The Nernst-Plank equation constants were applied to the finite difference equation 8.1.

$$J = -D_{eff} \cdot \frac{\Delta c}{l} \cdot \frac{zFU}{RT} \qquad (8.3)$$

where J is the flux through the downstream face of the specimen

D_{eff} is the effective diffusion coefficient

Δc is the concentration gradient across the specimen (the difference between the upstream and downstream concentration)

l is the thickness of the specimen

F is Faraday's constant, 96480 J/(V.mol)

z is the ion valence

U is the externally applied electrical potential difference

T is absolute temperature

R is the gas constant, 8.314 J/(mol.K)

The same prediction model procedure was used to obtain migration coefficients from the observed data. This method, however, yielded undesirable results – to be discussed. A discrete, finite difference analysis technique was then used – calculating discrete migration coefficients for each time step (approximately 24 hours). As standard rapid chloride migration tests are conducted within a few hours, the first three time steps of the migration tests were analysed and these discrete migration coefficients averaged to obtain a single migration coefficient to categorise the sample at its particular starting concentration. The migration coefficients of the first three time steps varied by up to 70 % (coefficient of variation), due to the

variability in titration results. At face value, this seems excessive, however, for migration coefficients of the order of 10^{-11} this is a reasonable coefficient of variation.

Four samples per mix, per starting NaCl concentration were used. As the prediction model approach could not be used in analysing the migration data, these four migration coefficients were then averaged to obtain one single migration coefficient to categorise all four samples for each initial NaCl concentration.

6.3 Chloride Binding Test

Objective

To investigate the chloride binding capabilities of the various binder systems and investigate any potential effects of the electrical field. The results of the chloride binding test would aid in determining what effect electrical field application had on the transport process, should any effect occur and be identified in the diffusion and migration tests.

A solution equalisation technique was used. This could not be done within the diffusion cells, as initially desired, due to time constraints. The specimen had to be removed and placed in a secondary solution.

Specimens were removed from the diffusion and migration cells, once sufficient data had been obtained. As the specimens had to be broken out of the cells, fragments with sizes ranging from 3 mm to 0.3 mm were obtained. These samples were then placed in a chloride solution of the same concentration as their initial chloride concentration in the transport tests (1; 3 or 5 M). If solution concentrations were used that were lower than the concentrations the sample was exposed to during the transport tests, a significant amount of chemical binding would have already occurred that would have been attributable to the higher concentration. The samples were housed in airtight containers. These were only opened after 3 months, in order to determine whether the solution had equalised. The samples were left to soak in the NaCl solution until all samples had equalised ($t > 3$ months). This ensured that the samples were all of the same maturity at the time of testing. The solution concentration was tested on a weekly basis starting three months after the last sample had been submerged. All samples had a coefficient of variation less than 2 % - the standard variability of the titrator used.

The samples were then removed from the solution and a portion of the sample oven-dried at 100 ˚C for seven days. The sample was then ground to a fine powder and returned to the oven for a further 24 hours. These samples were then potentiometrically titrated against silver nitrate to obtain the total chloride content as a mass percent of the sample. This was then converted to Molar units using the following formula:

$$c_M = \frac{c_{\%} \cdot \rho_{conc} \cdot (1-n)}{nM} \qquad (8.4)$$

where c_M is the concentration of chloride ions expressed in Molar units

$c_{\%}$ is the concentration of chloride ions expressed as a mass percent of concrete

ρ is density

n is porosity

M is the molar mass of chloride ions (35.453 g / mol)

Using mass balance, the amount of bound ions was then calculated using:

$$Cl^-_{total} = Cl^-_{free\ (external\ solution)} + Cl^-_{bound}\ (g) \qquad (8.5)$$

As the bulk porosity of the samples was known, the amount of free chlorides in the pore solutions could be calculated using the free chloride concentration. Once this was subtracted from the total chloride concentration obtained from acid digestion and titration, the amount of bound chlorides was obtained.

6.4 Porosity Analysis

The bulk porosity and density of the samples were obtained from mass loss due to oven drying at 50 ˚C for seven days (sufficient temperature and time to obtain a representative measure of the accessible capillary pore fraction). These measurements had to be used for the conversion of binding results from % sample units to % weight of cement and molar units. The porosities were also used in analysing the adsorption of chloride ions as greater porosity indicates greater pore surface areas and, hence, greater physical binding capacity.

6.5 Mix Designs

Chloride binding is highly dependent on the reactants available in the mix. As detailed in Chapter 4, Ground Granulated Corex Slag is hypothesized to exhibit superior binding properties due to its higher aluminate content. Both GGCS and CSF were incorporated into the experimental programme to observe the differences in binding and pore structure behaviour as compared to a CEM 1 mix.

6.5.1 Sand to binder ratio

This ratio is important in ensuring that sufficient aggregate and paste is present for mechanical properties to be optimally preserved. This ratio also dictates the workability and bleed potential of the mix. Trial mixes were cast to assess fresh mix characteristics. A sand to binder ratio of 4 yielded sufficient workability and a reasonable amount of bleeding (some but not excessive). A sand to binder ratio of 5 was used in a trial test but yielded very erratic transport behaviour (details of trial experiments are presented in Appendix 3). A sand to binder ratio of 4 was then used for the actual test mortars.

Good sample preparation was imperative and proper compaction in sufficient layers was required to ensure good sample – former bond. Flat, smooth PVC formers were required to ensure consistent edges and ensure the thickness of the sample was consistently 5 mm after casting. Floating such small samples proved difficult and resulted in a fairly rough surface. Due to the small nature of the samples, this would have affected the diffusion behaviour significantly and erratically. By using smooth PVC formers, this effect could be eliminated.

Superplasticiser was used to adjust the workability of all mortars – irrespective of binder system - as it is necessary to use superplasticiser with CSF. The mortar's workability was assessed using a flow table (SANS 6245 - Section 6.3) in order to ensure consistency across the three binder systems. A spread of approximately 140 % was used as a benchmark. This was the value obtained by the CSF mix (at 0.8 water binder ratio with a small amount of superplasticiser). Thus, it was ensured that all mixes contained superplasticiser, for consistency, and had the same workability.

6.5.2 Water to binder ratio (w:b)

Diffusion tests are, by nature, lengthy experiments. It was, therefore, desirable to use a high water to binder ratio to promote a more porous mix and a faster test. This was, however, limited by rapid permeability change with w:b, as seen in figure 66. The service life model, Life 365, was used to estimate the diffusion coefficients of the hardened mortar. The value for 28 days and the value at the hypothetical test end point was averaged and used to predict the test duration. Taking the limited study timeframe into account and the information provided by Neville (1981), water-binder ratios were decided upon. A w:b of 0,65 was used for the CEM 1 and GGCS mixes to ensure that the results obtained could be related to practical concrete mix designs. The CSF samples were cast at 0,8 w:b due to the significantly decreased permeability of CSF mortars. This would have slowed the diffusion process to such an extent that insufficient data would have been obtained at higher w:b ratios, in the limited timeframe.

Using the stated parameters, the mix designs in table 10 were compiled.

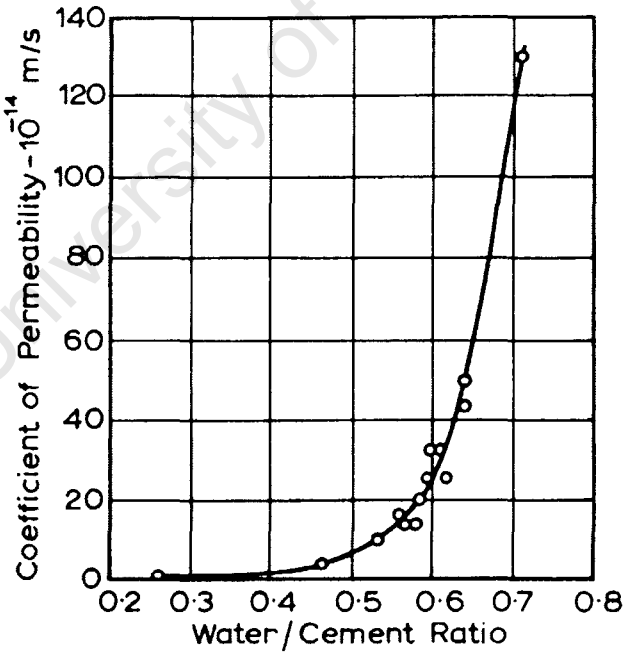

Figure 61: The effect of water to binder ratio on the coefficient of permeability

(Taken from Neville, 1981)

6.6 SEM

Cryogenic backscattered scanning electron microscopy was used for qualitative analysis of Friedel's salt formation. This allowed the pore structure to be observed with minimal amount of disruption from drying processes. Cryogenic SEM involves freezing the fractured sample in liquid nitrogen. The sample is then placed in the SEM chamber and the pressure lowered while maintaining very low temperatures. This sublimates the ice crystals on and in the sample, allowing the sample to be viewed with the SEM. The images obtained were qualitatively analysed by visual inspection.

Table 10: Diffusion and Migration test mix components

		Binders			Sand
		CEM 1	GGCS	SF	Klipheuwel
Density	(kg/m^3)	3150	2800	2200	2600
CEM 1					
	Water	**CEM 1**	**Sand**	**Total**	
Ratio	0.65	1	4		
kg/m^3	**259**	**399**	**1596**	**2254**	
50% GGCS					
	Water	**CEM 1**	**GGCS**	**Sand**	**Total**
Ratio	0.65	0.5	0.5	4	
kg/m^3	**257**	**198**	**198**	**1584**	**2237**
10% CSF					
	Water	**CEM 1**	**CSF**	**Sand**	**Total**
Ratio	0.8	0.9	0.1	4	
kg/m^3	**300**	**337**	**37**	**1498**	**2172**

Table 11 shows the final mix matrix for the experimental programme. Thirty-six split-cell diffusion tests, thirty-six split-cell migration tests and seventy-two chloride binding tests were conducted.

Table 11: Specimen matrix for the experimental study on the effect of electrical field application on chloride transport parameters.

Binder System	Diffusion Tests			Migration Tests		
	Initial Chloride Concentration			Initial Chloride Concentration		
	1 M	3 M	5 M	1 M	3 M	5 M
CEM 1	4 cells	4 cells	4 cells	4 cells	4 cells	4 cells
50 % GGCS	4 cells	4 cells	4 cells	4 cells	4 cells	4 cells
10 % CSF	4 cells	4 cells	4 cells	4 cells	4 cells	4 cells

7. EXPERIMENTAL RESULTS

7.1 Bulk Diffusion Tests

Bulk diffusion tests were conducted on all mortar mixes used in the diffusion and migration tests. The results of the bulk diffusion tests were then used in a comparative analysis of the diffusion coefficients obtained from the split-cell diffusion tests (to be discussed later). The BDT methodology was presented in Chapter 5.

Samples were taken from the mortars mixed for the split-cell diffusion and migration tests. Three cylinders were cast per mix and cured in saturated lime water for 28 days. These were then removed and the sides and bottom face coated with a thixotropic epoxy. The specimens were placed in 2.8 M NaCl solution once the epoxy had dried (29 days age). The specimens were then analysed after 90 days soaking in chloride solution. The specimens were found to have a diameter of 102 mm and could, therefore, not be accommodated in the grinding apparatus. Hence, five-millimetre saw cuts were taken, ground and titrated against silver nitrate to obtain the total chloride profile. Figures 62, 63 and 64 show typical bulk diffusion test specimen profiles for the three binder systems.

As can be seen in the figures, the 50 % GGCS profile shows a steeper concentration front. This is indicative of its chloride binding capacity. The immobilisation of ions decreases the free concentration at the front and slows down the diffusion process. Results of the bulk diffusion tests can be found in Table 12.

Table 12: Bulk diffusion test results of mortar sample soaked in 2.8 M NaCl solution for 90 days

CEM 1		50 % GGCS		10 % CSF	
0.65 w:b		0.65 w:b		0.8 w:b	
D_{eff}	COV	D_{eff}	COV	D_{eff}	COV
(m^2/s)		(m^2/s)		(m^2/s)	
1.02E-11	**4.15 %**	**2.28E-12**	**13.10 %**	**7.51E-12**	**12.25 %**

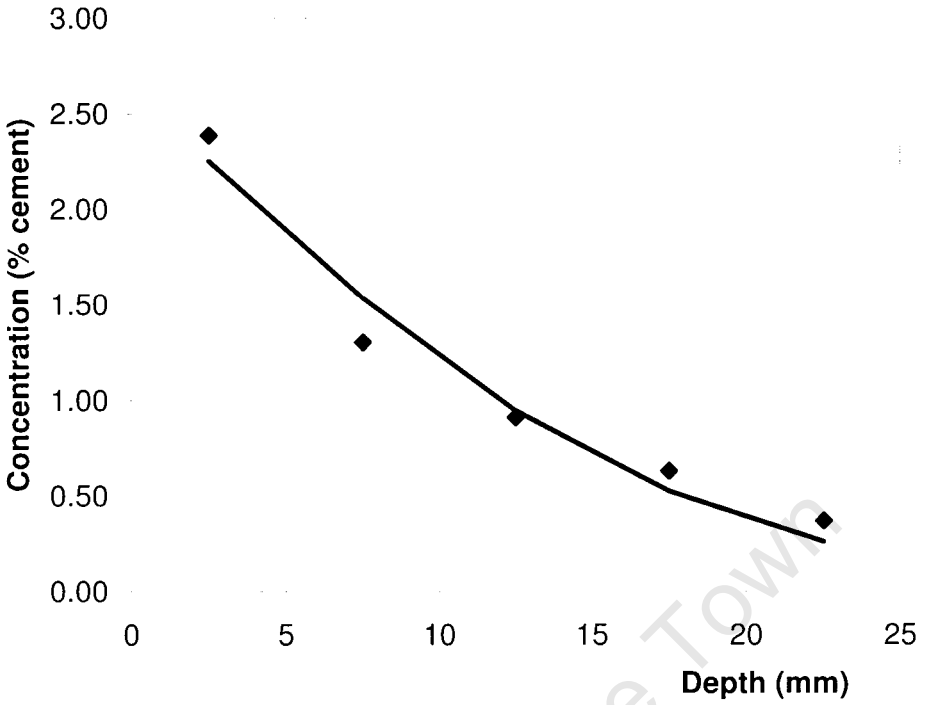

Figure 62: Bulk diffusion test profile of a 0.65 CEM 1 mortar after 90 days soaking in chloride solution

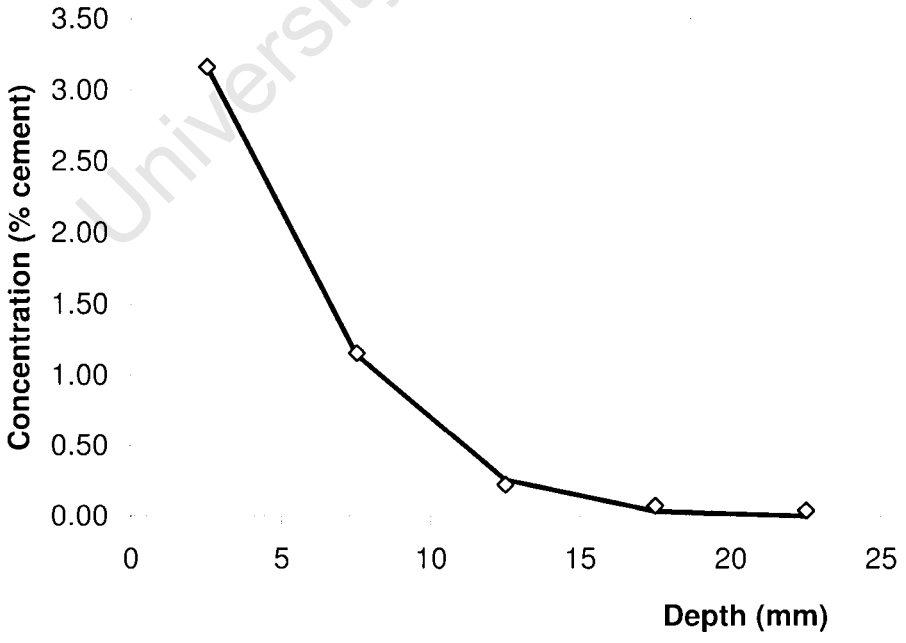

Figure 63: Bulk diffusion test profile of a 0.65 50 % GGCS mortar after 90 days soaking in chloride solution

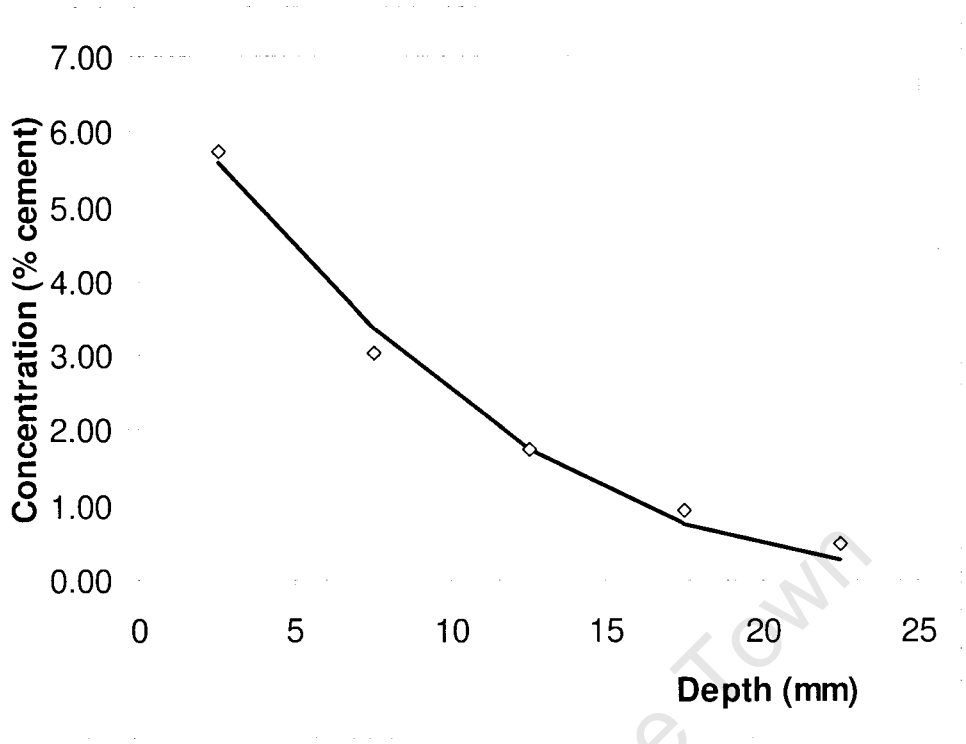

Figure 64: Bulk diffusion test profile of a 0.8 10 % CSF mortar after 90 days soaking in chloride solution

The 0.65 50 % GGCS mortar exhibited a diffusion coefficient that was an order of magnitude lower than the 0.65 CEM 1 mortar. This was expected due to GGCS's superior chloride binding capacity. As the CSF mortar was cast at a 0.8 w:b ratio, this cannot be directly compared to the other results. However, for comparison with the steady state diffusion coefficients obtained in the diffusion tests, diffusion coefficient ratios may be used (i.e. if the ratio of CSF to CEM 1 non steady state D_{eff} is x then it can be expected that the same ratio would be found for the steady state D_{eff}).

7.2 Diffusion and Migration Tests

The diffusion and migration tests were started at 28-day mortar age. The migration tests were run for two weeks and the diffusion tests for four months – in order to obtain sufficient data for analysis. Analysis of the data provided many insights into the different analysis methods available for use.

MacDonald and Northwood (1995) and Tang (1996) proposed Equation 2.13 for use in analysing finite, split-cell diffusion tests. Researchers such as MacDonald and Northwood (1995) and Tang (1996) apply this equation to finite volume split cell diffusion tests directly. Applying a linear equation to the observed data in order to calculate a single effective diffusion coefficient for the series was found to be incorrect in the case of finite volume cells. In the case of diffusion data, it was found that calculating an effective diffusion coefficient using the prediction model approach, previously discussed, is well suited, whereas in migration instances, a finite difference approach is better suited. This infers that the constants applied to Fick's First Law in arriving at the Nernst-Plank equation do not sufficiently represent migration behaviour over long periods of time. Changes in pore structure, significant changes in ion activity and changes in electrode performance significantly alter the observed behaviour.

A finite difference prediction model was used to calculate the effective diffusion coefficient from the observed data – as discussed in Chapter 6. For each cell, a least squares fit was used to obtain the effective diffusion or migration coefficients. As the change in downstream concentration is not linear, linear regression could not be directly performed. Using the least squares method, it was possible to obtain the "best fit" curve (Figure 65) – and the corresponding effective diffusion coefficient for each test.

For the migration tests, the finite difference approach was applied to the Nernst-Plank equation. This is derived from Fick's first law but constants are applied to account for the applied potential difference – as discussed in Chapter 6.

Calculating effective migration coefficients using the prediction model - incorporating the relevant Nernst-Plank constants - yielded incorrect prediction results. The prediction model calculated effective migration coefficients that were approximately an order of magnitude greater than the representative migration coefficient. This was found through visual inspection. As can be seen in Figure 66, the prediction model underestimated the early concentration levels while overestimating later levels. This resulted in a higher migration coefficient from the least squares analysis than was actually observed.

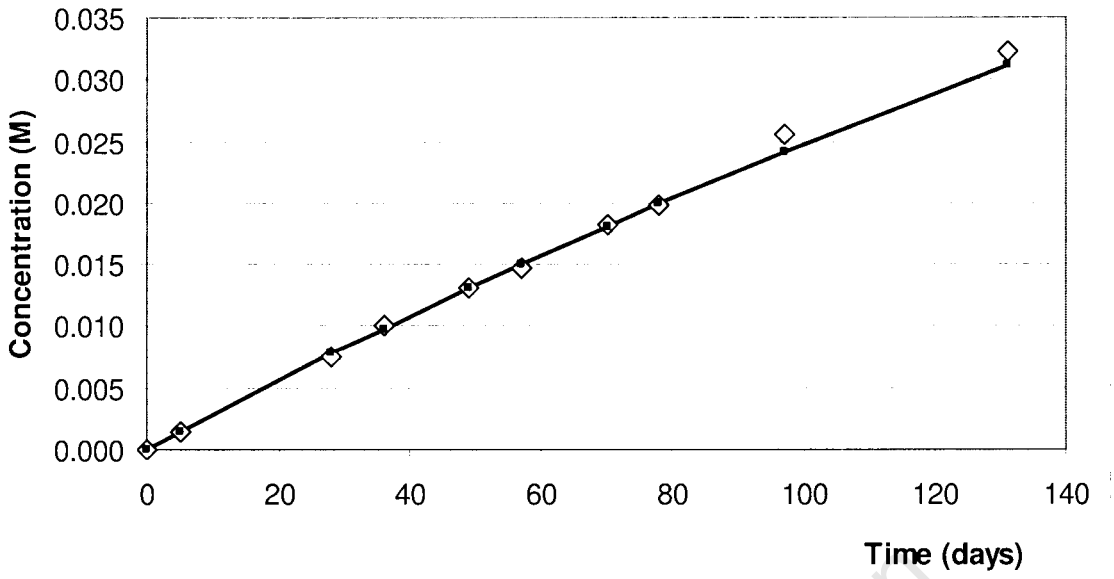

Figure 65: Prediction model vs observed data for a CEM 1 mortar at a 5 M initial chloride concentration

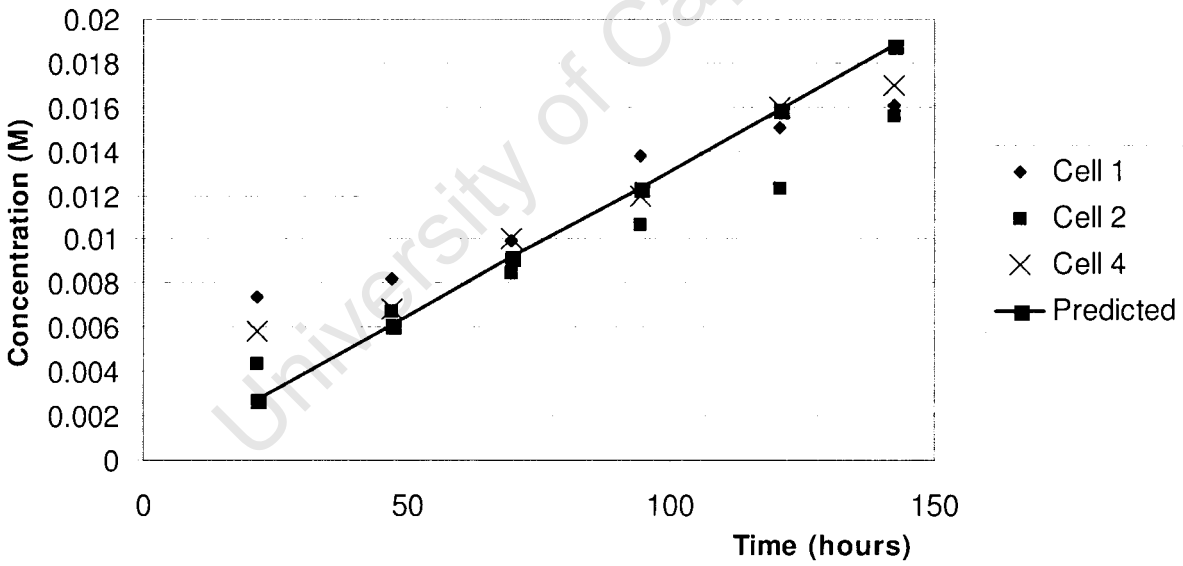

Figure 66: The prediction model, when applied to migration data, failed to correctly predict the observed data from a 50 % GGCS mortar at a 3 M initial NaCl concentration

The reason for this phenomenon is unclear but may be attributable to ion activity, which changes significantly with concentration. The migration process caused the upstream and downstream concentration to converge far more rapidly than in the diffusion tests. This would have had a significant impact on the ion activity and,

hence, behaviour in the system – as discussed in Chapter 6. It may be necessary to expand the Nernst-Plank equations (as some researchers have done – Samson and Marchand, 1999; Samson *et al*, 2003) and include an ion activity variable - as opposed to an activity constant. This would have to be based on a quadratic function approximating the ion activity versus concentration trend found in Chapter 2. However, this may prove to be impractical as different NaCl and NaOH or $Ca(OH)_2$ combinations will result in different ion activities and behaviour. It would therefore be simpler to use a finite difference method to obtain discrete coefficients which can then be averaged over a particular series of intervals.

As the migration tests were relatively rapid, changes in microstructure could not have had a significant effect. If microstructural changes were a significant factor, this would have affected the diffusion prediction model analysis far more than the migration test analysis due to the lengthy diffusion test duration.

As migration tests are rapid test methods, it was decided to use a finite difference method over the first three readings of test in order to obtain three discrete migration coefficients (as discussed in Chapter 6). These were not significantly different and were averaged to obtain an effective migration coefficient per sample.

The resulting sample coefficients were then averaged to obtain an effective diffusion or migration coefficient per concentration.

7.2.1 Test Variability

In order to analyse test variability in relation to initial chloride concentration, the linear equation given by MacDonald and Northwood (1995) was used to generate linear prediction curves. The diffusion and migration coefficients of each set of four identical cells with the same initial concentration were applied to the formula given by MacDonald and Northwood (9.1). This allowed linear data sets to be obtained – an example of which can be found in Figure 67. As the diffusion and migration coefficients are the same for all instances of steady state ion transport, this method could be applied to generate data from the actual effective transport coefficients obtained from the diffusion and migration tests.

Linear regression was then conducted on the generated data sets. This allowed the variation within the particular starting concentration to be determined. Analysis of

variation (ANOVA) yielded F statistics (describing the goodness of fit of the linear relationship) and *p values* (the significance of the regression coefficients obtained) for each initial concentration. By comparing these statistics, it was possible to identify the initial concentration corresponding to the lower test variability. It was also possible to consider the coefficients of variation obtained from averaging the cell diffusion coefficients.

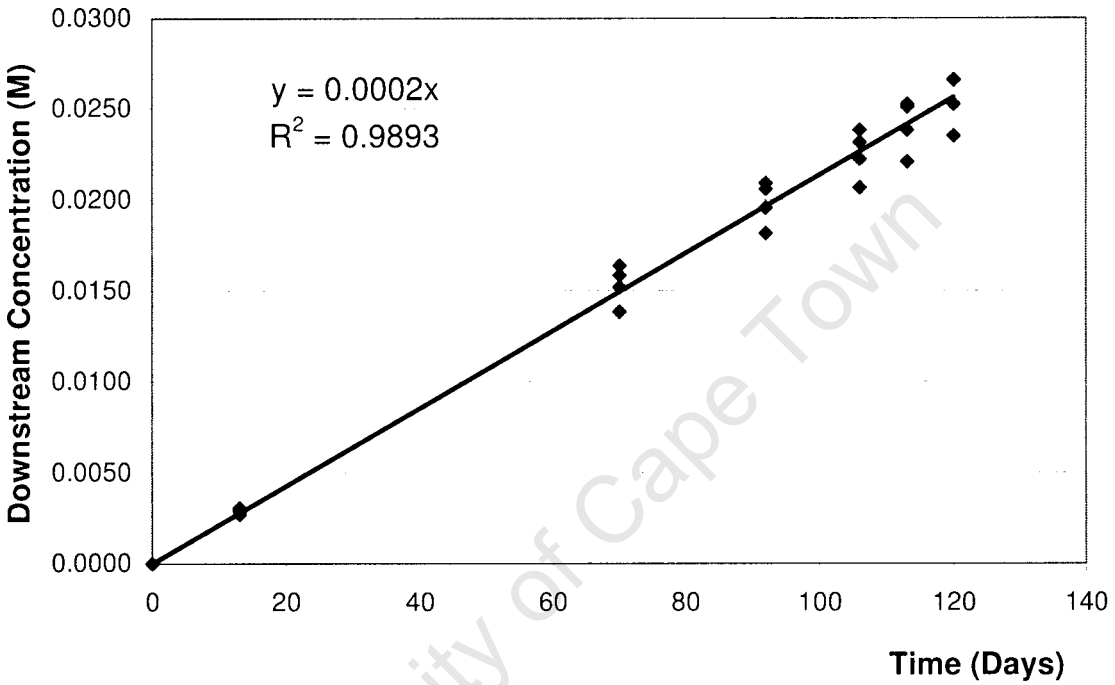

Figure 67: Data points generated from calculated diffusion coefficients of four identical cells, using linear, steady state migration theory

7.2.2 Diffusion Test Results

Examples of the diffusion data observed are presented in Figures 68 and 69. All data obtained and analysed can be found on the accompanying CD (Appendix 2).

The diffusion test results are presented in Tables 13 and 14. Table 13 shows the calculated diffusion and migration coefficients as well as the ratio of migration coefficient to diffusion coefficient. This gives an indication of the extent to which the migration coefficient over- or underestimates the diffusion behaviour. Table 14 shows the significance values of the ANOVA results (p values), the coefficient of determination of the linear regression analysis, as well as the coefficient of variance

found when calculating the averages of the four effective diffusion coefficients obtained for each initial chloride concentration and binder system.

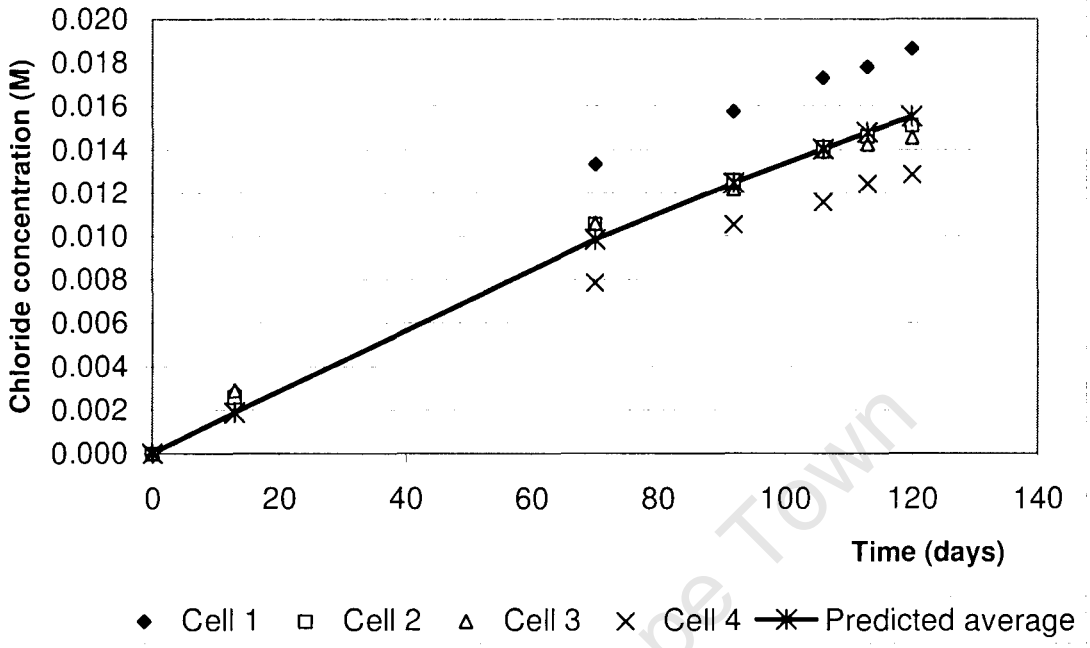

Figure 68: Observed diffusion data for the downstream cells of the four CEM 1 mortars at 3 M initial upstream chloride concentration

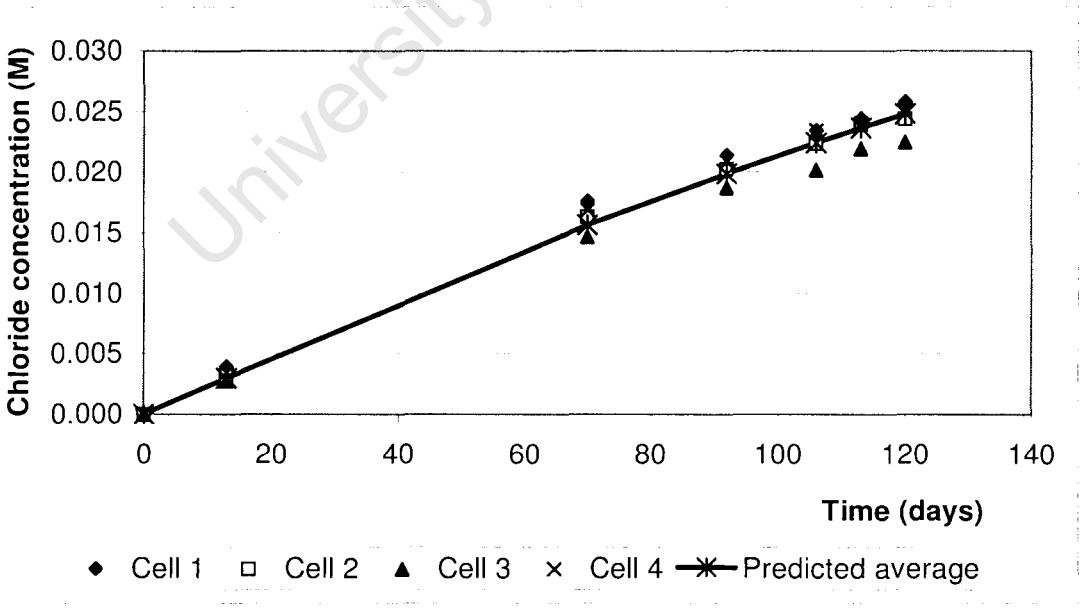

Figure 69: Observed diffusion data for the downstream cells of four CEM 1 mortars at 5 M initial upstream chloride concentration

CEM 1

The least variable results were obtained at a initial concentration of 5 M (corresponding to the highest r^2 value and the lowest coefficient of variation, F statistic and *p value*). This concentration also corresponded to the lowest average effective diffusion coefficient.

The low D_{eff} at 5 M is unexpected as ion activity increases considerably at this level. It must be noted that, due to the inherent variability of concrete and its constituents, these effective diffusion coefficients are, for all practical purposes, the same across concentrations.

GGCS

The GGCS samples exhibited the most consistent results at 1 M initial concentration. Due to the local minimum in ion activity found at approximately 1 M chloride concentration, these results could be expected and support the hypothesis that ion activity (initial chloride concentration) affects test variability.

The GGCS mix exhibited consistently lower effective diffusion coefficients than the CEM 1 mix. This is to be expected due to its enhanced chloride binding properties.

CSF

The CSF samples showed most consistent results at the 3 M level. The low D_{eff} at 1 M is as expected due to ion activity.

It can be seen in Table 15 that the trends observed in the split cell diffusion test, using the CEM 1 data as a benchmark, are similar to those found in the Bulk Diffusion Test. As previously discussed, the BDT is known to be a good representation of non-steady state diffusion behaviour, and non-steady state diffusion coefficients are directly proportional related to steady state diffusion coefficients at a given concentration. For comparative purposes, it can be seen that testing at 3 M gives the most representative results for GGCS – CEM 1 comparison; and at 1 M for CEM 1 – CSF comparison.

The concentration at which the most consistent results could be obtained varied with mix characteristics. No single concentration appears to be preferable for chloride diffusion testing of all or any concrete mix.

Table 13: Diffusion and Migration Coefficient Comparison

	Initial chloride concentration	Diffusion Coefficient (D_{eff})	Ratio of Migration coef. to Diffusion coef.	Migration Coefficient (M_{ss})
		(m^2/s)		(m^2/s)
CEM 1	1 M	5.71E-12	11.2	6.38E-11
	3 M	5.49E-12	9.9	5.41E-11
	5 M	4.94E-12	7.1	3.50E-11
GGCS	1 M	1.75E-12	30.3	5.30E-11
	3 M	1.25E-12	19.4	2.42E-11
	5 M	1.88E-12	10.2	1.92E-11
CSF	1 M	4.32E-12	22.0	9.51E-11
	3 M	4.89E-12	11.0	5.40E-11
	5 M	4.65E-12	10.2	4.74E-11

Table 14: Variability test results for calculated diffusion and migration coefficients

		Diffusion			Migration		
		Significance value (p)	r^2	D_{eff} COV	Significance value (p)	r^2	M_{ss} COV
CEM 1	1 M	1.31E-26	0.95	15.4%	**1.24E-13**	**0.97**	**9.3%**
	3 M	3.65E-24	0.93	18.6%	4.66E-10	0.97	27.3%
	5 M	**9.21E-36**	**0.99**	**6.5%**	3.35E-14	0.95	15.1%
GGCS	1 M	**2.77E-35**	**0.99**	**5.6%**	1.36E-10	0.97	1.4%
	3 M	1.23E-31	0.98	7.7%	1.90E-15	0.96	12.0%
	5 M	8.13E-21	0.88	23.0%	**1.77E-19**	**0.97**	14.5%
CSF	1 M	8.93E-16	0.76	13.5%	2.28E-15	0.947	17.2%
	3 M	**1.25E-28**	**0.98**	**9.1%**	**2.22E-26**	**0.996**	**4.2%**
	5 M	7.06E-23	0.93	14.2%	5.28E-15	0.91	24.7%

Table 15: Diffusion test results compared to the Bulk Diffusion Test results

		BDT	Steady State Diffusion Coefficient (m^2/s)		
			1	3	5
CEM 1		1.02E-11	5.71E-12	5.49E-12	4.94E-12
0.65 w:b	COV	4.15%	15.40%	18.60%	6.50%
GGCS / CEM 1		**0.22**	0.31	**0.23**	0.38
GGCS		2.28E-12	1.75E-12	1.25E-12	1.88E-12
0.65 w:b	COV	13.10%	5.60%	7.70%	23.00%
CSF / CEM 1		**0.74**	**0.76**	0.89	0.94
CSF		7.51E-12	4.32E-12	4.89E-12	4.65E-12
0.8 w:b	COV	12.25%	13.50%	9.10%	14.20%

7.2.3 Migration Test Results

The migration test results are also presented in Tables 13 and 14. Figure 66 gives an example of the data collected. This was for a 50 % GGCS mortar at 0.65 w:b ratio with a potential difference of approximately 3 V applied across it and a 3 M initial chloride concentration.

CEM 1

The most consistent results were obtained at a 1 M initial concentration. The significance values of these results were not as distinctly different as those found in the diffusion test.

The highest D_{eff} corresponding to the 1 M concentration is, again, unusual due to the decreased ion activity at that concentration. In terms of r^2 values, and *p values*, there is little distinction between the least and most variable concentration.

GGCS

The 5 M solution yielded the least variable results. The difference between the 5 M and the 1 and 3 M test variabilities (*p values*) was significantly larger than those

found for the CEM 1 migration test. The coefficient of variance in the 1 M test was significantly lower than the other tests. Note: The 1 M concentration lacked in data as two of the four migration cells leaked and could not be used.

The lack of sufficient data at the 1 M level resulted in the very low coefficient of variation value. This COV should be disregarded in analysis and only the *p value* considered. The 5 M samples were considerably less variable in their migration behaviour.

CSF

The 3 M test resulted in a very good correlation (0,99) and the lowest variability statistics. It appears that low concentrations should be avoided when migration testing. Concentrations of 3 or 5 M generally yield less variable results.

7.2.4 Diffusion versus Migration

A significant difference was observed between the diffusion coefficients and the migration coefficients. The trends can be seen in Figure 70. It can be seen that the migration coefficients were significantly higher than the corresponding diffusion coefficients for both the CEM 1 and 50 % GGCS mixes, across all initial concentrations. The 50 % GGCS mortar was more affected by the electrical field than the CEM 1 mortar at lower concentrations. This indicates that chloride binding is significantly affected by the application of an electrical field.

The differentials converge at higher concentrations. This is shown graphically in Figure 71. Because these values converge as the initial concentration increases from 1 M to 5 M, this indicates that increased concentration (and associated ion activity) partially dampens the effect of the electrical field on ion-matrix interaction. As the concentration increases, it becomes more difficult for the electrical field to impede binding due to increased ion activity and local electrostatic equilibria. These results are in accordance with the findings of Castelotte *et al* (1999), as discussed in Chapter 2. However, it appears that the concentration at which the electrical field enhances binding is greater than their reported 3 M approximation.

The results of the chloride binding tests would provide further insight into these hypotheses.

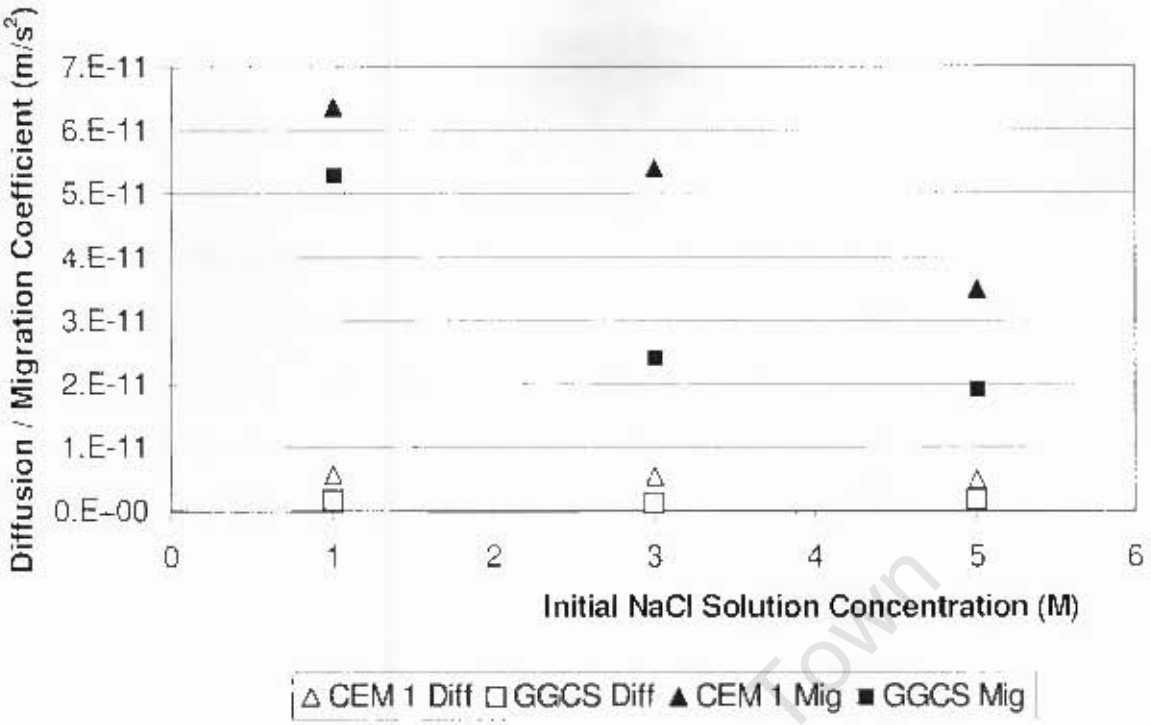

Figure 70: The effect of an electrical field on the observed transport coefficients

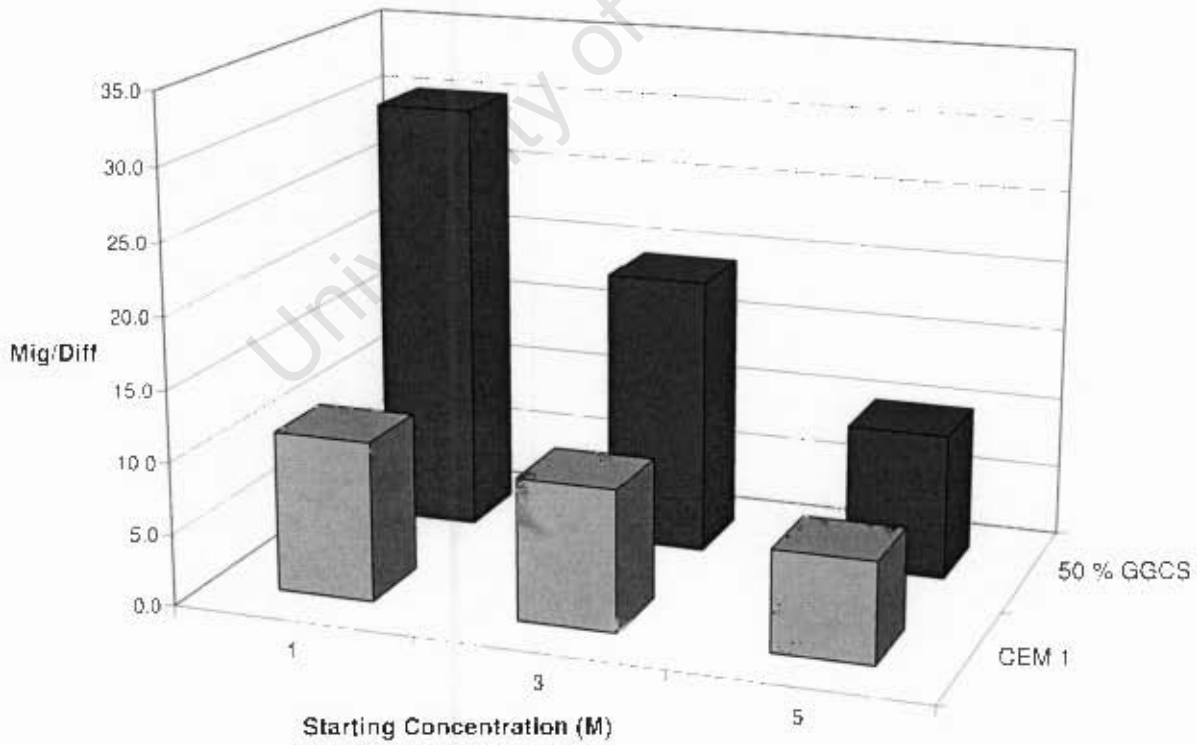

Figure 71: Ratio of migration coefficient to corresponding diffusion coefficient for the CEM 1 and 50 % GGCS mixes across all initial chloride concentrations

7.2.5 Conclusions – Diffusion and Migration Tests

The following conclusions were drawn from the diffusion and migration investigation:

- The linear equations presented by Tang (1996) and MacDonald and Northwood (1995) do not represent finite volume split cell diffusion data due to the constant decrease in upstream concentration.
- A prediction model based on the finite difference form of Fick's First Law is useful in obtaining effective diffusion coefficients for finite volume split cell diffusion tests.
- Migration coefficients could not be calculated using a prediction model based on the finite difference form of the Nernst-Plank equation. This indicates that a significant amount of extraneous factors effect the migration coefficient over time. Hence, migration testing should be limited to as short a time interval as possible.
- Test variability varied according to binder type and initial chloride concentration. No single initial chloride concentration could be associated with low test variability.
- Measured migration coefficients were generally greater than 10 times the measured effective diffusion coefficients.
- This differential decreased significantly with increased initial chloride concentration.

Diffusion tests exhibit lower variability at concentrations specific to the particular extender employed. However, in migration testing, concentrations above 3 M can be used to minimise test variability.

Migration testing affects chloride binding behaviour. This would disadvantage cement extenders used for their superior chloride binding capabilities. A migration test initial concentration at or above 5 M achieves results more representative of diffusion behaviour than those obtained at lower concentrations – indicating that increased initial chloride concentration dampens the effect of the electrical field on the measured transport properties. Migration testing, therefore, overestimates the effective diffusion coefficients of mortars. This would be detrimental to long term service life predictions where migration results are used to calculate diffusion

coefficients as concrete would be more conservatively designed against chloride ingress.

7.3 Results – Chloride Binding Tests

Chloride binding tests were conducted on all diffusion and migration test specimens. This was done to categorise the binding capacity of the binder systems used, as well as investigate any potential effects electrical field application may have had on binding capacity.

Diffusion specimens were removed from the diffusion cells after 120 days, crushed to a granular size varying from 0.3 to 3 mm, and placed in a NaCl solution corresponding to the specimen's initial chloride concentration in the transport tests (1, 3 or 5 M). The migration cell specimens were removed from the migration cells after 14 days. It may have been possible to allow the cell solutions to equalise using the electrical field, however, excessive corrosion of the anode may have occurred, affecting the results obtained. Once all solutions had equalised, the specimens were removed and tested. This ensured that all specimens had equal maturity and were exposed to chloride for the same length of time – the only difference being the two-week application of the electrical field in the case of the migration specimens. A portion of the specimen was dried at 100 ˚C for seven days, ground and then titrated against silver nitrate to obtain the total chloride content. The concentration of bound ions was obtained by subtracting the free chloride concentration from the total chloride concentration – as discussed in Chapter 6.

7.3.1 Diffusion Specimens

The chloride binding capacities of the diffusion specimens can be found in Figure 72. The 50 % GGCS mix showed the highest binding capacity at all total chloride concentrations. This was expected due to the increased aluminate content of this binder system. Hence, chemical binding was enhanced in this case. The 10 % CSF mix had the lowest chloride binding capacity at all concentrations due to a decrease in aluminate content.

By comparing the total chlorides to the bound chloride concentration, it is clear that a significant amount of chlorides are removed from the system by chloride binding.

These percentages can be found in Table 16. As expected, the proportion of bound ions decreased as the free chloride concentration increased from 1 M to 3 M. This is caused by the depletion of binding sites within the microstructure. However, the proportion increased from 3 M to 5 M free chloride concentration. Even though the majority of binding sites have been taken up by this point, the increased ion activity may result in further binding sites being made available. These sites would have been in existence throughout the process; however, higher ion activity and greater differences in local equilibrium between the pore solution and the matrix may make these sites available for binding at higher concentrations only. This trend is also shown in Figure 72.

The bulk porosities of the various mixes obtained by oven drying at 50 °C are also given in Table 16. Considering the results discussed above, it can be concluded that changes in chemical composition are far more effective in increasing binding capacity than changes in pore surface area (and, hence, physical binding potential). The CSF specimens had the greatest porosity – and, hence, greatest ion adsorption potential – however, these specimens had the lowest binding capacity. Also, 50 % GGCS replacement resulted in a decrease in bulk porosity (as expected). Hence, pore surface area and adsorption sites would decrease. However, chloride binding potential increased significantly with the use of GGCS due to the significant increase in chemical binding sites.

Table 16: Percentage of total chloride bound in diffusion specimens

	Initial Chloride Concentration	Bulk Porosity of control specimen (%)	Bound Chloride (%)
CEM 1	**1 M**		71 %
w:b 0.65	**3 M**	15.5 %	49 %
	5 M		61 %
50 % GGCS	**1 M**		85 %
w:b 0.65	**3 M**	10.5 %	73 %
	5 M		77 %
10 % CSF	**1 M**		58 %
w:b 0.8	**3 M**	19.4 %	42 %
	5 M		50 %

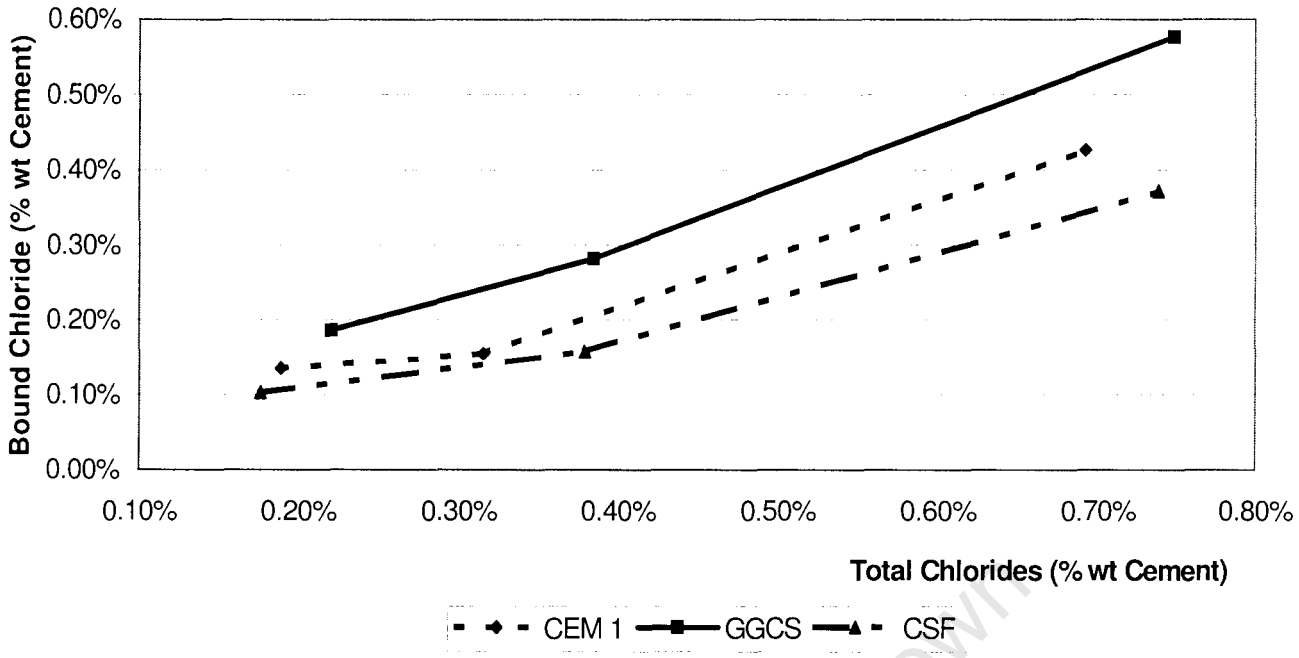

Figure 72: Chloride binding capacity of CEM 1, 50 % GGCS and 10 % CSF binder systems under diffusion conditions

7.3.2 Migration Specimens

The chloride binding capacity of the migration specimens can be found in Figure 73. Again, the 50 % GGCS specimens exhibited higher chloride binding capacity than the CEM 1 specimens. The 10 % CSF specimens exhibited unexpected behaviour. At 1 M initial concentration, the chloride binding capacity was not affected by CSF replacement. However, at higher concentrations, the CSF specimens exhibited higher chloride binding capacity than both the CEM 1 and GGCS specimens. As the CSF specimens had lower chemical binding potential, but exhibited greater total binding potential, it can be concluded that the electrical field had a greater effect on the chemical binding of the specimens. Chemical binding within the CSF specimens would have been suppressed. However, adsorption is the predominant mechanism of chloride binding in these specimens – hence the limited effect the electrical field had on these specimens.

The CEM 1 and 50 % GGCS specimens exhibited the expected decreasing trend in proportion of bound chloride with increasing chloride concentration (Table 17).

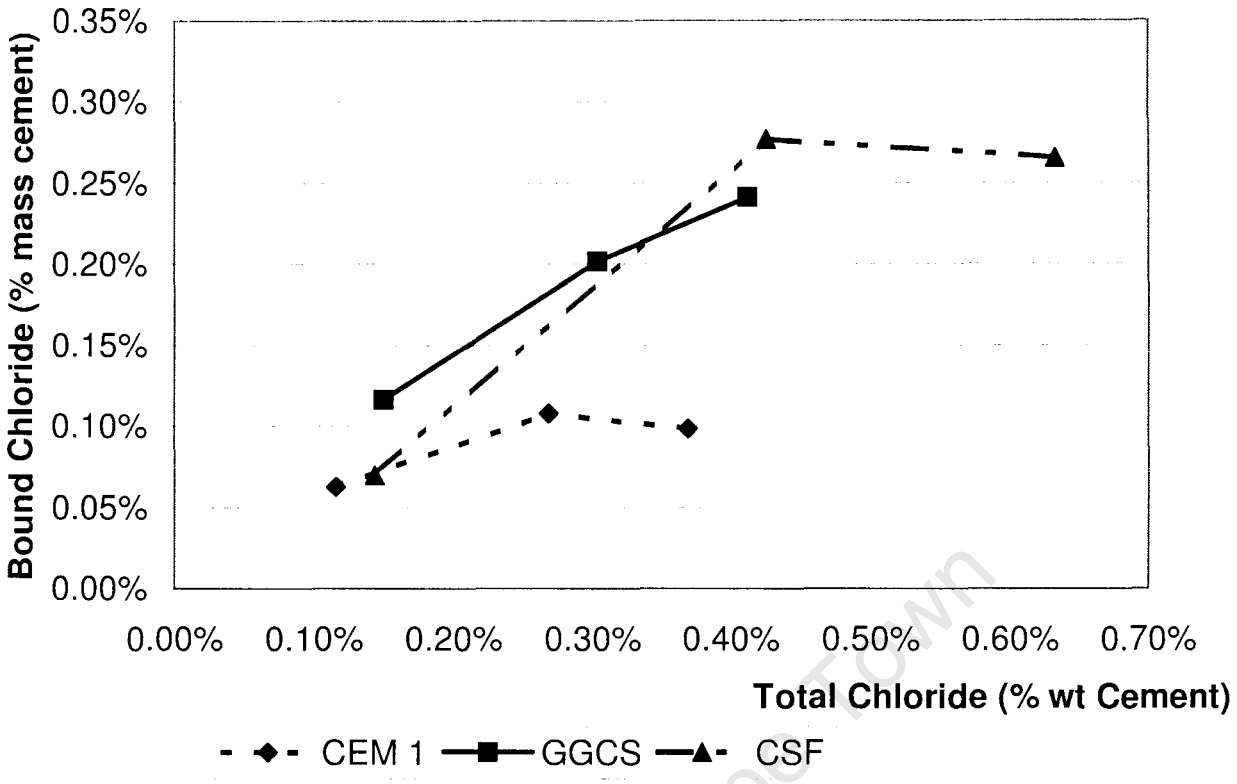

Figure 73: Chloride binding capacity of CEM 1, 50 % GGCS and 10 % CSF binder systems exposed to migration testing and then soaking in chloride solution

Table 17: Percentage of total chloride bound in migration specimens

	Initial Chloride Concentration	Bulk Porosity of control specimen (%)	Bound Chloride (%)
CEM 1	**1 M**		54 %
w:b 0.65	**3 M**	15.5 %	40 %
	5 M		27 %
50 % GGCS	**1 M**		78 %
w:b 0.65	**3 M**	10.5 %	67 %
	5 M		59 %
10 % CSF	**1 M**		48 %
w:b 0.8	**3 M**	19.4 %	54 %
	5 M		41 %

The 10 % CSF specimens did not exhibit the expected trend. As adsorption involves ion substitution on the pore walls, this would require less energy than chemical binding where ions must be displaced from a lattice structure. It is, therefore, possible for a significant amount of physical binding sites to be taken up at low chloride concentrations in the CSF specimens – hence the large proportion at 3 M chloride concentration.

The decrease in concentration of bound chloride from 3 M to 5 M in both the CEM 1 and CSF specimens may also be attributed to the impact of the electrical field on physical adsorption. As these bound ions can be desorbed under differing conditions, it is possible that a decrease in bound chlorides can occur.

7.3.3 Diffusion versus Migration Specimens

The chloride binding isotherms of all specimens are shown in Figure 74. As the total concentration of chloride within the mortar increases as chloride binding increases, it can clearly be seen that the chloride binding capacity of almost all specimens was significantly reduced by the application of an electrical field. Only the 10 % CSF specimen showed a slight increase in chloride binding capacity at the 3 M level. The CEM 1 and GGCS specimens were able to bind approximately 50 % less chloride than was possible under diffusion conditions.

The electrical field was only applied to the specimens for two weeks, followed by over 100 days of soaking in chloride solution (ordinary diffusion conditions). Significant changes in binding capacity occurred in these specimens, even though they were subjected to ordinary diffusion. It is, therefore, possible that the application of an electrical field to concretes and mortars not only alters the short-term behaviour of chloride ions and chloride binding capacity, but appears to alter the electrochemical nature of the matrix indefinitely.

Figure 75 shows the concentration of bound chloride ions versus free concentration for all specimens. At all free concentrations, the absolute amount of bound chloride significantly decreased when an electrical field was applied to the sample. The greater the specimens' ability to chemically bind chlorides the greater was the decrease in chloride binding capacity. This indicates that the application of an electrical field negatively affects chemical binding more than physical binding (adsorption).

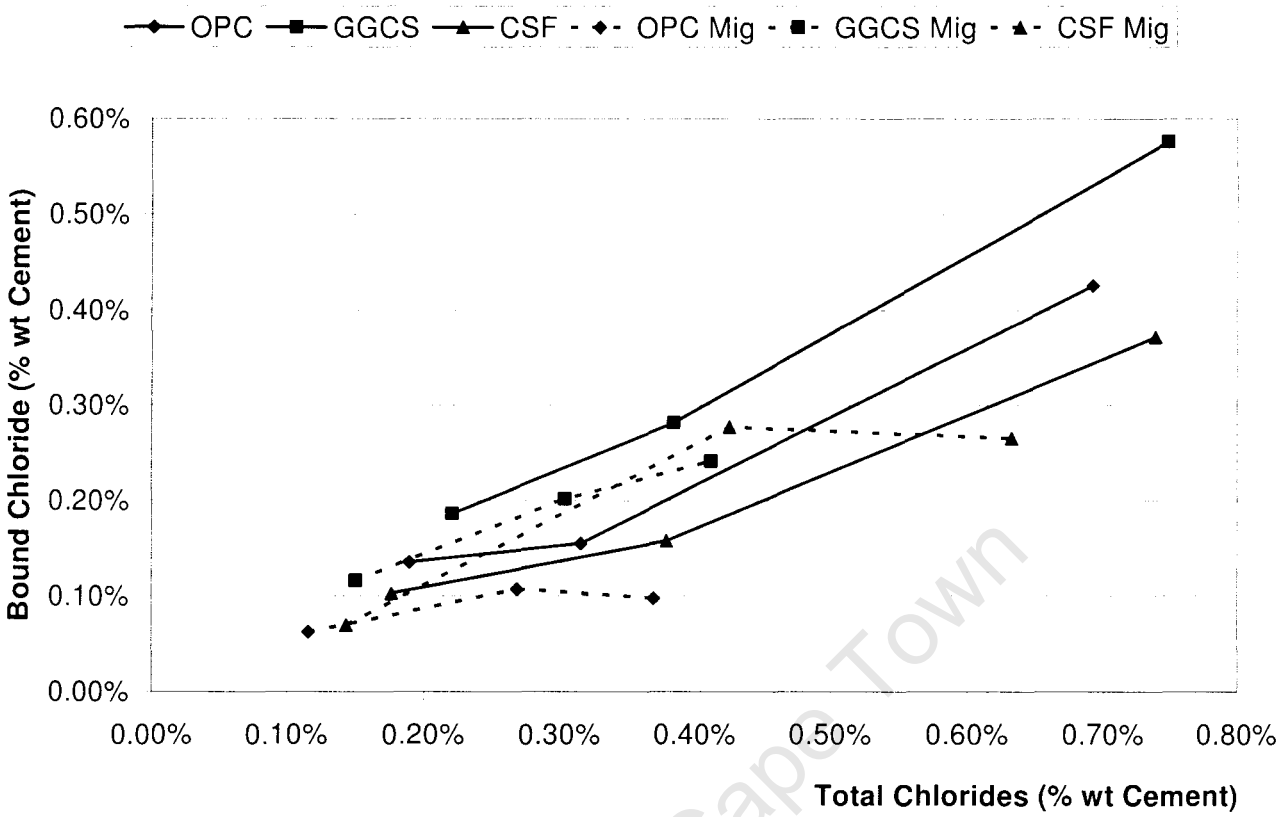

Figure 74: Comparison of binding isotherms of diffusion and migration specimens

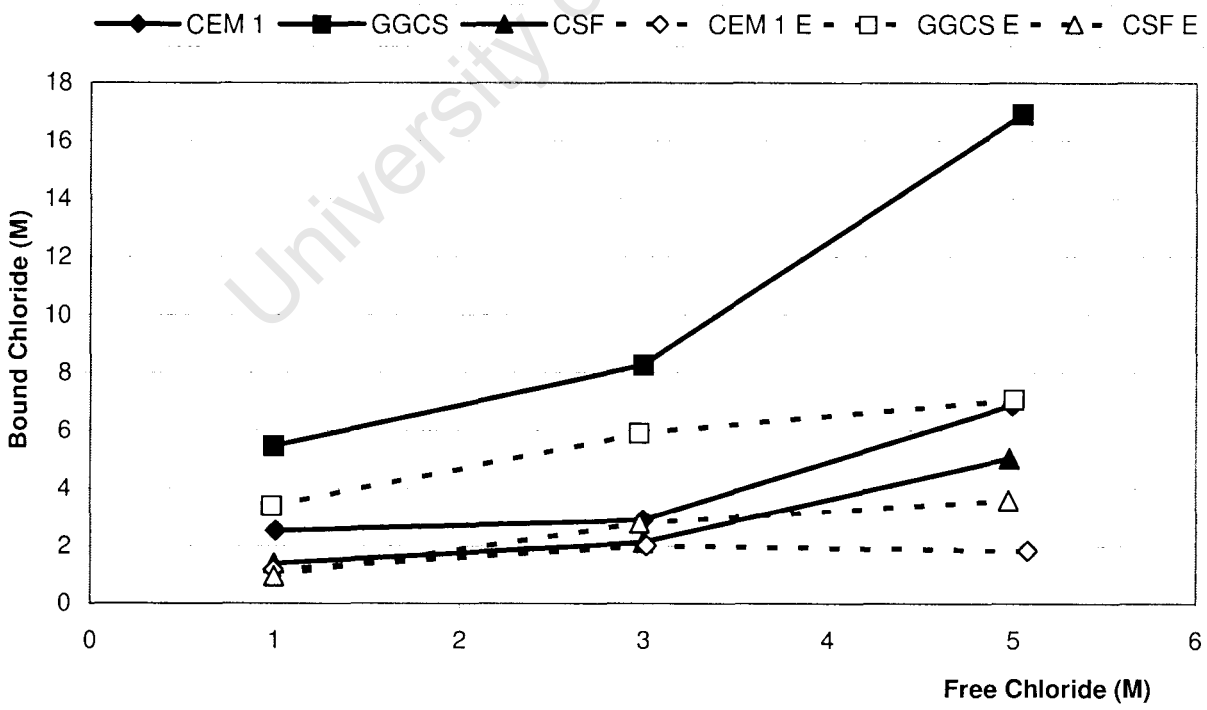

Figure 75: Free versus bound chloride concentrations for all specimens

7.3.4 Conclusions

The following conclusions were drawn from the chloride binding test analysis:

- GGCS exhibits superior chloride binding capacity under diffusion conditions and should, therefore, be used in concretes for chloride environments.
- CSF exhibits lower chloride binding capacity than CEM 1. This may be attributed to the lower aluminate content of CSF.
- The application of an electrical field significantly suppresses chemical chloride binding. This results in an overall reduction in chloride binding capacity of up to 50 %.
- The effect of an electrical field appears to be permanent, reducing the chloride binding capacity of the matrix indefinitely.

Ground granulated Corex slag mixes exhibited superior chloride binding capacity. This is due to its increase aluminate content. The decrease in porosity associated with the use of GGCS does not significantly alter the overall binding capacity.

Condensed silica fume has low chloride binding capacity due to a decrease in the aluminate content of the mix.

The application of an electrical field to mortar specimen significantly alters the binding capacity, decreasing it by as much as 50 %. GGCS and CEM 1 mixes are affected more by the electrical field than CSF mixes (where adsorption dominates). Hence, chemical binding appears to be affected more severely than adsorption.

Electrical field application appears to alter the electrochemistry of the cementitious matrix indefinitely. The effects of electrical field application alter chloride binding potential even after the electrical field has been removed. This finding would be concerning in the field of electrochemical chloride extraction as the alteration in electrochemistry would affect the concrete or mortar's long term performance in a chloride environment.

It is possible that the application of an electrical field significantly increases the chemical binding potential of other ions in the pore solution (such as sulphates) resulting in them being preferentially bound.

8. MICROSCOPY

Ordinary light microscopes employ various lens configurations and filters to create a magnified view of a sample. This method has various useful applications but also has many drawbacks. Light microscopy has a limited range of magnification that may, in some cases, be insufficient. Ordinary research microscopes have magnification ranges from 2 to 100 times. This allows a limited amount of detail to be obtained. Samples for light microscopy must also be carefully prepared. At low magnification, topography and relief can be observed. This, however, cannot be photographed, as a camera lens does not pick up the dual view needed for three-dimensional viewing. Stereoscopes could be employed but most light microscopy is predominantly done on carefully prepared flat samples or epoxy impregnated thin sections, rendering the capacity for topographical viewing very low.

In the case of cement and concrete, sample preparation can be destructive. Epoxy impregnation must be used due to the brittle nature of the material. Epoxy impregnation requires drying of the samples, which may result in microcracking. This method may also lead to problems when chlorides within the microstructure are to be observed. As the samples dry, chlorides are carried by the pore water, and diffusion forces, and are deposited on the sample surface. This affects the system due to precipitation and leaching of chlorides. The epoxy impregnation may also remove or displace chlorides, as well as upsetting the crystal structure. Relatively new developments in electron microscopy have provided other methods for concrete technologists to observe their samples. Cryogenic backscattered SEM allows fractured surfaces to be observed and does not require harsh sample drying or preparation techniques.

8.1 Cryogenic Backscattered Scanning Electron Microscopy (BSEM)

Cryogenic BSEM was used to analyse the cementitious samples. The samples were carefully fractured, to expose the internal microstructure not in contact with the curing solution. The fractured fragment was then mounted on a copper sample stage with

the aid of a mild adhesive. The sample was placed under vacuum and frozen in liquid nitrogen. The vacuum was maintained as the sample was placed in the vacuum chamber of the microscope for viewing. It was imperative that the sample did not come into contact with the atmosphere, as slight melting of the surface ice crystals (forming liquid water) would detrimental to the subsequent sublimation process. A low temperature was maintained in the vacuum chamber (80K to 190K) but allowed to rise slightly, resulting in sublimation of the water surrounding the sample and in the sample pores. This allowed the cementitious microstructure and Friedel's Salt crystal structure to be observed relatively undisturbed.

8.2 Sample Analysis

Trial observations showed that using the secondary electron detector and the backscattered electron detector in tandem allowed microstructural components to be more easily identified. The complex microstructure can be deciphered using knowledge of the expected elemental compositions of the various compounds, the expected abundance of any given compound and the structure of the compounds and crystals present.

Secondary electron images are very accurate visual depictions of the structure and topography. Crystal structures and different compound forms, textures and abundance are clearly discernable.

The backscattered detector is then used to verify these hypotheses and generate an elemental spectrum to identify likely elements present (similar to X-ray diffraction but using backscattered electron intensity). The BSEM was very beneficial in identifying small deposits of Friedel's Salt in capillary pores. At relatively low magnifications, small specks of the salt could be seen in the BSEM images that are not discernable in the secondary SEM images.

This allowed one to then zoom in on the capillary pores likely to house Friedel's Salt and investigate the structure and location of the Friedel's Salt crystals. The low magnification images were used to qualitatively analyse the overall abundance of the salt.

As fractured surface were investigated, the topography and porosity meant that the microscope could not perform optimally. Flat samples allow a maximum amount of

electrons to be detected by the detectors. The topographical samples caused a portion of the electrons to be scattered erratically and not be picked up by the detectors. For this reason, very high magnification shots were not possible due to lack of "focus" in the resulting images. Pores up to 1 μm in diameter could be observed but the internal structure was not clearly discernable. However, this high level of magnification is unnecessary as sufficient features can be seen at lower magnifications.

8.3 Observations

Apart from the observations presented in relevant chapters (Hydration Products and Chemical Binding), other significant observations was made.

8.3.1 CSH Gel Densification

It was possible to observe and identify various morphologies of CSH gel. In control samples, continually submerged in limewater for 28 days, Type I and II CSH gel dominated the microstructure. Bulk diffusion test samples, which had been exposed to NaCl ingress at 28 days, showed predominantly type II and III CSH gel. This can clearly be seen when comparing Figure 76 and Figure 77. This implied that the CSH morphology changed and densified after chloride ingress had taken place. This was later investigated with the use of pulse velocity testing.

8.3.2 Friedel's Salt Formation in Diffusion and Migration Samples

A difference existed between the Friedel's Salt formation in the Bulk Diffusion Test samples and in the Migration Test samples. In the BDT samples, Friedel's salt deposits occurred in large clusters (Figures 78, 79 and 80). These were easily discernable and prolific. In the migration samples, the Friedel's Salt formations were less prolific and found in small, discrete deposits (Figures 81 to 84). These are the same crystal structures as identified by Luo *et al* (2003). This is in support of Castelotte *et al's* (1999) work, in which the conclusion was drawn that the amount of chloride binding under an electrical field is far less than that under natural diffusion, for a free chloride concentration below 2 M. All observations were confirmed by EDX (Figure 85).

Figure 76: CEM 1 control sample showing Type I CSH gel with imbedded calcium hydroxide crystals

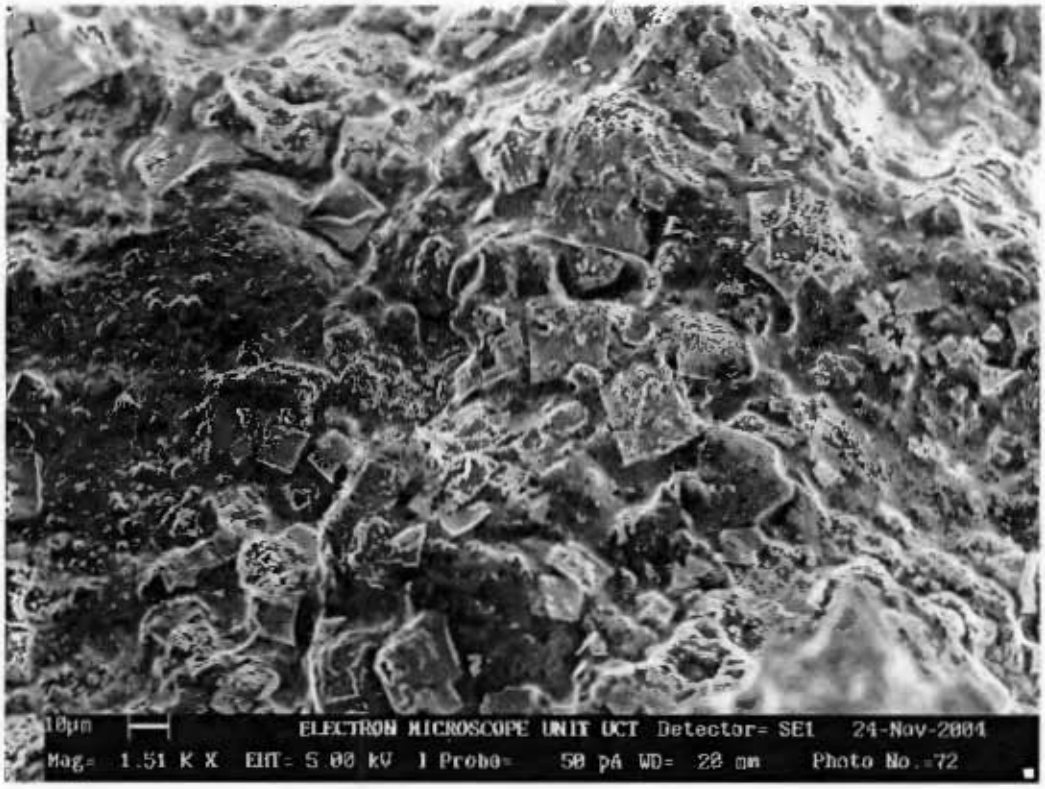

Figure 77: CEM 1 bulk diffusion test sample showing prolific Type III / IV CSH gel with imbedded calcium hydroxide crystals

Figure 78: BSEM showing a distinct Friedel's Salt cluster.

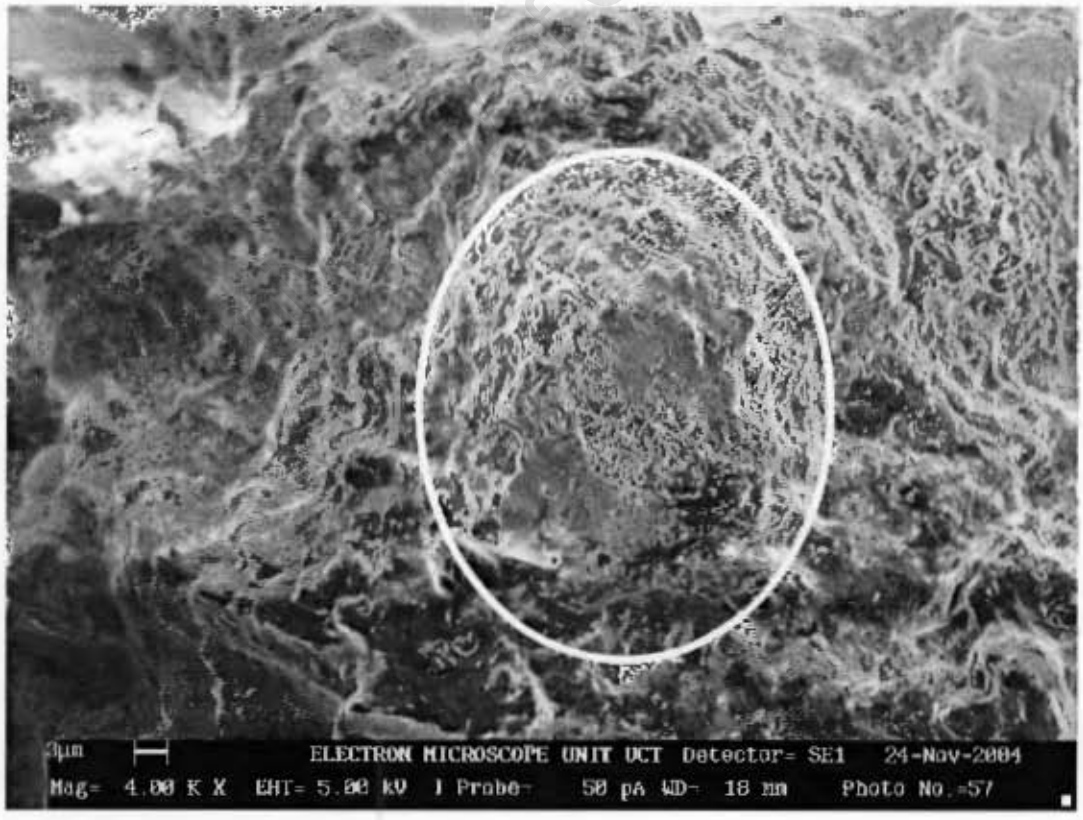

Figure 79: The same Friedel's Salt clusters (Figure XXXX) were difficult to identify with secondary electron imaging.

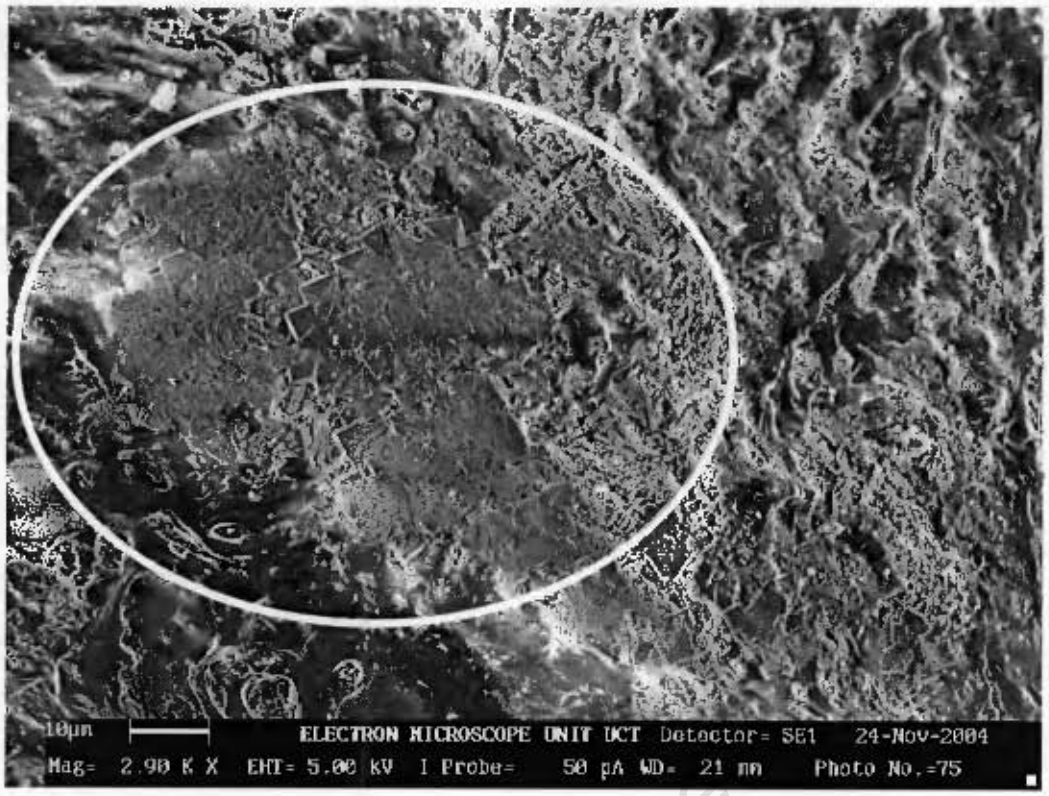

Figure 80: Distinct cluster structure characterises Friedel's Salt formation under ordinary diffusion conditions

Figure 81: Singular Friedel's Salt crystal, verified by EDX.

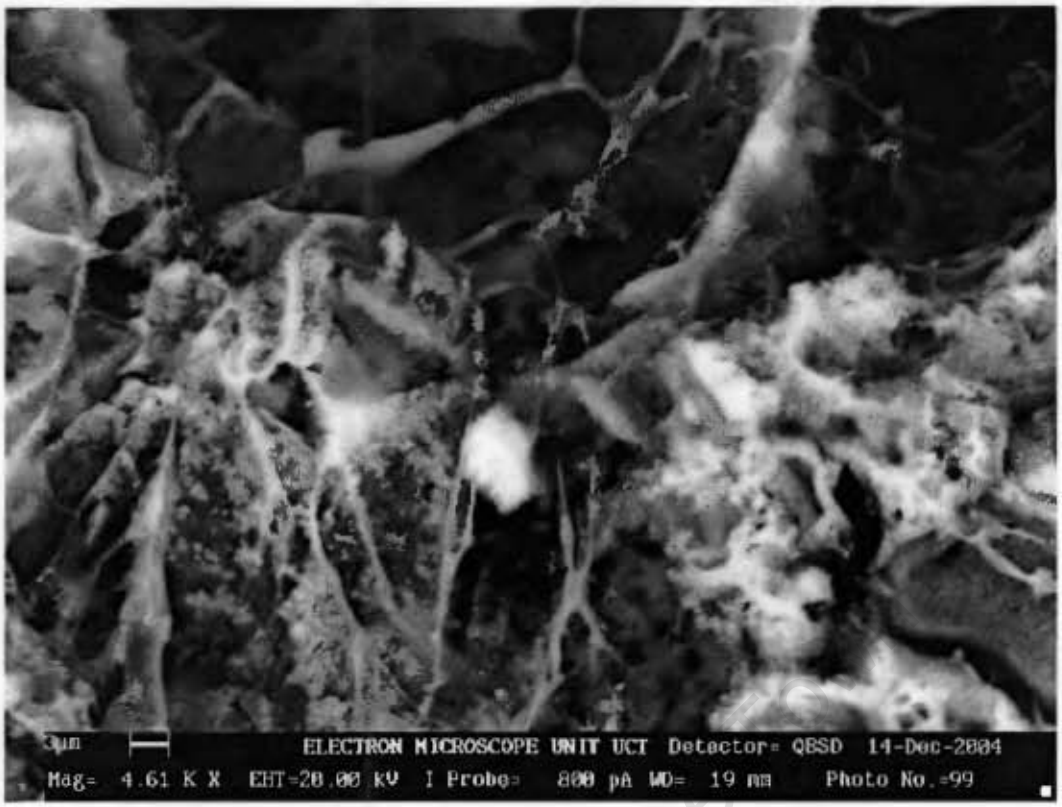

Figure 82: BSEM showing Friedel's Salt crystal in the centre.

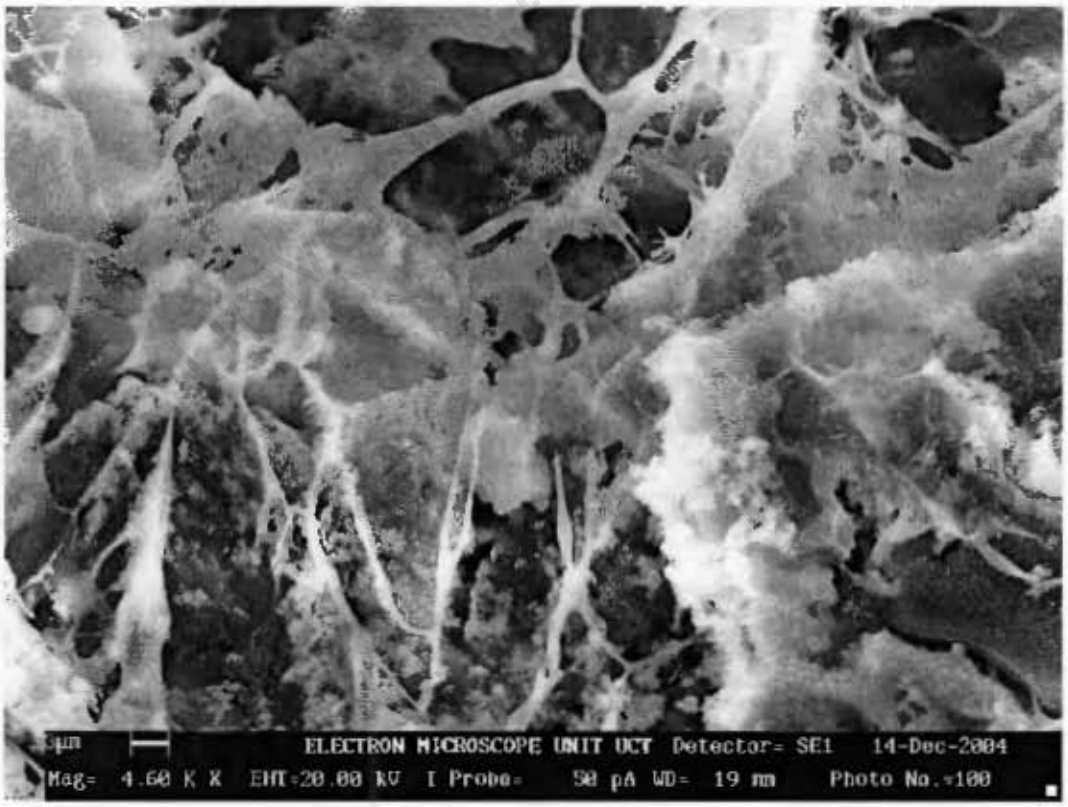

Figure 83: Secondary SEM image showing Friedel's Salt crystal in the centre.

Figure 84: Singular Friedel's Salt crystal of differing morphology.

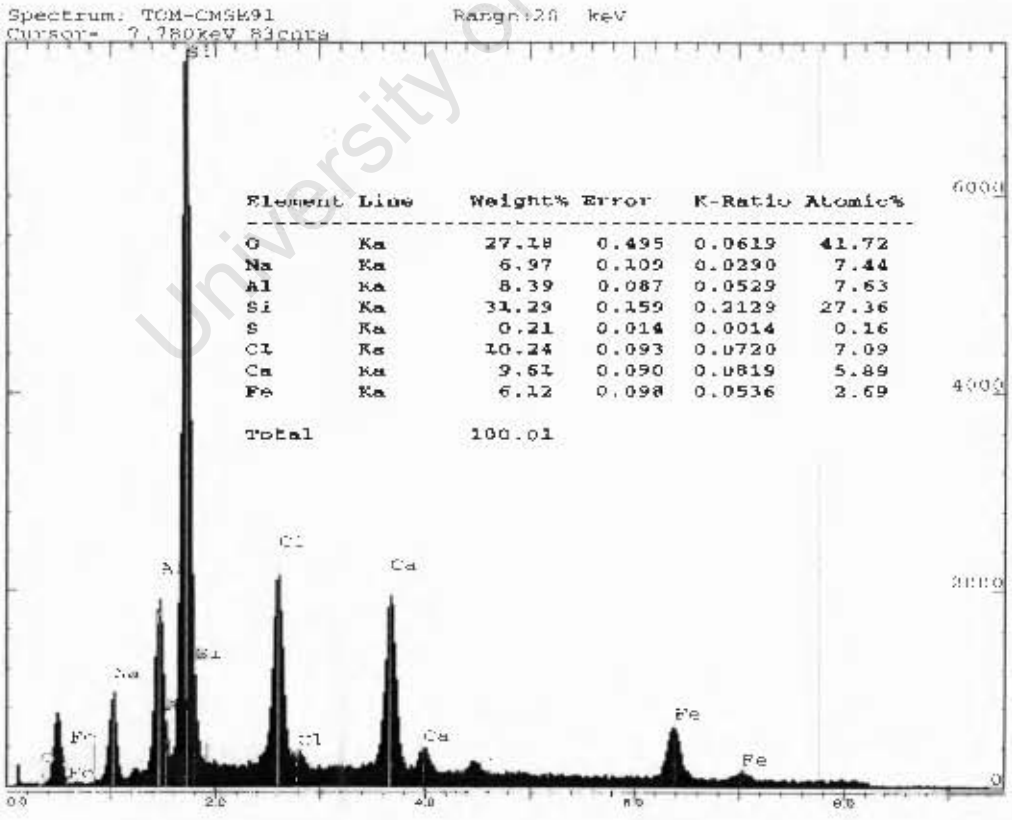

Figure 85: EDX of singular Friedel's Salt crystal.

8.3.3 Barium Sulphate Deposits in GGCS Samples

In the 50 % GGCS bulk diffusion test mortar samples, a substantial amount of barium sulphate deposits were found interacting with the CSH gel (Figure 86 and 87). Tsuyuki *et al* (2000) conducted a study on the effect of $BaSO_4$ on hydration products and chloride binding. $BaSO_4$ is inherently insoluble, with a solubility product constant (K_{sp}) of 1.3 X 10^{-6}. This can be compared to the solubility product of NaCl, which is 36. It was found that during the hydration of C_3A to form C_3AH_6, two intermediate phases are passed of the forms C_4AH_{19} and C_4AH_{13}. These phases have a layered structure like monosulphate and readily exchange OH^- ions with other compounds. When $BaSO_4$ is incorporated in this process, the chemical forces are strong enough to dissolve the $BaSO_4$, allowing the SO_4^{2-} ions to enter the lattice structure and effectively form further monosulphates. XRD on specimens subjected to chloride ingress showed conclusively that Friedel's Salt formation increased significantly in the presence of $BaSO_4$. MIP showed no significant difference in pore structure, however, chloride ion permeability decreased in the presence of $BaSO_4$, as result of increased chloride binding capacity.

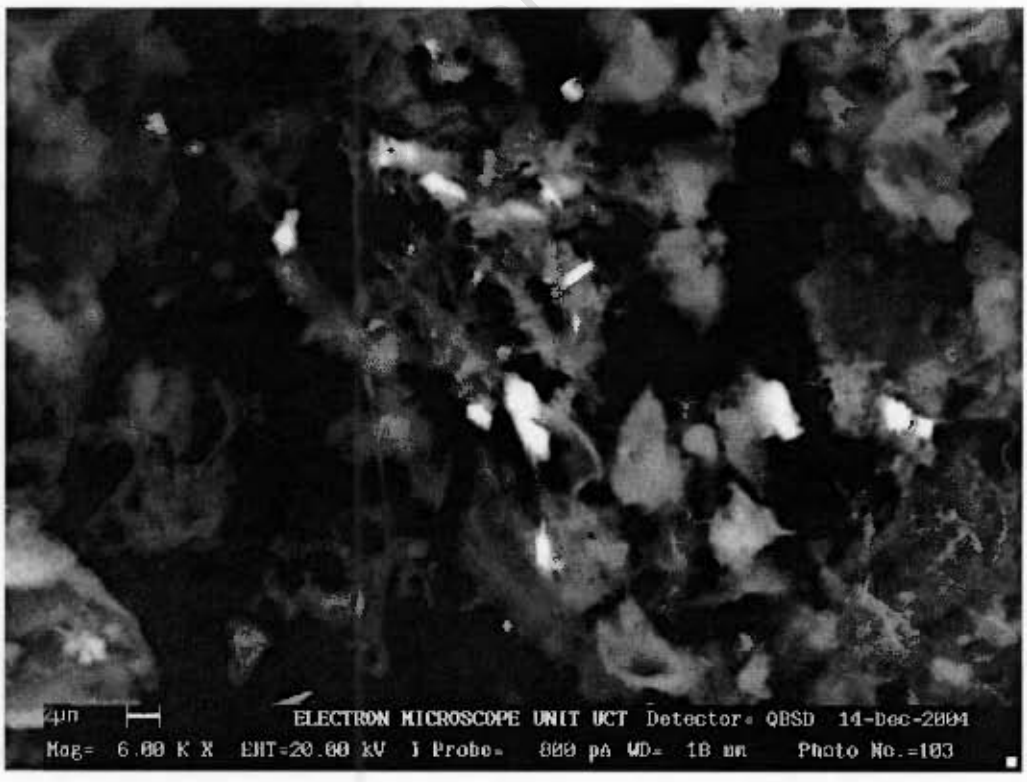

Figure 86: BSEM of barium sulphate deposits interacting with the C-S-H gel.

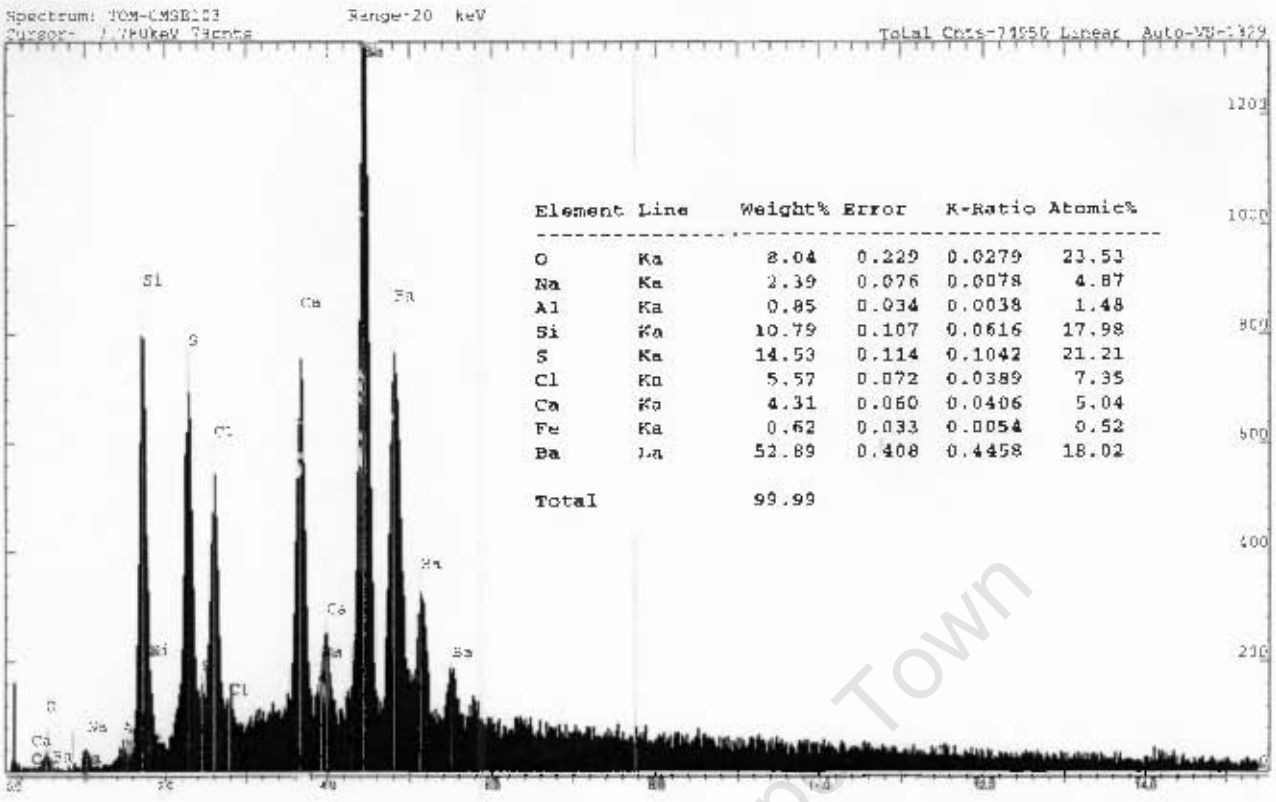

Figure 87: EDX of barium sulphate compound

The $BaSO_4$ found prolifically in the GGCS mortar indicates that over and above its increased aluminate content, the presence of barium sulphate is a further benefit of using GGCS as a supplementary cementitious material. The presence of either $BaSO_4$ (Tsuyuki *et al*, 2000) or $CaSO_4$ (Xu, 1999) greatly increases the chloride binding capacity of the hardened concrete.

Other noteworthy and interesting observations, unrelated to this study, can be found in Appendix 2.

8.4 Conclusions

The SEM observations provided few qualitative conclusions. The use of fracture surfaces to avoid Friedel's Salt disruption hindered quantitative analysis. However, several definite conclusions could be drawn:

- Friedel's Salt formation under natural diffusion predominantly occurs as large clustered deposits
- Friedel's Salt formation at low chloride concentrations under migration influences occurs as singular discreet deposits
- Ground granulated Corex Slag appears to be rich barium sulphate. This is reported to enhance chloride-binding capacity.
- It appears that the presence of chlorides facilitates the formations of a denser CSH gel, with morphologies moving from the Type 1, acicular range to the Type 4, solid formation range. This will be investigated by strength and pulse velocity testing

The change in Friedel's salt morphology observed in the migration specimens – from large clustered deposits to small, singular, sporadic deposits – occurs with associated loss of chloride binding potential. Hence, it is possible that the electrical field alters the electrochemistry of the matrix to the extent that large Friedel's salt crystal formation is hindered.

The densification of CSH morphology, that accompanied chloride ingress, may affect the long-term durability of the matrix. Literature shows that a decrease in porosity occurs with chloride ingress. This may be a combination of chloride binding effects and the observed change in CSH morphology. Further work in this area is recommended.

9. CONCLUSIONS AND RECOMMENDATIONS

Migration Testing

Diffusion and migration theory do not account for non-ideal factors such as ion activity and ion-matrix interaction. Hence, Fick's Laws and the Nernst-Plank equation must be used with care when calculating diffusion or migration coefficients for long-term prediction purposes. Due to the accelerated nature of migration testing and the significant alteration in matrix properties and ion behaviour with concentration, the Nernst-Plank equation should not be used to calculate effective migration coefficients. It may, however, be used to calculate migration coefficients based on short, discrete time intervals.

A fundamental aspect of chloride transport through concrete is chloride binding. Effective diffusion coefficients are used to account for chloride binding in the fundamental transport formulae. However, chloride binding is a complex process involving chemical reaction and physical adsorption. Both of these processes are dependent on pore solution chemistry and chloride concentration. Hence, the nature and behaviour of the cementitious matrix can be expected to change significantly with time and chloride concentration.

The application of an electrical field significantly alters chloride ion behaviour in concrete. Significant differences in transport coefficients, test variability and chloride binding capacity were measured.

Measured migration coefficients are significantly higher than measured diffusion coefficients. The extent of the observed difference was highly dependent on initial chloride concentration. At 5 M initial chloride concentration, the measured migration coefficients gave a far better approximation of the measured diffusion coefficient than at 1 M and 3 M initial chloride concentration. The difference between the transport coefficients was magnified in the 50 % GGCS specimens at 1 M and 3 M initial chloride concentrations. Hence, chemical binding is greatly affected by the presence of an electrical field. This effect decreases with increased initial chloride concentration, with a negligible difference between GGCS and CEM 1 specimens at

5 M concentration. It can, therefore, be concluded that migration testing should be preferentially conducted at 5 M initial concentration.

Test variability was dependent on the binder system of the specimens. However, the highest test variability measured fell within the limits of generally accepted transport test variability. The significance of regression analysis was found to be high at all concentrations. Hence, test variability is a secondary factor, with the impact of electrical field application on the absolute measured values being of primary importance (as discussed above).

Chloride binding capacity was significantly depleted in the presence of an electrical field. The CSF mortar was the least affected, whereas the GGCS mortar was most affected. Hence, chemical binding is affected most negatively by the presence of an electrical field. This observation explains the high disparity between the measured diffusion and migration coefficients in the 50 % GGCS specimen.

Electrical field application appears to alter the electrochemistry of the cementitious matrix indefinitely. Even though specimens were allowed to soak in a chloride solution post-migration testing, binding capacity was still depleted by up to 50 %. The electrochemistry of the matrix (pore walls) may be permanently altered by the application of an electrical field. It is also possible that the electrical field significantly increases the chemical binding potential of other ions in the pore solution (such as sulphates) resulting in them being preferentially bound.

Migration testing appears to significantly alter the ion-matrix interaction of chloride ions. This decreases chemical and physical binding mechanisms, resulting in measured migration coefficients being substantially higher than measured diffusion coefficients. This affect is highly dependent on initial chloride concentration. Migration coefficients should not be used in the place of diffusion coefficients. Rapid chloride testing affects chloride ion behaviour and alters ion-matrix interaction resulting in an over-estimate of transport parameters. Hence, economical concretes, mortars and pastes cannot be designed using the migration coefficients obtained from rapid chloride test results. Likewise, the results of rapid chloride tests should not be used to calculate migration coefficients for prediction models of the long-term performance of concretes, mortars or pastes – unless the test has been calibrated for this purpose. Diffusion coefficients should be obtained from the Bulk Diffusion Test for long-term prediction calculations.

Further research is recommended in order to investigate the long-term effects of electrical field application on the chloride binding capacity of concretes, mortars and pastes. This would be beneficial in correctly estimating the long-term performance of such materials after the application of electrochemical chloride extraction.

Rapid Chloride Test Methods

The Bulk Diffusion Test is the most representative of fundamental diffusion behaviour. However, it is not a rapid test and does not suit quality assurance purposes. This test is best suited for research purposes and should be used in testing and categorising new supplementary cementitious binders, concrete coatings and repair materials. The BDT should also be used in the construction of serviceability models and in the service life prediction of sensitive structures. Care must be taken when considering the results of the BDT. Non-steady state diffusion coefficients are not constant and change with time and chloride concentration. Hence, a standard BDT test time should be used for all specimen, where possible.

The Rapid Chloride Permeability Test introduces many extraneous variables, such as temperature gain, which affects the results obtained. The test results are also significantly affected by the binder system being tested and the presence of anodic inhibitors. Improved tests have been developed, making the RCPT an obsolete test. The Rapid Chloride Permeability Test should not be used for rapid chloride testing of concretes, mortars and pastes.

The Rapid Migration Test involves a lower potential difference than the RCPT, limiting temperature effects. The colorimetric measurement technique is simple and does not rely on current measurement (as in the RCPT). Hence, the test is not as sensitive to binder system or anodic inhibitors. As an electrical field is employed in this migration test, alteration of chloride binding behaviour and the matrix may occur. As the test time spans 12 - 72 hours, significant alteration of the pore structure and matrix may result, due to chloride binding and the application of the electrical field. Hence, this test should only be used as an indication of a concrete/mortars ability to resist chloride ingress and not as a basis from which to calculate diffusion coefficients for long term service life prediction. As the test has been calibrated

against long term BDT test and in situ measurements, the RMT is suitable for rapid chloride testing and categorisation of concretes.

The Chloride Conductivity Test has the most rapid testing procedure, allowing numerous specimens to be tested in a short time. The sample preparation technique is relatively lengthy and significantly alters the microstructure of the specimens. The oven drying procedure was found to significantly alter the test results, when compared to control samples dried using organic solvent displacement. The saturation technique was shown to be insufficient. A chloride concentration gradient was found from the surface to the centre of specimens, post-saturation. This affects the pore solution conductivity significantly, therefore affecting the fundamental theory underlying the results analysis. Care must therefore be taken when using the CCT in long term prediction of serviceability. The application of an electrical field would affect this test. However, as the test time is short (seconds), the impact of the electrical field on the matrix and ion behaviour may be minimal. It is therefore the most suitable test in terms of limiting the extraneous variables introduced by migration testing. The test has been calibrated using in-situ measurements. Hence, the test is suitable for quality assurance purposes.

Further Research Recommendations

Further research is recommended in the following areas:

- Differentiation between chemical binding and physical adsorption of chloride ions in cementitious matrices. These differing mechanisms appear to be dependent on and affected by differing variables (e.g. the application of an electrical field appears to more greatly affect chemical binding). A greater understanding of chloride binding mechanisms would allow them to be more accurately measured and exploited in practice.
- The impact of chloride ingress on concrete microstructure and the implication on long term transport properties and predicted behaviour
- The long-term (permanent) effect of applying an electrical field to the concrete matrix. This has certain implications for the electrochemical chloride extraction industry.

10. REFERENCES

1. Addis, B. and Owens, G. (2001). **Fulton's Concrete Technology - Eighth Edition.** Cement and Concrete institute, Midrand, SA.

2. Ait-Mokhtar, A.; Amiri, O.; Dumargue, P. and Bougerra, A. (2004) **On the applicability of Washburn law: study of mercury and water flow properties in cement-based materials.** Materials and Structures, Vol. 37, pp. 107 – 113. RILEM, France.

3. Aitcin, P-C.; Sarkar, S.L. and Diatta, Y. (1987) **Microstructural Study of Different Types of Very High Strength Concrete.** Microstructural Development During Hydration of Cement, Materials Research Society Symposia Proceedings Vol. 85. Edited by Struble, L.J. and Brown, P.W. Materials Research Society, Pennsylvania, USA.

4. Al-Hussaini, M.J.; Sangha, C.M.; Plunkett, B.A. and Walden, P.J. (1990) **The Effect of Chloride Ion Source on the Free Chloride Ion Percentages in OPC Mortars.** Cement and Concrete Research, Vol. 20, pp. 739 – 745. Elsevier Science Ltd, USA.

5. Alexander, M.G.; Mackechnie, J.R. and Ballim, Y. (1999) Research Monograph No. 2. **Guide to the use of durability indexes for achieving durability in concrete structures.** Dept of Civil Engineering, University of Cape Town, Cape Town, South Africa.

6. Alexander, M.G. and Mindess, S. (2005) **Aggregates in Concrete.** Oxford: Taylor & Francis.

7. Alexander, M.G.; Streicher, P.E. and Mackechnie, J.R. (1999). Research Monograph No. 3. **Rapid chloride conductivity testing of concrete.** The University of Cape Town and The University of the Witwatersrand, SA.

8. Andrade, C. (1993) **Calculation of Chloride Diffusion Coefficients in Concrete from Ionic Migration Measurements.** Cement and Concrete Research, Vol. 23, pp. 724 – 742. Pergamon Press Ltd, USA.

9. Andrade, C. and Sanjuan, M.A. (1994) **Experimental Procedure for the Calculation of Chloride Diffusion Coefficients in Concrete from Migration Tests**. Advances in Cement Research, Vol. 6, No 23, pp 127 – 134. Thomas Telford, USA.

10. Arya, C., Buenfeld, N.R. and Newman, J.B. (1990) **Factors Influencing Chloride-binding in Concrete.** Cement and Concrete Research, Vol. 20, pp. 291-300. Elsevier Science Ltd, USA

11. Arya, C. and Xu, Y. (1995) **Effect of Cement Type on Chloride Binding and Corrosion of Steel in Concrete.** Cement and Concrete Research, Vol. 25, No. 4, pp. 893-902. Elsevier Science Ltd, USA

12. ASTM C 1202 – 97. **Standard Test Method for Electrical Indication of Concrete's Ability to Resist Chloride Ion Penetration.** ASTM, USA.

13. Basheer, P.A.M.; Andrews, R.J.; Robinson, D.J. and Long, A.E. (2003) **PERMIT – A new in-situ migration test to determine the chloride transport through cover concrete.** Proceedings of the Tenth International Conference on Extending the Life of Bridges, Concrete and Composites, Buildings, Masonry and Civil Structures. The Commonwealth Institute, London. Edited by Forde, M.C. Engineering Technics Press, UK.

14. Basheer, L.; Basheer, P.A.M. and Long, A.E. (2005) **Influence of coarse aggregate on the permeation, durability and the microstructure characteristics of ordinary Portland cement concrete.** Cement and Concrete Research, Article in press. Elsevier Science Ltd, USA.

15. Basheer, P.A.M.; Gilleece, P.R.V.; Long, A.E. and Mc Carter, W.J. (2002) **Monitoring electrical resistance of concretes containing alternative cementitious materials to assess their resistance to chloride penetration.** Cement and Concrete Composites, Vol. 24, pp. 437 – 449. Elsevier Science Ltd, USA.

16. Birin-Yauri, U.A. and Glasser, F.P. (1998) **Frieldel's Salt, $Ca_2Al(OH)_6(Cl,OH).2H_2O$: It's Solid Solutions and Their Role in Chloride Binding.** Cement and Concrete Research, Vol. 28, pp 1713 - 1723. Pergamon Press Ltd, USA.

17. Bockris. J.O'M. and Reddy, A.K.N. (1998) **Modern Elecrochemistry 1 – Ionics**. Plenum Press, New York, USA.

18. Castelotte, M.; Andrade, C. and Alonso, M. (1999) **Chloride-binding isotherms in concrete submitted to non-steady state migration experiments.** Cement and Concrete Research, Vol. 29, pp. 1799 – 1806. Elsevier Science Ltd, USA.

19. Castelotte, M.; Andrade, C. and Alonso, M. (1999) **Changes in concrete pore size distribution due to electrochemical chloride migration trials.** ACI Materials Journal, Vol. 96. No.3, pp. 314 - 319. American Concrete Institute, USA.

20. Castelotte, M.; Andrade, C. and Alonso, M. (2002) **Accelerated simultaneous determination of the chloride depassivation threshold and of the non-stationary diffusion coefficient values.** Corrosion Science, Vol 44, pp. 2409 – 2424. Elsevier Science Ltd, USA

21. Chatterji, S. (2001) **A discussion of the paper "Mercury Porosimetry: In inappropriate method for the measurement of pore size distributions in**

cement-based materials, by S. Diamond". Cement and Concrete Research, Vol. 31, pp. 1657 – 1658. Elsevier Science Ltd, USA.

22. Crank, J. (1975) **Mathematics of Diffusion.** Clarendon Press, UK.

23. Csizmadia, J.; Balaz, G. and Tamas, F.D. (2001) **Chloride ion binding capacity of aluminoferrites.** Cement and Concrete Research, Vol. 31, pp. 577 – 588.

24. Dehghanian, C. and Arjemandi, M. (1997) **Influence of Slag Blended Cement on Chloride Diffusion Rate.** Cement and Concrete Research, Vol. 27, No. 6, pp. 937 – 945. Elsevier Science Ltd, USA.

25. Delagrave, A., Marchand, J., Ollivier, J.-P., Julien, S. and Hazrati, K. (1997) **Chloride Binding Capacity of Various Hydrated Cement Paste Systems.** Advanced Cement Based Materials, Vol. 6 pp. 28-35. Elsevier Science Ltd, USA.

26. Delegrave, A.; Bigas, J.P.; Ollivier, J.P.; Marchand, J. and Pigeon, M. (1997) **Influence of the Interfacial Zone on the Chloride Diffusivity of Mortars.** Advanced Cement Based Materials, Vol. 5, pp 86 – 92. Elsevier Science Ltd, USA.

27. Detwiler, R.J.; Fapohunda, C.A. and Natale, J. **Use of supplementary Cementing Materials to Increase Resistence to Chloride Ion Penetration of Concretes Cured at Elevated Temperatures.** ACI Materials Journal, Vol. 91, No. 1, pp. 63 – 66. American Concrete Institute, USA.

28. Dhir, R.K.; El-Mohr, M.A.K.; and Dyer, T.D. (1996) **Chloride binding in GGBS concrete.** Cement and Concrete Research, Vol. 26, pp 1767 - 1773. Pergamon Press Ltd, USA.

29. Diamond, S (1976) **Hydraulic Cement Pastes.** Cement and Concrete Association, Wexham Springs.

30. Diamond S. (1986) **The microstructures of cement paste in concrete**. International Proceedings of the VIII Congress on Cement Chemistry, Rio de Janeiro, Brazil. 1986. pp. 122–47.

31. Diamond, S. and Huang, J. (2001) **The ITZ in concrete – a different view based on image analysis and SEM observations.** Cement and Concrete Composites, Vol. 23, pp. 179 – 188. Elsevier Science Ltd, USA.

32. Diamond, S. (2000) **Mercury Porosimetry: In inappropriate method for the measurement of pore size distributions in cement-based materials.** Cement and Concrete Research, Vol. 30, pp 1517 – 1525. Elsevier Science Ltd, USA.

33. Diamond, S. (2001) **Reply to the discussion by S. Wild of the paper "Mercury porosimetry — an inappropriate method for the measurement of pore size distributions in cement-based materials"** Cement and Concrete Research, Vol. 31, pp. 1655 – 1656. Elsevier Science Ltd, USA.

34. Diamond, S. (2001) **Reply to the discussion by S. Chatterji of the paper "Mercury porosimetry—an inappropriate method for the measurement of pore size distributions in cement-based materials"** Cement and Concrete Research, Vol. 31, pp. 1659. Elsevier Science Ltd, USA.

35. Diamond, S. (2003) **A discussion of the paper "Effect of drying on cement-based materials pore structure as identified by mercury porosimetry—a comparative study between oven-, vacuum-, and freeze-drying" by C. Galle**. Cement and Concrete Research, Vol. 33, pp. 169 – 170. Elsevier Science Ltd, USA.

36. Diamond, S. (2003) **Percolation due to overlapping ITZs in laboratory mortars? A microstructural evaluation**. Cement and Concrete Research, Vol. 33, pp. 949 – 955. Elsevier Science Ltd, USA.

37. Diamond, S. (2004) **The microstructure of cement paste and concrete – a visual primer.** Cement and Concrete Composites, Vol. 26, pp. 919 – 933. Elsevier Science Ltd, USA.

38. Elsharief, A.; Cohen, M.D. and Olek, J. (2003) **Influence of aggregate size, water cement ratio and age on the microstructure of the interfacial transition zone.** Cement and Concrete Research, Vol. 33, pp. 1837 – 1849. Elsevier Science Ltd, USA.

39. Emanuelson, A. and Hansen, S. (1997) **Distribution of iron among ferrite hydrates.** Cement and Concrete Research, Vol. 28, No. 8, pp. 1167 – 1177. Elsevier Science Ltd, USA.

40. Endvoldsen, J.N.; Hansson, C.M. and Hope, B.B. (1994) **Binding of Chloride in Mortar Containing Admixed and Penetrated Chlorides.** Cement and Concrete Research, Vol. 24, No. 8, pp. 1525 – 1533. Elsevier Science Ltd, USA.

41. Feldman, R.F. (1981) **Pore Structure Formation During Hydration of Fly Ash and Slag Cement Blend.** Proceedings on the Effects of Fly Ash Incorporation in Cement and Concrete, Edited by Diamond, S., Materials Research Society, pp. 124 – 133.

42. Feldman, R.F. (1984) **Pore Structure Damage in Blended Cements Caused by Mercury Intrusion.** Journal, American Ceramic Society, Vol. 67, pp. 30 – 33. American Ceramic Society, USA.

43. Feldman, R.F. and Serada, P.J. (1968) **A Model for Hydrated Portland Cement Paste as Deduced from Sorption-Length Change and Mechanical**

Properties. Materials and Structures, Vol. 1, No. 6, pp. 509 – 520. RILEM, France.

44. Feldman, R.F. and Sereda, P.J. (1970) **A New Model of Hydrated Cement and its Practical Implications.** Engineering Journal, Vol. 53, pp. 53 – 59. Canada.

45. Feldman, R.F.; Chan, G.W.; Brousseau, R.J. and Tumidajski, P.J. (1994) **Investigation of the Rapid Chloride Permeability Test.** ACI Materials Journal, Vol. 91, No. 2, pp 246 – 255. American Concrete Institute, USA.

46. Galle, C. (2003) **Reply to the discussion by S. Diamond of the paper "Effect of drying on cement-based materials pore structure as identified by mercury intrusion porosimetry: a comparative study between oven-, vacuum- and freeze-drying"** Cement and Concrete Research, Vol 33, pp. 171 – 172. Elsevier Science Ltd, USA.

47. Glass, G.K. and Beunfeld, N.R. (1995) **The Determination of Chloride Binding Relationships.** Chloride Penetration into Concrete. Proceedings of the RILEM INT Workshop, France, October 1995. Eds. Nilsson, L.O. and Ollivier, J.P. RILEM Publications, France.

48. Glass, G.K.; Hassanein, N.M.; and Buenfeld, N.R. (1997) **Neural Network Modelling of Chloride Binding.** Magazine of Concrete Research, Vol. 49, pp 323 - 335. Thomas Telford Services Ltd, USA.

49. Glass, G.K.; Stevenson, G.M.; and Beunfeld, N.R. (1998) **Chloride – binding isotherms from the diffusion cell test.** Cement and Concrete Research, Vol. 28, No. 7. Elsevier Science Ltd, USA.

50. Glass, G.K.; Wang, Y.; and Beunfeld, N.R. (1996) **An Investigation of Experimental Methods Used to Determine Free and Total Chloride Contents.** Cement and Concrete Research, Vol. 26, No 9, pp 1433 – 1449. Elsevier Science Ltd, USA.

51. Gleize, P.J.P.; Muller, A. and Roman, H.R. (2003) **Microstructural Investigation of a Silica Fume–Cement–Lime Mortar.** Cement and Concrete Research, Vol. 25, pp 171 – 175. Elsevier Science Ltd, USA.

52. Goto, S. and Roy, D.M. (1981) **The Effect of W/C Ratio and Curing Temperature on the Permeability of Hardened Cement Paste.** Cement and Concrete Research, Vol. 11, No. 4, pp. 575 – 579. Elsevier Science Ltd, USA.

53. Hadley, D.W., Dolch, W.L. and Diamond, S. (2000) **On the occurrence of hollow-shell hydration grains in hydrated cement paste.** Cement and Concrete Research, Vol. 30, No. 1, pp. 1 – 6. Elsevier Science Ltd, USA.

54. Halamickova, P.; Detwiler, R.J.; Bentz, D.P. and Garboczi, E.J. (1995) **Water permeability and chloride ion diffusion in Portland cement mortars:**

Relationship to sand content and critical pore diameter. Cement and Concrete Research, Vol. 25, No. 4, pp. 790 – 802. Elsevier Science Ltd, USA.

55. Hearn, N. and Figg, J. (2001) **Transport Mechanisms and Damage: Current Issues in Permeation Characteristics of Concrete.** Materials Science of Concrete VI, Edited by Mindess, S. and Skalny, J. The American Ceramic Society, USA.

56. Hearn, N.; Hooton, R. D. and Mills, R. H. (1994) **Pore structure and permeability.** Significance of Tests and Properties of Concrete and Concrete Making Materials – Edited by Klieger, P. and Lamond, J.F. pp.240-262**.** ASTM, USA.

57. Hewlett, P.C. (1998) **Lea's Chemistry of Cement and Concrete.** Fourth Edition. Arnold, London.

58. Hooton, R.D., Thomas, M.D.A. and Stanish, K. (2001), **Prediction of Chloride Penetration in Concrete, Publication No. FHWA-RD-00-142**, US Department of Transportation, Federal Highway Administration, McLean, Va., USA. Available online: http://www.tfhrc.gov/hnr20/pubs/chlconcrete.pdf

59. Igarashi, S.; Watanabe, A. and Kawamura, M. (2005) **Evaluation of capillary pore size characteristics in high-strength concrete at early ages.** Cement and Concrete Research, Vol. 35, pp 513 – 519. Elsevier Science Ltd, USA.

60. Jensen, O.M.; Korzen, M.S.H.; Jakobsen, H.J. and Skibsted, J. (2000) **Influence of cement constitution and temperature on chloride binding in cement paste.** Advances in Cement Research, Vol. 12, No. 2, pp. 57 – 64. Thomas Telford, UK.

61. Jones, M.R.; Macphee, D.E.; Chudek, J.A.; Hunter, G.; Lannegrand, R.; Talero, R.; and Scrimgeour, S.N. (2003) **Studies Using Al MAS NMR of AF_m and AF_t phases and the formation of Friedel's salt.** Cement and Concrete Research, Vol. 33, pp 177 - 182. Pergamon Press Ltd, USA.

62. Justnes, H. (1998) **Review of Chloride Binding in Cementitious Systems.** Nordic Concrete Research Publications, No. 21. Nordic Concrete Research, Norway. Available Online: www.itn.is/ncr/publications/doc-21-4.pdf

63. Kayyali, O.A. and Haque, M.N. (1995) **The Cl^- / OH^- ratio in chloride-contaminated concrete – a most important criterion.** Magazine of Concrete Research, Vol. 47, No. 172, pp. 235 – 242. Thomas Telford Ltd, USA.

64. Khedr, S.A. and Abou-Zeid, M.N. (1994) **Characteristics of Silica Fume Concrete.** Journal of Materials in Civil Engineering, Vol. 6, No. 3, pp. 357 – 375. American Society of Civil Engineers, USA.

65. Lane, S (2000) **Thoughts on the Rapid Chloride Permeability Test.** Federal Highway Administration Resource Center, USA. Available Online: www.fhwa.dot.gov/resourcecenter/hpm_2.htm

66. Liao, K-Y.; Chang, P-K.; Peng, Y-N. and Yang, C-C (2004) **A study on characteristics of interfacial transition zone in concrete.** Cement and Concrete Research, Vol. 34, pp 977 – 989. Elsevier Science Ltd, USA.

67. Luo, R.; Cai, Y.; Wang. C.; and Huang, X. (2003) **Study of chloride binding and diffusion in GGBS concrete.** Cement and Concrete Research, Vol. 33, pp 1 – 7. Elsevier Science Ltd, USA.

68. MacDonald, K.A. and Northwood, D.O. (1995) **Experimental Measurements of Chloride Ion Diffusion Rates Using a Two-Compartment Diffusion Cell: Effects of Material and Test Variables.** Cement and Concrete Research, Vol. 25, No. 7, pp. 1407 – 1416. Elsevier Science Ltd, USA.

69. Mackechnie, J.R. and Alexander, M.G. (2000) **Rapid Chloride Test Comparisons.** Concrete International, Vol. 22, No 5, May 2000. American Concrete Institute (ACI), USA.

70. Mackechnie, J.R. and Alexander, M.G. (2000) **Practical Considerations for Rapid Chloride Conductivity Testing.** Proceedings of the 2nd International RILEM Workshop on Testing and Modelling the Chloride Ingress into Concrete, Paris, 2000. RILEM, France.

71. Mackechnie, J.R.; Alexander, M.G.; and Jaufeerally, H. (2003). **Structural and Durability Properties of Concrete Made With Corex Slag.** Research Monograph No. 6. The University of Cape Town and the University of the Witwatersrand, SA.

72. Mangat, P.S. and Molloy, B.T. (1995) **Chloride Binding in Concrete containing PFA, GBS or Silica Fume under sea water exposure.** Magazine of Concrete Research, Vol. 47, No. 171, pp. 129 – 141. Thomas Telford Services Ltd, USA.

73. McGrath, P.F. and Hooton, R.D. (1996) **Influence of Voltage on Chloride Diffusion Coefficients from Chloride Migration Tests.** Cement and Concrete Research, Vol. 26, No 8, pp. 1239 – 1244. Elsevier Science Ltd, USA.

74. Mehta, P.K. (1981) **Sulphate Resistance of Blended Portland Cements Containing Pozzolans and Granulated Blastfurnace Slag.** Proceedings of the 5th International Symposium on Concrete Technology, Mexico.

75. Mehta, P.K. (1991) **Durability of Concrete – fifty years of progress.** Proceeding of the Second International Conference on Durability of Concrete, Montreal, 1991. Ed. By Malhotra, V.M. Vol. 1, SP126-1, pp.1.

76. Mehta, P.K. and Manmohan, D. (1980) **Pore Size Distribution and Permeability of Hardened Cement Pastes.** Proceedings of the 7th International Congress on Chemistry of Cement, pp. VII 1 – 5.

77. Mehta, P.K. (1986) **Concrete: Structure, Properties and Materials.** Prentice-Hall Inc., NY, USA

78. Midgley, H.G. and Illston, J.M. (1984) **The Penetration of Chlorides into Hardened Cement Pastes.** Cement and Concrete Research, Vol. 14, No. 4, pp. 546 – 558. Elsevier Science Ltd, USA.

79. Montemor, M.F.; Simoes, A.M.P. and Ferreira, M.G.S. (2003) **Chloride-induced corrosion on reinforcing steel: from the fundamentals to the monitoring techniques.** Cement and Concrete Composites, Vol. 25, pp. 491 – 502. Elsevier Science Ltd, USA

80. Nagataki, S.; Otsuki, N.; Tiong-Huan, W. and Nakashita, K. (1992) **Condensation of Chloride Ion in Hardened Cement Matrix Materials and on Embedded Steel Bars.** ACI Materials Journal, Vol. 90, No. 4, pp. 323 – 332. ACI, USA.

81. Neville, A.M. (1981) **Properties of Concrete.** Pitman Publishing, UK.

82. Neville, A.M. (1995) **Properties of Concrete.** Prentice Hall, UK

83. Neville, A.M. (1995) **Chloride Attack of Reinforced Concrete: an Overview.** Materials and Structures, Vol. 28, pp 63 – 70. RILEM, France.

84. Ngala, V.T.; Page, C.L.; Parrott, L.J. and Yu, S.W. (1995) **Diffusion in cementitious materials: II. Further investigations of chloride and oxygen diffusion in well cured OPC and OPC/30% PFA pastes.** Cement and Concrete Research, Vol. 25, No 4, pp. 819 – 826. Elsevier Science Ltd, USA.

85. NTBUILD 202, 2nd Edition. Approved 1984-05. Concrete, Hardened: Chloride Content

86. O'Farrel, M., Wild, S. and Sabir, B.B. (2001) **Pore size distribution and compressive strength of waste clay brick mortar.** Cement and Concrete Composites, Vol. 23, pp. 81 – 91. Elsevier Science Ltd, USA.

87. Ollivier, J.P.; Maso, J.C. and Bourdette, B. (1995) **Interfacial Transition Zone in Concrete.** Advanced Cement Based Materials, Vol. 2, pp. 30 – 38. Elsevier Science Ltd, USA.

88. Page, C.L. (1975) Nature, Vol. 258, No. 514. Nature Publishing Group

89. Page, C.L.; Short, N.R. and El Tarras, A. (1981) **Diffusion of Chloride Ions in Hardened Cement Paste.** Cement and Concrete research, Vol. 11, No. 4, pp. 395 – 406. Elsevier Science Ltd, USA.

90. Page, C.L. and Treadway, K.W.J. (1982) **Aspects of the electrochemistry of Steel in Concrete.** Nature, Vol. 297, No. 109. Nature Publishing Group,

91. Page, C.L. and Vennesland, Ø. (1982). **Pore Solution Composition and Chloride Binding Capacity of Silica Fume Cement Pastes**. SINTEF Report STF65 A82025. SINTEF, Norway.

92. Polder, R.B. and Peelen, W.H.A. (2002) **Characterisation of chloride transport and reinforcement corrosion under cyclic wetting and drying by electrical resistivity.** Cement and Concrete Composites, Vol. 24, pp. 427 – 435. Elsevier Science Ltd, USA.

93. Powers, T.C. (1958) **Structure and Physical Properties of Hardened Cement Paste.** Journal of the American Ceramic Society, Vol. 41, pp. 1 – 6. American Ceramic Society, USA.

94. Principigallo, A.; van Breugel, K and Levita, G. (2003) **Influence of the aggregate on the electrical conductivity of Portland cement concretes.** Cement and Concrete Research, Vol. 33, pp. 1755 – 1763. Elsevier Science Ltd, USA.

95. Rapin, J.-P.; Renaudin, G.; Elkaim, E. and Francois, M. (2002) **Structural Transition of Friedel's Salt $3CaO.Al_2O_3.CaCl_2.10H_2O$ Studied by Synchrotron Powder Diffraction.** Cement and Concrete Research, Vol. 32, pp 513 - 519. Pergamon Press Ltd, USA.

96. Rasheeduzzafar; Ehtesham Hussain, S. and Al-Saadoun, S.S. (1992) **Effect of Tricalcium Aluminate Content of Cement on Chloride Binding and Corrosion of Reinforcing Steel in Concrete.** ACI Materials Journal, Jan-Feb 1992, pp. 3 – 12. ACI, USA.

97. Samaha, H.R. and Hover, K.C. (1992) **Influence of Microcracking on the Mass Transport Properties of Concrete.** ACI Materials Journal, Vol. 89, No. 4, pp. 416 – 424. American Concrete Institute, USA.

98. Samson, E.; Marchand, J. and Snyder, K. A. (2003) **Calculation of Ionic Diffusion Coefficients on the Basis of Migration Test Results.** Materials and Structures, Vol. 36, No. 257, 156-165. RILEM, France.

99. SANS 6245 / SABS SM 1245:1994 **- Potential reactivity of aggregates with alkalis (accelerated mortar prism method). Section 6.3 – Determination of Flow.** South African Bureau of Standards, South Africa.

100. Scrivener, K.L. (2004) **Backscattered electron imaging of cementitious microstructures: Understanding and quantification.** Cement and Concrete Composites, Vol 26, pp. 935 – 945. Elsevier Science Ltd, USA.

101. Scrivener, K.L. and Nemati, K.M. (1996) **The percolation of pore space in the cement paste/aggregate interfacial zone of concrete.** Cement and Concrete Research, Vol. 26, No. 1, pp. 35 – 40. Elsevier Science Ltd, USA.

102. Sergi, G.; Yu, S.W. and Page, C.L. (1992) **Diffusion of Chloride and Hydroxyl Ions in Cementitious Materials Exposed to a Saline Environment.** Magazine of Concrete Research, Vol. 44, No. 158, pp. 63 – 69. Thomas Telford Ltd, USA.

103. Siegwart, M.; Lyness, J.F.; and McFarland, B.J. (2003) **Change of pore size in concrete due to electrochemical chloride extraction and possible implications for the migration of ions.** Cement and Concrete Research, Vol. 33, Elsevier Science Ltd, USA.

104. Soroka, I. (1993) **Concrete in Hot Environments.** E & FN Spon; UK.

105. Stanish, K.D. (2002) **The migration of chloride ions in concrete.** PhD Thesis, Graduate Dept of Civil Engineering, University of Toronto, Canada.

106. Streicher, P.E. (1997) **The development of a rapid chloride test for concrete and its use in engineering practice.** PhD Thesis, Dept of Civil Engineering, University of Cape Town, Cape Town, South Africa.

107. Suryavanshi, A.K. and Scantlebury, J.D. and Lyon, S.B. (1995) **Pore Size Distribution of OPC and SRPC Mortars in Presence of Chlorides.** Cement and Concrete Research, Vol. 25, No. 5, pp. 980 – 988. Elsevier Science Ltd, USA.

108. Suryavanshi, A.K. and Swamy, R.N. (1998) **Influence of Penetrating Chlorides on the Pore Structure of Structural Concrete.** Cement, Concrete and Aggregates, CCAGDP, Vol. 20, No. 1, pp. 169 – 179. American Society for testing Materials, USA.

109. Sze (1981) **Semiconductor Devices – Physics and technology.** John Wiley and Sons, USA.

110. Tang, L. (1996) **Chloride Transport in Concrete – Measurement and Prediction.** PhD. Thesis, Chalmers University of Technology, Sweden.

111. Tang, L. and Nilsson, L-O. (1992) **Rapid Determination of Chloride Diffusivity in Concrete by Applying an Electrical Field.** ACI Materials Journal, Vol. 89, No. 1, pp. 49 – 53. ACI, USA.

112. Tang, L. and Nilsson, L.-O. (1993) **Chloride Binding Capacity and Binding Isotherms of OPC Pastes and Mortars.** Cement and Concrete Research, Vol. 23, pp 247 - 253. Pergamon Press Ltd, USA.

113. Thomas, M.D.A. and Bentz, E.C. (2000) **Life 365 – Service Life and Life-Cycle Cost Analysis of Reinforced Concrete Exposed to Chlorides.** Computer Software.

114. Thomas, M.D.A and Matthews, J.D. (2004) **Performance of pfa concrete in a marine environment – 10-year results.** Cement and Concrete Composites, Vol. 26, pp. 5 – 20. Elsevier Science Ltd, USA.

115. Tritthart, J. (1989) **Chloride Binding in Cement: II. The influence of hydroxide concentration in the pore solution of hardened cement paste on chloride binding.** Cement and Concrete Research, Vol. 19, No. 5, pp. 683 – 691. Elsevier Science Ltd, USA.

116. Tsuyuki, N.; Watanabe, R.; Koizumi, K.; Umemura, Y and Machinaga, O (2000) **Effects of barium salt on the fixation of chloride ions in hardened mortars.** Cement and Concrete Research, Vol. 30, pp 1435 – 1442. Elsevier Science Ltd, USA.

117. Wild, S. (2001) **A discussion of the paper "Mercury porosimetry—an inappropriate method for the measurement of pore size distributions in cement-based materials" by S. Diamond**. Cement and Concrete Research, Vol. 31, pp. 1653 – 1654. Elsevier Science Ltd, USA.

118. Winslow, D.N.; Cohen, M.D.; Bentz, D.P.; Snyder, K.A. and Garbozi, E.J. (1994) **Percolation and Pore Structure in Mortars and Concrete.** Cement and Concrete Research, Vol. 24, pp. 25 – 37. Elsevier Science Ltd, USA.

119. Wittman, F.H. (1973) **Interaction of Hardened Cement Paste and Water.** American Ceramic Society Journal, Vol. 56, No. 8, pp. 409 – 415. American Ceramic Society, USA.

120. Wittman, F.H. (1979) **Trends in Research on Creep and Shrinkage of Concrete.** Cement Production and Use, J.P. Skalny, Ed. Engineering Foundation, No. 79-08, pp. 143 – 462. Engineering Foundation, NY, USA.

121. Xu, Y. (1997) **Influence of sulphates on chloride binding and pore solution chemistry.** Cement and Concrete Research, Vol. 27, No. 12, pp. 1841 – 1850. Elsevier Science Ltd, USA.

122. Yang, C.C. (2004) **Relationship between Migration Coefficient of Chloride Ions and Charge Passed in Steady State.** ACI Materials Journal, Vol. 101, No. 2, pp 124 – 130. ACI, USA.

123. Yang, C.C. and Cho, S.W. (2003) **An electrochemical method for accelerated chloride migration test of diffusion coefficient in cement-based materials.** Materials Chemistry and Physics, Vol. 81, pp. 116 – 125. Elsevier Science Ltd, USA.

124. Yang, C.C. and Su, J.K. (2002) **Approximate Migration Coefficient of Interfacial Transition Zone and the effect of Aggregate Content on the Migration Coefficient of Mortar** Cement and Concrete Research, Vol. 32, No 10, pp. 1559 – 1565. Elsevier Science Ltd, USA.

125. Young, J.F. (1974) **Capillary Porosity in Hydrated tricalcium Silicate Paste.** Powder technology, Vol. 9, pp. 173 – 179.

APPENDIX 1 – SEM OBSERVATIONS

A number of noteworthy observations on the SEM were made that do not have direct links to the presented study.

Figure 88 is a unique cross section of a hydrating cement particle. The curing water has etched the hydration products resulting in a smoothed surface. This has occurred across the fractured particle surface, as well as the honeycomb like CSH gel, diffusing away from the particle. It was therefore uncertain whether the CSH was of Type 1 or Type 2 morphology.

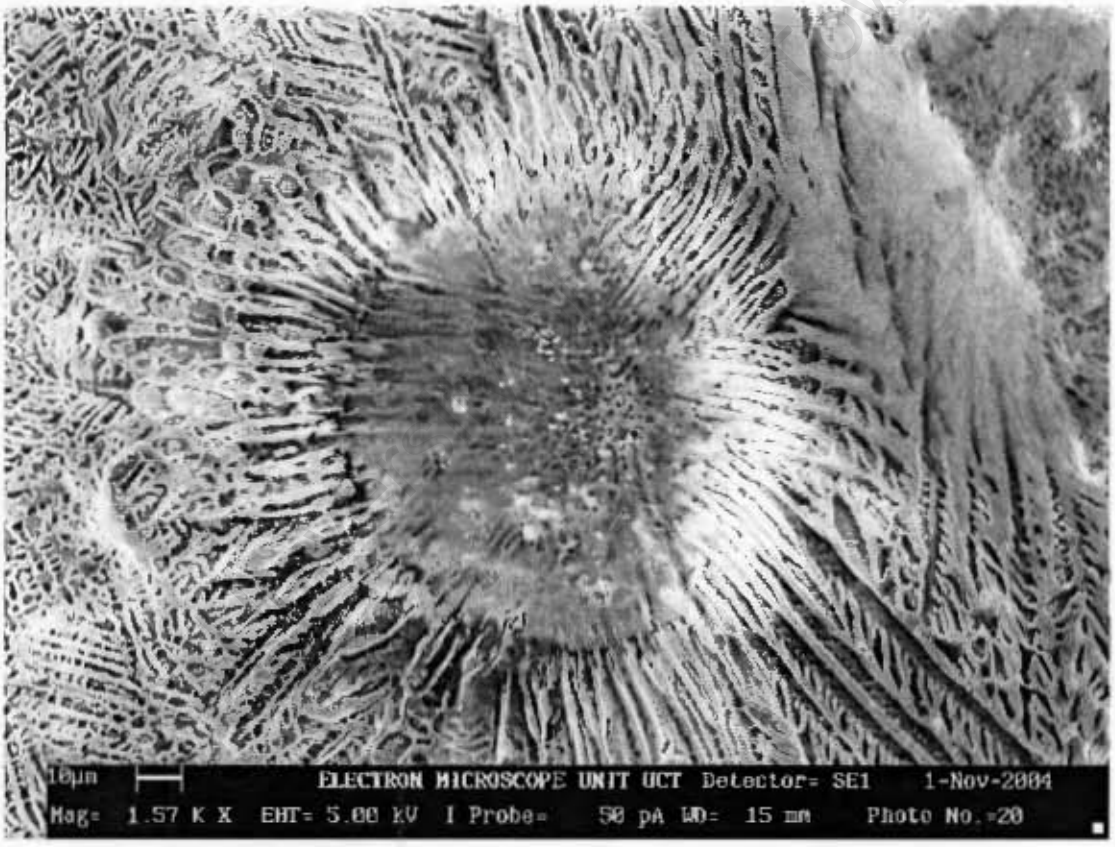

Figure 88: Hydrating cement particle, etched by curing water

The morphology of the CSH gel on the air void walls was noted. This could later be used to distinguish between air voids, voids left by plucked sand grains, and bleed lenses. Large air voids can be seen in Figures 89 and 90. The CSH morphology of the walls is clearly very smooth and regular. The small spherical bubbles or particles within the void could not be identified.

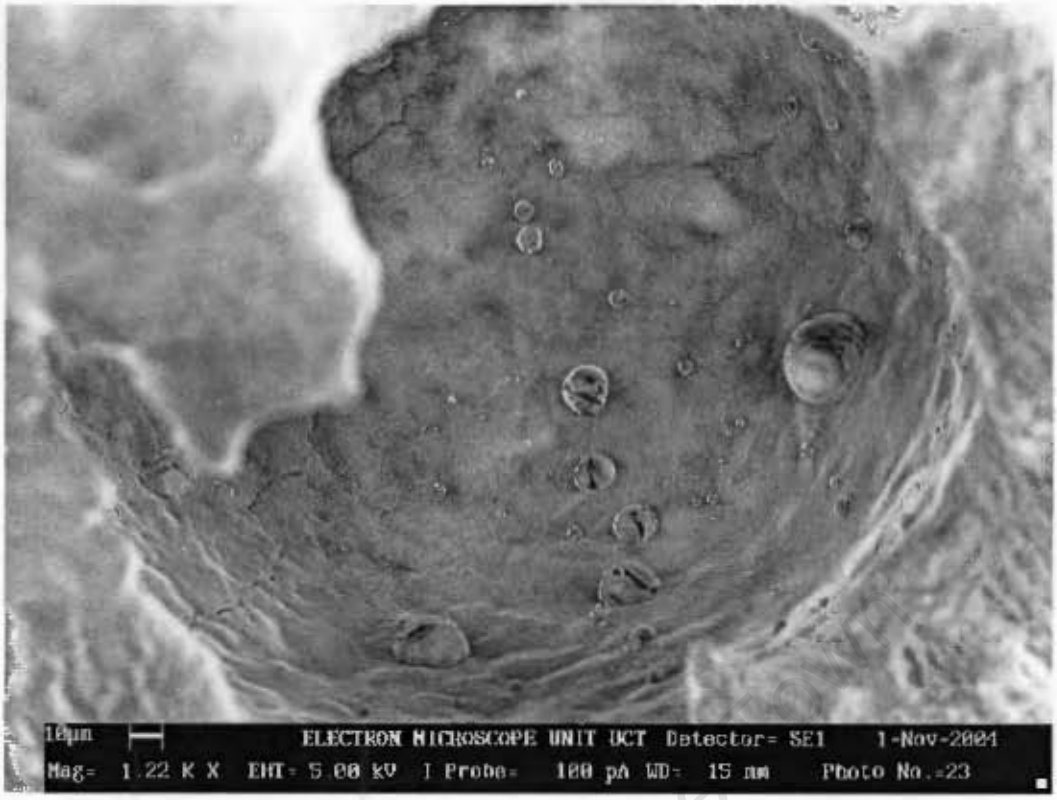

Figure 89: A large air void in a CEM I sample with walls exhibiting a smooth C-S-H gel morphology

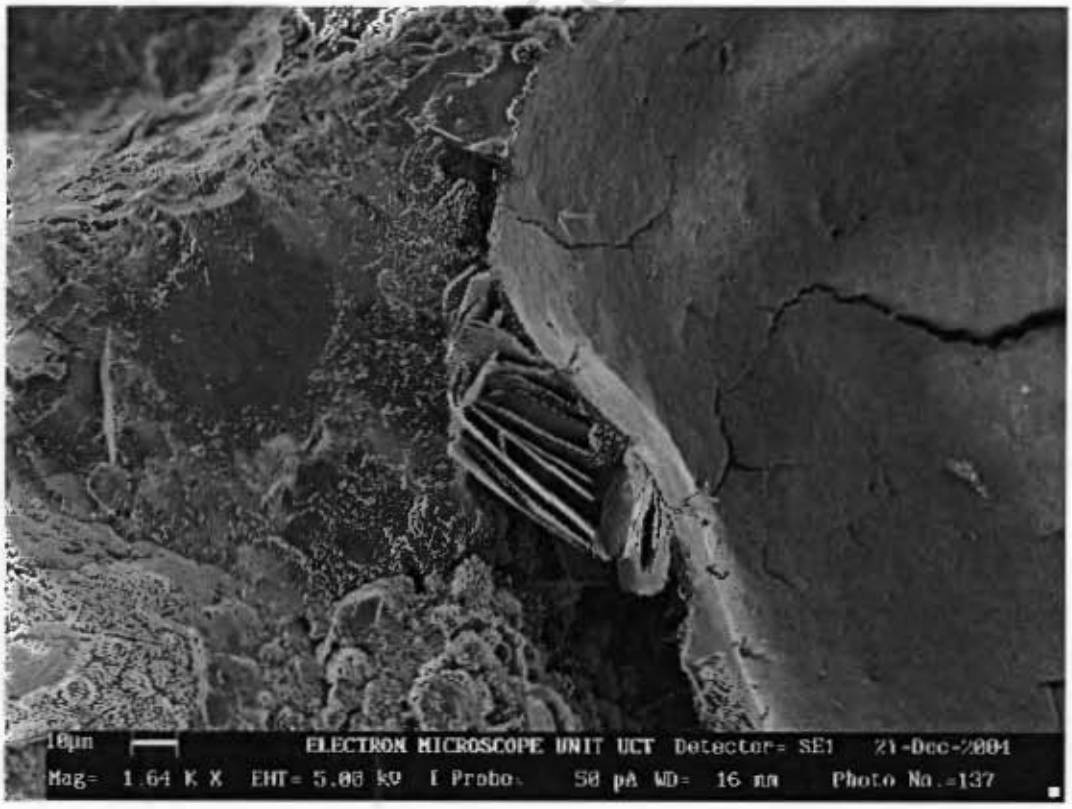

Figure 90: A large air void in a GGCS sample exhibiting a dense outer layer of hydration product and a large deposit of calcium hydroxide within a bleed lens

Figure 91 shows a dislodged sand particle that was surrounded by a bleed lens. Type I CSH can clearly be seen diffusing through the lens towards the sand particle's prior position. At the rear of the void, the Type I CSH had intercepted the particle and had begun to densify around it, probably to form a denser morphology of CSH. Type II CSH can be seen in the top right hand corner of the image and Type III CSH in the bottom right hand corner. Another, larger bleed lens can be seen in figure 92.

The small aggregate particle shown in Figures 93 and 94 clearly shows the Interfacial Transition Zone (ITZ) between aggregate and paste. Even in this very small aggregate dust particle, the ITZ is present.

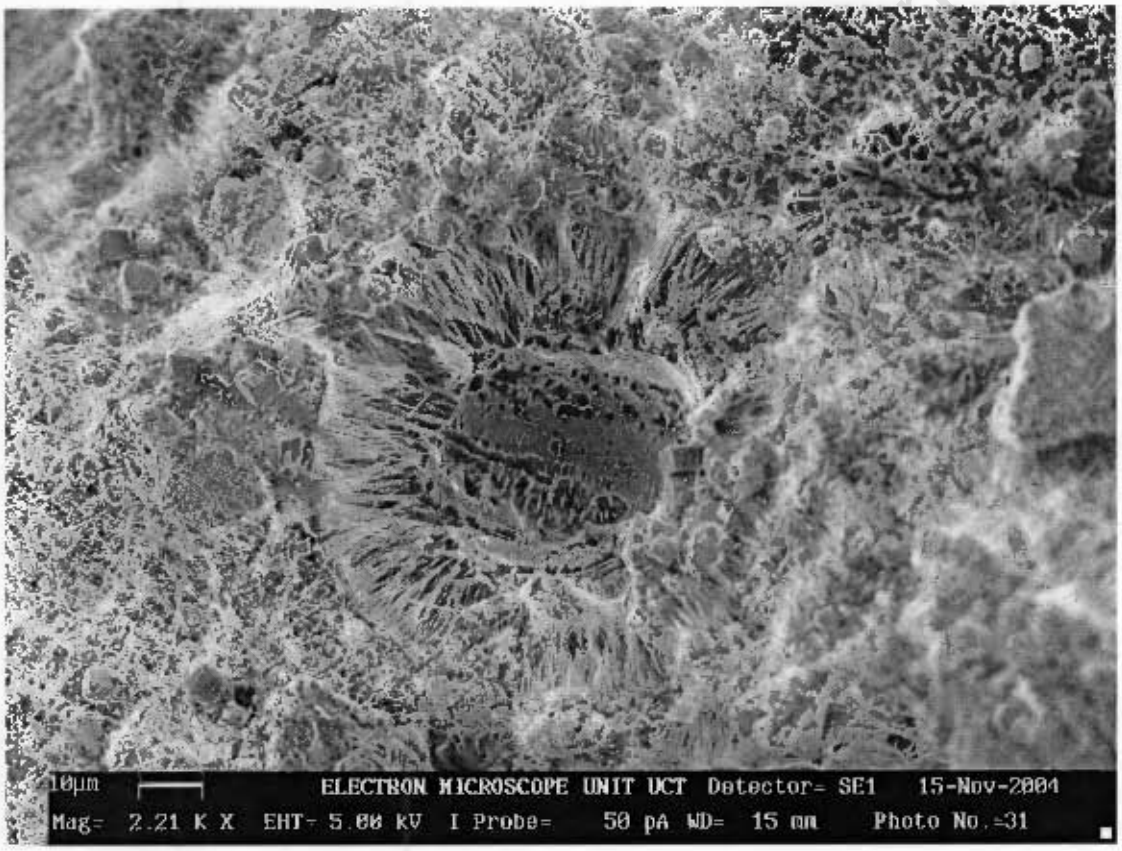

Figure 91: Remnants of a dislodged sand particle, once surrounded by a bleed lens.

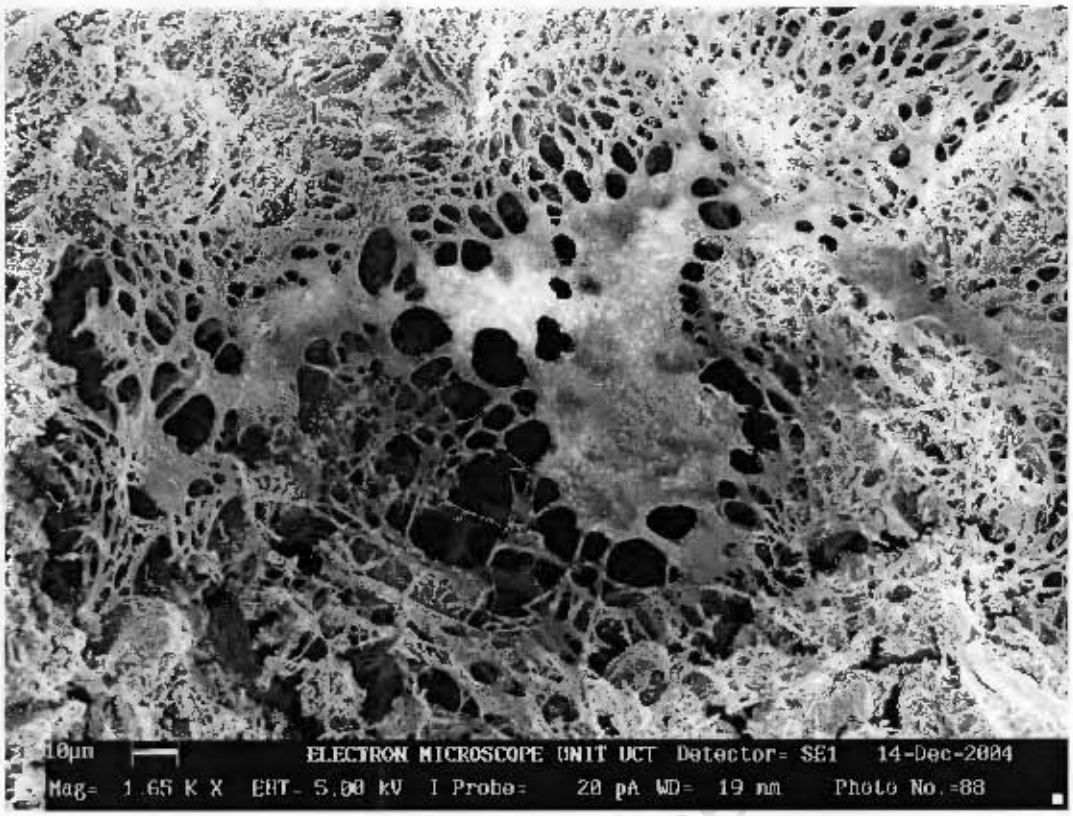

Figure 92: A bleed lens found beneath a sand particle in a 50 % GGCS mortar

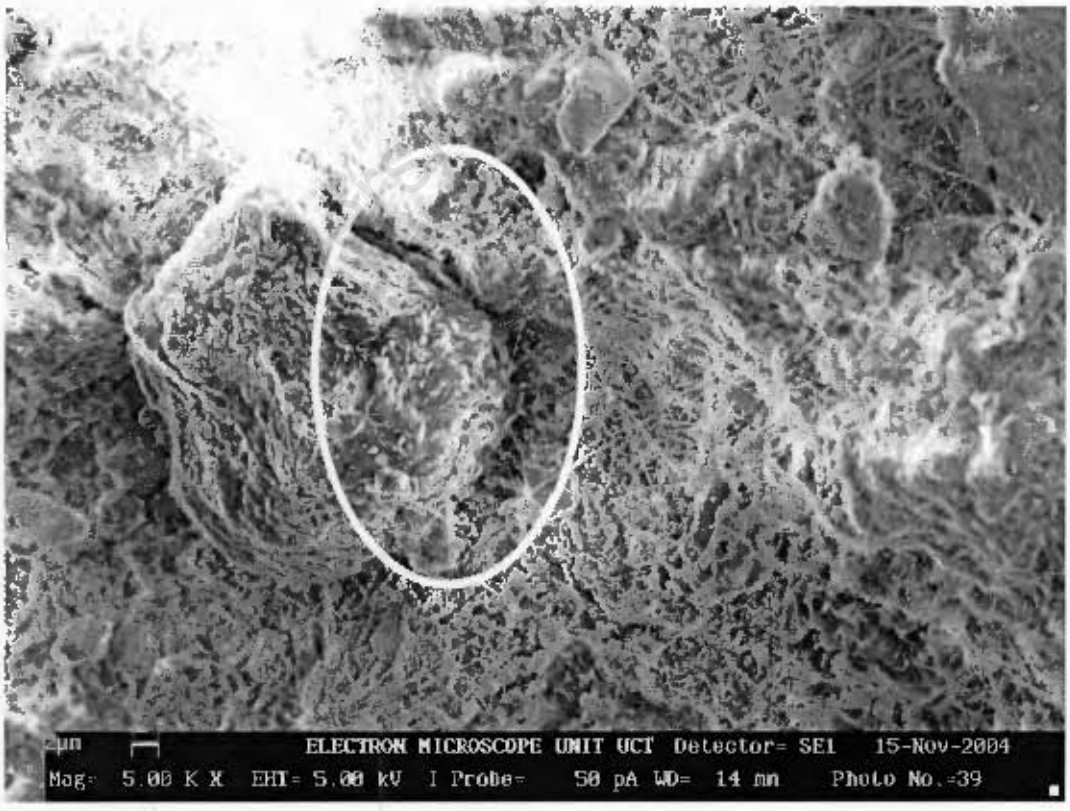

Figure 93: Small sand particle exhibiting the porous and permeable ITZ, characteristic of aggregate particles.

Figure 94: BSEM image of the sand particle showing distinctly differing compositions.

APPENDIX 2 – COMPACT DISC CONTENTS

Due to the size and complexity of the spreadsheets used in the results analysis, these are presented on the accompanying CD. The following is a contents list and brief explanation thereof (folder names are given in bold):

BDT

Results analysis of BDT tests on the mortar samples. The method of analysis and sample profiles can be found here.

Binding

The results of the chloride binding test and bulk porosity test. The method of analysis, unit conversions and plots can be found here.

Chloride Conductivity

The results of chloride conductivity tests on the mortar samples. The method of analysis and results can be found here.

CCT Development Test

The raw data of the CCT development tests and analysis thereof.

Diffusion Tests

Measurements made during the diffusion tests. Prediction model used to analyse this data. Various plots. Linear plot generation and linear regression results.

Migration Tests

Measurements made during the migration tests. Finite difference method used to analyse this data. Various plots. Linear plot generation and linear regression results.

RCPT

Results of RCPT tests on the mortar samples.

RMT

Results of RMT tests on the mortar samples. Photos of the colorimetric indicator.

APPENDIX 3 – TRIAL EXPERIMENTS

Diffusion cells identical to those used in the actual experiments were used in trial tests to determine the effectiveness of the cell design as well as the predictions of the time taken to equalise. The samples were cast with a sand-to-binder ratio of 4 and 5, and at a water binder ratio of 0.8 in order to accelerate the diffusion process and investigate the effect of sand to binder ratio on bleeding and diffusion behaviour.

Two mixes were cast for trial experiments - a CEM 1 mix (at a sand to binder ratio of 4) and a 50 % GGCS mix (at a sand to binder of 5). Four samples per mix were cast and placed in the diffusion cells at 28 days. Five molar NaCl solution was placed upstream and saturated $Ca(OH)_2$ solution placed downstream to avoid leaching. The concentration of both cells was monitored weekly to observe the diffusion behaviour.

It was predicted that the GGCS samples would take longer to equalise due to their superior chloride binding characteristics and more refined pore structure. Contrary to predictions, the GGCS samples exhibited a relatively fast and erratic rate of diffusion (Figure 95). The CEM 1 samples had good correlation in terms of rate of diffusion whereas the GGCS samples had poor correlation. Suspicion arose regarding the quality of the GGCS samples.

Two hypotheses were proposed and investigated in order to explain the erratic behaviour of the GGCS samples. It was hypothesized that the increased diffusion rate, and the erratic nature thereof, may have been due to drying shrinkage of the small samples (although this was unlikely as the specimen were cured at 100 % RH). This would have resulted in the samples pulling away from the edges of the sample holders and exhibiting shrinkage cracks, able to propagate chloride ions more readily than the bulk of the sample. This was investigated using reflected light microscopy.

Two GGCS samples were available, having undergone the same curing as the GGCS samples in the diffusion cells. Microscopy was carried out using two microscopes with magnifications from 2 to 10 times. No evidence of microcracking was seen. However, the interface between the sample and the PVC sample holder showed recesses, some of which were up to 3 mm deep. This would effectively lower the sample thickness, and, hence, the time taken to reach equilibrium, by

approximately 60 %. The recesses were not uniform and highly erratic. It was very possible that similar microscopic recesses occurred in the diffusion test samples. It was concluded that the mix was too harsh and that insufficient cement paste was available for sufficient adhesion between the sample and the former.

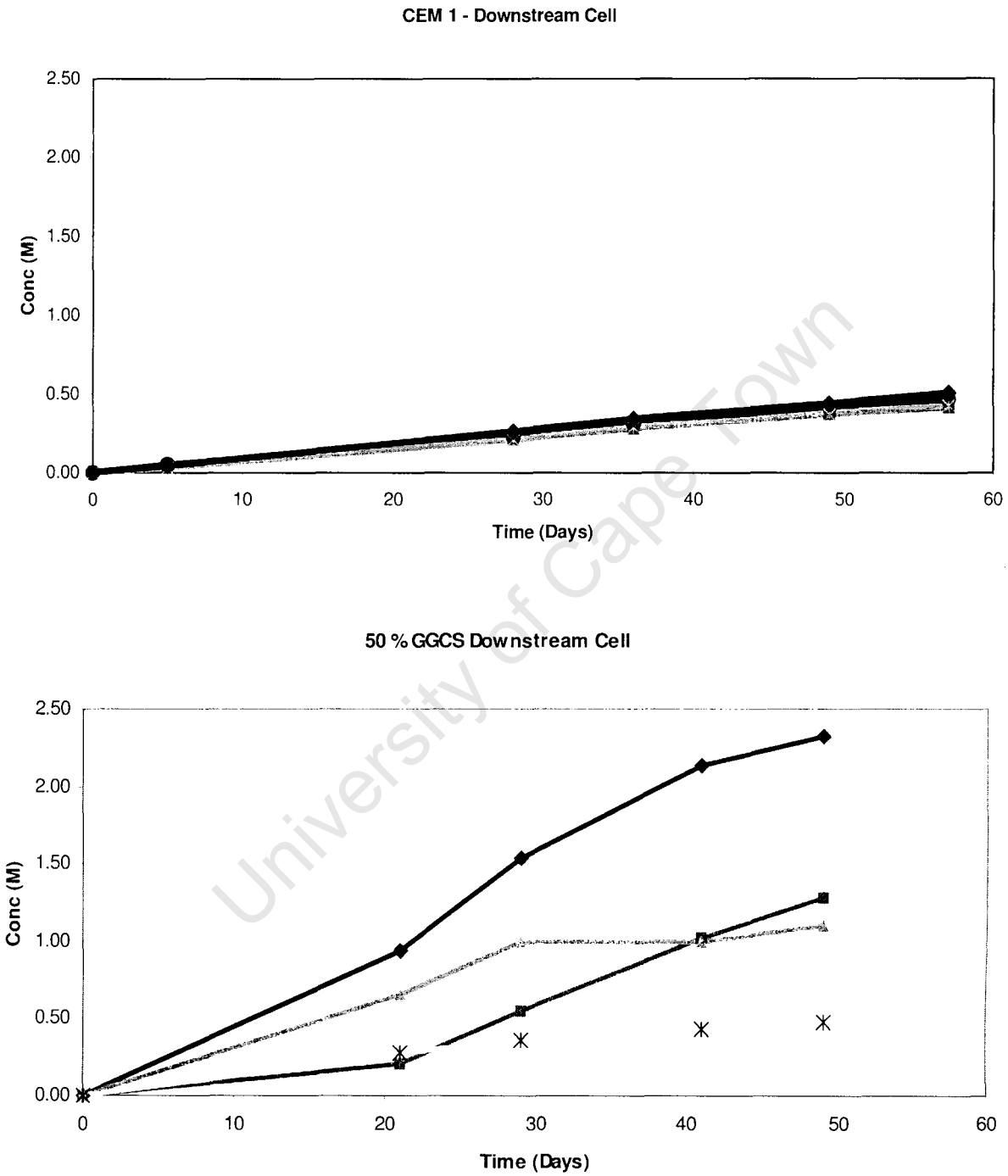

Figure 95: CEM 1 versus 50 % GGCS trial mix diffusion behaviour of four identical cells and samples (vertical axes scales identical for comparative purposes).

Halamickova *et al* (1995) found that sand to binder ratio affected diffusion rates and coefficients substantially, as discussed in Chapter 3. It was possible that the sand to binder ratio used in these samples (five) was near to a critical value at which percolation begins to occur. This would have resulted in erratic behaviour.

One area of potential concern when using a lower sand content is excessive bleeding. While this was seen with the CEM 1 and GGCS mortars at a w:b of 0.8, it was expected that the lower w:b of 0.65 would alleviate the problem. The inclusion of CSF acts to reduce bleeding and thus the use of higher w:b with the lower sand content was acceptable. It was, therefore, decided that a sand-to-binder ratio of four be used for all mortars.